Doctoral theses at NTNU, 2020:285

Yosuke Kodama

Translational Research in Personalized Medicine with Special References to Gastric Cancer and Obesity

Doctoral thesis

Yosuke Kodama

ISBN 978-82-326-4918-1 (printed ver.)
ISBN 978-82-326-4919-8 (electronic ver.)
ISSN 1503-8181

NTNU
Norwegian University of
Science and Technology

NTNU
Norwegian University of Science and Technology
Thesis for the Degree of
Philosophiae Doctor
Faculty of Medicine and Health Sciences
Department of Clinical and Molecular Medicine

Doctoral theses at NTNU, 2020:285

NTNU
Norwegian University of
Science and Technology

Yosuke Kodama

Translational Research in Personalized Medicine with Special References to Gastric Cancer and Obesity

Thesis for the Degree of Philosophiae Doctor

Trondheim, September 2020

Norwegian University of Science and Technology
Faculty of Medicine and Health Sciences
Department of Clinical and Molecular Medicine

NTNU
Norwegian University of
Science and Technology

NTNU
Norwegian University of Science and Technology

Thesis for the Degree of Philosophiae Doctor

Faculty of Medicine and Health Sciences
Department of Clinical and Molecular Medicine

ISBN 978-82-326-4918-1 (printed ver.)
ISBN 978-82-326-4919-8 (electronic ver.)
ISSN 1503-8181

Doctoral theses at NTNU, 2020:285

Printed by NTNU Grafisk senter

Table of Contents

Acknowledgements

This thesis was carried out at the Research Group of Experimental Surgery and Pharmacology at the Department of Clinical and Molecular Medicine, Faculty of Medicine and Health Sciences, Norwegian University of Science and Technology (NTNU) from 2008 to 2013. The research grants and PhD fellowship were supported by the Functional Genomics Programme (FUGE) of the Research Council of Norway (RCN) and the European Union Seventh Framework Programme (FP/2007-2013) under grant agreement no. 266408.

I would like to express my deepest gratitude to my supervisor Professor **Duan Chen** for giving me an opportunity to study under his supervision in Norway, and for his enthusiastic instruction throughout the entire of my study, providing me many new and challenging ideas and broadening my scientific view, which now becomes a fundamental to my skills, knowledge and philosophy as a scientist. He kindly supported me not only at research but also at private. We sometimes shared exciting feelings at experiments or research, being such a great memory for me.

I am truly grateful to my co-supervisor Dr. **Chun-Mei Zhao**. I learned a lot from her and was impressed by her unique and excellent ideas. Especially, she invented the sampling plate for stomach samples, it became essential tools for our experiments. We often conducted experiments together and at the same time, she taught me basic skills and knowledge of research. Together with Professor Duan Chen, she took care of me very kindly both at work and at private, like a “mother” to me in Norway, which remarkably helped me to establish my life in Norway.

I would like to give my special thanks to Dr. **Anders Øverby**. He is my excellent colleague as well as my great friend. We worked together quite often from early morning to very late evening, both in Norway and Japan. His hard work, passion and motivation always impressed and motivated me. He often invited me to the events in order to make me fun and relaxed. Anime meeting together with his friends, is an unforgettable memory. Whenever I struggled so much, you were always there, you

always encouraged me. Without his support, I would never have been possible to finish my PhD.

I also would like to give my special thanks to Dr. **Carl-Jørgen Arum**, and his family; **Karina**, **Ronja**, **Andrea**, **Silja**, **Thorbjørn** and **Linnea**. As my colleague, I enjoyed the experiments together with Dr. Carl-Jørgen Arum and I particularly could learn many things about clinical medicine from him. He and his family kindly treated me as a part of their family. I spent really good time with them, and have a lot of wonderful memories with them. They saved me from my lonely life in Norway.

I really would like to thank my good colleague and good friend Dr. **Helene Johannessen**. As we were PhD students together under supervision from Professor Duan Chen and Dr. Chun-Mei Zhao, we conducted numerous experiments together, supported each other, shared both fun and tough time. You might have learned several things from me but I also could learn many things from you. I am glad and honor that I could be your colleague and friend.

I would like to thank my colleague Dr. **Gøran Andersen**. Thankfully, he always cared about me, especially my mental status, it helped and saved me. He invited several times to his house and I could enjoy together with him and his family. As he is a surgeon in gastroenterology, I also learned clinical practice and medicine in the field of gastroenterology through his profession.

I would like to thank my colleague Dr. **Marianne Furnes** for teaching me basic skills and knowledge for animal research, and teaching me how to take care of animals properly. My thesis, especially part II focusing on obesity, is on the continuation of her great efforts and many works in obesity research. I found she is a very kind person and I thank her for taking care of me very well.

I would like to thank my colleague Dr. **Oluf Dimitri Røe**. He is a really kind and also talented person, and he cared about me all the time. Discussion with him about cancer research was very helpful. Not only him but also his family treated me very nicely. His music was brilliant and impressed me, I always enjoyed his music and humorous talk.

I would like to thank my colleague Dr. **Alexander Vigen** for his friendship with me and giving me a chance to learn clinical practice. His study about autophagy in gastric cancer helped me to gain the knowledge of the study in gastric cancer.

I also thank **Hanne-Line Rabben**. Her hard work and numerous results overwhelmed me but motivated me as well. She helped and encouraged me to write this thesis. I really appreciate her help.

All collaborators deserve my sincere thanks for their fruitful contributions to our studies. Especially, Professor **Timothy Wang** at Columbia University, New York, USA had great contribution to Paper I of my thesis and he kindly offered me to use his office when I visited there to finish and submit the manuscript of Paper I. Dr. **Hiroyuki Tomita** from Gifu University, Japan collected more than 100 immunohistochemical samples from primary gastric cancer patients and supported me to analyze the samples when I visited to his laboratory. Dr. **Sureshkumar Muthpalani** from Massachusetts Institute of Technology, USA performed pathological analysis on numerous samples from our research group. **Arnar Flatberg** who is a bioinformatician at NTNU, helped me patiently and remarkably to analyze and reanalyze the huge size of gene expression data obtained from microarray and qRT-PCR. Professor **Arne Sandvik** and Dr. **Vidar Beisvag** taught me the basic techniques and knowledge of microarray and bioinformatics.

I spent most of time in the animal facility for the experiments, thus I really would like to thank the staff at the animal facility at St. Olav's hospital; **Anne Åm**, **Trine Skoglund**, **Nils Hagen**, **Knut Grøn** and **Erling Wold**, **Venke-Lill Nygård** and **Karin Nykkelmo**, for their great help, taking very good care of our animals, kindness and friendship.

I wish to thank Dean, Professor **Björn Gustafsson** and Dr. **Miriam Gustafsson** for their deep kindnesses to me, for all the kind considerations to support finishing of my PhD, and for encouraging me to finish my PhD.

My gratefulness also goes to Dr. **Vidar Rao**, **Nina Sandberg** and **Oddrun Storrø**. We shared the office and they were so nice and sweet to me every day.

Professor **Susumu Okabe** first taught me pharmacology when I was in pharmacy school in Kyoto, Japan. After his retirement from the university, he visited to our research group in Norway and we conducted a research together. Eventually, we could publish the paper (Paper S4) and this method was used for Paper I. I was very impressed and inspired by his passion for research, and I am grateful for valuable experience from him.

Professor **Koji Takeuchi** first instructed me the basic skills and techniques of animal experiments when I was in his laboratory in pharmacy school. He provided us M_3 knockout mice, which were used and supplied important results for the study of Paper I. I would like to thank him especially for giving me the first opportunity to meet Professor Duan Chen.

I wish to thank Dr. **Masahiko Nakamura** for giving me the second opportunity to see Professor Duan Chen. Actually, this meeting became the critical step to start my study in Norway under Professor Duan Chen's supervision. I also appreciate that Dr. Masahiko Nakamura kindly offered me the work environment for focusing on my thesis.

I also wish to thank my friends at NTNU in Norway; **Kim Stiberg**, **Takaya Saito**, **Laurent Thomas**, **Stefan Blankvoort**, **Iwe Muiser**, **Peter Karpati**, **Bjørnar Sporsheim**, **Hiroshi Ito**, **Masato Uemura** and **Takuma Kitanishi** for the friendship and social activities with me, which certainly helped me to enjoy my life in Norway. Special thanks to Kim Stiberg and Peter Karpati for their deep kindness, support and encouragement.

I thank Professor **Kenichi Inui** (former director of Pharmacy Department at Kyoto University Hospital and former rector of Kyoto Pharmaceutical University), Dr. **Hiroshi Okada** (senior lecturer at School of Public Health, Kyoto University), Professor **Egil Pedersen** (former Professor at Department of Marine Technology, NTNU, and present Professor at Department of Technology and Safety, University of Tromsø) and his family for caring about me and encouraging me.

I would like to thank my parents, **Takashi Kodama** and **Mitsuko Kodama**, for their support for my study in Norway and for writing this thesis.

This thesis is dedicated to the memory of Dr. **Kazuhiro Kaneko** and Dr. **Yoshihiro Kondo**. Dr. Kazuhiro Kaneko who was a physician at National Cancer Center Hospital East, Japan, greatly contributed to our study (Paper I). He loved our study so that he worked very hard to provide us the data though he had been quite occupied by his clinical practice, even on the day his father passed away. Very sadly, he passed away at the day when he was supposed to give a speech for the ceremony of the collaboration between NTNU and Kitasato University, i.e., he continued the dedication to NTNU right until his death. I will never forget his contribution and wonderful smile. Dr. Yoshihiro Kondo had shown me his drastic effort to finish his PhD even though he had been extremely busy with working as a pharmacist at community pharmacy even while he had been suffering from the stage IV cancer. He had continued to encourage me to finish my PhD until just before his death. I really would like to thank him from the bottom of my heart.

List of Papers

This thesis is based on the following papers, which are referred to by their Roman numerals in the text (I-III).

I: Chun-Mei Zhao, Yoku Hayakawa, **Yosuke Kodama**, Sureshkumar Muthupalani, Christoph B. Westphalen, Gøran T. Andersen, Arnar Flatberg, Helene Johannessen, Richard A. Friedman, Bernhard W. Renz, Arne K. Sandvik, Vidar Beisvag, Hiroyuki Tomita, Akira Hara, Michael Quante, Zhishan Li, Michael D. Gershon, Kazuhiro Kaneko, James G. Fox, Timothy C. Wang & Duan Chen
Denervation suppresses gastric tumorigenesis
Sci Transl Med. 2014 Aug 20;6(250):250ra115.

II: **Yosuke Kodama**, Chun-Mei Zhao, Bård Kulseng, Duan Chen
Eating behavior in rats subjected to vagotomy, sleeve gastrectomy, and duodenal switch
J Gastrointest Surg. 2010 Oct;14(10):1502-10.

III: **Yosuke Kodama**, Helene Johannessen, Marianne W. Furnes, Chun-Mei Zhao, Gjermund Johnsen, Ronald Mårvik, Bård Kulseng, Duan Chen
Mechanistic comparison between gastric bypass vs. duodenal switch with sleeve gastrectomy in rat models
PLoS One. 2013 Sep 9;8(9):e72896.

List of additional publications

The following papers and book chapter (S1-S9) were published during the period of my doctoral work. Although these papers were not included in this thesis, the findings of these papers were discussed in the context of this thesis.

S1: Carl-Jørgen Arum, **Yosuke Kodama**, Natale Rolim, Marius Widerøe, Endre Anderssen, Trond Viset, Marit Otterlei, Steinar Lundgren, Duan Chen, Chun-Mei Zhao
A rat model of intravesical delivery of small interfering RNA for studying urinary carcinoma
World J Urol. 2010 Aug;28(4):479-85.

S2: Carl-Jørgen Arum, Endre Anderssen, Trond Viset, **Yosuke Kodama**, Steinar Lundgren, Duan Chen, Chun-Mei Zhao
Cancer immunoediting from immunosurveillance to tumor escape in microvillus-formed niche: a study of syngeneic orthotopic rat bladder cancer model in comparison with human bladder cancer
Neoplasia. 2010 Jun;12(6):434-42.

S3: Chun-Mei Zhao, Helene Johannessen, **Yosuke Kodama**, Bård Kulseng, Duan Chen
Handbook of Biologically Active Peptides
Edited by Abba J. Kastin. London, UK, Elsevier. 2nd edition 2011

S4: Susumu Okabe, **Yosuke Kodama**, Hailong Cao, Helene Johannessen, Chun-Mei Zhao, Timothy C. Wang, Rei Takahashi, Duan Chen
Topical application of acetic acid in cytoreduction of gastric cancer. A technical report using mouse model
J Gastroenterol Hepatol. 2012 Apr;27 Suppl 3:40-8.

S5: Helene Johannessen, **Yosuke Kodama**, Chun-Mei Zhao, Mirta ML Sousa, Geir Slupphaug, Bård Kulseng, Duan Chen

Eating behavior and glucagon-like peptide-1-producing cells in interposed ileum and pancreatic islets in rats subjected to ileal interposition associated with sleeve gastrectomy

Obes Surg. 2013 Jan;23(1):39-49.

S6: Reidar Alexander Vigen, **Yosuke Kodama**, Trond Viset, Reidar Fossmark, Helge Waldum, Mark Kidd, Timothy C. Wang, Irvin M. Modlin, Duan Chen, Chun-Mei Zhao

Immunohistochemical evidence for an impairment of autophagy in tumorigenesis of gastric carcinoids and adenocarcinomas in rodent models and patients

Histol Histopathol. 2013 Apr;28(4):531-42.

S7: Oddrun Anita Gudbrandsen, **Yosuke Kodama**, Svein Are Mjøs, Chun-Mei Zhao, Helene Johannessen, Hans-Richard Brattbakk, Christine Haugen, Bård Kulseng, Gunnar Mellgren, Duan Chen

Effects of duodenal switch alone or in combination with sleeve gastrectomy on body weight and lipid metabolism in rats

Nutr Diabetes. 2014 Jun 30;4:e124.

S8: Chun-Mei Zhao, **Yosuke Kodama**, Arnar Flatberg, Vidar Beisvag, Bård Kulseng, Arne K. Sandvik, Jens F. Rehfeld, Duan Chen

Gene expression profiling of gastric mucosa in mice lacking CCK and gastrin receptors

Regul Pept. 2014 Jun-Aug;192-193:35-44.

S9: Helene Johannessen, David Revesz, **Yosuke Kodama**, Nikki Cassie, Karolina P. Skibicka, Perry Barrett, Suzanne L. Dickson, Jens J. Holst, Jens F. Rehfeld, Geoffrey van der Plasse, Roger A. H. Adan, Bård Kulseng, Elinor Ben-Menachem, Chun-Mei Zhao, Duan Chen

Vagal Blocking for Obesity Control: a Possible Mechanism-Of-Action

Obes Surg. 2017 Jan;27(1):186.

Abbreviations

3Rs	Replace, Refine and Reduce (guideline for human use of animals)
5-FU	5-fluorouracil
ANCOVA	Analysis of covariance
ANOVA	Analysis of variance
ATP	Adenosine triphosphatase
BMDC	Bone marrow-derived cell
BMI	Body mass index
Botox	Botulinum toxin type A
CagA	Cytotoxin-associated antigen A
CCK	Cholecystokinin
CD44	Cluster of differentiation 44
CLAMS	Comprehensive Laboratory Animal Monitoring System
CSC	Cancer stem cell
Dclk1	Doublecortin-like kinase 1 protein
DNA	Deoxyribonucleic acid
DS	Duodenal switch
ECL cell	Enterochromaffin-like cell
EMR	Endoscopic mucosal resection
EMT	Epithelial-mesenchymal transition
ESD	Endoscopic submucosal dissection

FELASA	Federation of European Laboratory Animal Science Association
GB	Gastric bypass
GERD	Gastroesophageal reflux disease
GFP	Green fluorescent protein
GLP-1	Glucagon-like peptide-1
GM-CSF	Granulocyte-macrophage colony stimulating factor
GSC	Gastric stump cancer
HER-2	Human epidermal growth factor receptor 2
IFNγ	Interferon gamma
IL	Interleukin
INS-GAS	Insulin-gastrin transgenic mouse
KEGG	Kyoto Encyclopedia of Genes and Genomes
LAP	Laparotomy
Lgr5	Leucine-rich repeat-containing G-protein coupled receptor 5
LPS	Lipopolysaccharide
M_3R	Muscarinic acetylcholine receptor M_3
MAPK	Mitogen-activated protein kinase
MNNG	N-methyl-N'-nitro-N-nitrosoguanidine
MNU	N-methyl-N-nitrosourea
mRNA	Messenger ribonucleic acid
NIH	US National Institutes of Health
PCR	Polymerase chain reaction

PGE_2	Prostaglandin E_2
PGP9.5	Protein gene product 9.5
PP	Pyloroplasty
qRT-PCR	Quantitative real-time polymerase chain reaction
RER	Respiratory exchange ratio
RNA	Ribonucleic acid
SEM	Standard error of the mean
SG	Sleeve gastrectomy
SNAP-25	Synaptosomal nerve-associated protein 25
SPIA	Signaling pathway impact analysis
tA score	Score of total net accumulated pertubation obtained by SPIA
TLR	Toll-like receptor
TNFα	Tumor necrosis factor alpha
TPMT	Thiopurine S-methyltransferase
UVT	Unilateral anterior truncal vagotomy
VacA	Vacuolating cytotoxin A
VBLOC	Vagal blocking for obesity control
VEGF	Vascular endothelial growth factor
VTPP	Bilateral truncal vagotomy with pyloroplasty
WHO	World health organization

Abstract in English

Translational research in personalized medicine with special references to gastric cancer and obesity

Background: Translational research in medical science is essential because the rapid progression of science and technology has led to "the valley of death" between basic science and clinical practice. Cancer is one of the main leading causes of morbidity and mortality worldwide, and gastric cancer is the 5th most common cancer and the 3rd leading cause of cancer mortality (8.2% of all cancer deaths). Over the past decades, early diagnosis and minimal invasive surgery have been successfully applied in gastric cancer patients, however the treatment of patients with advanced gastric cancer still remains a challenging, as the current standard treatment such as chemotherapy is effective only in a small proportion of the patients due to high heterogeneity of gastric cancer. Thus, the development of new and personalized therapy for gastric cancer is needed. Several reports have demonstrated the importance of crosstalk between tumor cells and nerves, and vagus nerve is well-known to play an important role in the regulation of gastrointestinal function and gastric epithelial cell proliferation, indicating the potential role of vagus nerve in gastric tumorigenesis. Obesity is one of the risk factors to develop gastric cancer and the bariatric surgery is effective treatment for weight loss as well as reducing the cancer risk in obese patients, however the mechanisms underlying various bariatric procedures remain unclear, and thus it is important to elucidate the underlying mechanisms for personalized bariatric surgery.

Aims: Overall aim of this thesis is to conduct translational research with attempt to develop personalized therapies for gastric cancer (Part I) and obesity (Part II). The specific objectives included: (i) to investigate the role of vagus nerve on gastric tumorigenesis, and to develop new treatment based on the elucidated underlying mechanism, (ii) to elucidate the mechanisms of bariatric surgeries such as vagotomy with pyloroplasty (VTPP), sleeve gastrectomy (SG), duodenal switch (DS) and gastric bypass (GB).

Methods: In Part I, pathological evaluation, immunohistochemical analyses and gene expression profiling were performed using three different mouse models of gastric cancer (i.e.,

genetically-, chemically- or infection-induced gastric cancer models). Mice underwent denervation by VTPP (including unilateral vagotomy, UVT) or local injection of botulinum toxin type A (Botox). *In vitro* gastric organoids were also used. Three cohort studies were performed on human primary gastric cancer and gastric stump cancer. In Part II, rats were subjected to VTPP, PP, SG, DS, SG+DS, GB and laparotomy (as controls), and monitored by comprehensive laboratory animal monitoring system (CLAMS).

Results: In Part I, denervation of the stomach markedly inhibited gastric cancer initiation and progression, particularly in the denervated portion of the stomach (such as after UVT and unilateral Botox injection), in all three independent mouse models of gastric cancer. Denervation also enhanced the anti-tumor effects of chemotherapy and prolonged survival. Denervation-induced suppression of tumorigenesis was associated with suppression of the stem cell expansion by inhibiting Wnt signaling via muscarinic acetylcholine receptor M_3 (M_3R). In gastric cancer patients, tumor stage and lymph node metastasis correlated with neural density and activated Wnt signaling, whereas vagotomy reduced the risk of gastric cancer. In Part II, VTPP did not affect body weight, eating behavior and metabolic parameters. SG reduced body weight in short-term but not long-term, and transiently increased energy expenditure without reduction of food intake. DS regardless of whether it was accompanied by SG caused remarkable and continuous body weight loss, which was associated with increased energy expenditure, reduction of food intake and malabsorption. GB induced persistent body weight loss which was associated with increased energy expenditure without altered eating behavior and malabsorption.

Conclusions: In Part I, denervation suppresses gastric cancer initiation as well as progression through inhibition of the cancer stem cell niche by down-regulation of Wnt signaling pathway via M_3R. These findings could be translated to clinical trials using endoscopic Botox injection, and the therapy should be personalized depending on Wnt signaling expression on each gastric cancer patient. In Part II, weight loss after each bariatric surgical procedure differs in terms of degree, duration and the underlying mechanisms, pointing to the need of personalized bariatric surgery.

Abstract in Norwegian

Translasjonsforskning i personalisert medisin med fokus på magekreft og fedme

Introduksjon: Translasjonsforskning innen medisin er viktig fordi den raske utviklingen av vitenskap og teknologi har ført til et gap mellom grunnforskning og klinisk praksis. Kreft er en av de største årsakene til sykdom og dødelighet over hele verden, og magekreft er den femte vanligste krefttypen og den tredje ledende årsaken til kreftdødelighet. I løpet av de siste tiårene har tidlig diagnose og minimal invasiv kirurgi vært vellykket hos pasienter med magekreft. Samtidig er behandlingen av pasienter med avansert magekreft fortsatt utfordrende, siden nåværende standard behandling som inkludererer cellegift, kun er effektiv i en mindre andel av pasientene på grunn av høy heterogenitet i magekreft. Dermed er det behov for utvikling av en ny og mer individuelt rettet terapi for magekreft. Flere rapporter har beskrevet viktigheten av samspillet mellom tumorceller og nerver, og vagusnerven har blitt vist å spille en sentral rolle i regulering av gastrointestinale funksjoner og celleproliferasjon i gastroepitelcellevev, og videre en mulig rolle i gastrisk tumorigenese. Fedme utgjør en av risikofaktorene for å utvikle magekreft og bariatrisk kirurgi er en effektiv behandling for vekttap i tillegg til å redusere kreftrisikoen hos overvektige pasienter. Samtidig er de underliggende mekanismene for de forskjellige bariatriske prosedyrene fortsatt uklare som derfor argumenterer for et behov av å belyse disse for en økt forståelse av mekanismene for personlig bariatrisk kirurgi.

Hensikt: Hovedmålet i dette doktorgradsarbeidet var å utføre translasjonsforskning med fokus på å utvikle personaliserte terapier for magekreft (del I) og fedme (del II). Delmålene var: (i) å undersøke vagusnervens rolle i gastrisk tumorigenese, og å utvikle ny behandling basert på en økt forståelse av underliggende mekanismer, (ii) å avdekke mekanismene i bariatriske kirurgiske metoder som vagotomi med pyloroplasti (VTPP), gastrisk sleeve (SG), duodenal switch (DS) og gastrisk bypass (GB).

Metode: I del I ble patologisk evaluering, immunhistokjemiske analyser og genuttrykk-profilering utført ved bruk av tre ulike musemodeller som utvikler magekreft (genetisk-, kjemisk- eller infeksjonsindusert magekreftmodeller). Musene gjennomgikk denervering av VTPP (inkludert ensidig vagotomi, UVT) eller lokal injeksjon av botulinum toxin type A

(Botox). *In vitro* gastriske organoider ble også benyttet. Tre kohortstudier ble utført på human primær magekreft og gastrisk stumpkreft. I del II gjennomgikk rotter VTPP, PP, SG, DS, SG+DS, GB og laparotomi (som kontrollgruppe) og monitorert av et omfattende overvåkningssystem for forsøksdyr (CLAMS).

Resultat: Del I: denervering av magen inhiberte initiering og progresjon av magekreft. Tumorreduksjon ble obeservert spesielt i den denerverte delen av magesekken som en følge av UVT og unilateral Botoxinjeksjon, i samtlige tre musemodeller testet. Denerveringen forsterket også antitumoreffektene av cellegift og bidro til økt overlevelsesrate. Det ble videre vist en nedgang i stamcelle ekspansjon ved inihibering av Wnt-signalsporet via muscarinic acetylkolinreseptor M_3 (M_3R). Hos pasienter med magekreft korrelerte tumorstadium og lymfeknutemetastase med nevraltetthet og aktivert Wnt-signalering, mens vagotomi reduserte sannsynlighet for magekreft. I del II ble det vist at VTPP ikke påvirket kroppsvekt, spiseatferd og metabolske parametere. SG reduserte kroppsvekten på kort sikt, men ikke på lang sikt, og ga en forbigående økning i energiforbruk uten at dette reduserte matinntak. DS både med og uten SG forårsaket et bemerkelsesverdig og kontinuerlig vekttap, noe som var forbundet med et økt energiforbruk, reduksjon av matinntak og malabsorpsjon. GB induserte vedvarende vekttap som var assosiert med et økt energiforbruk uten endret spiseatferd og malabsorpsjon.

Konklusjon: Del I av dette studiet viste at denervering inhiberer både initiering og progresjon av magekreft ved å inhibere kreftstamcellenisje ved nedregulering av Wnt-signalspor gjennom M_3R. Disse funnene foreslås som overførbare til kliniske studier ved bruk av endoskopisk Botoxinjeksjon, sammen med en individuelt tilpasset behandling avhengig av genuttrykk av Wnt-signalspor hos den enkelte pasient. I del II fant vi at vekttapet etter bariatrisk kirurgiske prosedyrer varierer med grad, varighet og de underliggende mekanismene, noe som peker på behovet for individuelt tilpasset bariatrisk kirurgi.

Abstract in Japanese

胃癌および肥満領域におけるオーダーメイド医療を目的としたトランスレーショナル研究

背景: 科学技術の急速な発展は基礎科学と臨床診療の間に深刻な解離をもたらしている。よって、医学におけるトランスレーショナル研究は不可欠である。癌は世界的に最も大きな問題となっている疾患であり、なかでも現在胃癌は 5 番目に多い癌であり、また癌による死因では 3 番目に位置付けられ、全体の癌による死因の 8.2%を占めている。過去数十年にわたり、胃癌患者には早期診断と低侵襲手術が適用されてきたが、化学療法などの現在の標準的な治療は、胃癌に特徴的である腫瘍内および腫瘍間の高度な不均一性により、患者のごく一部にのみ有効であるため、進行胃癌患者の治療は依然として困難なままである。したがって、胃癌に対する新規かつ個別化治療法の開発が急務である。神経と癌の関係性に関する報告は多数存在するが、特に迷走神経は胃腸機能と胃上皮細胞増殖の調整に深く関わっていることが知られており、これらは迷走神経が胃の腫瘍形成に関与する可能性を強く示している。また、肥満は胃癌を発症させる危険因子の 1 つであり、肥満減量手術が体重減少に対して効果的な治療であるだけでなく、肥満患者の癌発症リスクも軽減させることが知られている。しかし、それらの手術の根本的な作用機序は未だ不明であり、個別化肥満減量手術の実現に向けて、これらの作用機序の解明が重要である。

目的: この論文における主目的は、胃癌(Part I)および肥満(Part II)領域におけるオーダーメイド医療の確立を目的としたトランスレーショナル研究を実施することである。以下に具体的な目的を述べる: (i) 胃の腫瘍形成における迷走神経の役割を調査し、解明されたメカニズムに基づいて新規治療法を検討すること。(ii) 幽門形成術を伴う両側迷走神経切断術(VTPP)、胃袖状切除術(SG)、十二指腸スイッチ術(DS)および胃バイパス術(GB)などの肥満減量手術の作用機序を解明すること。

方法: (Part I) 3 つの異なる胃癌マウスモデル(遺伝変異、化学、または感染誘発胃癌モデル)を使用し、病理学的評価、免疫組織化学解析および遺伝子発現解析を行った。マウスに VTPP(片側迷走神経切除, UVT を含む)または A 型ボツリヌス毒素(Botox)の局所的注射による除神経を施した。胃オルガノイドを *in vitro* 下で使用した。原発性胃癌患者および残胃癌

患者において、3 つのコホート研究を実施した。(Part II) ラットに VTPP、PP、SG、DS、SG + DS、GB、および開腹術（比較対照コントロール群）を行い、包括的動物実験モニタリングシステム(CLAMS)で測定を行った。

結果: (Part I) 3 つのすべての胃癌マウスモデルにおいて、胃の除神経により、特に胃の除神経部位(UVT 後および片側 Botox 注射後)での胃癌の発生および進行が著しく抑制された。また、除神経により、化学療法の抗腫瘍効果の増強、かつ生存期間の延長が見られた。除神経による腫瘍形成抑制は、ムスカリン性アセチルコリン M_3 受容体(M_3R)を介した Wnt シグナル伝達経路の阻害による幹細胞増殖の抑制が寄与しているものと考えられた。胃癌患者において、神経密度が癌のステージおよびリンパ節転移と相関していることが判明し、Wnt シグナル伝達経路の活性化もみられた、かつ迷走神経切除術は胃癌のリスクを低下させた。(Part II) VTPP は体重、摂食行動、代謝関連パラメーターに影響を与えなかった。SG は短期のみ体重を減少させ、一時的にエネルギー消費を増加させたが、食物摂取量は減少させなかった。DS は、SG を伴うかどうかに関係なく、エネルギー消費の増加、食物摂取量の減少、吸収抑制を起因とした著明かつ長期的な体重減少を引き起こした。GB は、エネルギー消費の増加を起因とした持続的な体重減少を引き起こしたが、摂食行動や吸収には影響を与えなかった。

結論: (Part I) 除神経は、M_3R を介した Wnt シグナル伝達経路の低下によって生じる癌幹細胞ニッチの抑制を起因とし、胃癌の発生と進行を抑制する。これらの結果は、胃癌患者に対する内視鏡下 Botox 注射を使用した新規治療への適応の可能性を示唆しており、かつその治療において、胃癌患者の Wnt シグナル発現に応じたオーダーメイド医療の必要性を示唆している。(Part II) 肥満減量手術による体重減少の程度、期間、作用機序は術式間で異なる。よって、個別化肥満減量手術の必要性を強く示している。

Introduction

General Background

Translational research

The remarkable and rapid progression of science and technology, especially since the expansion of molecular biology in 1970s, has elucidated the mechanisms of diseases and developed new treatments, alternatively has led to a subdivision and complexity in a medical science, which have started to cause a gap between basic science and clinical practice [1]. In fact, it takes quite long time (the median of time lag=24 years) to "translate" from the initial discovery in basic research to the medical intervention [2]. And in drug development process, only 5% of all molecules discovered make it to human clinical trials [3] and less than 20% of those molecules entering the trials are able to get marketing approval, and it requires 8-10 years for this process [4]. Thus, the research to remove this gap (i.e., translational research) is essential in a medical science.

Despite an importance of translational research, there is yet no standard definition until today [5][6]. The term of "translational research" in PubMed appeared as early as in 1993, in the study of cancer research about the characterization of cancer genes for the purpose of immediate applications in early detection and treatment of cancers [7]. Use of the term remained low until year of 2000, when the US National Institutes of Health (NIH) made translational research a priority, and established centers of translational research [8]. In a grant announcement by the NIH in 2003, translational research was first defined as "*Translational research includes two areas of translation. One is the*

process of applying discoveries generated during research in the laboratory, and in preclinical studies, to the development of trials and studies in humans. The second area of translation concerns research aimed at enhancing the adoption of best practices in the community. Cost-effectiveness of prevention and treatment strategies is also an important part of translational science." [5]. In 2014, European Society for Translational Medicine (EUSTM) defined translational research in medicine as "*Translational medicine as an interdisciplinary branch of the biomedical field supported by three main pillars: benchside, bedside and community. The goal of translational medicine is to combine disciplines, resources, expertise, and techniques within these pillars to promote enhancements in prevention, diagnosis, and therapies.*" [9]. Thus, translational research is widely and simply defined as "*Taking research from bench-to-bedside and vice versa.*", "*Bridging basic research and medical innovation.*", "*Translating research into medical practice.*", or "*Translating science into better healthcare.*" [6][10][11]. Although little agreement between definitions of translational research exists, there is an emerging consensus for 5-phase (T0-T4) definition for translational research [6]. T0 is the phase to define mechanisms, targets, and lead molecules through basic or preclinical research including animal or *in vitro* studies, etc., but not including interventions with human subjects. T1 is the phase of translation to humans, and involves processes that bring ideas from basic/preclinical research through early testing in humans such as phase I-II clinical trials. T2 is the phase of translation to practice in patients, and involves the establishment of effectiveness in humans and clinical guidelines through phase III clinical trials, etc. T3 is the phase of translation to community, and primarily focuses on implementation and dissemination research such

as phase IV clinical trial and clinical studies, etc., while T4 is the phase of translation to public health, and focuses on outcomes and effectiveness in populations [6][12][13][14] (Fig. 1). Needless to say, between those phases T0-T4 are multidirectional, however the biggest gap is present between T0 and T1, called “valley of death” because most fundamental research studies do not go beyond the gap, therefore not to enter the clinical phases [15][16].

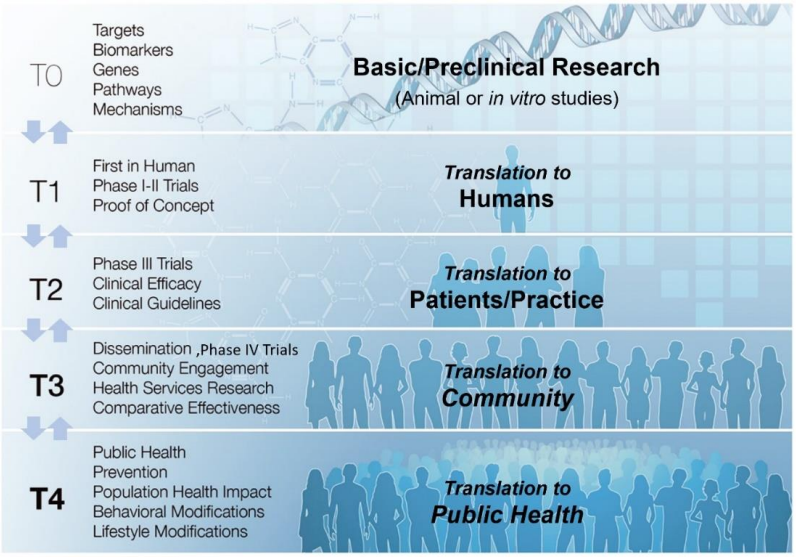

Figure 1 | Five-phase (T0-T4) definition for translational research. (*modified from Waldman et al. Clin Transl Sci. 2010* [12])

The gaps exist not only between basic science and clinical medicine, but also between basic scientists themselves and between clinicians themselves. In the present and future, teamwork should be more successful than the individuals in the past, because the translational research involves various research and clinical fields, and is surely better facilitated by interactions between co-workers representing different specialties. For

example, the study using mathematical models to quantify complexity in translational research revealed that collaboration networks and multidisciplinary team capacity are crucial for translating new discoveries into practice, particularly at T0 and T1 phases [17].

Thus, multidisciplinary collaboration ("translation" between collaborators) is essential to successfully conduct translational research [9][14][18][19].

Personalized medicine

Personalized medicine is defined as "*The right treatment (including the right drug at the right dose), to the right patient, at the right time.*" [20]. The concept of personalized medicine is not new since medicine has always been personalized [21][22][23]. However, traditional medicine has been narrative- or experience-based medicine, for instance, physicians have chosen drugs and the dose based on clinical signs and symptoms of patients, the so-called "one-size-fits-all" approach, and they eventually would adjust the dose or reselect the drugs depending on the patient's response to the given prescribed drugs [24][25]. Traditional methods are not always the most effective as not all patients respond equally to drugs even though they have similar clinical manifestations. In fact, there is high variability in drug response rates across diseases, 38% to 75% of patients fail to respond to a drug treatment, and the average response rate of a cancer drug is the lowest at 25% [26][27]. Recent advances in molecular biology such as "-omics" science have contributed significantly to an increased

understanding of the differences between patients, and have enabled evidence-based personalized medicine [28]. Especially the development of pharmacogenomics, which is the study of how genetic variants influence variability in drug response (the name reflects the combination of “pharmacology” and “genomics”), has dramatically facilitated the personalized medicine in drug therapy [29][30][31][32][33]. Concurrently, the new term “precision medicine” has emerged, which can be defined as “*Systems approach to convey a more precise classification of disease into subgroups based on OMICS data and perform personalized treatment and preventive intervention for each patient subgroups.*” [34][35][36][37][38][39][40], thus “precision medicine” is focused on the subgroup of patients rather than individual patient, and this term is used in a narrower sense, whereas “personalized medicine” is used in a broader sense. The term of “precision medicine” has started to be frequently used in the literature since 2009, instead of “personalized medicine” [41]. In this thesis, “personalized medicine” will be mainly focused and this term will be used to refer to “evidence-based approach to individualized medicine” throughout this thesis.

Evidence-based personalized medicine has been in fact accepted particularly in oncology due to the potentially lethal characters of cancer and the adverse effects of chemotherapy [21]. As an example of personalized medicine involving patient’s genotype, thiopurines (6-mercaptopurine or the pro-drug, azathioprine) are immune suppressants and widely used in the treatments of acute lymphocytic leukemia, chronic myeloid leukemia as well as inflammatory bowel disease [42]. Thiopurine S-methyltransferase (TPMT) is a polymorphic enzyme, and metabolizes the thiopurines into inactive metabolite, methyl-6-mercaptopurine [43]. In the general population, 0.3%

of people have two non-functional alleles and low or absent TPMT activity, 11% have one non-functional allele and intermediate TPMT activity, and the remaining approximately 89% or people have no non-functional alleles and normal TPMT activity [44]. The deficiency of TPMT activity generates high concentrations of thioguanine nucleotides, resulting in severe adverse effects such as myelosuppression. Thus, patients with low or absent TPMT activity are at an increased risk of life-threatening adverse effects if receiving the treatment at standard doses of thiopurines [45]. Therefore, testing for TPMT genotype (or phenotype if possible) has been commonly performed prior to the treatment with either 6-mercaptopurine or azathioprine, and in case of the detection of low or absent TPMT activity, the patients can receive a low thiopurine dosage or an alternative drug before starting therapy [46][47]. As another example of personalized medicine involving tumor genotype, trastuzumab, a monoclonal antibody against human epidermal growth factor receptor 2 (HER-2), is the first molecular targeted chemotherapy approved in 1998 [48] and used to treat breast cancer [49] and gastric cancer [50][51]. In breast cancer, 20-25% of patients have shown overexpression of HER-2, and is associated with poor clinical outcomes and aggressive tumor progression [52], while in gastric cancer, several studies reported wider range of the rates from 8.2% to 53.4% (mean of the rate is 19.0%) of HER-2 positive gastric cancer, and the rates of positive HER-2 expression also varies depending on the histology (intestinal type; 16%, diffuse type; 7%, unknown; 14%), which is probably due to the high heterogeneity of gastric cancer [53][54]. The overexpression of HER-2 in gastric cancer is also correlated with tumor size and invasion, lymph node metastasis and poor survival [51][54]. The assessment of HER-2 expression prior to treatment is now universal standard [55], and

trastuzumab is used in combination with chemotherapy or as monotherapy only for cancer patients with overexpression of HER-2 [56]. These facts have indicated that each cancer from each patient has a complicated and unique set of genetic alterations even though their phenotypes are quite similar, suggesting the importance of personalized medicine using molecular classification of cancers on the basis of gene expression including singling pathways [57].

Since personalized medicine includes a complex and board interdisciplinary research area ranging from basic science to clinical medicine, the research in personalized medicine requires a multidisciplinary and translational research framework [58][59][60][61]. Thus, the main objective of this thesis was to conduct translational research with attempt to develop personalized therapies.

Part I: Background in gastric cancer

Gastric cancer in general

Cancer is one of the world's major health problems and has now become the 1st or 2nd leading cause of death in developed countries [62]. Despite its decreasing incidence, gastric cancer remains an important cancer worldwide and is responsible for over 1,000,000 new cases and an estimated 783,000 deaths in 2018, making it the 5th most frequently diagnosed cancer and the 3rd leading cause of cancer death (8.2% of all cancer deaths). The incidence rates are almost twice higher in men than in women, and the rates are markedly elevated in Eastern Asia such as in Japan, Korea, China and

Mongolia, whereas the rates in Northern America and Northern Europe are generally low [62][63][64]. The overall case fatality rate of gastric cancer is 74.5% compared with 50.4% for colorectal cancer and 96.8% for pancreatic cancer [65]. The overall 5-year survival rate is about 20% in most areas of the world [66]. The recent report in the United States has shown that the 5-year survival rate for early stage of gastric cancer is 88-94%, compared with 18% for advanced gastric cancer [63], and less than 10% for the gastric cancer patients in metastatic status [67]. Most gastric cancers occur in the lesser curvature and antrum in a stomach [68][69]. Gastric cancer is highly heterogeneous compared with other gastrointestinal cancers, both genetically and phenotypically [70][71][72][73][74]. In the Lauren classification, gastric cancer can be divided into 2 types, i.e., intestinal (well-differentiated) or diffuse (undifferentiated) type, according to the site of tumor origin and the pathological appearance of the lesion [75]. The diffuse-type has a poor prognosis due to the lack of ability to establish intercellular connections leading to increasing the risk of metastasizing and invading into the neighbor tissues [76]. However, the most frequent gastric cancer is the intestinal-type [70]. According to the histological classification of gastric cancer (the World Health Organization, WHO, classification), there are several different types such as adenocarcinoma, lymphoma, sarcoma, or carcinoid [72]. Among those types, adenocarcinoma accounts for 90-95% of all gastric cancer [69], thus in this thesis, adenocarcinoma will be of the main focus, and will subsequently be referred to as "gastric cancer" throughout this thesis. The pathogenesis of gastric cancer includes multiple steps starting with chronic inflammation which is well-known as a critical and

first step in the progression towards cancer, and eventually resulting in carcinoma through atrophic gastritis, intestinal metaplasia and dysplasia [77][78].

Multiple factors are involved in the etiology of gastric cancer. Lifestyle behaviors such as alcohol and smoking as well as high salt intake or low vegetable/fruit intake (vitamins), play a role in the development of gastric cancer [62][63][79][80]. Apart from those lifestyle-related factors, several diseases are reported as risk factors for gastric cancer, such as obesity, gastric ulcer, gastroesophageal reflux disease (GERD), or pernicious anemia [63][81]. It has been often reported that the main risk factor for gastric cancer as well as gastric ulcer is *Helicobacter pylori*, and this bacterium is Gram-negative and has been characterized as a class I carcinogen of gastric cancer by WHO [63][79]. Infection of *Helicobacter pylori* is a strong inducer of chronic gastric inflammation and can develop into atrophic gastritis, intestinal metaplasia, or eventually gastric cancer [82]. Certain *Helicobacter pylori* strains with the virulence factors (such as cytotoxin-associated antigen A, CagA or vacuolating cytotoxin A, VacA) are more likely to increase gastric cancer risk [79]. CagA is directly injected from *Helicobacter pylori* into the cytoplasm of epithelial cells through the bacterial type IV secretion system, affecting cell morphology, proliferation and apoptosis. VacA disrupts cell polarity, promotes epithelial cells apoptosis, and inhibits T cell proliferation and effector function [83]. In rodents, however, infection of *Helicobacter pylori* alone without additional carcinogenic stimuli has not been shown to induce gastric cancer [84]. In humans, most people infected with *Helicobacter pylori* are asymptomatic for life, while only a fraction of infected people develops a disease [85]. Apparently, not only one

factor but various combination and complex interactions of these risk factors may ultimately lead to the development of gastric cancer.

Treatments of gastric cancer

Surgical removal of gastric cancer is a primary treatment and the only potentially curative treatment approach for gastric cancer patients [51][67]. The current standard recommendation for resectable gastric cancer is surgical resection with D2 lymphadenectomy [51][86]. The D2 lymph node dissection is recommended due to the high incidence of lymph node metastasis in gastric cancer and the improvement of overall outcomes [86][87]. More extended lymph node dissection, D3 lymphadenectomy, has shown no additional survival benefit but more surgical complications, thus this D3 procedure has not been recommended yet as a standard treatment [51]. Advances in endoscopic technology have contributed to a trend towards minimal invasive surgery such as endoscopic mucosal resection (EMR) or endoscopic submucosal dissection (ESD) [88]. EMR or ESD has been widely used for treating early gastric cancer which is defined as the cancer confined to the mucosa or submucosa without lymph node metastasis [89][90]. In comparison with EMR, ESD is relatively new procedure and can be performed using endoscopy knives such as insulation-tripped diathermic knife (IT-knife) and the flex-knife instead of using a snare to remove small gastric lesion lifted by a grasper in EMR, which enables en-bloc resection of larger tumors and more precise pathologic diagnosis of the dissected cancer tissue [91][92][93].

Chemotherapy is the standard first-line treatment for advanced gastric cancer [94]. It has been passed over 50 years since 5-fluorouracil (5-FU) was developed, but it is still the key drug in the chemotherapeutic regimens for gastric cancer. The anti-tumor effects of 5-FU can be enhanced by combination with platinum-based drugs such as cisplatin or oxaliplatin, and this regimen has currently been used as global standard of first-line treatment for advanced gastric cancer [50][95]. Recently, S-1 instead of 5-FU and oxaliplatin among platinum-based drugs have been recommended for the combination regimen because some clinical studies have demonstrated that S-1 and oxaliplatin-containing regimens have higher response rates and better survival improvement, compared with the regimen of 5-FU or cisplatin [50]. 5-FU is an intravenous drug, whereas S-1 is an oral fluoropyrimidine composed of a mixture of tegafur (a prodrug of 5FU) and two modulators; gimeracil and oteracil, and the 5-FU metabolized from tegafur arrests cell-cycle by blockage of DNA synthesis via inhibition of thymidylate synthase and interferes with RNA function [96], while gimeracil maintains high 5-FU levels in blood and tumor tissue by inhibiting dihydropyrimidine dehydrogenes (the enzyme metabolizing 5-FU) and oteracil reduces the gastrointestinal toxicity of the 5-FU by inhibiting orotate phosphoribosyltransferase leading to lower 5-FU levels in the gut [97]. Oxaliplatin also inhibits DNA synthesis (both DNA replication and transcription) by forming inter- and intra-strand crosslinks in DNA [98]. In the case of HER-2 positive gastric cancer, the patients have lately received trastuzumab, which is a targeted antagonist for HER-2, in addition to the combination therapy [50][51]. Currently, two additional targeted therapies have been approved for gastric cancer; the tumor angiogenesis inhibitor ramucirumab (monoclonal antibody for vascular

endothelial growth factor receptor 2, VEGFR2) and the immune check point inhibitor pembrolizumab (monoclonal antibody for programmed cell death protein 1, PD-1) [74], the evidence for the efficacy of those drugs has however not been accumulated enough yet.

Radiotherapy alone has not been used commonly for gastric cancer patients due to poor outcomes, alternatively the combination therapy of radiotherapy and chemotherapy, the so-called chemoradiotherapy, has been used as an adjuvant therapy for advanced gastric cancer patients [99][100][101].

The treatment of patients with advanced gastric cancer still remains a challenging area of oncology. Despite some clinical trials showing the benefits of chemotherapy, the rate of efficacy was around 10-20%, indicating that current standard chemotherapy is effective in only a small subgroup of the patients, which is probably due to high heterogeneity of gastric cancer [89][102]. Therefore, the development of personalized and new therapy for gastric cancer is needed.

Due to low survival rates in most areas of the world and few treatment options, reducing incidence seems to be the key to reducing mortality from gastric cancer [63]. In contrast to the low survival rates in other countries, Japan has shown more about 60% of 5-year survival rates of gastric cancer patients [65]. Such high survival rate may be due to mass screening programs to detect gastric cancer at early and curable stage, and eradication of *Helicobacter pylori* for larger population [66], however effective and standard methodology for prevention of gastric cancer has not been established yet. Thus, it is also important to find a preventive treatment for gastric cancer.

Gastric cancer stem cells and the niche

Stem cell is an undifferentiated cell characterized by self-renewal (producing more stem cells) and potency (the ability to differentiate into different cell types). There are two types of self-renewal; symmetric division provides that one stem cell divides into two new stem cells, and asymmetric division provides that one stem cell divides into another stem cell and one differentiating cell. The differentiation of stem cells is towards terminal differentiated cells through transiently amplifying cells and progenitor cells [103]. Progenitor cells are early descendants of stem cells that can differentiate to one or more kinds of cells, but lack self-renewal potential and indefinite cell division [104]. The balance of self-renewal and differentiation is extremely important for the maintenance and survival of stem cells, and is regulated by their surrounding microenvironment, the so-called “stem cell niche”. The stem cell niche provides signals to stem cells to control the rate of stem cell proliferation, determine the fate of stem cell daughters, and protect stem cells from exhaustion or death. Thus, the existence of stem cell niche is essential for stem cells. The stem cell niche consists of various components such as stromal cells, extracellular matrix, vascular and lymphatic networks, macrophages, mast cells, fibroblasts, mesenchymal stem cells, schwann cells, paneth cells, neurons, etc., although not all niches necessarily incorporate all of these components [105]. Most of the stem cell niches are hypoxic (<10% O_2) [106] and keep the stem cells in quiescent state (stay in the G_0 phase of the cell cycle) to maintain the long-term survival by avoiding exhaustion due to cell division and minimizing the risk of DNA replication errors [107].

The concept of stem cells has been extended to the cancer field by the discovery of stem-like cells within tumors, referred to as cancer stem cells (CSCs). CSCs (also called as cancer initiating cells) are the small subset of tumor cells and characterized by not only self-renewal and differentiation abilities as shown in normal stem cells, but also the ability to form cancer [108] (Fig. 2). CSCs also contribute to cancer relapse after treatment and cancer metastasis [109]. Like normal stem cells, CSCs are strongly dependent on its niche (Fig. 2).

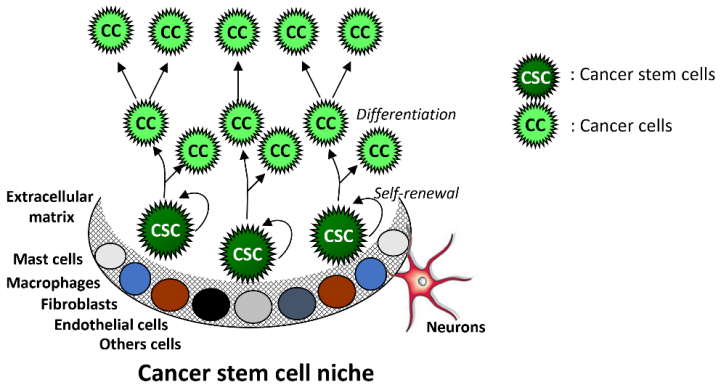

Figure 2 | Illustration of cancer stem cell niche. (*modified from Arum et al. Neoplasia. 2010* [110] (Paper S2))

Interestingly, CSCs can modify their niche by themselves, e.g., CSCs secrete vascular endothelial growth factor (VEGF) that directly supports the development of the angiogenesis within the tumor [111], and moreover, CSCs can transdifferentiate into intra-tumor vascular endothelial cells by Notch and VEGF signals [112][113][114]. The evidence of the existence of CSCs has been demonstrated in human acute myeloid leukemia by Dick *et al* in 1997 [115], and then in solid tumor by Al-Hajj *et al* in 2003,

who isolated CSCs from human breast cancer [116]. Accumulating data support that CSCs exist in many types of solid tumors. In 2009, Takaishi *et al* identified CSCs in gastric cancer by analyzing a series of human gastric cancer cell lines [117]. At the same time, Fukuda *et al* described putative gastric CSCs by isolating and characterizing the side population cells in five human gastric cancer cell lines and three cases of primary human gastric cancers [118]. Since gastric CSCs can generate multiple different types of cells within the tumor, high intra-tumor heterogeneity of gastric cancer also indicates the existence of gastric CSCs [119][120]. The gastric CSCs are located mainly in the mucous neck region of stomach at the stage of intestinal metaplasia, and at the stage of gastric cancer, the cells are located at the luminal surface, tumor center, and invasion front [121]. It was reported that the high expression of gastric CSCs is positively correlated with TNM grading, invasion depth, malignant transformation, metastasis and relapse of gastric cancer [122]. Myofibroblasts, cancer-associated fibroblasts and macrophages have been considered as major components of the niche for gastric CSCs [123][124][125][126]. Some potential gastric cancer stem and progenitor cell markers have been identified. CD44 (Cluster of differentiation 44), including its variant CD44v6, is a class I transmembrane glycoprotein that acts as the receptor for extracellular matrix such as hyaluronic acid. CD44 is one of the first specific markers of CSCs in solid tumors, and has been proven to be the most useful for the identification of CSCs in solid tumors [117][127]. Leucine-rich repeat-containing G-protein coupled receptor 5 (Lgr5) is a G-protein-coupled receptor with a large N-terminal extracellular domain containing several leucine-rich repeats. *Lgr5* was initially identified as a Wnt target gene in colon cancer cell lines and intestinal crypts *in vivo* [128]. Lgr5 has been

widely used as a marker of stem cells, and is a marker of gastric stem cells in both normal and cancer tissues [129]. In the stomach, Lgr5-positive cells are concentrated on the lesser curvature and in the antrum where tumor is often found [130]. Dclk1 (doublecortin-like kinase 1 protein) is encodes a microtubule-associated protein with a C-terminal serine-threonin kinase domain that is expressed in neural radial glia cells and gastric tuft cells, and the up-regulation of Dclk1 has been associated with inflammation-induced carcinogenesis [131]. Dclk1 is a putative gastric progenitor cell marker [132], and furthermore, Dclk1 marks intestinal CSCs in Apc(Min/+) mice [133]. Although the origin of gastric CSCs has not yet been conclusively elucidated, some studies have suggested that gastric CSCs may originate from normal gastric stem or progenitor cells, or bone marrow-derived cells (BMDCs). There was a report showing *Helicobacter pylori* induced malignant transformation of gastric stem cells into gastric CSCs [73]. BMDCs migrate to and differentiate into the gastrointestinal tract epithelia contributing to the recovery from severe epithelial damage in human patients with gastric ulcer or intestinal inflammation [134]. Previous studies have shown that BMDCs contributed directly to angiogenesis in tumor formation, and the BMDCs partly derived cancer-associated fibroblasts, which is known to be an important component of gastric CSC niche [135]. Another study has also demonstrated that in a mouse model of severe gastric mucosal injury induced by chronic inflammation via infection of *Helicobacter felis*, transplanted BMDCs engrafted into the gastric mucosa and appeared to replace a great portion of the epithelium with donor cell progeny. Importantly, in the absence of injury, there was no substantial contribution of BMDCs, suggesting that this event may not occur in the normal homeostatic maintenance of the epithelium. The mice infected

with *Helicobacter felis* induced gastric mucosal atrophy, metaplasia and eventually gastric cancer, which were associated with the recruitment of BMDCs [136]. Interestingly, the recruitment of BMDCs to the gastric mucosa was not observed during acute gastric infection with *Helicobacter* species, nor was it observed during either acute ulceration. Instead, BMDCs derived metaplasia arose only in the setting of severe chronic inflammation [135]. Taken together, these data strongly suggest that gastric CSCs originate from BMDCs, especially under chronic inflammation status.

Current conventional treatments for cancer, such as chemotherapy or radiotherapy, are targeting on cancer cells (non-CSCs) and are insufficient to eradicate CSCs due to the chemo- and radiation-therapy resistance of CSCs. The resistance against chemotherapy in CSCs is considered to be due to following reasons. Chemotherapy is mainly targeting the cell cycle of cancer cells, whereas most CSCs stay in the G0 phase of the cell cycle [107]. CSC niche is hypoxic [106], thus the cells are located far from the blood vessels which deliver the anti-tumor drugs. Moreover, the structure of intra-tumor blood vessels generated by angiogenesis is abnormal and chaotic, therefore the vessel network is immature, thin-walled, tortuous and leaky, leading to high interstitial fluid pressure which interrupts the anti-tumor drug delivery [137][138]. In addition, CSCs overexpresses ATP-binding cassette transporters (ABC transporters) which play an important role for the elimination of drug from the cells [139]. These factors may explain why the recent studies using CSC-targeted drug therapy have not shown significant outcomes yet. Hypoxic CSC niche also induces the resistance against radiotherapy because oxygen is a well-known radiosensitizing agent due to its ability to form radiation-induced reactive oxygen species damaging DNA, thus low oxygen status

can avoid the radiation-induced damage [140]. According to the CSC model, targeting specifically on cancer cells (non-CSCs) by conventional cancer therapy may lead to tumor relapse, as it will not be successful in treating the patients with recurrence of cancer, but in fact will promote more malignant features in the relapsed cancer as showed in study using computational modeling [141]. This was supported by the studies using *in vivo* and *in vitro* models of skin and breast cancer [142][143]. On the other hand, targeting only CSCs may be insufficient for the rapid tumor regression or shrinkage because CSCs represent only a small proportion of the entire tumor so that the eradication of CSCs may have little impact on the size of the tumor in short-term and the residue of non-CSCs may still have malignant features, but in long-term, the tumor would be expected to exhaust itself and wither away because the tumor has lost the capacity of prolonged self-renewal [144]. In fact, the study using a genetically engineered mouse model of glioma has demonstrated that treatment targeting specifically on CSCs did not reduce the number of cancer cells but the combination therapy targeting both CSCs and non-CSCs reduced the cell number and prolonged survival compared with non-CSCs-targeted therapy [145]. Therefore, simultaneous attacking both cancer cells (non-CSCs) and CSCs should be considered to be used to eradicate a cancer [146] (Fig. 3).

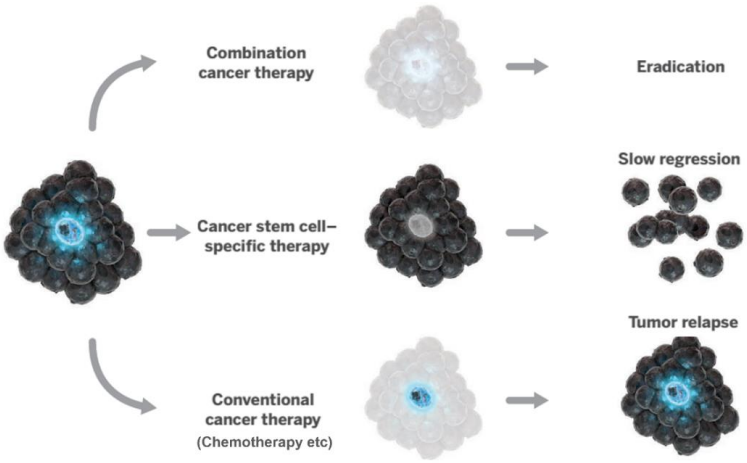

Figure 3 | Theoretical strategy to eradicate cancer including non-CSCs and CSCs. (*modified from Kaiser. Science. 2015* [146])

These observations emphasize the necessity of novel therapeutic approaches targeted toward CSCs in addition to the current conventional therapy in order to achieve better clinical outcomes for patients with gastric cancer.

Wnt signaling in gastric cancer and the stem cells

Wnt signaling pathway consists of three pathways; canonical Wnt pathway (Wnt/β-catenin pathway), noncanonical Wnt/planar cell polarity pathway, and noncanonical Wnt/Ca^{2+} pathway. All these three pathways are activated by the binding of Wnt ligands to a Frizzled family receptor, which transmits the biological signal to the Dishevelled protein inside the cell. In the canonical Wnt pathway, binding of Wnt ligands to Frizzled family receptor and/or lipoprotein receptor-related protein (LRP) receptor leads

to activation of Dishevelled, which in turn inhibits GSK-3β mediated phosphorylation of β-1catenin, subsequently the β-catenin stabilizes, accumulates in the cytosol, and translocates to the nucleus, where it activates the transcription [147][148] (Fig. 4).

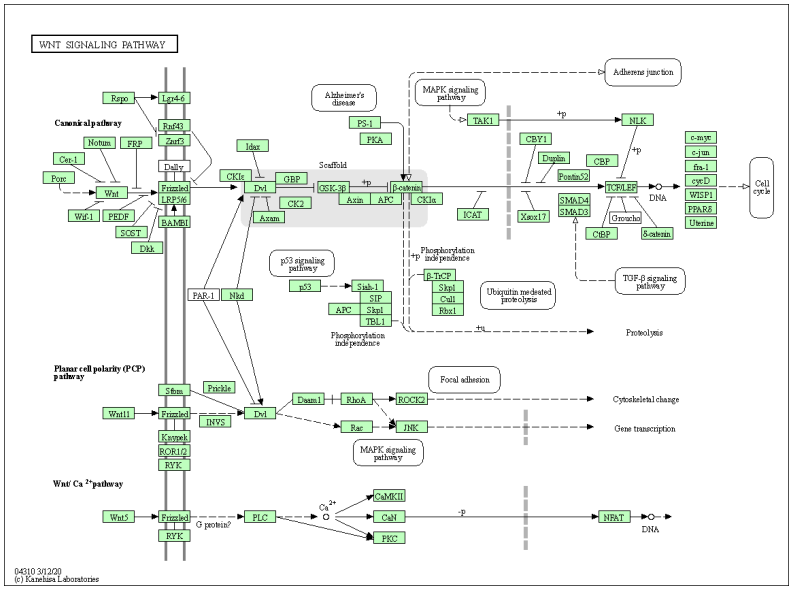

Figure 4 | Overall picture of Wnt signaling pathway. (*from KEGG database*)

The biological effects of the Wnt signaling pathway are mediated by the regulation of target genes such as *Cyclin D1*, *Axin2*, *Myc*, *Lgr5*, *CD44* and *Sox9* [130].

Wnt signaling pathway is involved in cancer initiation, progression, recurrence and metastasis [149][150][151][152][153]. As to the metastasis, Wnt signaling pathway mediates VEGF signaling pathway and is implicated with both angiogenesis [154] and lymphangiogenesis [155]. Moreover, it has been reported that migrating CSCs, located at the tumor invasive front, exhibited epithelial-mesenchymal transition (EMT) and the

activated Wnt signaling pathway [156]. Wnt signaling pathway as well as Hedgehog and Notch signaling pathways plays a key role in the regulation of normal and CSCs [157][158]. Aberrant activation of Wnt signaling pathway in normal stem cells can promote their transformation into CSCs [159].

Wnt signaling controls gastric stem cells and epithelial homeostasis in the stomach [130][160]. Most gastric cancer patients (over 50%) overexpresses Wnt signaling pathway [161][162], and the Wnt signaling pathway is related to gastric cancer initiation, progression, tumor invasion, metastasis and lower 5-year survival of gastric cancer patients [153][161][163][164][165]. Furthermore, the Wnt signaling pathway is essential for the self-renewal and the maintenance of gastric CSCs [70][123][166][167][168]. Interestingly, it has been reported that *Helicobacter pylori* or HER-2 regulates gastric CSCs via Wnt signaling pathway [169][170]. Taken together, these data strongly suggest that Wnt signaling pathway is a very important target in gastric cancer therapy.

Crosstalk between nerve and cancer

Numerous studies have reported the nerve-cancer crosstalk [171]. It is well described that tumor cells migrate and proliferate along the nerves, which is known as perineural invasion. The perineural invasion has been reported in many types of cancer including gastric cancer [172], and is frequently associated with poor clinical outcomes in terms of tumor size, tumor depth and invasion, stage of cancer, lymph node metastasis, cancer

recurrence, and survival [173][174][175][176][177]. Protein gene product 9.5 (PGP9.5) is a neuron-specific marker, and is also correlated with poor prognosis in cancer patients [178][179][180][181]. Tumors can initiate their own innervation by releasing neurotrophic factors and some molecules to induce neurogenesis around the tumors and axon guidance or neurite outgrowth towards the tumors [182], while the neurotransmitters or neuropeptides secreted from the nerves stimulate the tumor cell proliferation, migration, invasion and survival, leading to the tumor development, progression and metastasis [183][184][185] (Fig. 5). Neoangiogenesis and lymphangiogenesis support metastasis development of cancer. The tumor cells release VEGF in addition to neurotrophic factors, which promotes not only neurogenesis but neoangiogenesis and lymphangiogenesis as well [186][187]. Nerve is often wiring together with blood and lymphatic vessels, and sharing common factors with them [188][189], thus these three processes (innervation, neoangiogenesis and lymphangiogenesis) are likely to occur simultaneously and contribute to the cancer metastasis [190]. It should be noted that Wnt signaling pathway plays important role in neurogenesis [191] and axon guidance [192] in addition to angiogenesis [154] and lymphangiogenesis [155], suggesting that Wnt signaling pathway may also contribute to those processes in the nerve-cancer crosstalk (Fig. 5).

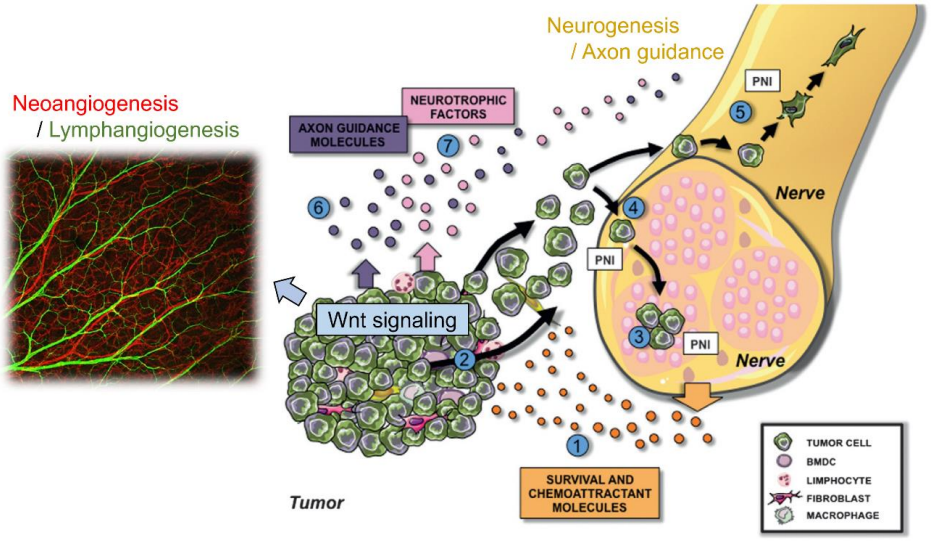

Figure 5 | Illustration of nerve-cancer crosstalk. (*modified from Mancino et al. Biochim Biophys Acta. 2011*. [184])

The nerve is involved in the regulation of stem and progenitor cells [193][194], and could also modulate the conversion of stem or progenitor cells into cancer cells [195]. In fact, it has been reported that tumor infiltration by autonomic nerves is essential for prostate cancer development and metastasis [196].

Vagus nerve is strongly related to the gastric physiology and homeostasis including the gastric acid secretion, gastric motility and maintenance of the mucosal integrity [197][198]. The autonomic innervation of the stomach is largely parasympathetic, and main branch of vagus nerve fiber is distributed along the lesser curvature of the stomach in both humans and rodents [199][200], where gastric cancer is frequently found. M_3R is the most abundant acetylcholine receptor in parietal cells and chief cells of the stomach [201]. It has been known that muscarinic receptors and the ligands play key

roles in cancer progression [202], and the stimulation of M_3R is associated with the tumor growth in colon [203], prostate [204] and lung cancers [205]. Additionally, we previously reported that M_3R plays an important role in cell proliferation of the oxyntic mucosa of stomach [206]. These findings suggest that vagus nerve is a novel target for gastric cancer therapy, so that we investigated the potential role of the vagus nerve in gastric tumorigenesis (Paper I).

Part II: Background in obesity

Obesity in general

Obesity has become a global public health concern, since it is well recognized as a risk factor for many diseases such as type 2 diabetes mellitus, hypertension, myocardial infraction, stroke, fatty liver disease, dementia, osteoarthritis, and obstructive sleep apnoea [207]. Body mass index (BMI) is the most commonly used to assess the overweight and obesity. It can be calculated by the following formula; BMI (kg/m^2) =body weight (kg) /height $(m)^2$. According to the WHO classification, a normal BMI range is 18.5 to 24.9, whereas a BMI≥25 kg/m^2 is considered to be overweight, and a BMI≥30 kg/m^2 is classified as obese (class I obesity; BMI≥30 kg/m^2, class II obesity; BMI≥35 kg/m^2), with severe obesity (class III obesity) and super obesity (class IV obesity) defined as a BMI≥40 kg/m^2 and BMI≥50 kg/m^2, respectively [208][209]. In 2015, 600 million adults and 100 million children were obese worldwide. The overall prevalence of obesity was 12% among adults and 5% among children. In adults, the

prevalence of obesity was commonly higher among women than among men in all ages. Overweight and obesity rates have increased considerably during the past 35 years globally, i.e., the age-standardized prevalence of overweight (BMI≥25 kg/m^2) increased from 26.5% in 1980 to 39.0% in 2015, and the prevalence of obesity (BMI≥30 kg/m^2) likewise increased from 7% in 1980 to 12.5% in 2015. There was some variability between countries and regions in the prevalence of obesity, the highest prevalence of obesity was observed in the United States (34%), whereas African and Asian regions had much lower prevalence of obesity, which was lowest in Vietnam (1.6%). High BMI was associated with 4 million deaths annually, and more than two thirds of the deaths related to the high BMI were due to cardiovascular disease [210][211]. Obesity is believed to be caused by the imbalance between energy intake and energy expenditure, thus basic strategy of treatment for obesity aims at reducing calorie intake and increasing energy expenditure [207][212].

Bariatric surgery

Although there are various approaches to treat obesity, such as diet control, physical exercise and medications, the long-term effects on weight loss are relatively poor [213]. Bariatric surgery is the only treatment which have shown the efficacy on long-term weight loss [214][215]. According to the practice guidelines, obese patients with a BMI≥40 kg/m^2, or BMI≥35 kg/m^2 associated with comorbidities can be subjected to bariatric surgery [209][213]. During the evolution of surgery for morbid obesity, many different bariatric surgical procedures have been developed.

Vagotomy with pyloroplasty (VTPP) (Fig. 6) had commonly been used to treat peptic ulcers until the H_2 antagonists or proton pump inhibitors (gastric acid blockers) were developed [216]. VTPP was also suggested for treatment of severe obesity [217]. Recently, the so-called "Vagal BLocking for Obesity Control" (VBLOC) therapy was created. In contrast to VTPP, this VBLOC procedure is reversible and much less invasive weight loss surgery. The VBLOC therapy is performed by using a small implanted device blocking the vagus nerve with high frequency electrical pulses. Although this therapy demonstrated body weight reduction in the initial clinical trial, the therapeutic mechanisms are not yet fully understood [218]. Hence, in this thesis, we investigated the potential role of vagus nerve in body weight, eating behavior and energy expenditure by using rats subjected to VTPP (Paper II).

Gastric bypass (GB) (Fig. 6) had been the most common bariatric surgery worldwide until around 2013 due to the abundant evidences showing high efficacy and safety [219]. The initial procedure of GB was invented by Dr. Edward Mason in 1965, and later it was converted to Roux-en-Y procedure which was created by Dr. Cesar Roux in 1897. GB is designed to create a small pouch in the stomach to produce early satiety and a consequent reduction in food intake, and moreover to induce malabsorption by creating an intestinal bypass and/or by accomplishing distal mixing of bile acid and pancreatic juice with ingested nutrients, thereby reducing absorption [220].

Duodenal switch (DS) with sleeve gastrectomy (SG) (Fig. 6) is the most effective procedure among bariatric surgeries, producing marked weight loss and comorbidity reduction [221], alternatively DS+SG has greater side effects including nutritional

deficiencies, anemia, osteopenia and severe diarrhea [214][222]. In addition to these side effects, the DS+SG procedure has the highest mortality among bariatric surgeries because of its complex and difficult surgical procedure [220][223]. Thus, the DS+SG procedure tends to be used only for the patients with super obesity (BMI≥50 kg/m^2) [224]. The DS+SG procedure was initially created as surgical solution for primary bile reflux gastritis and/or to decrease postoperative symptoms after distal gastrectomy and gastroduodenostomy [225]. The surgical procedure of DS+SG usually consists of two phases; as the first phase, an approximately 75% longitudinal gastrectomy (i.e., SG procedure) is performed, and the second phase is done by creation of an alimentary limb approximately 50% of total small bowel length (i.e., bypassing jejunum), a common channel length of 100 cm, and cholecystectomy [221]. Even though DS+SG and GB shares similar surgical concepts, many clinical studies have demonstrated that DS+SG is superior to GB in body weight loss [226][227][228][229][230][231][232], although the mechanism of the difference remains unknown. In this thesis, we compared the postoperative effects of DS+SG *vs.* GB on eating behavior and metabolic parameters in addition to body weight by using rat models (Paper III).

Sleeve gastrectomy (SG) (Fig. 6) has currently become the most common bariatric surgery due to the simpler surgical technique compared to GB [233][234]. This procedure was originally proposed as the first stage followed by Rouex-en-Y GB or DS, and has recently been used as an independent bariatric surgery due to lower risks of surgical complications [220][235]. SG is usually performed by laparoscopically assisted vertical gastrectomy using a Dexterity Pneumo Sleeve device, leading to reducing the stomach size to about 25% [224].

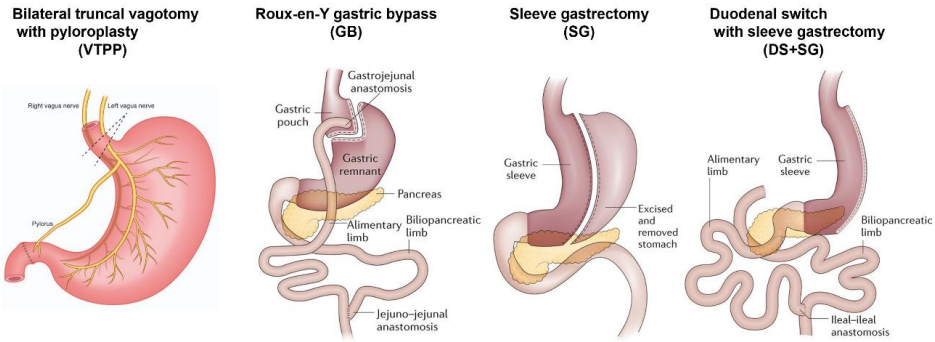

Figure 6 | Illustration of bariatric surgeries. (*modified from Rabben et al. Curr Neuropharmacol. 2016* [236], *Nguyen et al. Nat Rev Gastroenterol Hepatol. 2017.* [237])

Previously, we compared the eating behavior in rats that underwent a total gastrectomy *vs.* GB and found that the food intake and meal size were reduced after total gastrectomy but not GB, thus suggesting that the control of food intake was independent of the food reservoir function of the stomach [238]. Therefore, we hypothesized that SG might not reduce food intake, and thus the DS procedure could be and independent weight loss surgery. Hence, we evaluated the effects of SG alone and DS with/without SG on body weight, eating and metabolic parameters in this thesis (Paper II).

Obesity and cancer

Many reports have demonstrated that obesity is the risk factor for several types of cancer [207][208][239][240][241] including gastric cancer [81]. Obesity is well-known to induce low-grade but systemic chronic inflammation, which is a crucial component to

develop and progress the cancer [242][243][244]. The cancer-promoting caused by obesity-associated chronic inflammation is considered to be largely attributable to the innate immune cells especially macrophages mediated from inflamed adipose tissues [245]. In fact, obesity increases not only cancer risk but also cancer mortality rate [246]. Bariatric surgery is reported to reduce cancer risk and its mortality [247], however only in the case of success in body weight loss after surgery [215]. Therefore, it is very important to select the right bariatric surgery to the right obese patient. To achieve this, it is essential to know the underlying mechanism of each bariatric surgery. However, many surgeons have generally performed a surgery based on experience without understanding the mechanisms, i.e., evidence-based surgery, leading to unstable post-operative outcomes [248]. Moreover, in obesity research, translation of newly acquired evidence to surgical practice is slow and incomplete because of following reasons; (i) From an ethical as well as a methodological point of view, it is hard to conduct placebo-controlled clinical trials including “blinding” or “sham operation”. (ii) Standardization of surgical treatment is difficult due to the variability of surgical skills, surgical technique, surgical materials, strategy, and pre-/post-operative cares depending on each surgeon or other members of the team. (iii) Economic bias for making decision, i.e., the selection of surgery is not simply decided by only surgeons, but also by patient’s demand due to the high cost for surgery. (iv) Lack of conducting preclinical research using adequate animal models [249]. In contrast to clinical studies in obesity research, preclinical study using animal models enables to provide same conditions in all groups, to include sham-operated control group, to use comprehensive monitoring system for collecting sophisticated eating and metabolic data, to collect various samples, and to

exclude the economic, mental or operation performer-dependent biases. Thus, the evidence obtained from preclinical animal studies should be considered as a high-level evidence in obesity research, which probably is feasible to translate the findings into the surgical practice. Therefore, in this thesis, we conducted the translational research using appropriate animal models in order to elucidate the mechanisms underlying bariatric surgeries with attempt to develop the evidence-based bariatric surgery (Papers II, III).

Aims of the Studies

Principal Objective

To conduct translational research with attempt to develop personalized therapies for gastric cancer and obesity.

Specific Objectives

- To investigate the potential role of vagus nerve on gastric tumorigenesis, and to elucidate the underlying mechanisms for development of the new therapy (Paper I).

- To investigate the effects of VTPP, SG, DS with/without SG, and GB on body weight, eating and metabolic parameters, and to elucidate the underlying mechanisms (Papers II, III).

- To test the hypothesis that DS alone (without SG) could be an independent weight loss surgery (Papers II).

- To compare GB *vs.* SG+DS which have similar surgical concepts, and to elucidate the mechanisms of the differences in those effects (Papers III).

Methods

Part I: Gastric cancer (Paper I)

Animals

The insulin-gastrin (INS-GAS) transgenic mice were generated by Dr. T.C. Wang and his co-workers [250], and imported to Norway by Dr. D. Chen for these studies. Animals were further bred through sibling mating for more than 20 generations. More than 800 INS-GAS mice have been examined before these studies (presented in Paper I). Percentage of the mice without preneoplastic lesions was 3.7% at 6 months of age, and incidence rate of spontaneous gastric corpus cancer increased from 75% (at the beginning of this study in Jan. 2005) to 100% (May 2013) at 12 months of age without an additional infection with *Helicobacter pylori*. For instance, 187 INS-GAS mice were examined at 1 to 20 months of age during 2005, and 61 mice were found to have the gastric tumor mostly after 9 months of age (Paper I; Fig. 1A). During 2012, 139 INS-GAS mice were examined at 12 months of age and all the mice had the gastric tumor (Y. Kodama, C-M Zhao and D. Chen, unpublished observation). The gastric cancer in INS-GAS mice is developed through the stages of atrophy, metaplasia and dysplasia [77][250]. Chemically-induced gastric cancer model was established according to our previous report [251]. In brief, wild-type mice and muscarinic acetylcholine receptor M_3 (M_3R) knockout mice were exposed to N-methyl-N-nitrosourea (MNU, Sigma Chemical, St. Louis, MO) which was dissolved in distilled water at a concentration of 240 ppm and freshly prepared twice per week for the administration in drinking water in light-shielded bottles *ad libitum*. Mice at 4 weeks of age were given drinking water

containing MNU on alternate weeks for a total of 10 weeks. The development of tumors was observed in wild-type mice by 56 weeks. M_3R knockout mice were obtained from Kyoto Pharmaceutical University [206]. The mice had higher water intake than age- and sex-matched wild type mice (3.74±0.41 *vs.* 2.28±0.27 mL/24 hours, $p<0.01$).

All mice were housed 3-4 together in individually ventilated cages on wood chip bedding with a 12-hour light/dark cycle, room temperature of 22°C and 40-60% relative humidity, free access to tap water and standard pellet food (RM1 801002, Scanbur BK AS, Sweden). All INS-GAS mice and FVB wild-type mice were housed at the standard housing conditions in a specific pathogen-free in agreement with FELASA (Federation of European Laboratory Animal Science Association) recommendations. M_3R knockout mice, *Helicobacter pylori*-infected H^+/K^+-ATPase-IL-1ß mice [252], and wild-type controls (C57BL/6 mice, Taconic, Denmark) were housed in a guaranteed animal facility in Trondheim. Animal experiments were performed according to the guidelines for the design and statistical analysis of experiments using laboratory animals [253] after being approved by the Norwegian National Animal Research Authority (Forsøksdyrutvalget, FDU).

Design of animal experiments

Five hundred eighty-one mice were divided into 14 experimental groups (Paper I; Table S1). In each experiment, mice were randomly divided into different subgroups. The animals, samples and treatments were coded until the data were analyzed. In the 1st

experiment, 107 mice at 6 months of age underwent bilateral truncal vagotomy with pyloroplasty (VTPP)(6 males, 19 females), pyloroplasty alone (PP)(7 males, 18 females), unilateral anterior truncal vagotomy (UVT)(11 males, 19 females) or sham operation (11 males, 16 females). Six months after surgery (i.e. at 12 months of age), the animals were euthanized, and the anterior and posterior parts of the stomachs collected for histopathological and immunohistochemical analyses.

In the 2nd experiment, 20 wild-type mice (FVB, the same genetic background as INS-GAS mice) were exposure to MNU for one week every other week for 5 cycles (10 weeks). At 14 weeks of age (i.e., at one week after the completion of MNU treatment), half group of MNU-treated mice was subjected to VTPP and another half group received no surgery (no effects by PP in the 1st experiment). All mice were euthanized at 13 months of age, and the stomachs were examined macroscopically as well as collected for histopathological analysis.

In the 3rd experiment, 24 H^+/K^+-ATPase-IL-1ß mice (14 males and 10 females, backcrossed to C57BL/6 for 10 generation) were inoculated with *Helicobacter pylori* at 3.5 months of age [252]. Infection of H^+/K^+-ATPase-IL-1ß mice with *Helicobacter pylori* accelerated gastric tumorigenesis, resembling *Helicobacter pylori*-related atrophy-metaplasia-dysplasia sequence in humans. At 12 months of age (8.5 months after *Helicobacter pylori* infection), half of the infected mice underwent UVT and the other half underwent a sham operation (laparotomy). All the mice were euthanized 6 months later. The stomachs were examined macroscopically and collected for histopathological analysis.

In the 4th experiment, 16 INS-GAS mice (5 males and 11 females) at 6 months of age underwent unilateral Botox treatment and were euthanized at 12 months of age. The anterior and posterior parts of the stomachs were collected for histopathological analysis.

In the 5th experiment, 64 INS-GAS mice at 8 months (7 males and 10 females), 10 months (6 males and 8 females) and 12 months (6 males and 6 females) of age underwent UVT, and 21 age-matched mice (8 males and 13 females) had no surgery. At 18 months of age, all surviving mice including 12 (6 males and 6 females) from the 8-month group, 9 from the 10-month group (3 males and 6 females), 8 from the 12-month group (4 males and 4 females), and 10 from the un-operated group (4 males and 6 females) were euthanized, and the anterior and posterior parts of the stomachs were collected for histopathological analysis and genome-wide gene expression profiling analysis. Survival analysis was also performed.

In the 6th experiment, 26 INS-GAS mice at 12 months of age underwent Botox treatments (only anterior or both anterior and posterior sides of the stomach with or without UVT) or vehicle injection (both anterior and posterior sides of the stomach). Mice were euthanized at 14 months of age. Both the anterior and posterior parts of the stomachs were collected for histopathological analysis.

In the 7th experiment, 133 INS-GAS mice at 12-14 months of age received no treatment (6 males and 6 females), saline (5 males and 5 females), 5-FU (5 males and 5 females), oxaliplatin (5 males and 8 females), saline + unilateral Botox treatment (4 males and 6 females), unilateral Botox treatment + 5-FU (4 males and 6 females), unilateral Botox

treatment + oxaliplatin (6 males and 7 females), sham operation (laparotomy) + 5-FU +oxaliplatin (6 males and 9 females), unilateral Botox treatment + 5-FU + oxaliplatin (11 males and 13 females), or UVT+ 5-FU + oxaliplatin (6 males and 10 females). Denervation treatment was applied to only half of the stomach, such that the non-denervated half of the stomach in each animal served as a control, either as chemotherapy only or as an untreated control. All mice were euthanized 2 months after starting the treatments, except for mice that died before the end of study, and both the anterior and posterior parts of the stomachs were collected for histopathological analysis. Survival analysis was also performed.

In the 8th experiment, 16 INS-GAS mice at 6 months of age underwent UVT and were euthanized at 2 months (1 male and 4 females), 4 months (2 males and 3 females), or 6 months (2 males and 4 females) postoperatively. The anterior and posterior parts of the stomachs were collected for genome-wide gene expression profiling.

In the 9th experiment, 44 INS-GAS mice at 12-14 months of age received saline (3 males and 3 females), 5-FU + oxaliplatin (5 males and 8 females), darifenacin (6 males and 6 females), or a combination of 5-FU + oxaliplatin and darifenacin (8 males and 5 females). Two months after starting the treatments, the mice were euthanized, and both the anterior and posterior parts of the stomachs were collected for histopathological analysis.

In the 10th experiment, both INS-GAS mice (6 males and 6 females) and wild-type mice (10 males and 10 females) were subjected either to UVT or no treatment. Six months

after surgery (at 12 months of age), the animals were euthanized and the anterior and posterior parts of the stomachs were collected for gene expression analysis.

In the 11th experiment, 12 MNU-treated mice (6 males and 6 females) were subjected to PP or VTPP at 6 months of age and euthanized 4 months later. The stomachs were collected for qRT-PCR analysis.

In the 12th experiment, 7 M_3R knockout mice (4 males and 3 females) and 13 wild-type mice (5 males and 8 females) (C57BL/6, the same genetic background as M_3R knockout mice) were exposed to MNU and euthanized at 11 months of age. The stomachs were examined macroscopically and were collected for histopathological analysis.

In the 13th experiment, 37 mice (20 males, 17 females) at 12-18 months of age underwent a topical application of acetic acid on the anterior side of the stomach with or without simultaneous UVT and were euthanized 1 week (5 males, 7 females), 2 weeks (3 males, 9 females), or 3 weeks (12 males, 1 female) later, and the anterior parts of the stomachs were collected for histopathological analysis.

In the 14th experiment, 10 *Lgr5*-GFP mice (all males) were treated with MNU at 2 months of age, subjected to PP or VTPP at 19 weeks of age, and euthanized at 25 weeks of age.

All animal experiments were designed by strictly following 3Rs (the guideline for human use of animals; Replace, Refine and Reduce) [254].

Animal surgery

All surgical procedures were performed under isoflurane inhalation anesthesia (2–3%), with buprenorphine (0.1 mg/kg subcutaneously) given as postoperative analgesia. The abdominal cavity was accessed through a midline incision. Sham operation consisted of a laparotomy with mild manipulation of organs, including identification of the vagus nerve. PP was done by longitudinal incision of the pyloric sphincter followed by transverse suturing. VTPP was performed by subdiaphragmatic dissection of both the anterior and posterior vagal trunks, and simultaneous PP to prevent post-vagotomy delayed gastric emptying. In UVT, only the anterior truncal vagus nerve was cut (Paper I; Fig. S2), leading to a specific vagal denervation of the anterior aspects of the stomach with preserved pyloric function making PP unnecessary. Sample collection was done under inhalation anesthesia as described, and the animals euthanized by exsanguination while still under anesthesia. Body weight was not affected by surgery including VTPP, PP and UVT (Paper I; Fig. S3).

Botox treatment

Botox (Botulinum Toxin Type A) inhibits release of neurotransmitters including acetylcholine from vagus nerve terminals by following pharmacological mechanism; the light-chain of Botox binds to and cleaves SNAP-25 (synaptosomal nerve-associated protein 25) leading to the inhibition of exocytosis of synaptic vesicles containing neurotransmitter at nerve endings [255][256]. However, this inhibition is reversible due

to the neogenesis of the vagal presynaptic terminals, in contrast, inhibition by vagotomy operation is irreversible. Thus, repeated injection of Botox was needed for this study.

Botox 100 U (Botox® Allergan Cooperation, Irvine, CA) was dissolved in 0.9% cold saline and 1% methylene blue (for the purpose of visualization of the injection) achieving a concentration of 0.25 U of Botox/mL. The Botox solution was injected subserosally along the greater curvature into the anterior (unilateral Botox treatment)(Fig. 7) or both anterior and posterior sides (bilateral Botox treatment) of the stomach (only corpus area where tumor developed) at the dose of 0.05 U/mouse (0.2mL/mouse) or 0.1 U/mouse (0.4mL/mouse) respectively, once per month until the end of the study.

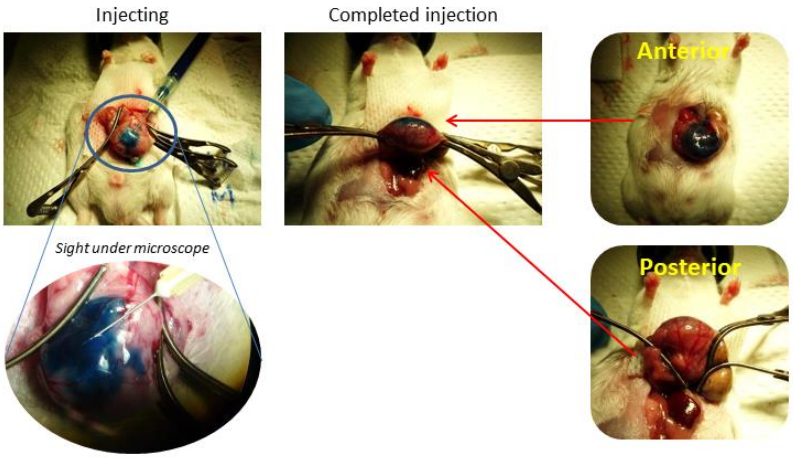

Figure 7 | Photos of unilateral Botox injection. Botox was injected into only corpus area in anterior side of the stomach.

In the control group, the vehicle solution was prepared with 0.9% cold saline and 1% methylene blue and injected to both anterior and posterior sides of the stomach (only corpus area where tumor developed) at the volume of 0.4mL/mouse. Body weight was not affected by Botox treatment (Fig. 8).

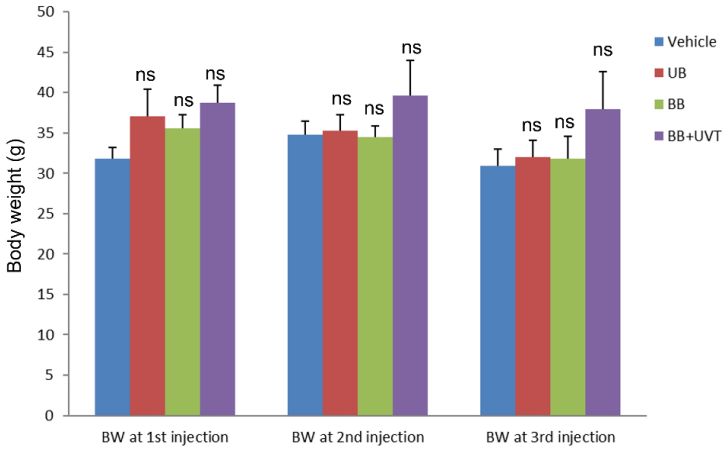

Figure 8 | Body weight comparison of INS-GAS mice under Botox treatment. Botox treatment did not affect body weight in all groups. UB; unilateral anterior Botox, BB; bilateral Botox, BB+UVT; bilateral Botox plus unilateral anterior vagotomy. Means±SEM. ns; $p>0.05$ (*vs.* Vehicle group, ANOVA followed by Dunnett's test).

Chemotherapy

5-Fluorouracil (5-FU, Flurablastin®, Pfizer, Inc., NY) was diluted in saline and given at a dose of 25 mg/kg in volume of 1 mL. Oxaliplatin (Hospira, Inc. IL) was diluted in saline and given at 5 mg/kg in 1 mL. Combination of 5-FU (25 mg/kg in 0.5 mL) and oxaliplatin (5 mg/kg in 0.5 mL) was given at the same time, but the drugs were injected separately. Chemotherapy was given by intraperitoneal injection weekly in 2 cycles, namely 3 injections in the 1st month (one week after the 1st Botox or UVT surgery), and 3 injections in the 2nd month (starting at one week after the 2nd Botox or no UVT). Age- and sex-matched mice received intraperitoneal injection of saline (1 mL) as controls.

The injection needle was 27G. The dosages and regimens were made based on our pilot experiments for selecting the doses and our own results showing no effect on tumor size by 5-FU or oxaliplatin alone (p>0.05, n=8-13)(Paper I; Fig. S16).

Muscarinic acetylcholine receptor M_3 antagonist treatment

Darifenacin was used for this study because this antagonist has the highest and specific affinity to M_3R compared with the other muscarinic receptor antagonists such as solifenacin, tolterodine, oxybutynin, propiverine, pirenzepine [257][258]. Darifenacin hydrobromide (Santa Cruz Biotechnology) was given at a dose of 1 mg/kg/h for 2 months via an osmotic mini-pump (ALZET 2006) as reported previously [259].

Tumor regeneration model

The method was previously reported by us and the topical application of acetic acid was found to promptly necrotize the tumor tissue in INS-GAS mice [260](Paper S4). In brief, under isofluran anesthesia, the stomach was exposed through a midline abdominal incision and 60% acetic acid was topically applied serosally to the anterior side of the stomach for 60 seconds using a 5 mm ID of cylindrical metal mold. In the experiment of acetic acid-induced necrotic ulcer with UVT, the mice received UVT and then the acetic acid application during the surgery.

Pathological and immunohistochemical analyses

The samples for histology comprised multiple linear strips along the greater curvature of the stomach wall, extending from the squamocolumnar junction through the antrum. Samples were briefly rinsed in saline, fixed in 4% formaldehyde for 8–12 hours at room temperature and embedded in paraffin. Sections (4 µm thick) were stained with hematoxylin, eosin and saffron. Pathological evaluation was performed by one comparative pathologist (S.M.) and one histologist (C-M.Z.) who were blinded to the sample source. The gastric lesions were scored on an ascending scale from 0 to 4 using the criteria adopted from previous reports [261][262]. The size of visible tumor in the stomach was measured by planimetric analysis according to the principle of stereology, and expressed as volume density, i.e., the percentage of glandular volume occupied by the tumor. Immunohistochemistry was performed using a DAKO AutoStainer (Universal Staining System with DAKO EnVision System, Dako, Glostrup, Denmark). Antibodies used were Ki67 (Dako, 1:100), PCNA (Dako, 1:100), M_3R (Acris, 15 µg/mL), CD44 (BD Pharmigen, 1:100), CD44v6 (Millipore, 1:200), and Dclk1 (AbGent 1:100). Cell proliferation rate is expressed as number of Ki67 or PCNA immunoreactive cells/gland. There was no difference between the two markers between two labs (TW and DC). Slides were visualized on a Nikon TE2000-U and representative microphotos were taken. Positive-stained cells with nuclei were counted only in dysplastic glands and at least 50 glands were counted per animal in a blinded fashion, and results expressed as numerical densities (number of cells per gland or number of cells per 10 glands).

Vagus nerve fibers and terminals in the mouse stomach traced with DiI

The esophagus, diaphragm and stomach were removed from adult mice and fixed for 3 days with formaldehyde (from paraformaldehyde). DiI crystals were placed on the anterior and posterior thoracic vagal trunks about 1 cm above the diaphragm, which was left undisturbed. The preparation was incubated at 37° C in PBS containing 0.5% sodium azide in a sealed container for 3 months. Following incubation, the stomach was opened along the greater curvature, the mucosa and submucosa were removed and the preparation were mounted, serosa side up, in buffered glycerol for microscopic examination. DiI fluorescence was viewed with a Leica CTR6000 microscope equipped with a cooled CCD camera and computer assisted video imaging. The entire gastric wall was scanned with a 2.5× objective, and a montage was made of the resulting images [263]. In order to observe the density of DiI-labled vagal fibers within the myenteric plexus, additional images were obtained at higher magnification in the lesser curvature close to the esophago-gastric junction, and the greater curvature. The density of DiI-labeled fibers was estimated by point counting technique. A test system comprising a 1.0 cm square lattice was placed over each photograph, and the numbers of test points overlying the DiI-labeled fibers and the visual field were determined.

RNA isolation, gene expression profiling by microarray and qRT-PCR arrays in mice and humans

The collected mouse and human stomach samples were kept frozen at -80°C until further processing. Total RNA from the frozen stomach samples was isolated and purified using an Ultra-Turrax rotating-knife homogenizer and the mirVana miRNA Isolation Kit (AM1560, Ambion) according to the manufacturer's instructions. Concentration and purity of total RNA were assessed using a NanoDrop photometer (NanoDrop Technologies, Inc., Wilmington, DE). The A260/280 ratios were 2.05±0.01 for mouse samples and 1.96±0.10 for human samples (mean±SEM). RNA integrity was assessed using a Bioanalyzer (Agilent Technologies, Palo Alto, CA) and found satisfactory with RIN values 9.1±0.1 for mouse samples, and 8.7±0.9 for human samples (means±SEM). The microarray gene expression analysis followed standard protocols, analyzing 300 ng total RNA per sample with the Illumina MouseWG-6 and HumanHT-12 Expression BeadChips (Illumina, San Diego, CA). Microarray data were confirmed by qRT-PCR array (RT^2 Profiler PCR Array, SABiosciences, Qiagen, MD) (StepOnePlus™, Applied Biosystem, Foster City, CA). Mouse microarray data were deposited in the Gene Expression Omnibus (GEO accession no. GSE30295), and human data in ArrayExpress (accession no. E-MTAB-1338).

Fluorescence-activated cell sorting (FACS)

Single epithelial cells were isolated from *Lgr5*-GFP mouse stomachs. Isolated crypts were dissociated with TrypLE Express (Invitrogen) including 1 mg/ml DNase I (Roche Applied Science) for 10 minutes at 37°C. Dissociated cells were passed through a 20-μm cell strainer, washed with 2% FBS/PBS, and sorted by FACS (BD FACSAria Cell

Sorter III). Viable single epithelial cells were gated by forward scatter, side scatter and a pulse-width parameter, and negative staining for propidium iodide. Cells expressing high and low levels of GFP and 14 GFP-negative cells were sorted separately, and RNA was isolated by using RNAqueous-Micro Kit (Ambion).

***In vitro* culture system**

Wild-type, Ubiquitin C-green fluorescent protein (UBC-GFP), or Gt (ROSA) 26Sortm4 (ACTB-tdTomato,-EGFP) Luo/J mice (purchased from Jackson laboratory) were used for *in vitro* culture. Crypt isolation and culture were performed, as described previously [130] with minor modifications. Removed mouse stomach were opened longitudinally, chopped into approximately 5 mm pieces, and incubated in 8 mM EDTA in PBS for 60 minutes on ice. The tissue fragments were suspended vigorously, yielding supernatants enriched in crypts. Crypt fractions were centrifuged at 900 rpm for 5 minutes at 4°C and diluted with advanced DMEM/F12 (Invitrogen) containing B27, N2, 1 μM n-Acetylcysteine, 10 mM HEPES, penicillin/streptomycin, and Glutamax (all Invitrogen). Crypts were embedded in extracellular matrix (provided from NCI) and 400 crypts/well were seeded on pre-warmed plate. Advanced DMEM/F12 medium containing 50 ng/mL EGF, 100 ng/mL Noggin, and 1 μg/mL R-spondin1 was overlaid [264]. Growth factors were added every other day and the entire medium was changed twice a week. Passage was performed at day 7 as described previously [130]. Mouse primary neuronal cells were prepared following the protocol described previously [265]. Neuronal cells were mixed with extracted gastric crypts in the extracellular matrix at the ratio of

crypt:neuron 1:5. Enteric nervous system was isolated from guinea pig as described previously [266]. Botox, scopolamine hydrochloride, and pilocarpine hydrochloride (Sigma) were dissolved in PBS and added in the cultured medium every other day. The images of gastric organoids were acquired using fluorescent microscopy (Nikon, TE2000-U) and two-photon microscopy (Nikon, A1RMP). Isolation of mRNA from cultured organoids was performed by using NucleoSpin RNA XS kit (Clontech Laboratories Inc, CA) as manufacture's instruction. The first-strand complementary DNA was synthesized using the ImProm-II Reverse Transcription System (Promega). Amplification was performed using the ABI PRISM 7300 Quantitative PCR System (Applied Biosystems). Use of the animals involved in this experiment was approved by the local ethical committer of Columbia University, New York.

Patients and methods

Three cohort studies were included. In the 1st study, human stomach specimens (both tumors and the adjacent non-tumor tissues) were taken immediately after gastrectomy from 17 patients during 2005 to 2010 at St. Olav's University Hospital, Trondheim, Norway for gene expression profiling analysis. All patients were diagnosed histologically as primary gastric carcinoma of stage I-IV. 10 of 17 patients were *Helicobacter pylori* positive at the time of surgery. In the 2nd study, human stomach tissues were obtained from 120 gastric cancer patients who underwent curative surgical resection from 2001 to 2008 at Gifu University Hospital, Gifu, Japan. All patients were diagnosed histologically as primary gastric carcinoma of stage II, III or IV.

Immunohistochemical analysis of the nerve density was performed with PGP9.5 antibody (DAKO at dilution 1: 100). Low and high expression of PGP9.5 were defined by bisecting subjects in order of the volume density of PGP9.5. In the 3rd study, clinical data of 37 patients with early gastric stump cancer (GSC) who had received distal gastrectomy with or without vagotomy during 1962 to 1995 at the National Cancer Center Hospital East, Chiba, Japan were evaluated. Early GSC was defined as gastric cancer that occurred ≥5 years (from 5 to 36 years) after curative distal gastrectomy, regardless of the original benign or malignant disease. Early GSC was histologically defined as adenocarcinoma infiltrating the mucosal or submucosal layer. The tumor location was recorded according to the recommendation by the Japanese Gastric Cancer Association: anterior or posterior wall, or lesser and greater curvature [267]. All the study protocols were approved by the ethics committees in Japan and Norway, and written informed consent was obtained from all patients.

Data analysis

Values were expressed as means±SEM. Comparisons between experimental groups, between anterior and posterior sides of the stomachs and between groups of patients were performed using independent *t*-test, paired *t*-test, ANOVA followed by Dunnett's or Bonferroni test as appropriate. Survival curve was obtained by using Kaplan-Meier method and analyzed by log-rank test. Tumor incidence was analyzed by Fisher's exact test. Microarray data were log2 transformed and quantile normalized. Gene expression profiles from both microarray and qRT-PCR were analyzed independently by a paired

robust *t*-test for mouse samples or a paired *t*-test for human samples. Paired *t*-statistics were computed by fitting a linear robust or non-robust regression to the anterior and posterior stomach samples within each mouse or to the cancer and the adjacent non-cancerous tissue samples within each patient. False discovery rate adjusted *p*-values less than 0.05 were defined as differentially expressed. Regulated pathways were identified using signaling pathway impact analysis (SPIA) based on data from the Kyoto Encyclopedia of Genes and Genomes (KEGG) database, also scores of total net accumulated perturbation (tA score) of pathways were obtained by SPIA (tA score>0: activation, tA score<0: inhibition). The calculations were performed within the R software environment (http://www.r-project.org/) using Lumi [268], Limma [269] and SPIA [270].

Part II: Obesity (Papers II and III)

Animals

Male rats (Sprague–Dawley) were purchased from Taconic M&B, Skensved, Denmark. The males were preferred because females change their food intake during ovulation and males grow faster than females, making it easier to detect body weight change. The rats were housed in individually ventilated Makrolon cages on wood chip bedding with a 12-hour light/dark cycle, room temperature of 22°C and 40–60% relative humidity. They were allowed free access to tap water and standard rat pellet food (RM1 801002, Scanbur BK AS, Sweden) containing metabolizable energy of 2.57 kcal/g. The study

was approved by the Norwegian National Animal Research Authority (Forsøksdyrutvalget, FDU).

Experimental design

In Paper II, the animals were divided into the following groups: laparotomy (LAP), pyloroplasty (PP), bilateral truncal vagotomy plus pyloroplasty (VTPP), sleeve gastrectomy (SG), duodenal switch alone (DS), SG as the first stage and then DS as the second stage (SG_1+DS_2), and SG and DS simultaneously (SG+DS). 14 rats in control groups have been re-used after a 9-week recovery from previous operation and revealed an unchanged eating behavior and metabolic parameters. The rats were first subjected to LAP (n=7), PP (n=7), or VTPP (n=7), respectively. After 9 weeks, LAP and PP rats were subjected to SG and DS, respectively. After an additional 11 weeks, SG rats were subjected to DS, and VTPP rats were simultaneously subjected to both SG and DS. An additional group of age-matched rats were subjected to LAP (n=7).

In Paper III, 34 rats were randomly divided into the following groups: gastric bypass (GB) (14 rats), SG_1+DS_2 (7 rats), and LAP (13 rats). The body weight was not different between the groups before surgery (p=0.276). Total of 13 rats underwent LAP were subjected to the age-matched controls for SG_1+DS_2 (LAP_{DS}, 7 rats) or the age-matched controls for GB (LAP_{GB}, 6 rats), and were used for comparisons because metabolic parameters are age-dependent [271][272]. Due to markedly loss of body weight after SG_1+DS_2, the group of SG_1+DS_2 rats, together with LAP_{DS} rats, were followed up only

for 8 weeks, while GB rats and LAP_{GB} rats were followed up for 14 weeks. Rats that had been used for studies of the effects of individual surgical procedures were re-used.

In Paper II and III, each rat was monitored weekly with respect to the body weight development throughout the study period. Each rat was placed in the Comprehensive Laboratory Animal Monitoring System (CLAMS) cage three times for 48 hours, i.e., 1 week before surgery, 1–3 (at short-term) and 8–14 weeks (at long-term) after surgery for measurements of the eating and metabolic parameters. All animal experiments were designed by strictly following 3Rs [254].

Bariatric surgeries

Rats were fasted excluding water for 12 hours pre- and 24 hours post-operation. All operations were performed under general anesthesia with isofluran (4% for induction and 2% for maintenance). Buprenorphine (0.05 mg/kg) was administrated as a pain reliever subcutaneously immediately after surgery.

Laparotomy (LAP): LAP was performed through a middle-line incision with gentle manipulation of viscera. There was no mortality in rats underwent LAP.

Bilateral truncal vagotomy (VT) and Pyrloroplasty (PP): PP was done by cutting off the pyloric sphincter (2 mm) and sturing it vertically against the incision. VTPP was performed by subdiaphragmatic dissection of both the anterior and posterior vagal

trunks (Fig. 9A), and simultaneous PP to prevent gastroparesis-induced food retention and gastric dilation (Fig. 6).

Sleeve gastrectomy (SG): SG was performed by resecting 90% of the rumen and 70% of the glandular stomach along the greater curvature (Fig. 9B, C).

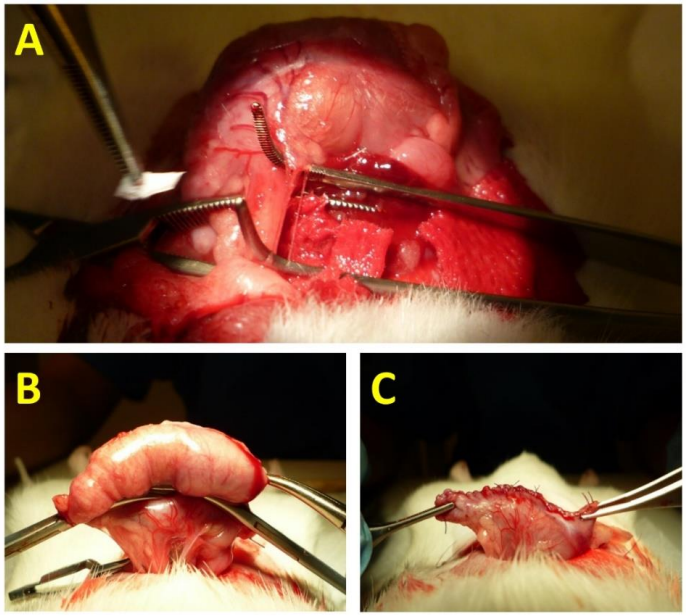

Figure 9 | The photo of VTPP (A) and SG (B and C) procedures. (A) Identification and isolation of subdiaphragmatic truncal vagus nerve (both anterior and posteior) before dissection. (B) Gross appearance of stomach before SG. (C) Gross appearance of stomach after SG.

Duodenal switch (DS): DS was constructed by transecting the duodenum 1 cm to the pylorus, and a common channel was created by dividing the ileum 5 cm proximal to the ileocecal junction (rats have a much longer jejunum than humans). The distal limb of the ileum was anastomosed to the post-pyloric duodenum in an end-to-end manner, and the stump of the duodenum was closed with cross-suture. The distal anastomosis was

performed by joining the distal biliopancreatic limb at 1 cm to the ileocecal junction in an end-to-side manner (Paper III; Fig. 1H).

Gastric bypass (GB): GB was performed by anastomosing the distal esophagus to the proximal jejunum about 2–3 cm distal to the Treitz ligament in an end-to-side manner (Paper III; Fig. 1G).

Measurements of eating behavior and metabolic parameters

Eating and metabolic parameters were automatically and accurately recorded by the comprehensive laboratory animal monitoring system (CLAMS; Columbus Instruments International, Columbus, OH, USA). This system is composed of a four-chamber open circuit indirect calorimeter designed for the continuous monitoring of individual rats from each chamber (Fig. 10A, B).

The high-resolution eating data was generated by monitoring feeding balances every 0.5 seconds. The end of an eating event (meal) was recorded when the balance was stable for more than 10 seconds and a minimum of 0.05 g was eaten. The eating parameters during daytime and nighttime (12 hours each time) for each rat included: accumulated food intake (g or kcal), number of meals, meal size (g/meal), meal duration (min/meal), intermeal interval (min), rate of eating (g/min), satiety ratio (min/g) , and water intake (mL). The intermeal interval was defined as the interval in minutes between two meals. The rate of eating was calculated by dividing meal size by meal duration. The satiety

ratio, an index of non-eating time produced by each gram of food consumed, was calculated as intermeal interval divided by meal size.

The volume of O_2 consumption (VO_2 mL/kg/hr) and the volume of CO_2 production (VCO_2 mL/kg/hr) were measured by an air sample withdrawn every 5 min from each chamber through the gas dryer (Fig. 10C). Energy expenditure (kcal/hr) was calculated according to the equation: $(3.815+1.232\ RER) \times VO_2$, where the respiratory exchange ratio (RER) was obtained by VCO_2 divided by VO_2. RER is used as an indicator which fuel, e.g., carbohydrate or fat, is being metabolized to supply energy to the body. RER close to 1.0 indicates that carbohydrate is the predominant fuel resource, whereas RER close to 0.7 indicates that fat is the predominant fuel resource, according to the chemical equations below.

Under the condition of carbohydrate combustion

$$6\ O_2 + C_6H_{12}O_6 \rightarrow 6\ CO_2 + 6\ H_2O + 38\ ATP$$

$$RER = VCO_2/VO_2 = 6\ CO_2/6\ O_2 = 1.0$$

Under the condition of fat combustion

$$23\ O_2 + C_{16}H_{32}O_2 \rightarrow 16\ CO_2 + 16\ H_2O + 129\ ATP$$

$$RER = VCO_2/VO_2 = 16\ CO_2/23\ O_2 = 0.7$$

Ambulatory activity was obtained by the activity sensors attached to each chamber (Fig. 10D).

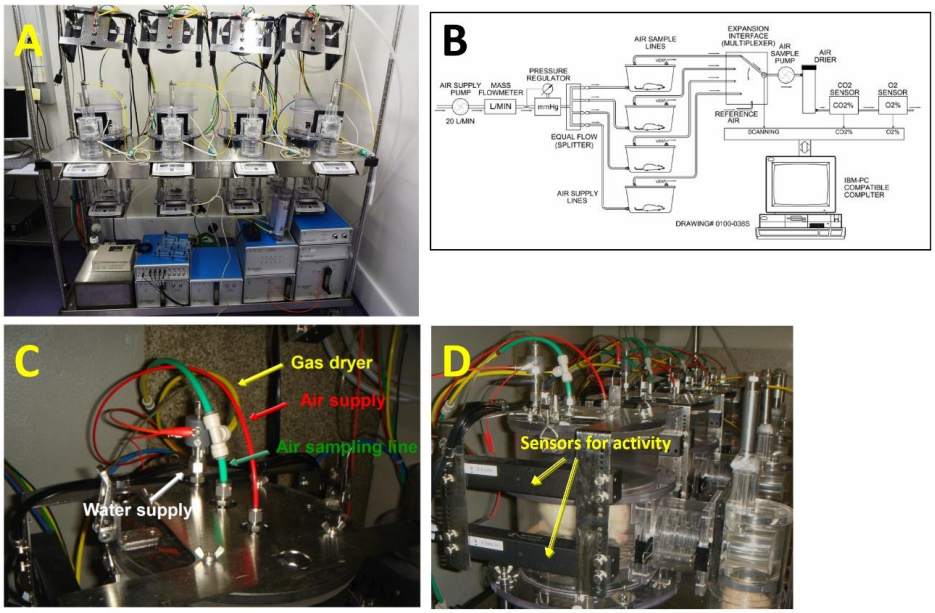

Figure 10 | The photo (A) and the illustration (B) of overview of CLAMS. (C) Air sampling system of CLAMS. (D) Overview of CLAMS chamber and the activity sensor.

In order for rats to acclimate to CLAMS, they were placed in these metabolic chambers for 24 hours at one week before the first CLAMS monitoring. For the measurement of eating and metabolic parameters, the rats were placed in the CLAMS for 48 hours. In order to minimalize possible effect of stress, data from the last 24 hours in CLAMS were only used for the analysis. The CLAMS measurements of normal rats at day 1 and 21 one week after 24 hours training with CLAMS cages showed no significant

differences in any eating parameters and activity, indicating that the animals were acclimated to CLAMS (Paper III; Table S1). The rats have had free access to standard rat powder food (RM1 811004, Scanbur BK AS, Sweden) containing metabolizable energy of 2.57 kcal/g and tap water while they were in CLAMS.

Determination of fecal energy density

Feces were collected while the rats were placed in CLAMS chambers and dried for 72 hours at 60ºC. The energy density was determined using an adiabatic bomb calorimeter (IKACalorimeter C 5000, IKA-Werke GmbH & Co. KG, Staufen,Germany).

Determination of plasma levels of cytokines and CCK

Blood was drawn from the abdominal aorta under the anesthesia just before the rats were euthanized, and the plasma samples were stored at -80ºC until determination of levels of cytokines and cholecystokinin (CCK). The multiplex cytokine assay was used (Bio-Plex Human cytokine 27-Plex Panel; Bio-Rad Laboratories, Hercules, CA, USA). It contained the following analytics: IL-1α, IL-1β, IL-2, IL-4, IL-5, IL-6, IL-10, IL-13, granulocyte-macrophage colony stimulating factor (GM-CSF), interferon gamma (IFNγ), and tumor necrosis factor alpha (TNFα). CCK levels were determined by radioimmunoassay with sulfated CCK-8 as standard, using a CCK kit (Euro Diagnostica AB, Malmö, Sweden).

Statistical analysis

The values were expressed as mean±SEM. Two-tailed independent-samples *t*-test or Mann Whitney U test was performed for two-group comparisons, ANOVA followed by Tukey's or Bonferroni test was performed for multiple comparisons as appropriate, and the homogeneity of regression assumption test and ANCOVA were performed for analysis of energy expenditure. Analysis was performed using SPSS version 19.0 (SPSS Inc. Chicago, IL, USA). A *p*-value of <0.05 was considered statistically significant.

Results

Part I: Gastric cancer (Paper I)

High incidence of gastric tumors in lesser curvature of stomach was associated with high vagal innervation

In human patients, it has been shown that there is a higher incidence of gastric cancer in the lesser (~80%) than the greater curvature [68][273]. We also observed this distribution in the INS-GAS mouse model, a genetic mouse model of spontaneous gastric cancer, in which, we found a similar preponderance (77%) of tumors on the lesser curvature (Paper I; Fig. 1A). Topographic analysis of vagus nerve fibers and terminals in the murine stomach by Dil-tracing revealed a higher density of neurons and larger size of ganglia in the lesser curvature compared to the greater curvature (Paper I; Fig. 1B), correlating with the observed pattern of tumor formation. Thus, this strong correlation between the normal distribution of vagal nerve fibers with the appearance of gastric tumors in the INS-GAS mouse prompted us to study the role of nerves in gastric tumorigenesis in a number of large cohorts of animals (Paper I; Table S1), using surgical and pharmacological approaches.

Surgical denervation at preneoplastic stage attenuated tumorigenesis in mouse models of gastric cancer

In the first series of experiments, surgical vagotomy was performed in INS-GAS mice at an early preneoplastic stage (6 months of age), and the effects of vagotomy were examined 6 months later. INS-GAS mice (n=107) were subjected to either subdiaphragmatic bilateral truncal vagotomy accompanied with a pyloroplasty drainage procedure (VTPP), unilateral truncal vagotomy (UVT) (Paper I; Fig. S1), sham operation (Sham), or pyloroplasty alone (PP). The unilateral vagotomy approach takes advantage of the fact that each (anterior or posterior) vagal trunk innervates only one half of the stomach. Consequently, denervation of one side of the stomach does not impair the overall functional capacity of the stomach, leaving gastric acid output, circulating gastrin levels and motility unchanged [198][274]. In addition, UVT provides excellent model to know the role of vagus nerve specifically, by direct comparisons between innervation and denervation sides within the same mice, i.e., same conditions.

Six months later, tumor incidences were 17% after VTPP *vs.* 86% after PP alone, 14% in the anterior side *vs.* 76% in the posterior side after UVT and 78% in the sham-operated mice (Fig. 11A)(Paper I; Fig. 1C). Histological examination showed that the thickness of the oxyntic mucosa was reduced after VTPP (compared to PP) or UVT (compared to the corresponding posterior side) (Paper I; Fig. 1D, Fig. S4), suggesting successful denervation [197][198]. Pathological evaluation revealed attenuated inflammation, epithelial defects, oxyntic atrophy, epithelial hyperplasia, dysplasia, and pseudopyloric metaplasia, along with reduced cell proliferation (Paper I; Fig. 1E, F, Fig. S5). Interestingly, the expression of M_3R was found to be up-regulated in gastric epithelial cells (Fig. 11B).

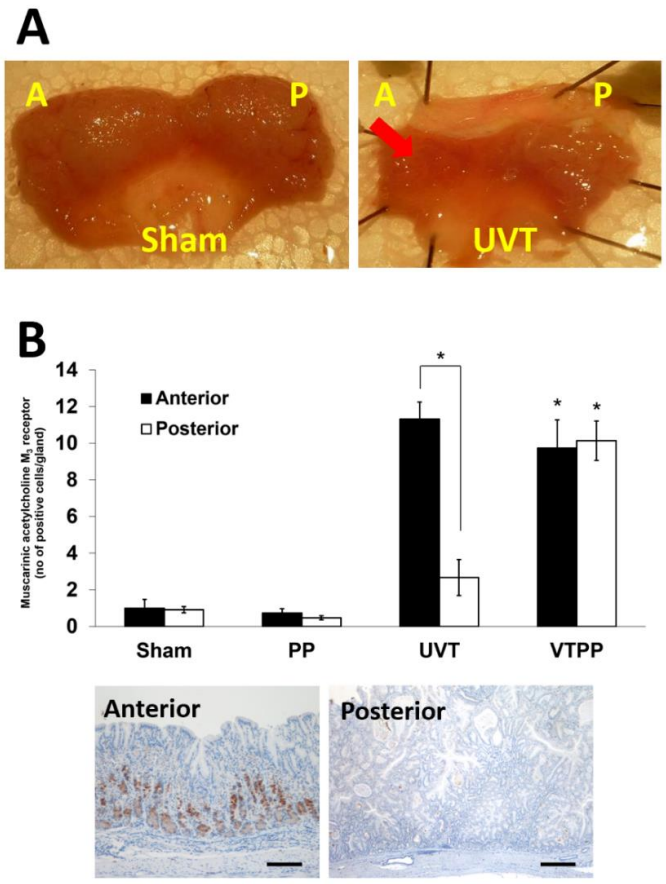

Figure 11 | (A) Gross appearance of anterior and posterior stomachs at 12 months of age after (left) Sham at 6 months of age and (right) UVT at 6 months of age. Red arrow; vagotomized side. Tumor was not observed at vagotomized anterior side of the stomach after UVT. (B) Number of M_3R-positive cells in the anterior and posterior mucosa of the stomach underwent Sham, PP, UVT or VTPP, respectively. Means±SEM. *; $p<0.05$ (Anterior *vs.* Posterior or PP *vs.* VTPP). Representative immunohistochemical microphotographs in UVT group are shown below. Scale bars; 25 μm.

To confirm the effects of surgical denervation on gastric tumorigenesis seen in INS-GAS mice, we investigated the chemically-induced (MNU) mouse model of gastric cancer, which develops large tumors in gastric antrum [251].Vagotomy (VTPP) significantly inhibited tumorigenesis (Paper I; Fig. 1G, H), further validating the general importance of functional innervation in gastric tumorigenesis, across mouse models of gastric cancer, we further investigated the infection-induced mouse model of gastric cancer (*Helicobacter pylori*-infected H^+/K^+-ATPase-IL-1ß mice) [252]. Vagotomy (UVT) reduced tumor size and number of proliferating cells in the denervated side of the stomach (Paper I; Fig. 1I, J). Therefore, the findings from these three independent mouse models of gastric cancer indicate the certainty and importance of functional innervation in gastric tumorigenesis.

Pharmacological denervation at an early preneoplastic stage attenuated gastric tumorigenesis

To establish that the effects of surgical denervation were primarily local (acting at the terminals of vagus nerve within the gastric mucosa), unilateral intragastric injection of Botox was performed in INS-GAS mice at 6 months of age. After 6-months Botox treatment (monthly reinjection of Botox), tumor size and cell proliferation rate were markedly reduced in the anterior side compared with the posterior side of the stomach. Moreover, these changes were associated with attenuated inflammation, epithelial defects, atrophy, hyperplasia, dysplasia and metaplasia (Paper I; Fig. 1K-N, Fig. S6).

Hence, these findings confirm the role of local signaling from vagus nerve endings, which is predominantly cholinergic, in gastric tumor development.

Surgical or pharmacological denervation attenuated gastric tumorigenesis at the neoplastic stage

While vagotomy or Botox treatment appeared to inhibit the tumorigenesis at preneoplastic stages, we next examined whether denervation of the stomach could retard tumor progression at later stages. INS-GAS mice begin to develop dysplasia at 8 months of age, with almost 100% of mice exhibiting dysplasia by 12 months. Accordingly, INS-GAS mice at 8, 10, or 12 months of age were subjected to UVT and euthanized at 18 months of age. In these mice, tumors were significantly smaller with less severe dysplasia in the anterior compared to the posterior side of the stomach, suggesting that vagotomy also suppresses tumor progression in mice with established neoplastic changes (Paper I; Fig. 2A-C).

While the average lifespan of wild-type FVB/N mice is well over 24 months, the survival rate of INS-GAS mice at 18 months of age was 53%. Importantly, the 18-month survival rate of age-matched vagotomized INS-GAS mice was improved: 71% when UVT was performed at 8 months, 64% when performed at 10 months, and 67% when performed at 12 months, respectively (Paper I; Fig. 2D). With the similar experimental design, INS-GAS mice at 12 months of age were subjected to vehicle or Botox treatment unilaterally or bilaterally with or without UVT (n=6-7 in each group at

the beginning). Due to surgical mortality (n=4-6 in each group at the end), this experiment was terminated at 2 months postoperatively. Nevertheless, cell proliferation was significantly reduced in the anterior side of the stomach where Botox was injected, when compared to the posterior side or vehicle-treated anterior side (Paper I; Fig. 2E). The reduction in proliferation in the posterior side of stomach after bilateral Botox injection did not reach statistical significance, probably due to the small sample size and the technical difficulty of Botox injection to the posterior side of solid stomach caused by gastric cancer (Paper I; Fig. 2E). The combination of UVT and Botox did not further reduce the cell proliferation, indicating that vagotomy and Botox likely act through the same mechanism. Overall, these results show that vagotomy (surgical denervation) or Botox treatment (pharmacological denervation) inhibits gastric cancer progression even when applied at the stage of dysplasia.

Vagotomy or Botox synergized with chemotherapy in treatment of the gastric cancer in mice

We next examined whether denervation could enhance the effects of systemic chemotherapy in invasive gastric cancer. INS-GAS mice at 14 months of age received systemic administration of 5-FU+oxaliplatin, along with unilateral Botox treatment or UVT or no additional therapy. An additional group of INS-GAS mice served as untreated controls. As early as 2 months after starting treatment, tumor size was already significantly reduced in mice treated with chemotherapy, particularly in areas of denervated stomach following unilateral vagotomy or Botox injection (Paper I; Fig. 2F,

G). Most importantly, the combination of either Botox or UVT with chemotherapy led to a statistically significant increase in survival compared to chemotherapy alone (Paper I; Fig. 2H). Thus, these findings suggest a synergistic effect of chemotherapy and denervation on both tumor growth and survival.

Vagotomy led to inhibition of gastric Wnt signaling

Genome-wide gene expression profiling was performed in INS-GAS mice post vagotomy (i.e., UVT performed at 6 months of age). Direct comparison between the vagotomized anterior and the untreated posterior side of the same stomach, revealed 4495 differentially expressed genes annotated to 93 signaling pathways (6 months post-surgery), with evidence for inhibition of the Wnt signaling pathway (Table 1)(Paper I; Fig. 3, Fig. S9), a finding confirmed by immunohistochemical analysis of nuclear β-catenin and qRT-PCR array. As expected, vagotomy also inhibited signaling pathways linked to gastric acid secretion, neurotrophin, actin cytoskeleton, mitogen-activated protein kinase (MAPK) and hedgehog signaling, whereas it stimulated signaling pathways of apoptosis and autophagy (Table 1)(Paper I; Fig. S8). Inflammation-related signaling pathways - including T cell receptor signaling, natural killer cell mediated cytotoxicity, leukocyte transendothelial migration, chemokine signaling and VEGF signaling - were activated at 2 months, and then inhibited at 4 and 6 months after vagotomy, whereas Toll-like receptor signaling was inhibited at all the time points (Paper I; Fig. 4A). In contrast, inhibition of Wnt signaling was persistent at 2, 4, 6, 8, and 10 months post vagotomy (tA=-0.208, -0.427, -8.614, -0.773, and -0.036,

respectively). Thus, the gene expression profiling analysis pointed to a relatively specific and long-lasting effect of denervation on suppressing gastric Wnt signaling.

Table 1 | List of annotated KEGG pathways (in INS-GAS mice at 12 months of age, 6 months after UVT). Status: inhibition or activation by vagotomy in the anterior side *vs.* the posterior side of the stomach.

KEGG ID	Pathway	tA score	Status
4310	Wnt signaling pathway	-8.614	Inhibited
4971	Gastric acid secretion	-5.220	Inhibited
4650	Natural killer cell mediated cytotoxicity	-3.678	Inhibited
4350	TGF-beta signaling pathway	-3.391	Inhibited
4810	Regulation of actin cytoskeleton	-2.547	Inhibited
4910	Insulin signaling pathway	-2.255	Inhibited
5100	Bacterial invasion of epithelial cells	-2.041	Inhibited
4930	Type II diabetes mellitus	-1.863	Inhibited
4620	Toll-like receptor signaling pathway	-1.727	Inhibited
4670	Leukocyte transendothelial migration	-1.465	Inhibited
4530	Tight junction	-1.406	Inhibited
4370	VEGF signaling pathway	-1.401	Inhibited
4722	Neurotrophin signaling pathway	-1.353	Inhibited
4664	Fc epsilon RI signaling pathway	-1.314	Inhibited
4720	Long-term potentiation	-1.190	Inhibited
5223	Non-small cell lung cancer	-1.152	Inhibited
4270	Vascular smooth muscle contraction	-1.084	Inhibited
4914	Progesterone-mediated oocyte maturation	-1.071	Inhibited
4950	Maturity onset diabetes of the young	-0.871	Inhibited
5214	Glioma	-0.777	Inhibited
5140	Leishmaniasis	-0.726	Inhibited
5010	Alzheimer's disease	-0.715	Inhibited
4621	NOD-like receptor signaling pathywa	-0.631	Inhibited
4062	Chemokine signaling pathway	-0.518	Inhibited
5016	Huntington's disease	-0.492	Inhibited
4912	GnRH signaling pathway	-0.385	Inhibited
5014	Amyotrophic lateral sclerosis	-0.361	Inhibited
5332	Graft-versus-host disease	-0.361	Inhibited
5330	Allograft rejection	-0.345	Inhibited
4940	Type I diabetes mellitus	-0.345	Inhibited
5210	Colorectal cancer	-0.332	Inhibited
5320	Autoimmune thyroid disease	-0.331	Inhibited
5416	Viral myocarditis	-0.317	Inhibited
4012	ErbB signaling pathway	-0.296	Inhibited
4010	MAPK signaling pathway	-0.292	Inhibited
4360	Axon guidance	-0.290	Inhibited
4920	Adipocytokine signaling pathway	-0.276	Inhibited
5142	Chagas disease	-0.257	Inhibited
4115	p53 signaling pathway	-0.252	Inhibited
4660	T cell receptor signaling pathway	-0.252	Inhibited
4340	Hedgehog signaling pathway	-0.234	Inhibited
4320	Dorso-ventral axis formation	-0.228	Inhibited

4612	Antigen processing and presentation	-0.204	Inhibited
3320	PPAR signaling pathway	-0.200	Inhibited
4630	Jak-STAT signaling pathway	-0.175	Inhibited
4672	Intestinal immune network for IgA production	-0.162	Inhibited
5216	Thyroid cancer	-0.156	Inhibited
5310	Asthma	-0.119	Inhibited
4512	ECM-receptor interaction	-0.105	Inhibited
5012	Parkinson's disease	-0.096	Inhibited
4141	Protein processing in endoplasmic reticulum	-0.038	Inhibited
5412	Arrhythmogenic right ventricular cardiomyopathy	0	Mixed
5144	Malaria	0	Mixed
4142	Lysosome	0	Mixed
4080	Neuroactive ligand-receptor interaction	0	Mixed
4962	Vasopressin-regulated water reabsorption	0.026	Activated
5020	Prion diseases	0.058	Activated
4742	Taste transduction	0.097	Activated
4730	Long-term depression	0.158	Activated
4970	Salivary secretion	0.184	Activated
4020	Calcium signaling pathway	0.186	Activated
4110	Cell cycle	0.192	Activated
4130	SNARE interactions in vesicular transport	0.254	Activated
4666	Fc gamma R-mediated phagocytosis	0.261	Activated
4960	Aldosterone-regulated sodium reabsorption	0.271	Activated
5218	Melanoma	0.291	Activated
4610	Complement and coagulation cascades	0.300	Activated
5322	Systemic lupus erythematosus	0.316	Activated
5146	Amoebiasis	0.340	Activated
5221	Acute myeloid leukemia	0.375	Activated
4740	Olfactory transduction	0.393	Activated
4150	mTOR signaling pathway	0.469	Activated
4210	Apoptosis	0.510	Activated
5220	Chronic myeloid leukemia	0.539	Activated
5414	Dilated cardiomyopathy	0.592	Activated
5217	Basal cell carcinoma	0.644	Activated
4510	Focal adhesion	0.728	Activated
4623	Cytosolic DNA-sensing pathway	0.746	Activated
5212	Pancreatic cancer	0.777	Activated
5213	Endometrial cancer	0.839	Activated
4710	Circadian rhythm - mammal	0.860	Activated
5219	Bladder cancer	0.866	Activated
5211	Renal cell carcinoma	1.083	Activated
4622	RIG-I-like receptor signaling pathway	1.326	Activated
4744	Phototransduction	1.371	Activated
4140	Regulation of autophagy	1.484	Activated
4662	B cell receptor signaling pathway	1.530	Activated
4540	Gap junction	1.544	Activated
5222	Small cell lung cancer	1.609	Activated
4060	Cytokine-cytokine receptor interaction	2.156	Activated
4916	Melanogenesis	3.397	Activated
4114	Oocyte meiosis	4.233	Activated
4330	Notch signaling pathway	6.010	Activated

Muscarinic acetylcholine receptor M3 activation drove Wnt signaling in gastric stem and progenitor cells

The Wnt signaling pathway is a major regulator of gastrointestinal stem and progenitor cells and tumorigenesis [275][276]. CD44 is a known target of the Wnt signaling pathway [277], and has been shown to label a cancer initiating cell population (i.e. CSCs) [117]. Lgr5 is a marker of gastric stem cells in both normal and cancer tissues, and also a target of the Wnt signaling pathway [129]. Either vagotomy (VTPP and UVT) or Botox treatment induced down-regulation of CD44 (and CD44v6) in the gastric mucosa of INS-GAS mice, although the combination of vagotomy and Botox did not lead to a further decrease in CD44 expression (Paper I; Fig. 4B, C, Fig. S10, Fig. S11). Vagotomy also reduced the expression of Wnt target genes, such as *Cyclin D1*, *Axin2*, *Myc*, *Lgr5*, and *Cd44*, in MNU-treated mice (Paper I; Fig. 4D). The number of cells with nuclear β-catenin and the number of *Lgr5*-positive cells in MNU-treated mice were reduced after vagotomy (Paper I; Fig. 4E, F). Dclk1 is a maker of gastric progenitor cells and gastrointestinal CSCs [132][133]. Vagotomy (both VTPP and UVT) was associated with downregulation of Dclk1 together with the downregulation of CD44 in the gastric mucosa (Fig. 12A), consistent with the inhibition of Wnt and inflammation-related signaling pathways. Similarly, Botox treatment reduced the expression of CD44, CD44v6 and Dclk1 in the stomach (Fig. 12B)(Paper I; Fig. 4C).

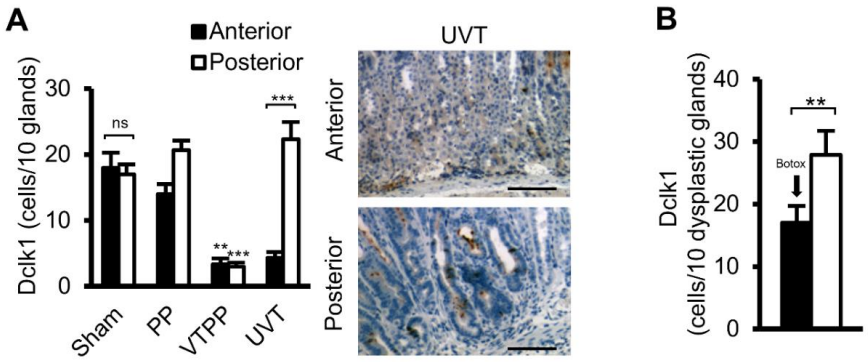

Figure 12 | (A) Graph showing numbers of Dclk1-positive cells in the anterior and posterior mucosa of the stomach underwent Sham, PP, VTPP or UVT, respectively (left), and the representative immunohistochemical microphotographs in UVT group (right). Means±SEM. **; $p<0.01$, ***; $p<0.001$ (Anterior *vs.* Posterior or PP *vs.* VTPP). Scale bars; 25 μm. (B) Effects of Botox treatment on numbers of Dclk1-positive cells. Means±SEM. **; $p<0.01$ (Anterior *vs.* Posterior).

These observations are consistent with previous studies showing that the vagus nerve stimulates progenitor cell proliferation in the brain and liver through the M_3R [278][279], and that activation of muscarinic receptors can lead to an increased Wnt signaling, which is independent of Wnt ligands [280]. Taken together, these results suggest that disruption of neuronal signaling inhibits Wnt signaling and thereby stem and progenitor cell expansion, resulting in the suppression of tumor development in both INS-GAS and MNU mouse models.

Wnt signaling is also involved in tumor regeneration [145]. We have established an INS-GAS mouse model of tumor regeneration through topical application of acetic acid

[260](Paper S4), and found that vagotomy delayed tumor regeneration in the denervated side of the stomach (Paper I; Fig. S12).

We next examined whether vagotomy down-regulated *Lgr5* expression through the muscarinic acetylcholine receptors. Gastric epithelial cells from *Lgr5*-GFP mice were sorted on the basis of GFP expression, then gene expression of the muscarinic acetylcholine receptors was tested in *Lgr5*-negative, *Lgr5*-low, and *Lgr5*-high cell populations (Paper I; Fig. 5A). There was coexpression of *Lgr5* and *Chrm3* (the gene encoding M_3R) in the cells from *Lgr5*-GFP mouse stomach, but the expressions of other subtypes of muscarinic receptor were remarkably low in those cells (Paier I; Fig. 5B, C), suggesting that *Lgr5*-positive stem cell function is possibly modulated by M_3R signaling. To confirm the involvement of M_3R in the gastric tumorigenesis, we treated INS-GAS mice by continuous infusion of darifenacin which is the specific M_3R antagonist [257][258], in combination with chemotherapy. Using an experimental design similar to that of the Botox and vagotomy experiments, we found

that the combination of darifenacin and chemotherapy reduced cellular proliferation of the tumors (Paper I; Fig. 5D). Furthermore, Wnt signaling pathway was analyzed in M_3R knockout *vs.* wild-type mice and it was found that several key genes, including one encoding β-catenin, were downregulated (Paper I; Fig. S13). Next, M_3R knockout mice and wild-type controls were treated with MNU. At 7.5 months after MNU treatment (11 months of age), M_3R knockout mice had fewer tumor incidence (57.1% *vs.* 100%, $p<0.05$) and smaller tumor size when compared to wild-type controls (Paper I; Fig.5E, F). Thus, it is suggested that the vagus nerve regulates gastric tumorigenesis at least in

part through M_3R–mediated Wnt signaling, which is operative in gastric stem and progenitor cells.

Nerves stimulated gastric stem and progenitor cells *in vitro* via muscarinic acetylcholine receptor M3-dependent Wnt signaling

To demonstrate the potential regulatory role of nerves in the growth of the gastric epithelium, we utilized an established *in vitro* culture system for gastric organoids [130]. Primary neurons were isolated from murine spinal cord or the enteric nervous system of guinea pigs, and co-cultured with gastric crypts [130][265][266]. Cultured neurons showed outgrowth of neurites and evidence of direct contact with the gastric organoids (Paper I; Fig. 6A, B). Furthermore, neurons stimulated gastric organoid growth when compared to gastric organoids in the absence of neurons (Paper I; Fig. 6C-E). Interestingly, the addition of either Botox or scopolamine (a muscarinic cholinergic receptor antagonist) inhibited this stimulatory effect (Paper I; Fig. 6D, E), whereas pilocarpine (a muscarinic cholinergic receptor agonist) increased organoid growth (Paper I; Fig. 6F). Importantly, pilocarpine caused upregulation of the stem cell markers and Wnt target genes *Lgr5*, *Cd44*, and *Sox9* [130] in a dose-dependent manner, whereas pilocarpine showed no effects on the expression of these genes in gastric organoids of M_3R knockout mice (Paper I; Fig. 6G), indicating the importance of the M_3R for stem cell growth. Furthermore, neurons substitute for Wnt3a in gastric organoid cultures that are otherwise strictly dependent on addition of Wnt ligands [281] (Paper I; Fig. 6H),

confirming the ability of cholinergic signaling to induce ligand-independent Wnt signaling in this *in vitro* system.

Involvement of Wnt signaling, innervation and vagotomy in gastric cancer patients

In order to further validate our findings in humans, we evaluated three separate cohort studies of gastric cancer patients (Paper I; Table S2). In the group of 17 primary gastric cancer patients, a gene expression profile in gastric cancer tissue was compared to adjacent non-cancerous tissue. Both the Wnt signaling pathway, neurotrophin signaling and axon guidance pathways (along with many other pathways) were significantly activated in the cancer tissue (Paper I; Fig. 7, Fig. S14). In another group of 120 primary gastric cancer patients, neuronal density measured by PGP9.5 expression was correlated with more advanced tumor stages, tumor depth and lymph node metastases (Paper I; Fig. 8A-C). Interestingly, in the third cohort of 37 patients who developed gastric stump cancer after distal gastrectomy with or without selective vagotomy (which is consequently performed during D2 lymphadenectomy procedure), 35% (13 of 37) patients had undergone vagotomy, and in those patients the tumors were located neither in the anterior (0/13) nor in the posterior walls (1/13) ($p<0.05$) where the vagal nerve branches were selectively cut, whereas in patients without vagotomy, the tumors were observed in both anterior and posterior walls (Paper I; Fig. S15).

Part II: Obesity (Papers II and III)

Vagotomy did not affect body weight and both eating behavior and metabolic parameters

Both LAP and PP had no effect on body weight development. VTPP transiently reduced the body weight (about 10% at 1 week postoperatively) but regained the weight within a short time of period (Paper II; Fig. 1a). Similarly, in INS-GAS mice, body weight was not affected by both PP and VTPP (Paper I; Fig. S3). In addition, specific denervation of vagus nerve terminals at gastric corpus by Botox treatment also had no effects on body weight in INS-GAS mice (Fig. 8). There were no differences between LAP and PP in terms of food intake and eating behavior parameters at either 1 or 9 weeks postoperatively. VTPP was without any measurable effects on food intake, eating behavior and metabolic parameters measured at either 1 or 9 weeks postoperatively (Paper II; Fig. 2a, Table 1). There was no mortality in rats underwent LAP, PP, or VTPP.

Sleeve gastrectomy reduced body weight in short-term but not long-term by transiently increased energy expenditure without reduction of food intake

SG reduced the body weight (approximately 10%) in short-term but the effect on body weight loss was abolished at 6 weeks after SG (Paper II; Fig. 1b). SG had no effects on food intake and eating behavior parameters, except for meal duration during the night measured at 2 weeks after surgery (Paper II; Fig. 2b, Table 2). In addition, SG reduced

the water intake during one interval (0.91±0.07 mL/time at 1 week before surgery *vs.* 0.47±0.07 mL/time at 2 weeks and *vs.* 0.45±0.08 mL/time at 11 weeks after surgery, both $p<0.01$). Energy expenditure (kcal/h/100 g body weight) was significantly increased at 2 weeks after SG but not at 11 weeks after surgery, and RER was increased at 11 weeks postoperatively (Paper II; Table 2). One of 7 rats was died after SG.

Duodenal switch caused remarkable and continuous body weight loss associated with increased energy expenditure, reduction of food intake and malabsorption

DS alone or SG followed by DS (SG_1+DS_2) reduced the body weight in a similar manner, i.e., a rapid and continuous weight loss of about 10% at 1 week and 50% at 8 weeks postoperatively (Paper II; Fig. 1b)(Paper III; Fig. 2B). There were no differences between DS and SG_1+DS_2 in terms of food intake and eating behavior parameters (Table 2).

Table 2 | Comparison of eating parameters between DS alone (DS) *vs.* SG followed by DS (SG_1+DS_2) at 2 weeks and 8 weeks after surgery. Means±SEM. ns; not significant.

		2W after surgery		8W after surgery	
	Parameters	**DS**	**SG_1+DS_2**	**DS**	**SG_1+DS_2**
Daytime	Food intake (g/100g body weight)	0.82±0.20	0.93±0.11^{ns}	1.97±0.25	1.22±0.21^{ns}
	Calories intake (kcal/100g body weight)	2.10±0.52	2.39±0.28^{ns}	5.06±0.64	3.14±0.54^{ns}
	Number of meals	18.40±7.97	16.60±0.93^{ns}	32.80±7.81	18.60±4.50^{ns}
	Meal size (g/meal)	0.27±0.06	0.22±0.02^{ns}	0.26±0.12	0.23±0.05^{ns}
	Meal duration (min/meal)	2.57±0.81	2.13±0.29^{ns}	5.14±3.72	2.34±0.45^{ns}
	Intermeal interval (min)	70.34±28.63	39.38±2.04^{ns}	34.22±17.34	50.16±17.90^{ns}
	Rate of eating (g/min)	0.16±0.05	0.11±0.01^{ns}	0.09±0.02	0.10±0.01^{ns}
Nighttime	Food intake (g/100g body weight)	1.14±0.31	1.24±0.19^{ns}	2.20±0.18	2.20±0.26^{ns}
	Calories intake (kcal/100g body weight)	0.80±5.64	3.19±0.50^{ns}	5.64±0.47	5.65±0.68^{ns}
	Number of meals	16.20±5.45	24.40±3.85^{ns}	28.20±5.92	34.20±7.13^{ns}
	Meal size (g/meal)	0.35±0.11	0.21±0.03^{ns}	0.34±0.17	0.24±0.07^{ns}
	Meal duration (min/meal)	5.08±2.49	2.20±0.28^{ns}	5.29±3.17	2.39±0.44^{ns}
	Intermeal interval (min)	51.15±11.34	29.43±5.57^{ns}	32.76±13.75	21.49±4.03^{ns}
	Rate of eating (g/min)	0.11±0.03	0.10±0.01^{ns}	0.08±0.01	0.09±0.01^{ns}

DS regardless of whether it was accompanied by SG reduced the daily food/calories intake by over 50% when measured at 2 as well as 8 weeks postoperatively (Paper II; Fig. 3a, Table 3)(Paper III; Fig. 3A,B, Table 1,2). The reduced food intake was associated with reduced meal size, rate of eating and an increased satiety ratio, but not with the number of meals (Paper II; Fig. 3b-d, Table 3)(Paper III; Fig. Fig. 4A-D, Table 1,2). DS accompanied by SG increased daytime energy expenditure both at 2 and 8 weeks as well as nighttime energy expenditure at 8 weeks postoperatively (Paper III; Fig. 5B, D, Tables 3, 4). RER tended to be reduced during nighttime at 2 weeks after DS (p=0.051) (Paper III; Table.3). The fecal energy density of DS rats both with and without SG was higher than that of control LAP rats at 8 weeks (Paper III; Fig. 6B)(Fig. 13A). It was difficult to collect the fecal samples at 2 weeks after DS due to a severe diarrhea. At 8 weeks after DS, the feces became solid and were collected for the analysis of energy density (Fig. 13B).

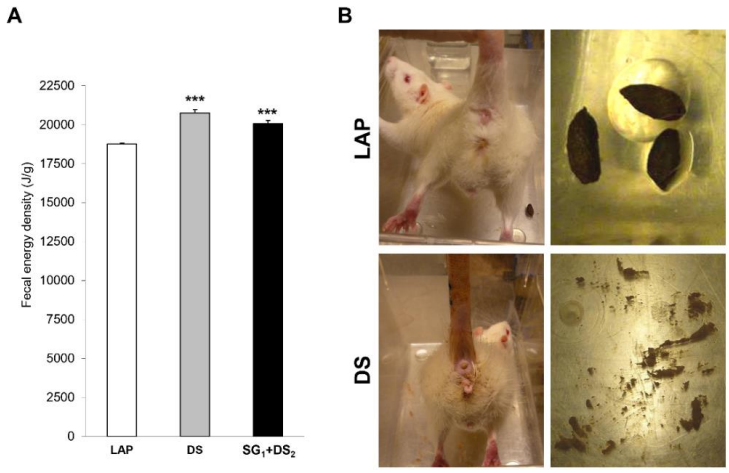

Figure 13 | (A) Fecal energy density of LAP, DS or SG_1+SG_2 at 8 weeks after surgery. Means±SEM. ***; p<0.001 (LAP *vs.* DS or SG_1+SG_2). (B) Photos of solid feces in LAP and of diarrheal feces in DS at 2 weeks after surgery.

Plasma CCK levels were 12.6±3.0 pmol/L in SG_1+DS_2 rats, which was over 10 times higher than the value of the rats subjected to the sham operation in our previous report (plasma CCK levels were 1.1±0.5 pmol/L) [282]. Unfortunately, there was a technical error in the determination of the CCK levels in LAP and DS rats. The plasma levels of the cytokines, including IL-1α, IL-1β, IL-2, IL-4, IL-5, IL-6, IL-10, IL-13, GM-CSF, IFNγ, and TNFα, were not significantly different between LAP *vs.* DS with SG (Paper III; Table S2). The mortality rate was 2 of 7 to DS alone, 1 of 6 to SG_1+DS_2, and 6 of 7 to SG+DS simultaneously. One surviving rat subjected to SG+DS simultaneously showed well-matched eating parameters to the rats subjected to SG_1+DS_2. However, this was not analyzed statistically.

Gastric bypass induced persistent body weight loss caused by increased energy expenditure without altered eating behavior and malabsorption

GB caused approximately 20% weight loss throughout the study period for 14 weeks (Paper III; Fig. 2B). In comparison with LAP, GB increased either total food intake (kcal) or food intake adjusted by body weight (kcal/100g body weight) only in daytime at 3 weeks, and had no effect afterwards (14 weeks postoperatively) (Paper III; Fig. 3A-D). GB was without effects neither on satiety ratio (min/g) nor rate of eating (g/min) both at short-term (3 weeks) and long-term (14 weeks) after surgery (Paper III; Fig. 4A-D, Table 1,2). GB increased nighttime energy expenditure (kcal/hr/100 g body weight) at short-term (3 weeks) and daytime energy expenditure at long-term (14 weeks) postoperatively (Paper III; Fig.5A, B, Table 3, 4). RER was unchanged after GB (Paper

III; Table 3, 4). There was no change in the fecal energy density after GB (Paper III; Fig. 6A). There was no difference in the plasma levels of the cytokines (IL-1α, IL-1β, IL-2, IL-4, IL-5, IL-6, IL-10, IL-13, GM-CSF, IFNγ, and TNFα) between LAP *vs.* GB (Paper III; Table S2). The mortality rate of GB in rats was 6 of 14 due to surgical complications, trauma and learning curve factors.

In comparison with DS, GB had less effect on body weight loss (20% persistent weight loss after GB *vs.* continuous weight loss up to 50% after DS) (Paper III; Fig. 2B). In terms of eating behavior, GB did not reduce food intake with no effects on eating behavior such as satiety ratio or rate of eating (Paper III; Table 1,2). In contrast, DS decreased food intake, rate of eating and increased satiety ratio both at short-term and long-term after surgery (Paper III; Table 1,2). Both GB and DS increased energy expenditure at short-term and long-term (Paper III; Fig. 5A-D). Analysis of the homogeneity of regression assumption showed no significant correlations between the body weight and energy expenditure (kcal/hr) regardless of type of surgery (Paper III; Fig. S1). Consequently, ANCOVA indicated that there was no significant difference in adjusted energy expenditure between LAP *vs.* GB or DS (Paper III; Fig. S2). Analysis of the fecal energy density revealed that DS caused malabsorption but not GB (Paper III; Fig. 6).

Discussion

Part I: Gastric cancer (Paper I)

The present study, using three independent mouse models of gastric cancer, revealed that either surgical or pharmacological denervation suppresses tumorigenesis, and the denervation therapy alone has effective inhibition on both gastric cancer initiation and progression, and it also enhances the anti-tumor effect (i.e. tumor shrinkage) of chemotherapy leading to prolongation of survival in mice with advanced tumors. The effect of denervation therapy is primarily on terminals and intramucosal branches of the vagus nerve, as shown through its response to unilateral vagotomy and localized Botox injection. Gene expression and immunohistochemical analysis of stem and progenitor cell markers, along with the *in vitro* gastric organoid model, strongly suggests that nerves directly modulate epithelial stem and progenitor cells through activation of Wnt signaling via M_3R.

Several previous reports have indicated that M_3R plays a role in gastric proliferation and M_3R is overexpressed in human gastric cancer which is correlated with the cancer stage and with lymph node metastasis [206][283][284]. In the present study, gastric M_3R strongly up-regulated after vagotomy most likely due to the result of a compensatory mechanism, and importantly, both genetic knockout and pharmacological inhibition of M_3R attenuate gastric tumor progression, pointing to the importance of M_3R in vagal pathway for gastric cancer development.

Canonical Wnt signaling controls epithelial homeostasis in the intestine and the stomach, and plays a role in a subset of gastric cancers [130][285]. Gene expression profiling analysis in the present study has revealed that Wnt signaling is upregulated in the tumorigenic stomach and is remarkably down-regulated after vagotomy at all the time points, suggesting that vagus nerve is a critical regulator of Wnt signaling in gastric tumorigenesis. Furthermore, gastric Wnt signaling was down-regulated in M_3R knowckout mice, which were resistant to MNU induced tumorigenesis.

Gene expression profiling has also shown many other differentially expressed signaling pathways. Hedgehog signaling pathway is related to gastric cancer and its stem cells [162][286][287], and was inhibited after vagotomy in the present study. Inflammation-related signaling pathways including VEGF signaling pathway which is also related to angiogenesis [288][289], were inhibited by vagotomy. Interestingly, previous report about transgenic mouse model of gastric cancer showed that double activation of both Wnt and prostaglandin E_2 (PGE_2) pathways successfully developed gastric cancer with 100% of the tumor incidence rate, whereas the mice with single activation of Wnt pathway developed small preneoplasia and the mice with PGE_2 induction developed hyperplasia associated with inflammation [161][290]. This report is well in line with our observation, i.e., both Wnt signaling and inflammation-related signaling pathways were inhibited in vagotomized stomach without gastric tumorigenesis. VEGF signaling pathway is also known as the essential mediator for lymphangiogenesis and the metastasis [288][289][291]. In the present study, the effect of denervation in metastatic lymph nodes or other organs remains unclear due to the limited availability of metastasis in our models, and needs to be further investigated in suitable models. We

previously reported that autophagy is impaired in gastric cancer using rodent models of hypergastrinemia (cotton rats and INS-GAS mice) and gastric tumor samples from human patients [292](Paper S6). Likewise, signaling pathway of autophagy was activated in vagotomized non-cancerous side of stomach, suggesting improved autophagy by denervation may also contribute to the gastric tumor suppression by denervation. MAPK signaling pathway plays an important role in cell proliferation, differentiation and apoptosis as well as cancer development and progression [293][294]. The MAPK signaling is upstream regulator of Wnt signaling not through Wnt ligands [295][296]. In addition, it is reported that MAPK signaling pathway was stimulated by M_3R expressed in human gastric cancer cells [283]. In the present study, MAPK signaling pathway was down-regulated after vagotomy, which was associated with down-regulation of Wnt signaling pathway and compensatory up-regulation of M_3R. Thus, inhibition of MAPK signaling pathway via M_3R by denervation probably involves in the suppression of gastric tumorigenesis and the Wnt signaling. Toll-like receptors (TLRs) play a key role in the innate immune system, especially in inflammatory response against various invading pathogens, by rapidly recognizing pathogen-associated molecular patterns of pathogenic components of bacteria, viruses, fungi and parasites. TLRs are membrane-surface receptors and contain several subtypes including TLR4 which is known to be the receptor for lipopolysaccharide (LPS), a membrane component of Gram-negative bacteria including *Helicobacter pylori* [297]. TLRs also has a critical role in the regulation of tissue injury and healing process as well as neurogenesis [298][299][300][301]. TLRs are widely expressed in cells within the body, including not only immune-related cells [302] but also gastric epithelial and

enterochromaffin-like (ECL) cells [303][304], and both peripheral nerve and nodose ganglion of vagus nerve [305][306][307][308][309]. In addition, TLRs expressed in gastric cancer cells contribute to the tumor development and progression through promoting inflammation, cell proliferation, cell invasion and metastasis [303][310][311][312]. Furthermore, Wng signaling is triggered by TLRs expressed in CSCs and stimulates its cells [313][314]. Thus, these facts have indicated the importance of correlation between TLRs and vagus nerve in gastric cancer. In fact, the present study demonstrated Toll-like receptor signaling pathway was down-regulated at all the time points after vagotomy, and tumor regeneration was attenuated by vagotomy.

There are some studies suggesting that nerves contribute to the normal stem cell niche [193][194][315][316], and there is a report showing that the correlation of sympathetic nerves to prostate cancer progression [196]. However, the stomach differs from other solid organs in that its autonomic innervation is largely parasympathetic, and cholinergic nerves have been shown to regulate gastrointestinal proliferation [317]. The present study demonstrated that *Lgr5*-positive gastric stem cells express the M_3R, and that Wnt signaling in those cells is activated by cholinergic stimulation via direct physical contact of nerve, resulting in epithelial proliferation and stem cell expansion. Gastrointestinal stem cells are supported by a number of niche cells including paneth cells, mesenchymal stem cells, myofibroblasts, smooth muscle cells, lymph and vascular endothelial cells, and bone marrow–derived stromal cells [318][319][320]. Here, we identified nerves regulating gastric stem cell expansion during the tumorigenesis, and showed the strong evidence that vagus nerve “i.e., parasympathetic nerve” is the regulator of gastric CSCs and the niche during the tumorigenesis.

In contrast to our current results, previous vagotomy studies in dog and rat models of chemically induced gastric cancer show promoting effect [321][322][323]. In the study using dog with chemical gastric carcinogen, namely N-methyl-N'-nitro-N-nitrosoguanidine (MNNG) [321], vagotomy was performed before initiating MNNG treatment. N-nitrosamines such as MNNG or MNU are easily decomposed by strong acid, thus MNNG concentration becomes higher in stomach of vagotomized group because vagotomy attenuates gastric acid output and, in consequence, inhibit the decomposition of MNNG. In addition to this mechanism, physical contact of MNNG to gastric mucosa is promoted due to the decreased thickness of mucosa by vagotomy. Thus, it can be said that the study above used wrong experimental design. In the studies using rat model with MNNG treatment [322][323], bilateral vagotomy was performed without pyloroplasty, which delayed gastric emptying and therefore increased the exposure time of orally administered chemical carcinogens on the gastric mucosa and decreased the physical performance of the vagotomized rats [324]. Further, it is reported that uncompleted vagotomy causes recovery of vagal innervation and its function [325][326][327][328], moreover, it has been reported that the regeneration of vagus nerve after uncompleted truncal vagotomy causes hyperinnervation in stomach [329]. Those reports in rat models with MNNG, failed to reduce mucosal thickness, questioning sufficient vagotomy, therefore, it is likely that increased vagal nerve density rather than denervation promoted gastric cancer in those reports. In our study, truncal vagus nerve was dissected as much as possible and then entire dissected area was carefully checked under microscope to ensure the completeness of vagotomy (Paper I; Fig. S2), consequently decreased thickens of mucosa was observed after vagotomy

(Paper I; Fig. S4), indicating successful vagotomy. We performed bilateral vagotomy always together with PP or PP alone as control after completion of the MNU treatment to ensure that dose and time of MNU exposure were equalized in all the groups and to prevent retention of gastric contents and to prevent enhancing gastric tumorigenesis by surgical trauma, allowing analysis of the specific effects of the vagus nerve on the gastric tumorigenesis.

The present study was conducted with the view of translational research and has important clinical implications. First, darifenacin was used for this study because this is the most specific anti-muscarinic agent to M_3R and already in clinical use for overactive urinary bladder [330]. Darifenacin has been shown to inhibit growth of small cell lung cancer xenografts [205], thus darifenacin therapy with/without chemotherapy could be considered in future clinical trials for gastric cancer treatment. Second, denervation by Botox instead of vagotomy has a relevance for basic medical science to test if the effects of denervation on gastric tumorigenesis is primarily local (vagus nerve terminals), and also has a clinical relevance. Botox is already in a market, and the safety of Botox is generally well accepted due to its use for several decades both clinically and for cosmetic purposes [331][332][333]. Endoscopic Botox injection to stomach in human has already been established for the treatment of gastroparesis and morbid obesity [334][335][336]. Whereas the vagotomy is an invasive procedure, the direct injection of Botox into gastric cancer through endoscope is minimum invasive and super localized, thus Botox therapy is probably usable for inoperable advanced gastric cancer patients, and can avoid systematic side effects, drug interactions, drug resistance, unsuccessful drug delivery and complicated dosage calculation which are the common

issues in chemotherapy, suggesting the possible rapid application of Botox therapy to gastric cancer patients in the future. It has been reported that removing primary cancer by gastric resection in advanced gastric cancer patients with metastases improves patient prognosis [337][338][339][340], so that Botox therapy against primary gastric cancer without high risk surgical intervention has a clinical significance for those patients. Third, 5-FU plus platinum (e.g., oxaliplatin and cisplatin) regimen is a current global standard treatment for advanced cancer [50][95], so that this chemotherapy regimen was used for the present study. We found that denervation by either vagotomy or Botox enhances the therapeutic effect of chemotherapy. According to the CSC model, simultaneous attacking both cancer cells and CSCs are considered to be essential to eradicate a cancer [144][146], suggesting that the combination of chemotherapy targeting gastric cancer cells and Botox therapy targeting gastric CSCs is conceivable as effective treatment for inoperable cancer patients. Fourth, analysis of human patients with gastric cancer was included to the present study and showed good correlations between neural pathways and Wnt signaling and increased innervation in more advanced tumors, with decreased cancer risk in surgically denervated portions of the stomach, and also showed up-regulated signaling pathways of Hedgehog, VEGF, MAPK and Toll-like receptor associated with axon guidance and neurotrophin in human gastric cancer tissue via gene expression profiling. These results in human patients are well in line with our findings obtained from animal experiments, consequently indicating high potential of rapid application of the present study to human patients. In fact, based on the findings of this study, a phase II clinical trial of endoscopic Botox injection to gastric cancer patients has been initiated at St. Olaves Hospital, Norway

(NCT number; NCT01822210, EudraCT number; 2012-002493-31). Finally, this study was conducted based on multidisciplinary platform to facilitate translational cancer research, namely international collaboration and contribution of both clinicians (medical doctors, pharmacist and nurse) and basic scientists (molecular biologists, bioinformaticians, pharmacologists, pathologists and neurologists).

Part II: Obesity (Papers II and III)

Regarding the translational research of bariatric surgeries, it is important to use the right animal models in the right experimental settings in order to elucidate the underlying mechanisms. In this thesis, surgical procedures were performed by taking into the consideration of the difference in anatomy and physiology between humans and rats. VTPP procedure performed in this thesis was as same as the procedure in human because vagal innervation and the function are basically same between humans and rodents [199][200][341]. SG in rats was performed by resecting about 90% of the thin-walled non-glandular rumen in addition to 70% of the glandular stomach (Fig. 9). The rumen does not exist in human, and was removed from rats as much as possible to prevent failed SG due to rumen dilatation [342]. DS was achieved by bypassing jejunum, which is approximately 90% of small intestine in rats, whereas the jejunum is about 40% of total small intestine in human (Paper III; Fig. 1). GB was performed without the Roux-en-Y reconstruction because this surgical method was originally created in order to prevent post-gastrectomy bile vomiting in patients but rats are non-emetic and has no gallbladder [343][344] (Paper III; Fig. 1).

Vagus nerve acts as the sensor for stomach tension and transmits the satiety signal to brain and controls energy homeostasis through gut-brain axis [345], Based on the understanding that vagus nerve controls satiety/hunger, VBLOC therapy was developed by using a small implanted device blocking the vagus nerve, and the initial clinical trial showed decreasing satiation, hunger and body weight in obese patients [218]. In contrast to these results from VBLOC therapy, the present study (Paper II) demonstrated that disruption of the gut-brain axis by VTPP in rats caused slight (about 10%) and transient (1 week postoperatively) body weight loss without any measurable effect on the eating behavior and energy homeostasis. Body weight loss was not observed in INS-GAS mice underwent either VTPP or Botox injection (selective denervation on gastric corpus) (Paper I). It should be noticed that eating behavior of rodents is nibbling (eating much more frequently compared with humans) and this nibbling behavior would not increase the stomach tension enough to stimulate the satiety signaling via vagus nerve. Importantly, we reported that vagus nerve stimulation in rats reduced body weight and food intake, and increased satiety by activating vagal signaling to the brainstem and hippocampus [346] (Paper S9). Therefore, it is suggested that vagal afferent signaling activation rather than blocking is essential to induce satiety and body weight loss.

Although SG is increasingly performed due to its safety and efficiency in obese patients [347], we found that SG reduced the body weight by about 10% in the short-term (1-6 weeks) but not in the long-term (after 7 weeks) (Paper II). The reduction was not associated with reduced food intake but with increased energy expenditure, which is in line with previous observations in rats subjected to total gastrectomy [238], indicating

that to make stomach size smaller is not essential to reduce food intake. Importantly, the recent meta-analysis and systematic review for SG has pointed the regain of body weight after SG in obese patients and the rate of regain was from 5.7% at 2 years to 75.6% at 6 years after SG [348][349], which is similar to our results. On the other hand, clinical data have shown the improvement of type 2 diabetes mellitus in about 80% of patients underwent SG [350][351]. We also reported that GB increases glucagon-like peptide-1 (GLP-1) levels in α-cells pancreatic islets [352] (Paper S5). Increased RER at long-term after GB in rats is probably because higher GLP-1 secretion induces higher insulin levels leading to increased cell uptake of glucose, resulting in increased utilization of carbohydrates as fuel. It should also be mentioned that SG rats, like rats with total gastrectomy, seemed to drink frequently postoperatively, probably owing to lower ghrelin and obestatin levels [238].

DS alone and SG+DS exhibited well-matched postoperative effects on body weight, metabolic parameters and eating behavior, leading to a long-lasting and remarkable body weight loss (Papers II, III). DS regardless of whether it was accompanied by SG dramatically reduced food intake probably due to increased plasma levels of CCK (hyperCCKemia), which is a gastric peptide hormone suppressing apatite and synthesized predominantly in endocrine I cells of the duodenum and upper jejunum [353]. In fact, hypertrophic effect of DS was observed in the duodenum (Fig. 14).

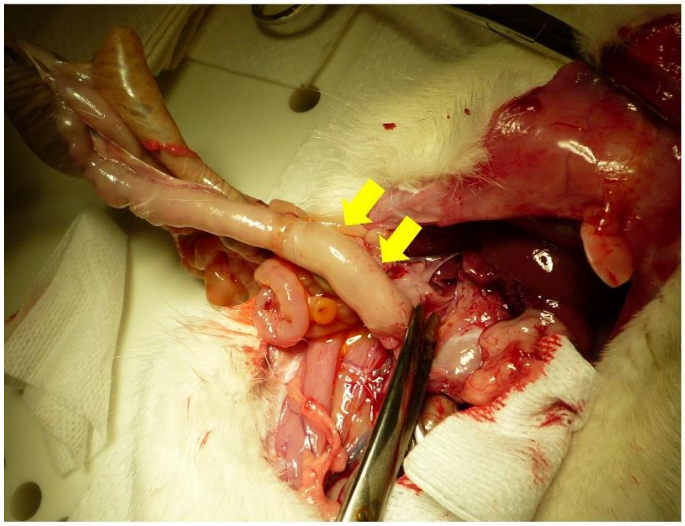

Figure 14 | Photo showing the hypertrophy of duodenum by DS (yellow arrows).

In addition to CCK which has a trophic effect on pancreas [354], GLP-1 levels in the circulation have been reported to be elevated in rats subjected to pancreaticobiliary diversion, which could be contributed to food intake reduction as well, and have a beneficial effect on ß cells in the pancreas [355][356], as the meta-analysis has reported DS demonstrates 98.9% of diabetes resolution in patients [357]. The rate of eating also has impacts on body weight. It has been reported that there is a correlation between rate of eating and BMI [358][359][360]. Previously, our group has shown that high-fat-diet-induced obesity was associated with increased rate of eating, increased size of meals, but not with daily calories intake [361]. In the present studies (Papers II, III), DS decreased the eating rate during both day- and night-time. Malabsorption is believed to be due to long-limb intestinal bypass after DS. In spite of highly invasive surgical

procedure, the ambulatory activity had no difference between before and after DS, suggesting that DS rats recovered well from surgery. Even though the principle of DS with SG for patients has been considered as simultaneous effects; malabsorption by DS and less food intake by SG, SG alone failed to reduce food intake as described previously, whereas DS alone induced great reduction of food intake due to hyperCCKemia and malabsorption due to intestinal bypass. Therefore, these results strongly support our hypothesis that the DS procedure *per se* could be considered as an independent weight loss surgery. Moreover, we also reported that SG+DS, in comparison with DS alone, showed higher plasma levels of the inflammatory cytokines and poorer regulation of lipid metabolism, e.g., SG+DS rats had a reduced fecal output of triacylglycerol and an increased accumulation of triacylglycerol in live that might lead to liver damage over time [362] (Paper S7). Taking these observations and the high surgical risks of SG+DS procedure into account, DS *per se* rather than the combination of DS and SG could be better procedure for obesity treatment.

In the present study (Paper III), GB reduced the body weight without causing early satiety, reducing food intake or inducing malabsorption. Our previous study showed that body weight gain was associated with decreased energy expenditure along with aging in normal rats [363], thus we suggest that the mechanism underlying GB-induced body weight loss is unlikely through the effects on food intake and/or absorption, but is due to increasing energy expenditure. Both GB and SG+DS has same concept as a bariatric surgery, namely to cause restrictive food intake by reducing stomach size and malabsorption by intestinal bypass, however GB or SG+DS showed different effects on body weight, eating behavior and metabolic parameters respectively. SG+DS resulted in

greater weight loss than GB, that are in accordance with many reports from clinical series in patients [226][227][228][229][230][231][232]. GB did not alter eating behavior including food intake, whereas DS with/without SG induced dramatic changes in eating behavior. In addition to the pervious findings from SG alone, these results strongly suggest that the control of food intake and meal size is independent on the food reservoir function of the stomach. Behavior of rats is mostly driven on instincts, while behavior of human is much more complicated, e.g., most patients underwent bariatric surgery change their eating habits by following the "postoperative instruction" given by clinicians to achieve the best possible conditions for weight reduction and to avoid post-surgical side-effects like gastro-esophageal reflux and dumping syndrome which unlikely occur in rats[364]. Resting energy expenditure has been suggested to be a therapeutic target for obesity [365][366]. In this study (Paper III), we showed that the increased energy expenditure took place only during nighttime (relevant to active energy expenditure) shortly after GB and switched to daytime (relevant to resting energy expenditure) at long-term after GB, whereas the daytime energy expenditure (resting energy expenditure) was increased both at short-term and long-term after DS and nighttime energy expenditure (active energy expenditure) was additionally increased at long-term after DS. We also observed that DS, but not GB, caused diarrhea shortly after surgery (2 weeks) and malabsorption (measured at 2 months postoperatively) in rats, which is in line with observations in patients [214].

In general, research in obese patients has direct impacts on clinical practice. However, there are discrepancies in the clinical obesity studies due to the heterogeneity of patient populations and the technical limitation of measurements of eating behavior and energy

expenditure, e.g., simply using questionnaires to examine eating behavior or portable metabolic carts under artificial rather than “free-living” conditions [367][368], whereas studies in animals provide much greater latitude in control and experimental manipulation of the system. Thus, research using animal models is an excellent way of developing and learning bariatric surgical techniques as well as understanding the postsurgical physiology and the underlying mechanisms, and it ultimately enables to translate the findings from animals into humans [369][370]. Taken the data from the previous and the present studies (Papers II, III) together, the appropriately designed rat models provide significant insights into the mechanisms of bariatric surgery which explain well the clinical observations.

Personalized medicine for the treatment of gastric cancer and obesity (Papers I-III)

We demonstrated that Wnt signaling pathway is the key factor to inhibit gastric tumorigenesis by denervation (Paper I). The Wnt signaling is up-regulated in the most gastric cancer patients [162], yet gastric cancer is highly heterogeneous between patients from morphological and molecular standpoints so that not all the patients overexpress Wnt signaling [70][71][72][73][74]. Therefore, personalized denervation therapy is conceivable to be more effective for the gastric cancer patients associated with up-regulated Wnt signaling. As a future aspect, to consider the heterogeneity of CSC niche would enable more specific personalized denervation therapy. CSC niche is complexed and consists of various components, however it is unlikely that every niche

necessarily includes all of the components [105][119]. In fact, we previously reported the cancer CSC niche forming microvillus mesh through desmosomes, which is independent of innervation [110] (Paper S2). Hypoxia is closely related to CSC niche, and CSCs are predominantly localized in hypoxic regions within tumors and the increase in CSCs in response to hypoxia is medicated via the activation of Wnt signaling pathway [106][143][371][372]. Recently, real-time imaging of hypoxia or nerves including vagus nerve under endoscopy has been developed [373][374][375]. Thus, combination of hypoxia imaging (to identify the location of CSC niche) and nerve imaging (to identify the innervation in gastric tumor) would be able to detect the nerve-dependent CSC niche, leading to more personalized Botox therapy by identification of more specific and appropriate injection points.

Obesity is one of the risk factors for gastric cancer [81] and bariatric surgery is only treatment showing the long-term efficacy on weight loss which also reduces the risk of cancer in obese patients [214][215]. Thus, bariatric surgery can be considered as one of the preventive methods for cancer in obese patients. Obesity is multifactorial disease [240] and we demonstrated that each bariatric surgery has different mechanism of weight loss (Papers II, III), strongly suggesting selection of right bariatric surgical procedure should be personalized.

Conclusions

Part I: Translational research in gastric cancer (revealed in Paper I);

- Denervation suppresses gastric cancer initiation as well as progression through inhibition of the CSC niche by down-regulation of Wnt signaling pathway via M_3R (Fig. 15).

- Denervation therapy by endoscopic Botox injection has a strong clinical significance to treat gastric cancer patients.

- Denervation therapy should be personalized depending on Wnt signaling expression on each gastric cancer patient.

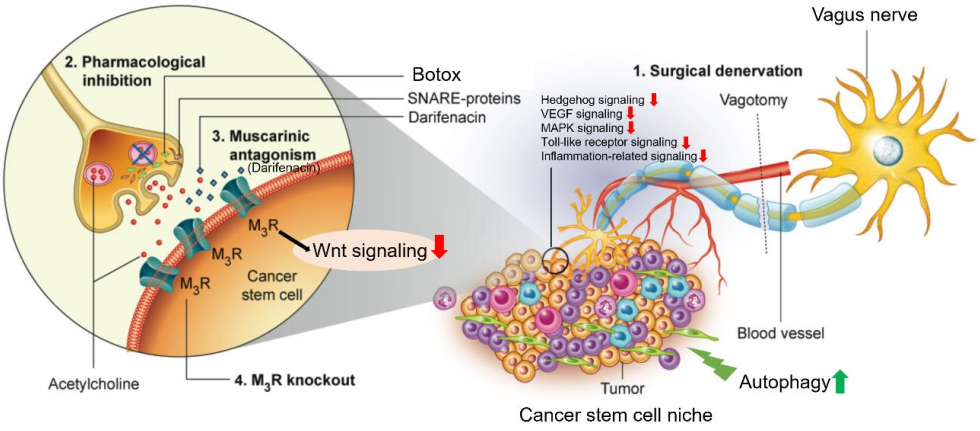

Figure 15 | Illustration showing the mechanism of denervation on suppressing gastric tumorigenesis. (*modified from Rabben et al. Curr Neuropharmacol. 2016* [236])

Part II: Translational research in obesity (revealed in Papers II, III);

- Weight loss after each bariatric surgical procedure (VTPP, SG, DS and GB) differs in terms of degree, duration and the underlying mechanisms, indicating the need of personalized bariatric surgery.

- DS procedure *per se* (without SG) could be an independent weight loss surgery with lower risk of surgical complications.

- DS with SG procedure is superior to GB in body weight loss through different mechanisms.

- Control of food intake is independent on the stomach size.

Errata

Paper II

"Serum CCK level" should be replaced to "Plasma CCK level"

Paper III

Page 5, section "Energy Expenditure", column 2: "Fig. 5A, C" should be "Fig. 5A, B"

Page 5, section "Energy Expenditure", column 5: "Fig. 5B, D" should be "Fig. 5C, D"

References

[1]. Butler D. Translational research: crossing the valley of death. Nature. 2008 Jun 12;453(7197):840-2. doi: 10.1038/453840a.

[2]. Contopoulos-Ioannidis DG, Alexiou GA, Gouvias TC, Ioannidis JP. Medicine. Life cycle of translational research for medical interventions. Science. 2008 Sep 5;321(5894):1298-9. doi: 10.1126/science.1160622.

[3]. Chandra S, Muir C, Silva M, Carr S. Imaging biomarkers in drug development: an overview of opportunities and open issues. J Proteome Res. 2005 Jul-Aug;4(4):1134-7.

[4]. Kelloff GJ, Sigman CC. New science-based endpoints to accelerate oncology drug development. Eur J Cancer. 2005 Mar;41(4):491-501. Epub 2005 Jan 22.

[5]. Rubio DM, Schoenbaum EE, Lee LS, Schteingart DE, Marantz PR, Anderson KE, Platt LD, Baez A, Esposito K. Defining translational research: implications for training. Acad Med. 2010 Mar;85(3):470-5. doi: 10.1097/ACM.0b013e3181ccd618.

[6]. Fort DG, Herr TM, Shaw PL, Gutzman KE, Starren JB. Mapping the evolving definitions of translational research. J Clin Transl Sci. 2017 Feb;1(1):60-66. doi: 10.1017/cts.2016.10. Epub 2017 Feb 2.

[7]. Mulshine JL, Jett M, Cuttitta F, Treston AM, Quinn K, Scott F, Iwai N, Avis I, Linnoila RI, Shaw GL. Scientific basis for cancer prevention. Intermediate cancer markers. Cancer. 1993 Aug 1;72(3 Suppl):978-83.

[8]. Zerhouni E. Medicine. The NIH Roadmap. Science. 2003 Oct 3;302(5642):63-72.

[9]. Schwartz J, Macomber C. So, You Think You Have an Idea: A Practical Risk Reduction-Conceptual Model for Academic Translational Research. Bioengineering (Basel). 2017 Apr 4;4(2). pii: E29. doi: 10.3390/bioengineering4020029.

[10]. Callard F, Rose D, Wykes T. Close to the bench as well as at the bedside: involving service users in all phases of translational research. Health Expect. 2012 Dec;15(4):389-400. doi: 10.1111/j.1369-7625.2011.00681.x. Epub 2011 May 25.

[11]. van der Laan AL, Boenink M. Beyond bench and bedside: disentangling the concept of translational research. Health Care Anal. 2015 Mar;23(1):32-49. doi: 10.1007/s10728-012-0236-x.

[12]. Waldman SA, Terzic A. Clinical and translational science: from bench-bedside to global village. Clin Transl Sci. 2010 Oct;3(5):254-7. doi: 10.1111/j.1752-8062.2010.00227.x.

[13]. Blumberg RS, Dittel B, Hafler D, von Herrath M, Nestle FO. Unraveling the autoimmune translational research process layer by layer. Nat Med. 2012 Jan 6;18(1):35-41. doi: 10.1038/nm.2632.

[14]. Mensah GA, Czajkowski SM. Translational science matters: forging partnerships between biomedical and behavioral science to advance the public's health. Transl Behav Med. 2018 Sep 8;8(5):808-814. doi: 10.1093/tbm/ibx023.

[15]. Tugwell P, Knottnerus JA. The new paradigm: from 'bench to bedside' to the translational research 'valleys of death'. J Clin Epidemiol. 2015 Jul;68(7):725-6. doi: 10.1016/j.jclinepi.2015.05.010. Epub 2015 May 14.

[16]. Hostiuc S, Moldoveanu A, Dascălu MI, Unnthorsson R, Jóhannesson ÓI, Marcus I. Translational research-the need of a new bioethics approach. J Transl Med. 2016 Jan 15;14:16. doi: 10.1186/s12967-016-0773-4.

[17]. Munoz DA, Nembhard HB, Kraschnewski JL. Quantifying complexity in translational research: an integrated approach. Int J Health Care Qual Assur. 2014;27(8):760-76.

[18]. Long JC, Cunningham FC, Braithwaite J. Network structure and the role of key players in a translational cancer research network: a study protocol. BMJ Open. 2012 Jun 25;2(3). pii: e001434. doi: 10.1136/bmjopen-2012-001434. Print 2012.

[19]. Hassmiller Lich K, Frerichs L, Fishbein D, Bobashev G, Pentz MA. Translating research into prevention of high-risk behaviors in the presence of complex systems: definitions and systems frameworks. Transl Behav Med. 2016 Mar;6(1):17-31. doi: 10.1007/s13142-016-0390-z.

[20]. Abrahams E. Right drug-right patient-right time: personalized medicine coalition. Clin Transl Sci. 2008 May;1(1):11-2. doi: 10.1111/j.1752-8062.2008.00003.x.

[21]. Cascorbi I. The promises of personalized medicine. Eur J Clin Pharmacol. 2010 Aug;66(8):749-54. doi: 10.1007/s00228-010-0858-6. Epub 2010 Jun 19.

[22]. Salari K, Watkins H, Ashley EA. Personalized medicine: hope or hype? Eur Heart J. 2012 Jul;33(13):1564-70. doi: 10.1093/eurheartj/ehs112. Epub 2012 Jun 1.

[23]. Schleidgen S, Klingler C, Bertram T, Rogowski WH, Marckmann G. What is personalized medicine: sharpening a vague term based on a systematic literature review. BMC Med Ethics. 2013 Dec 21;14:55. doi: 10.1186/1472-6939-14-55.

[24]. Lesko LJ. Personalized medicine: elusive dream or imminent reality? Clin Pharmacol Ther. 2007 Jun;81(6):807-16.

[25]. Hong KW, Oh B. Overview of personalized medicine in the disease genomic era. BMB Rep. 2010 Oct;43(10):643-8. doi: 10.5483/BMBRep.2010.43.10.643.

[26]. Spear BB, Heath-Chiozzi M, Huff J. Clinical application of pharmacogenetics. Trends Mol Med. 2001 May;7(5):201-4.

[27]. Cho SH, Jeon J, Kim SI. Personalized medicine in breast cancer: a systematic review. J Breast Cancer. 2012 Sep;15(3):265-72. doi: 10.4048/jbc.2012.15.3.265. Epub 2012 Sep 28.

[28]. Rosenblum D, Peer D. Omics-based nanomedicine: the future of personalized oncology. Cancer Lett. 2014 Sep 28;352(1):126-36. doi: 10.1016/j.canlet.2013.07.029. Epub 2013 Aug 11.

[29]. Evans WE, Relling MV. Moving towards individualized medicine with pharmacogenomics. Nature. 2004 May 27;429(6990):464-8.

[30]. Nebert DW, Vesell ES. Advances in pharmacogenomics and individualized drug therapy: exciting challenges that lie ahead. Eur J Pharmacol. 2004 Oct 1;500(1-3):267-80.

[31]. Ginsburg GS, Willard HF. Genomic and personalized medicine: foundations and applications. Transl Res. 2009 Dec;154(6):277-87. doi: 10.1016/j.trsl.2009.09.005. Epub 2009 Oct 1.

[32]. Ritchie MD. The success of pharmacogenomics in moving genetic association studies from bench to bedside: study design and implementation of precision medicine in the post-GWAS era. Hum Genet. 2012 Oct;131(10):1615-26. doi: 10.1007/s00439-012-1221-z. Epub 2012 Aug 25.

[33]. Weinshilboum RM, Wang L. Pharmacogenomics: Precision Medicine and Drug Response. Mayo Clin Proc. 2017 Nov;92(11):1711-1722. doi: 10.1016/j.mayocp.2017.09.001. Epub 2017 Nov 1.

[34]. Katsnelson A. Momentum grows to make 'personalized' medicine more 'precise'. Nat Med. 2013 Mar;19(3):249. doi: 10.1038/nm0313-249.

[35]. Collins FS, Varmus H. A new initiative on precision medicine. N Engl J Med. 2015 Feb 26;372(9):793-5. doi: 10.1056/NEJMp1500523. Epub 2015 Jan 30.

[36]. Jameson JL, Longo DL. Precision medicine--personalized, problematic, and promising. N Engl J Med. 2015 Jun 4;372(23):2229-34. doi: 10.1056/NEJMsb1503104. Epub 2015 May 27.

[37]. Ginsburg GS, Phillips KA. Precision Medicine: From Science To Value. Health Aff (Millwood). 2018 May;37(5):694-701. doi: 10.1377/hlthaff.2017.1624.

[38]. Rosen A, Zeger SL. Precision medicine: discovering clinically relevant and mechanistically anchored disease subgroups at scale. J Clin Invest. 2019 Mar 1;129(3):944-945. doi: 10.1172/JCI126120. Epub 2019 Jan 28.

[39]. Lee KM, Wason J. Design of experiments for a confirmatory trial of precision medicine. J Stat Plan Inference. 2019 Mar;199:179-187. doi: 10.1016/j.jspi.2018.06.004.

[40]. Maier M. Personalized medicine-a tradition in general practice! Eur J Gen Pract. 2019 Apr;25(2):63-64. doi: 10.1080/13814788.2019.1589806.

[41]. Jaccard E, Cornuz J, Waeber G, Guessous I. Evidence-Based Precision Medicine is Needed to Move Toward General Internal Precision Medicine. J Gen Intern Med. 2018 Jan;33(1):11-12. doi: 10.1007/s11606-017-4149-0.

[42]. Relling MV, Gardner EE, Sandborn WJ, Schmiegelow K, Pui CH, Yee SW, Stein CM, Carrillo M, Evans WE, Klein TE; Clinical Pharmacogenetics Implementation Consortium. Clinical Pharmacogenetics

Implementation Consortium guidelines for thiopurine methyltransferase genotype and thiopurine dosing. Clin Pharmacol Ther. 2011 Mar;89(3):387-91. doi: 10.1038/clpt.2010.320. Epub 2011 Jan 26.

[43]. Lennard L. The clinical pharmacology of 6-mercaptopurine. Eur J Clin Pharmacol. 1992;43(4):329-39.

[44]. Weinshilboum RM, Sladek SL. Mercaptopurine pharmacogenetics: monogenic inheritance of erythrocyte thiopurine methyltransferase activity. Am J Hum Genet. 1980 Sep;32(5):651-62.

[45]. Lennard L, Gibson BE, Nicole T, Lilleyman JS. Congenital thiopurine methyltransferase deficiency and 6-mercaptopurine toxicity during treatment for acute lymphoblastic leukaemia. Arch Dis Child. 1993 Nov;69(5):577-9.

[46]. Daly AK. Individualized drug therapy. Curr Opin Drug Discov Devel. 2007 Jan;10(1):29-36.

[47]. Relling MV, Schwab M, Whirl-Carrillo M, Suarez-Kurtz G, Pui CH, Stein CM, Moyer AM, Evans WE, Klein TE, Antillon-Klussmann FG, Caudle KE, Kato M, Yeoh AEJ, Schmiegelow K, Yang JJ. Clinical Pharmacogenetics Implementation Consortium Guideline for Thiopurine Dosing Based on TPMT and NUDT15 Genotypes: 2018 Update. Clin Pharmacol Ther. 2019 May;105(5):1095-1105. doi: 10.1002/cpt.1304. Epub 2019 Jan 20.

[48]. Peddi PF, Hurvitz SA. Trastuzumab emtansine: the first targeted chemotherapy for treatment of breast cancer. Future Oncol. 2013 Mar;9(3):319-26. doi: 10.2217/fon.13.7.

[49]. Hicks DG, Kulkarni S. HER2+ breast cancer: review of biologic relevance and optimal use of diagnostic tools. Am J Clin Pathol. 2008 Feb;129(2):263-73. doi: 10.1309/99AE032R9FM8WND1.

[50]. Wagner AD, Syn NL, Moehler M, Grothe W, Yong WP, Tai BC, Ho J, Unverzagt S. Chemotherapy for advanced gastric cancer. Cochrane Database Syst Rev. 2017 Aug 29;8:CD004064. doi: 10.1002/14651858.CD004064.pub4.

[51]. Recio-Boiles A, Waheed A, Babiker HM. Cancer, Gastric. StatPearls [Internet]. Treasure Island (FL): StatPearls Publishing; 2020-.2019 Aug 4.

[52]. Arteaga CL, Sliwkowski MX, Osborne CK, Perez EA, Puglisi F, Gianni L. Treatment of HER2-positive breast cancer: current status and future perspectives. Nat Rev Clin Oncol. 2011 Nov 29;9(1):16-32. doi: 10.1038/nrclinonc.2011.177.

[53]. Gravalos C, Jimeno A. HER2 in gastric cancer: a new prognostic factor and a novel therapeutic target. Ann Oncol. 2008 Sep;19(9):1523-9. doi: 10.1093/annonc/mdn169. Epub 2008 Apr 25.

[54]. Jørgensen JT. Targeted HER2 treatment in advanced gastric cancer. Oncology. 2010;78(1):26-33. doi: 10.1159/000288295. Epub 2010 Feb 25.

[55]. Abrahao-Machado LF, Scapulatempo-Neto C. HER2 testing in gastric cancer: An update. World J Gastroenterol. 2016 May 21;22(19):4619-25. doi: 10.3748/wjg.v22.i19.4619.

[56]. Wang J, Xu B. Targeted therapeutic options and future perspectives for HER2-positive breast cancer. Signal Transduct Target Ther. 2019 Sep 13;4:34. doi: 10.1038/s41392-019-0069-2. eCollection 2019.

[57]. van't Veer LJ, Bernards R. Enabling personalized cancer medicine through analysis of gene-expression patterns. Nature. 2008 Apr 3;452(7187):564-70. doi: 10.1038/nature06915.

[58]. Ozdemir V, Williams-Jones B, Cooper DM, Someya T, Godard B. Mapping translational research in personalized therapeutics: from molecular markers to health policy. Pharmacogenomics. 2007 Feb;8(2):177-85.

[59]. Louca S. Personalized medicine--a tailored health care system: challenges and opportunities. Croat Med J. 2012 Jun;53(3):211-3.

[60]. Evers AW, Rovers MM, Kremer JA, Veltman JA, Schalken JA, Bloem BR, van Gool AJ. An integrated framework of personalized medicine: from individual genomes to participatory health care. Croat Med J. 2012 Aug;53(4):301-3.

[61]. Crews KR, Hicks JK, Pui CH, Relling MV, Evans WE. Pharmacogenomics and individualized medicine: translating science into practice. Clin Pharmacol Ther. 2012 Oct;92(4):467-75. doi: 10.1038/clpt.2012.120. Epub 2012 Sep 5.

[62]. Bray F, Ferlay J, Soerjomataram I, Siegel RL, Torre LA, Jemal A. Global cancer statistics 2018: GLOBOCAN estimates of incidence and mortality worldwide for 36 cancers in 185 countries. CA Cancer J Clin. 2018 Nov;68(6):394-424. doi: 10.3322/caac.21492. Epub 2018 Sep 12.

[63]. Rawla P, Barsouk A. Epidemiology of gastric cancer: global trends, risk factors and prevention. Prz Gastroenterol. 2019;14(1):26-38. doi: 10.5114/pg.2018.80001. Epub 2018 Nov 28.

[64]. Petryszyn P, Chapelle N, Matysiak-Budnik T. Gastric cancer: Where are we heading? Dig Dis. 2020 Feb 17. doi: 10.1159/000506509. [Epub ahead of print]

[65]. Fock KM. Review article: the epidemiology and prevention of gastric cancer. Aliment Pharmacol Ther. 2014 Aug;40(3):250-60. doi: 10.1111/apt.12814. Epub 2014 Jun 10.

[66]. Karimi P, Islami F, Anandasabapathy S, Freedman ND, Kamangar F. Gastric cancer: descriptive epidemiology, risk factors, screening, and prevention. Cancer Epidemiol Biomarkers Prev. 2014 May;23(5):700-13. doi: 10.1158/1055-9965.EPI-13-1057. Epub 2014 Mar 11.

[67]. Orditura M, Galizia G, Sforza V, Gambardella V, Fabozzi A, Laterza MM, Andreozzi F, Ventriglia J, Savastano B, Mabilia A, Lieto E, Ciardiello F, De Vita F. Treatment of gastric cancer. World J Gastroenterol. 2014 Feb 21;20(7):1635-49. doi: 10.3748/wjg.v20.i7.1635.

[68]. Cassaro M, Rugge M, Gutierrez O, Leandro G, Graham DY, Genta RM. Topographic patterns of intestinal metaplasia and gastric cancer. Am J Gastroenterol. 2000 Jun;95(6):1431-8.

[69]. Shang J, Pena AS. Multidisciplinary approach to understand the pathogenesis of gastric cancer. World J Gastroenterol. 2005 Jul 21;11(27):4131-9.

[70]. Chiurillo MA. Role of the Wnt/β-catenin pathway in gastric cancer: An in-depth literature review. World J Exp Med. 2015 May 20;5(2):84-102. doi: 10.5493/wjem.v5.i2.84. eCollection 2015 May 20.

[71]. Figueiredo C, Costa S, Karameris A, Machado JC. Pathogenesis of Gastric Cancer. Helicobacter. 2015 Sep;20 Suppl 1:30-5. doi: 10.1111/hel.12254.

[72]. Gullo I, Carneiro F, Oliveira C, Almeida GM. Heterogeneity in Gastric Cancer: From Pure Morphology to Molecular Classifications. Pathobiology. 2018;85(1-2):50-63. doi: 10.1159/000473881. Epub 2017 Jun 16.

[73]. Carrasco-Garcia E, García-Puga M, Arevalo S, Matheu A. Towards precision medicine: linking genetic and cellular heterogeneity in gastric cancer. Ther Adv Med Oncol. 2018 Aug 29;10:1758835918794628. doi: 10.1177/1758835918794628. eCollection 2018.

[74]. Ho SWT, Tan P. Dissection of gastric cancer heterogeneity for precision oncology. Cancer Sci. 2019 Nov;110(11):3405-3414. doi: 10.1111/cas.14191. Epub 2019 Sep 25.

[75]. LAUREN P. THE TWO HISTOLOGICAL MAIN TYPES OF GASTRIC CARCINOMA: DIFFUSE AND SO-CALLED INTESTINAL-TYPE CARCINOMA. AN ATTEMPT AT A HISTO-CLINICAL CLASSIFICATION. Acta Pathol Microbiol Scand. 1965;64:31-49.

[76]. Carneiro F, Huntsman DG, Smyrk TC, Owen DA, Seruca R, Pharoah P, Caldas C, Sobrinho-Simões M. Model of the early development of diffuse gastric cancer in E-cadherin mutation carriers and its implications for patient screening. J Pathol. 2004 Jun;203(2):681-7.

[77]. Fox JG, Wang TC. Inflammation, atrophy, and gastric cancer. J Clin Invest. 2007 Jan;117(1):60-9.

[78]. Burkitt MD, Varro A, Pritchard DM. Importance of gastrin in the pathogenesis and treatment of gastric tumors. World J Gastroenterol. 2009 Jan 7;15(1):1-16.

[79]. Cheng XJ, Lin JC, Tu SP. Etiology and Prevention of Gastric Cancer. Gastrointest Tumors. 2016 Sep;3(1):25-36. Epub 2016 Feb 12.

[80]. Poorolajal J, Moradi L, Mohammadi Y, Cheraghi Z, Gohari-Ensaf F. Risk factors for stomach cancer: a systematic review and meta-analysis. Epidemiol Health. 2020;42:e2020004. doi: 10.4178/epih.e2020004. Epub 2020 Feb 2.

[81]. Yang P, Zhou Y, Chen B, Wan HW, Jia GQ, Bai HL, Wu XT. Overweight, obesity and gastric cancer risk: results from a meta-analysis of cohort studies. Eur J Cancer. 2009 Nov;45(16):2867-73. doi: 10.1016/j.ejca.2009.04.019. Epub 2009 May 6.

[82]. Lauwers GY. Defining the pathologic diagnosis of metaplasia, atrophy, dysplasia, and gastric adenocarcinoma. J Clin Gastroenterol. 2003 May-Jun;36(5 Suppl):S37-43; discussion S61-2.

[83]. Cardaropoli S, Rolfo A, Todros T. Helicobacter pylori and pregnancy-related disorders. World J Gastroenterol. 2014 Jan 21;20(3):654-64. doi: 10.3748/wjg.v20.i3.654.

[84]. Chen D, Stenström B, Zhao CM, Wadström T. Does Helicobacter pylori infection per se cause gastric cancer or duodenal ulcer? Inadequate evidence in Mongolian gerbils and inbred mice. FEMS Immunol Med Microbiol. 2007 Jul;50(2):184-9.

[85]. Roesler BM, Costa SC, Zeitune JM. Eradication Treatment of Helicobacter pylori Infection: Its Importance and Possible Relationship in Preventing the Development of Gastric Cancer. ISRN Gastroenterol. 2012;2012:935410. doi: 10.5402/2012/935410. Epub 2012 Jun 13.

[86]. Tan Z. Recent Advances in the Surgical Treatment of Advanced Gastric Cancer: A Review. Med Sci Monit. 2019 May 13;25:3537-3541. doi: 10.12659/MSM.916475.

[87]. Songun I, Putter H, Kranenbarg EM, Sasako M, van de Velde CJ. Surgical treatment of gastric cancer: 15-year follow-up results of the randomised nationwide Dutch D1D2 trial. Lancet Oncol. 2010 May;11(5):439-49. doi: 10.1016/S1470-2045(10)70070-X. Epub 2010 Apr 19.

[88]. Roukos DH. Current status and future perspectives in gastric cancer management. Cancer Treat Rev. 2000 Aug;26(4):243-55.

[89]. Choi YY, Noh SH, Cheong JH. Evolution of Gastric Cancer Treatment: From the Golden Age of Surgery to an Era of Precision Medicine. Yonsei Med J. 2015 Sep;56(5):1177-85. doi: 10.3349/ymj.2015.56.5.1177.

[90]. Hatta W, Gotoda T, Koike T, Masamune A. History and future perspectives in Japanese guidelines for endoscopic resection of early gastric cancer. Dig Endosc. 2020 Jan;32(2):180-190. doi: 10.1111/den.13531. Epub 2019 Sep 17.

[91]. Takahashi T, Saikawa Y, Kitagawa Y. Gastric cancer: current status of diagnosis and treatment. Cancers (Basel). 2013 Jan 16;5(1):48-63. doi: 10.3390/cancers5010048.

[92]. Kim MY, Cho JH, Cho JY. Ever-changing endoscopic treatment for early gastric cancer: yesterday-today-tomorrow. World J Gastroenterol. 2014 Oct 7;20(37):13273-83. doi: 10.3748/wjg.v20.i37.13273.

[93]. Ko WJ, Song GW, Kim WH, Hong SP, Cho JY. Endoscopic resection of early gastric cancer: current status and new approaches. Transl Gastroenterol Hepatol. 2016 Apr 6;1:24. doi: 10.21037/tgh.2016.03.22. eCollection 2016.

[94]. Digklia A, Wagner AD. Advanced gastric cancer: Current treatment landscape and future perspectives. World J Gastroenterol. 2016 Feb 28;22(8):2403-14. doi: 10.3748/wjg.v22.i8.2403.

[95]. Takashima A, Yamada Y, Nakajima TE, Kato K, Hamaguchi T, Shimada Y. Standard First-Line Chemotherapy for Metastatic Gastric Cancer in Japan Has Met the Global Standard: Evidence From Recent Phase III Trials. Gastrointest Cancer Res. 2009 Nov;3(6):239-44.

[96]. Longley DB, Harkin DP, Johnston PG. 5-fluorouracil: mechanisms of action and clinical strategies. Nat Rev Cancer. 2003 May;3(5):330-8.

[97]. Koizumi W. Chemotherapy for advanced gastric cancer: review of global and Japanese status. Gastrointest Cancer Res. 2007 Sep;1(5):197-203.

[98]. Alcindor T, Beauger N. Oxaliplatin: a review in the era of molecularly targeted therapy. Curr Oncol. 2011 Jan;18(1):18-25.

[99]. Song Z, Wu Y, Yang J, Yang D, Fang X. Progress in the treatment of advanced gastric cancer. Tumour Biol. 2017 Jul;39(7):1010428317714626. doi: 10.1177/1010428317714626.

[100]. Schernberg A, Rivin Del Campo E, Rousseau B, Matzinger O, Loi M, Maingon P, Huguet F. Adjuvant chemoradiation for gastric carcinoma: State of the art and perspectives. Clin Transl Radiat Oncol. 2018 Mar 13;10:13-22. doi: 10.1016/j.ctro.2018.02.005. eCollection 2018 Mar.

[101]. Toneto MG, Viola L. CURRENT STATUS OF THE MULTIDISCIPLINARY TREATMENT OF GASTRIC ADENOCARCINOMA. Arq Bras Cir Dig. 2018;31(2):e1373. doi: 10.1590/0102-672020180001e1373. Epub 2018 Jul 2.

[102]. Davidson M, Okines AF, Starling N. Current and Future Therapies for Advanced Gastric Cancer. Clin Colorectal Cancer. 2015 Dec;14(4):239-50. doi: 10.1016/j.clcc.2015.05.013. Epub 2015 Jun 6.

[103]. Kolios G, Moodley Y. Introduction to stem cells and regenerative medicine. Respiration. 2013;85(1):3-10. doi: 10.1159/000345615. Epub 2012 Dec 13.

[104]. Seaberg RM, van der Kooy D. Stem and progenitor cells: the premature desertion of rigorous definitions. Trends Neurosci. 2003 Mar;26(3):125-31.

[105]. Jones DL, Wagers AJ. No place like home: anatomy and function of the stem cell niche. Nat Rev Mol Cell Biol. 2008 Jan;9(1):11-21.

[106]. Mohyeldin A, Garzón-Muvdi T, Quiñones-Hinojosa A. Oxygen in stem cell biology: a critical component of the stem cell niche. Cell Stem Cell. 2010 Aug 6;7(2):150-61. doi: 10.1016/j.stem.2010.07.007.

[107]. Arai F, Suda T. Maintenance of quiescent hematopoietic stem cells in the osteoblastic niche. Ann N Y Acad Sci. 2007 Jun;1106:41-53. Epub 2007 Mar 1.

[108]. Rosen JM, Jordan CT. The increasing complexity of the cancer stem cell paradigm. Science. 2009 Jun 26;324(5935):1670-3. doi: 10.1126/science.1171837.

[109]. Velasco-Velázquez MA, Homsi N, De La Fuente M, Pestell RG. Breast cancer stem cells. Int J Biochem Cell Biol. 2012 Apr;44(4):573-7. doi: 10.1016/j.biocel.2011.12.020. Epub 2012 Jan 9.

[110]. Arum CJ, Anderssen E, Viset T, Kodama Y, Lundgren S, Chen D, Zhao CM. Cancer immunoediting from immunosurveillance to tumor escape in microvillus-formed niche: a study of syngeneic orthotopic rat bladder cancer model in comparison with human bladder cancer. Neoplasia. 2010 Jun;12(6):434-42.

[111]. Gilbertson RJ, Rich JN. Making a tumour's bed: glioblastoma stem cells and the vascular niche. Nat Rev Cancer. 2007 Oct;7(10):733-6. doi: 10.1038/nrc2246.

[112]. Ricci-Vitiani L, Pallini R, Biffoni M, Todaro M, Invernici G, Cenci T, Maira G, Parati EA, Stassi G, Larocca LM, De Maria R. Tumour vascularization via endothelial differentiation of glioblastoma stem-like cells. Nature. 2010 Dec 9;468(7325):824-8. doi: 10.1038/nature09557. Epub 2010 Nov 21.

[113]. Wang R, Chadalavada K, Wilshire J, Kowalik U, Hovinga KE, Geber A, Fligelman B, Leversha M, Brennan C, Tabar V. Glioblastoma stem-like cells give rise to tumour endothelium. Nature. 2010 Dec 9;468(7325):829-33. doi: 10.1038/nature09624. Epub 2010 Nov 21.

[114]. Bautch VL. Cancer: Tumour stem cells switch sides. Nature. 2010 Dec 9;468(7325):770-1. doi: 10.1038/468770a.

[115]. Bonnet D, Dick JE. Human acute myeloid leukemia is organized as a hierarchy that originates from a primitive hematopoietic cell. Nat Med. 1997 Jul;3(7):730-7.

[116]. Al-Hajj M, Wicha MS, Benito-Hernandez A, Morrison SJ, Clarke MF. Prospective identification of tumorigenic breast cancer cells. Proc Natl Acad Sci U S A. 2003 Apr 1;100(7):3983-8. Epub 2003 Mar 10.

[117]. Takaishi S, Okumura T, Tu S, Wang SS, Shibata W, Vigneshwaran R, Gordon SA, Shimada Y, Wang TC. Identification of gastric cancer stem cells using the cell surface marker CD44. Stem Cells. 2009 May;27(5):1006-20. doi: 10.1002/stem.30.

[118]. Fukuda K, Saikawa Y, Ohashi M, Kumagai K, Kitajima M, Okano H, Matsuzaki Y, Kitagawa Y. Tumor initiating potential of side population cells in human gastric cancer. Int J Oncol. 2009 May;34(5):1201-7.

[119]. Boesch M, Sopper S, Zeimet AG, Reimer D, Gastl G, Ludewig B, Wolf D. Heterogeneity of Cancer Stem Cells: Rationale for Targeting the Stem Cell Niche. Biochim Biophys Acta. 2016 Dec;1866(2):276-289. doi: 10.1016/j.bbcan.2016.10.003. Epub 2016 Oct 15.

[120]. Katoh M. Canonical and non-canonical WNT signaling in cancer stem cells and their niches: Cellular heterogeneity, omics reprogramming, targeted therapy and tumor plasticity (Review). Int J Oncol. 2017 Nov;51(5):1357-1369. doi: 10.3892/ijo.2017.4129. Epub 2017 Sep 19.

[121]. Simon E, Petke D, Böger C, Behrens HM, Warneke V, Ebert M, Röcken C. The spatial distribution of LGR5+ cells correlates with gastric cancer progression. PLoS One. 2012;7(4):e35486. doi: 10.1371/journal.pone.0035486. Epub 2012 Apr 18.

[122]. Li K, Dan Z, Nie YQ. Gastric cancer stem cells in gastric carcinogenesis, progression, prevention and treatment. World J Gastroenterol. 2014 May 14;20(18):5420-6. doi: 10.3748/wjg.v20.i18.5420.

[123]. Xu G, Shen J, Ou Yang X, Sasahara M, Su X. Cancer stem cells: the 'heartbeat' of gastric cancer. J Gastroenterol. 2013 Jul;48(7):781-97. doi: 10.1007/s00535-012-0712-y. Epub 2012 Nov 27.

[124]. Singh SR. Gastric cancer stem cells: a novel therapeutic target. Cancer Lett. 2013 Sep 10;338(1):110-9. doi: 10.1016/j.canlet.2013.03.035. Epub 2013 Apr 10.

[125]. Fu Y, Du P, Zhao J, Hu C, Qin Y, Huang G. Gastric Cancer Stem Cells: Mechanisms and Therapeutic Approaches. Yonsei Med J. 2018 Dec;59(10):1150-1158. doi: 10.3349/ymj.2018.59.10.1150.

[126]. Fu L, Bu L, Yasuda T, Koiwa M, Akiyama T, Uchihara T, Baba H, Ishimoto T. Gastric Cancer Stem Cells: Current Insights into the Immune Microenvironment and Therapeutic Targets. Biomedicines. 2020 Jan 6;8(1). pii: E7. doi: 10.3390/biomedicines8010007.

[127]. Qiao XT, Gumucio DL. Current molecular markers for gastric progenitor cells and gastric cancer stem cells. J Gastroenterol. 2011 Jul;46(7):855-65. doi: 10.1007/s00535-011-0413-y. Epub 2011 Jun 1.

[128]. Van der Flier LG, Sabates-Bellver J, Oving I, Haegebarth A, De Palo M, Anti M, Van Gijn ME, Suijkerbuijk S, Van de Wetering M, Marra G, Clevers H. The Intestinal Wnt/TCF Signature. Gastroenterology. 2007 Feb;132(2):628-32. Epub 2006 Aug 18.

[129]. Schuijers J, Clevers H. Adult mammalian stem cells: the role of Wnt, Lgr5 and R-spondins. EMBO J. 2012 Jun 13;31(12):2685-96. doi: 10.1038/emboj.2012.149. Epub 2012 May 22.

[130]. Barker N, Huch M, Kujala P, van de Wetering M, Snippert HJ, van Es JH, Sato T, Stange DE, Begthel H, van den Born M, Danenberg E, van den Brink S, Korving J, Abo A, Peters PJ, Wright N, Poulsom R, Clevers H. Lgr5(+ve) stem cells drive self-renewal in the stomach and build long-lived gastric units in vitro. Cell Stem Cell. 2010 Jan 8;6(1):25-36. doi: 10.1016/j.stem.2009.11.013.

[131]. Tu SP, Quante M, Bhagat G, Takaishi S, Cui G, Yang XD, Muthuplani S, Shibata W, Fox JG, Pritchard DM, Wang TC. IFN-γ inhibits gastric carcinogenesis by inducing epithelial cell autophagy and T-cell apoptosis. Cancer Res. 2011 Jun 15;71(12):4247-59. doi: 10.1158/0008-5472.CAN-10-4009. Epub 2011 Apr 21.

[132]. Kikuchi M, Nagata H, Watanabe N, Watanabe H, Tatemichi M, Hibi T. Altered expression of a putative progenitor cell marker DCAMKL1 in the rat gastric mucosa in regeneration, metaplasia and dysplasia. BMC Gastroenterol. 2010 Jun 18;10:65. doi: 10.1186/1471-230X-10-65.

[133]. Nakanishi Y, Seno H, Fukuoka A, Ueo T, Yamaga Y, Maruno T, Nakanishi N, Kanda K, Komekado H, Kawada M, Isomura A, Kawada K, Sakai Y, Yanagita M, Kageyama R, Kawaguchi Y, Taketo MM, Yonehara S, Chiba T. Dclk1 distinguishes between tumor and normal stem cells in the intestine. Nat Genet. 2013 Jan;45(1):98-103. doi: 10.1038/ng.2481. Epub 2012 Dec 2.

[134]. Okamoto R, Yajima T, Yamazaki M, Kanai T, Mukai M, Okamoto S, Ikeda Y, Hibi T, Inazawa J, Watanabe M. Damaged epithelia regenerated by bone marrow-derived cells in the human gastrointestinal tract. Nat Med. 2002 Sep;8(9):1011-7. Epub 2002 Aug 26.

[135]. Takaishi S, Okumura T, Wang TC. Gastric cancer stem cells. J Clin Oncol. 2008 Jun 10;26(17):2876-82. doi: 10.1200/JCO.2007.15.2603.

[136]. Houghton J, Stoicov C, Nomura S, Rogers AB, Carlson J, Li H, Cai X, Fox JG, Goldenring JR, Wang TC. Gastric cancer originating from bone marrow-derived cells. Science. 2004 Nov 26;306(5701):1568-71.

[137]. Heldin CH, Rubin K, Pietras K, Ostman A. High interstitial fluid pressure - an obstacle in cancer therapy. Nat Rev Cancer. 2004 Oct;4(10):806-13.

[138]. Schaaf MB, Garg AD, Agostinis P. Defining the role of the tumor vasculature in antitumor immunity and immunotherapy. Cell Death Dis. 2018 Jan 25;9(2):115. doi: 10.1038/s41419-017-0061-0.

[139]. Haraguchi N, Utsunomiya T, Inoue H, Tanaka F, Mimori K, Barnard GF, Mori M. Characterization of a side population of cancer cells from human gastrointestinal system. Stem Cells. 2006 Mar;24(3):506-13. Epub 2005 Oct 20.

[140]. Morrison R, Schleicher SM, Sun Y, Niermann KJ, Kim S, Spratt DE, Chung CH, Lu B. Targeting the mechanisms of resistance to chemotherapy and radiotherapy with the cancer stem cell hypothesis. J Oncol. 2011;2011:941876. doi: 10.1155/2011/941876. Epub 2010 Oct 12.

[141]. Sottoriva A, Verhoeff JJ, Borovski T, McWeeney SK, Naumov L, Medema JP, Sloot PM, Vermeulen L. Cancer stem cell tumor model reveals invasive morphology and increased phenotypical heterogeneity. Cancer Res. 2010 Jan 1;70(1):46-56. doi: 10.1158/0008-5472.CAN-09-3663.

[142]. Driessens G, Beck B, Caauwe A, Simons BD, Blanpain C. Defining the mode of tumour growth by clonal analysis. Nature. 2012 Aug 23;488(7412):527-30. doi: 10.1038/nature11344.

[143]. Conley SJ, Gheordunescu E, Kakarala P, Newman B, Korkaya H, Heath AN, Clouthier SG, Wicha MS. Antiangiogenic agents increase breast cancer stem cells via the generation of tumor hypoxia. Proc Natl Acad Sci U S A. 2012 Feb 21;109(8):2784-9. doi: 10.1073/pnas.1018866109. Epub 2012 Jan 23.

[144]. Yang ZJ, Wechsler-Reya RJ. Hit 'em where they live: targeting the cancer stem cell niche. Cancer Cell. 2007 Jan;11(1):3-5.

[145]. Chen J, Li Y, Yu TS, McKay RM, Burns DK, Kernie SG, Parada LF. A restricted cell population propagates glioblastoma growth after chemotherapy. Nature. 2012 Aug 23;488(7412):522-6. doi: 10.1038/nature11287.

[146]. Kaiser J. The cancer stem cell gamble. Science. 2015 Jan 16;347(6219):226-9. doi: 10.1126/science.347.6219.226.

[147]. Komiya Y, Habas R. Wnt signal transduction pathways. Organogenesis. 2008 Apr;4(2):68-75.

[148]. Willert K, Nusse R. Beta-catenin: a key mediator of Wnt signaling. Curr Opin Genet Dev. 1998 Feb;8(1):95-102.

[149]. Barker N, Clevers H. Mining the Wnt pathway for cancer therapeutics. Nat Rev Drug Discov. 2006 Dec;5(12):997-1014.

[150]. Vincan E, Barker N. The upstream components of the Wnt signalling pathway in the dynamic EMT and MET associated with colorectal cancer progression. Clin Exp Metastasis. 2008;25(6):657-63. doi: 10.1007/s10585-008-9156-4. Epub 2008 Mar 19.

[151]. Huang D, Du X. Crosstalk between tumor cells and microenvironment via Wnt pathway in colorectal cancer dissemination. World J Gastroenterol. 2008 Mar 28;14(12):1823-7.

[152]. Anastas JN, Moon RT. WNT signalling pathways as therapeutic targets in cancer. Nat Rev Cancer. 2013 Jan;13(1):11-26. doi: 10.1038/nrc3419.

[153]. Shaw HV, Koval A, Katanaev VL. Targeting the Wnt signalling pathway in cancer: prospects and perils. Swiss Med Wkly. 2019 Oct 3;149:w20129. doi: 10.4414/smw.2019.20129. eCollection 2019 Sep 23.

[154]. Olsen JJ, Pohl SÖ, Deshmukh A, Visweswaran M, Ward NC, Arfuso F, Agostino M, Dharmarajan A. The Role of Wnt Signalling in Angiogenesis. Clin Biochem Rev. 2017 Nov;38(3):131-142.

[155]. Cha B, Geng X, Mahamud MR, Zhang JY, Chen L, Kim W, Jho EH, Kim Y, Choi D, Dixon JB, Chen H, Hong YK, Olson L, Kim TH, Merrill BJ, Davis MJ, Srinivasan RS. Complementary Wnt Sources Regulate Lymphatic Vascular Development via PROX1-Dependent Wnt/β-Catenin Signaling. Cell Rep. 2018 Oct 16;25(3):571-584.e5. doi: 10.1016/j.celrep.2018.09.049.

[156]. Eccles SA, Welch DR. Metastasis: recent discoveries and novel treatment strategies. Lancet. 2007 May 19;369(9574):1742-57.

[157]. Takebe N, Harris PJ, Warren RQ, Ivy SP. Targeting cancer stem cells by inhibiting Wnt, Notch, and Hedgehog pathways. Nat Rev Clin Oncol. 2011 Feb;8(2):97-106. doi: 10.1038/nrclinonc.2010.196. Epub 2010 Dec 14.

[158]. Takebe N, Miele L, Harris PJ, Jeong W, Bando H, Kahn M, Yang SX, Ivy SP. Targeting Notch, Hedgehog, and Wnt pathways in cancer stem cells: clinical update. Nat Rev Clin Oncol. 2015 Aug;12(8):445-64. doi: 10.1038/nrclinonc.2015.61. Epub 2015 Apr 7.

[159]. Lu D, Carson DA. Inhibition of Wnt signaling and cancer stem cells. Oncotarget. 2011 Aug;2(8):587.

[160]. Mishra L, Shetty K, Tang Y, Stuart A, Byers SW. The role of TGF-beta and Wnt signaling in gastrointestinal stem cells and cancer. Oncogene. 2005 Aug 29;24(37):5775-89.

[161]. Oshima H, Matsunaga A, Fujimura T, Tsukamoto T, Taketo MM, Oshima M. Carcinogenesis in mouse stomach by simultaneous activation of the Wnt signaling and prostaglandin E2 pathway. Gastroenterology. 2006 Oct;131(4):1086-95.

[162]. Holbrook JD, Parker JS, Gallagher KT, Halsey WS, Hughes AM, Weigman VJ, Lebowitz PF, Kumar R. Deep sequencing of gastric carcinoma reveals somatic mutations relevant to personalized medicine. J Transl Med. 2011 Jul 25;9:119. doi: 10.1186/1479-5876-9-119.

[163]. Lowy AM, Clements WM, Bishop J, Kong L, Bonney T, Sisco K, Aronow B, Fenoglio-Preiser C, Groden J. beta-Catenin/Wnt signaling regulates expression of the membrane type 3 matrix metalloproteinase in gastric cancer. Cancer Res. 2006 May 1;66(9):4734-41.

[164]. Song Y, Li ZX, Liu X, Wang R, Li LW, Zhang Q. The Wnt/β-catenin and PI3K/Akt signaling pathways promote EMT in gastric cancer by epigenetic regulation via H3 lysine 27 acetylation. Tumour Biol. 2017 Jul;39(7):1010428317712617. doi: 10.1177/1010428317712617.

[165]. Oliveira LA, Oshima CTF, Soffner PA, Silva MS, Lins RR, Malinverni ACM, Waisberg J. THE CANONICAL WNT PATHWAY IN GASTRIC CARCINOMA. Arq Bras Cir Dig. 2019 Jan 7;32(1):e1414. doi: 10.1590/0102-672020180001e1414.

[166]. Cai C, Zhu X. The Wnt/β-catenin pathway regulates self-renewal of cancer stem-like cells in human gastric cancer. Mol Med Rep. 2012 May;5(5):1191-6. doi: 10.3892/mmr.2012.802. Epub 2012 Feb 21.

[167]. Mao J, Fan S, Ma W, Fan P, Wang B, Zhang J, Wang H, Tang B, Zhang Q, Yu X, Wang L, Song B, Li L. Roles of Wnt/β-catenin signaling in the gastric cancer stem cells proliferation and salinomycin treatment. Cell Death Dis. 2014 Jan 30;5:e1039. doi: 10.1038/cddis.2013.515.

[168]. Stojnev S, Krstic M, Ristic-Petrovic A, Stefanovic V, Hattori T. Gastric cancer stem cells: therapeutic targets. Gastric Cancer. 2014 Jan;17(1):13-25. doi: 10.1007/s10120-013-0254-x. Epub 2013 Apr 6.

[169]. Song X, Xin N, Wang W, Zhao C. Wnt/β-catenin, an oncogenic pathway targeted by H. pylori in gastric carcinogenesis. Oncotarget. 2015 Nov 3;6(34):35579-88. doi: 10.18632/oncotarget.5758.

[170]. Jung DH, Bae YJ, Kim JH, Shin YK, Jeung HC. HER2 Regulates Cancer Stem Cell Activities via the Wnt Signaling Pathway in Gastric Cancer Cells. Oncology. 2019;97(5):311-318. doi: 10.1159/000502845. Epub 2019 Sep 24.

[171]. Jobling P, Pundavela J, Oliveira SM, Roselli S, Walker MM, Hondermarck H. Nerve-Cancer Cell Cross-talk: A Novel Promoter of Tumor Progression. Cancer Res. 2015 May 1;75(9):1777-81. doi: 10.1158/0008-5472.CAN-14-3180. Epub 2015 Mar 20.

[172]. Liebig C, Ayala G, Wilks JA, Berger DH, Albo D. Perineural invasion in cancer: a review of the literature. Cancer. 2009 Aug 1;115(15):3379-91. doi: 10.1002/cncr.24396.

[173]. Tanaka A, Watanabe T, Okuno K, Yasutomi M. Perineural invasion as a predictor of recurrence of gastric cancer. Cancer. 1994 Feb 1;73(3):550-5.

[174]. Duraker N, Sişman S, Can G. The significance of perineural invasion as a prognostic factor in patients with gastric carcinoma. Surg Today. 2003;33(2):95-100.

[175]. Tianhang L, Guoen F, Jianwei B, Liye M. The effect of perineural invasion on overall survival in patients with gastric carcinoma. J Gastrointest Surg. 2008 Jul;12(7):1263-7. doi: 10.1007/s11605-008-0529-4. Epub 2008 May 8.

[176]. Deng J, You Q, Gao Y, Yu Q, Zhao P, Zheng Y, Fang W, Xu N, Teng L. Prognostic value of perineural invasion in gastric cancer: a systematic review and meta-analysis. PLoS One. 2014 Feb 21;9(2):e88907. doi: 10.1371/journal.pone.0088907. eCollection 2014.

[177]. Chen SH, Zhang BY, Zhou B, Zhu CZ, Sun LQ, Feng YJ. Perineural invasion of cancer: a complex crosstalk between cells and molecules in the perineural niche. Am J Cancer Res. 2019 Jan 1;9(1):1-21. eCollection 2019.

[178]. Hibi K, Westra WH, Borges M, Goodman S, Sidransky D, Jen J. PGP9.5 as a candidate tumor marker for non-small-cell lung cancer. Am J Pathol. 1999 Sep;155(3):711-5.

[179]. Tezel E, Hibi K, Nagasaka T, Nakao A. PGP9.5 as a prognostic factor in pancreatic cancer. Clin Cancer Res. 2000 Dec;6(12):4764-7.

[180]. Yamazaki T, Hibi K, Takase T, Tezel E, Nakayama H, Kasai Y, Ito K, Akiyama S, Nagasaka T, Nakao A. PGP9.5 as a marker for invasive colorectal cancer. Clin Cancer Res. 2002 Jan;8(1):192-5.

[181]. Akishima-Fukasawa Y, Ino Y, Nakanishi Y, Miura A, Moriya Y, Kondo T, Kanai Y, Hirohashi S. Significance of PGP9.5 expression in cancer-associated fibroblasts for prognosis of colorectal carcinoma. Am J Clin Pathol. 2010 Jul;134(1):71-9. doi: 10.1309/AJCPRJP39MIDSGBH.

[182]. Ayala GE, Dai H, Powell M, Li R, Ding Y, Wheeler TM, Shine D, Kadmon D, Thompson T, Miles BJ, Ittmann MM, Rowley D. Cancer-related axonogenesis and neurogenesis in prostate cancer. Clin Cancer Res. 2008 Dec 1;14(23):7593-603. doi: 10.1158/1078-0432.CCR-08-1164.

[183]. Entschladen F, Drell TL 4th, Lang K, Joseph J, Zaenker KS. Tumour-cell migration, invasion, and metastasis: navigation by neurotransmitters. Lancet Oncol. 2004 Apr;5(4):254-8.

[184]. Mancino M, Ametller E, Gascón P, Almendro V. The neuronal influence on tumor progression. Biochim Biophys Acta. 2011 Dec;1816(2):105-18. doi: 10.1016/j.bbcan.2011.04.005. Epub 2011 May 14.

[185]. Arese M, Bussolino F, Pergolizzi M, Bizzozero L, Pascal D. Tumor progression: the neuronal input. Ann Transl Med. 2018 Mar;6(5):89. doi: 10.21037/atm.2018.01.01.

[186]. Entschladen F, Palm D, Lang K, Drell TL 4th, Zaenker KS. Neoneurogenesis: tumors may initiate their own innervation by the release of neurotrophic factors in analogy to lymphangiogenesis and neoangiogenesis. Med Hypotheses. 2006;67(1):33-5. Epub 2006 Mar 3.

[187]. Ondicova K, Mravec B. Role of nervous system in cancer aetiopathogenesis. Lancet Oncol. 2010 Jun;11(6):596-601. doi: 10.1016/S1470-2045(09)70337-7.

[188]. Carmeliet P, Tessier-Lavigne M. Common mechanisms of nerve and blood vessel wiring. Nature. 2005 Jul 14;436(7048):193-200.

[189]. Weinstein BM. Vessels and nerves: marching to the same tune. Cell. 2005 Feb 11;120(3):299-302.

[190]. Voss MJ, Entschladen F. Tumor interactions with soluble factors and the nervous system. Cell Commun Signal. 2010 Sep 7;8:21. doi: 10.1186/1478-811X-8-21.

[191]. Zhang L, Yang X, Yang S, Zhang J. The Wnt/β-catenin signaling pathway in the adult neurogenesis. Eur J Neurosci. 2011 Jan;33(1):1-8. doi: 10.1111/j.1460-9568.2010.7483.x. Epub 2010 Nov 14.

[192]. Zou Y. Wnt signaling in axon guidance. Trends Neurosci. 2004 Sep;27(9):528-32.

[193]. Katayama Y, Battista M, Kao WM, Hidalgo A, Peired AJ, Thomas SA, Frenette PS. Signals from the sympathetic nervous system regulate hematopoietic stem cell egress from bone marrow. Cell. 2006 Jan 27;124(2):407-21.

[194]. Lundgren O, Jodal M, Jansson M, Ryberg AT, Svensson L. Intestinal epithelial stem/progenitor cells are controlled by mucosal afferent nerves. PLoS One. 2011 Feb 9;6(2):e16295. doi: 10.1371/journal.pone.0016295.

[195]. Pardal R, Clarke MF, Morrison SJ. Applying the principles of stem-cell biology to cancer. Nat Rev Cancer. 2003 Dec;3(12):895-902.

[196]. Magnon C, Hall SJ, Lin J, Xue X, Gerber L, Freedland SJ, Frenette PS. Autonomic nerve development contributes to prostate cancer progression. Science. 2013 Jul 12;341(6142):1236361. doi: 10.1126/science.1236361.

[197]. Håkanson R, Vallgren S, Ekelund M, Rehfeld JF, Sundler F. The vagus exerts trophic control of the stomach in the rat. Gastroenterology. 1984 Jan;86(1):28-32.

[198]. Axelson J, Ekelund M, Håkanson R, Sundler F. Gastrin and the vagus interact in the trophic control of the rat oxyntic mucosa. Regul Pept. 1988 Aug;22(3):237-43.

[199]. Berthoud HR, Neuhuber WL. Functional and chemical anatomy of the afferent vagal system. Auton Neurosci. 2000 Dec 20;85(1-3):1-17.

[200]. Fox EA, Phillips RJ, Martinson FA, Baronowsky EA, Powley TL. Vagal afferent innervation of smooth muscle in the stomach and duodenum of the mouse: morphology and topography. J Comp Neurol. 2000 Dec 18;428(3):558-76.

[201]. Xie G, Drachenberg C, Yamada M, Wess J, Raufman JP. Cholinergic agonist-induced pepsinogen secretion from murine gastric chief cells is mediated by M1 and M3 muscarinic receptors. Am J Physiol Gastrointest Liver Physiol. 2005 Sep;289(3):G521-9. Epub 2005 Jun 2.

[202]. Shah N, Khurana S, Cheng K, Raufman JP. Muscarinic receptors and ligands in cancer. Am J Physiol Cell Physiol. 2009 Feb;296(2):C221-32. doi: 10.1152/ajpcell.00514.2008. Epub 2008 Nov 26.

[203]. Frucht H, Jensen RT, Dexter D, Yang WL, Xiao Y. Human colon cancer cell proliferation mediated by the M3 muscarinic cholinergic receptor. Clin Cancer Res. 1999 Sep;5(9):2532-9.

[204]. Rayford W, Noble MJ, Austenfeld MA, Weigel J, Mebust WK, Shah GV. Muscarinic cholinergic receptors promote growth of human prostate cancer cells. Prostate. 1997 Feb 15;30(3):160-6.

[205]. Song P, Sekhon HS, Lu A, Arredondo J, Sauer D, Gravett C, Mark GP, Grando SA, Spindel ER. M3 muscarinic receptor antagonists inhibit small cell lung carcinoma growth and mitogen-activated protein kinase phosphorylation induced by acetylcholine secretion. Cancer Res. 2007 Apr 15;67(8):3936-44.

[206]. Aihara T, Fujishita T, Kanatani K, Furutani K, Nakamura E, Taketo MM, Matsui M, Chen D, Okabe S. Impaired gastric secretion and lack of trophic responses to hypergastrinemia in M3 muscarinic receptor knockout mice. Gastroenterology. 2003 Dec;125(6):1774-84.

[207]. Blüher M. Obesity: global epidemiology and pathogenesis. Nat Rev Endocrinol. 2019 May;15(5):288-298. doi: 10.1038/s41574-019-0176-8.

[208]. Arroyo-Johnson C, Mincey KD. Obesity Epidemiology Worldwide. Gastroenterol Clin North Am. 2016 Dec;45(4):571-579. doi: 10.1016/j.gtc.2016.07.012.

[209]. Gadde KM, Martin CK, Berthoud HR, Heymsfield SB. Obesity: Pathophysiology and Management. J Am Coll Cardiol. 2018 Jan 2;71(1):69-84. doi: 10.1016/j.jacc.2017.11.011.

[210]. GBD 2015 Obesity Collaborators, Afshin A, Forouzanfar MH, Reitsma MB, Sur P, Estep K, Lee A, Marczak L, Mokdad AH, Moradi-Lakeh M, Naghavi M, Salama JS, Vos T, Abate KH, Abbafati C, Ahmed MB, Al-Aly Z, Alkerwi A, Al-Raddadi R, Amare AT, Amberbir A, Amegah AK, Amini E, Amrock SM, Anjana RM, Ärnlöv J, Asayesh H, Banerjee A, Barac A, Baye E, Bennett DA, Beyene AS, Biadgilign S, Biryukov S, Bjertness E, Boneya DJ, Campos-Nonato I, Carrero JJ, Cecilio P, Cercy K, Ciobanu LG, Cornaby L, Damtew SA, Dandona L, Dandona R, Dharmaratne SD, Duncan BB, Eshrati B, Esteghamati A, Feigin VL, Fernandes JC, Fürst T, Gebrehiwot TT, Gold A, Gona PN, Goto A, Habtewold TD, Hadush KT, Hafezi-Nejad N, Hay SI, Horino M, Islami F, Kamal R, Kasaeian A, Katikireddi SV, Kengne AP, Kesavachandran CN, Khader YS, Khang YH, Khubchandani J, Kim D, Kim YJ, Kinfu Y, Kosen S, Ku T, Defo BK, Kumar GA, Larson HJ, Leinsalu M, Liang X, Lim SS, Liu P, Lopez AD, Lozano R, Majeed A, Malekzadeh R, Malta DC, Mazidi M, McAlinden C, McGarvey ST, Mengistu DT, Mensah GA, Mensink GBM, Mezgebe HB, Mirrakhimov EM, Mueller UO, Noubiap JJ, Obermeyer CM, Ogbo FA, Owolabi MO, Patton GC, Pourmalek F, Qorbani M, Rafay A, Rai RK, Ranabhat CL, Reinig N, Safiri S, Salomon JA, Sanabria JR, Santos IS, Sartorius B, Sawhney M, Schmidhuber J, Schutte AE, Schmidt MI, Sepanlou SG, Shamsizadeh M, Sheikhbahaei S, Shin MJ, Shiri R, Shiue I, Roba HS, Silva DAS, Silverberg JI, Singh JA, Stranges S, Swaminathan S, Tabarés-Seisdedos R, Tadese F, Tedla BA, Tegegne BS, Terkawi AS, Thakur JS, Tonelli M, Topor-Madry R, Tyrovolas S, Ukwaja KN, Uthman OA, Vaezghasemi M, Vasankari T, Vlassov VV, Vollset SE, Weiderpass E, Werdecker A, Wesana J, Westerman R, Yano Y, Yonemoto N, Yonga G, Zaidi Z, Zenebe ZM, Zipkin B, Murray CJL. Health Effects of Overweight and Obesity in 195 Countries over 25 Years. N Engl J Med. 2017 Jul 6;377(1):13-27. doi: 10.1056/NEJMoa1614362. Epub 2017 Jun 12.

[211]. Chooi YC, Ding C, Magkos F. The epidemiology of obesity. Metabolism. 2019 Mar;92:6-10. doi: 10.1016/j.metabol.2018.09.005. Epub 2018 Sep 22.

[212]. Canoy D, Buchan I. Challenges in obesity epidemiology. Obes Rev. 2007 Mar;8 Suppl 1:1-11.

[213]. Kissler HJ, Settmacher U. Bariatric surgery to treat obesity. Semin Nephrol. 2013 Jan;33(1):75-89. doi: 10.1016/j.semnephrol.2012.12.004.

[214]. Leff DR, Heath D. Surgery for obesity in adulthood. BMJ. 2009 Sep 22;339:b3402. doi: 10.1136/bmj.b3402.

[215]. Adams TD, Hunt SC. Cancer and obesity: effect of bariatric surgery. World J Surg. 2009 Oct;33(10):2028-33. doi: 10.1007/s00268-009-0169-1.

[216]. Clarke RJ, Lewis DL, Williams JA. Vagotomy and pyloroplasty for gastric ulcer. Br Med J. 1972 May 13;2(5810):369-71.

[217]. Kral JG. Vagotomy for treatment of severe obesity. Lancet. 1978 Feb 11;1(8059):307-8.

[218]. Camilleri M, Toouli J, Herrera MF, Kulseng B, Kow L, Pantoja JP, Marvik R, Johnsen G, Billington CJ, Moody FG, Knudson MB, Tweden KS, Vollmer M, Wilson RR, Anvari M. Intra-abdominal vagal blocking (VBLOC therapy): clinical results with a new implantable medical device. Surgery. 2008 Jun;143(6):723-31. doi: 10.1016/j.surg.2008.03.015. Epub 2008 May 9.

[219]. Khorgami Z, Shoar S, Andalib A, Aminian A, Brethauer SA, Schauer PR. Trends in utilization of bariatric surgery, 2010-2014: sleeve gastrectomy dominates. Surg Obes Relat Dis. 2017 May;13(5):774-778. doi: 10.1016/j.soard.2017.01.031. Epub 2017 Jan 25.

[220]. Ward M, Prachand V. Surgical treatment of obesity. Gastrointest Endosc. 2009 Nov;70(5):985-90. doi: 10.1016/j.gie.2009.09.001.

[221]. Anderson B, Gill RS, de Gara CJ, Karmali S, Gagner M. Biliopancreatic diversion: the effectiveness of duodenal switch and its limitations. Gastroenterol Res Pract. 2013;2013:974762. doi: 10.1155/2013/974762. Epub 2013 Nov 21.

[222]. Aasheim ET, Björkman S, Søvik TT, Engström M, Hanvold SE, Mala T, Olbers T, Bøhmer T. Vitamin status after bariatric surgery: a randomized study of gastric bypass and duodenal switch. Am J Clin Nutr. 2009 Jul;90(1):15-22. doi: 10.3945/ajcn.2009.27583. Epub 2009 May 13.

[223]. Anthone GJ, Lord RV, DeMeester TR, Crookes PF. The duodenal switch operation for the treatment of morbid obesity. Ann Surg. 2003 Oct;238(4):618-27; discussion 627-8.

[224]. Colquitt JL, Pickett K, Loveman E, Frampton GK. Surgery for weight loss in adults. Cochrane Database Syst Rev. 2014 Aug 8;(8):CD003641. doi: 10.1002/14651858.CD003641.pub4.

[225]. Colquitt JL, Pickett K, Loveman E, Frampton GK. Surgery for weight loss in adults. Cochrane Database Syst Rev. 2014 Aug 8;(8):CD003641. doi: 10.1002/14651858.CD003641.pub4.

[226]. Strain GW, Gagner M, Inabnet WB, Dakin G, Pomp A. Comparison of effects of gastric bypass and biliopancreatic diversion with duodenal switch on weight loss and body composition 1-2 years after surgery. Surg Obes Relat Dis. 2007 Jan-Feb;3(1):31-6. Epub 2006 Nov 20.

[227]. Prachand VN, Ward M, Alverdy JC. Duodenal switch provides superior resolution of metabolic comorbidities independent of weight loss in the super-obese (BMI > or = 50 kg/m2) compared with gastric bypass. J Gastrointest Surg. 2010 Feb;14(2):211-20. doi: 10.1007/s11605-009-1101-6.

[228]. Søvik TT, Taha O, Aasheim ET, Engström M, Kristinsson J, Björkman S, Schou CF, Lönroth H, Mala T, Olbers T. Randomized clinical trial of laparoscopic gastric bypass versus laparoscopic duodenal switch for superobesity. Br J Surg. 2010 Feb;97(2):160-6. doi: 10.1002/bjs.6802.

[229]. Laurenius A, Taha O, Maleckas A, Lönroth H, Olbers T. Laparoscopic biliopancreatic diversion/duodenal switch or laparoscopic Roux-en-Y gastric bypass for super-obesity-weight loss versus side effects. Surg Obes Relat Dis. 2010 Jul-Aug;6(4):408-14. doi: 10.1016/j.soard.2010.03.293. Epub 2010 Apr 8.

[230]. Søvik TT, Aasheim ET, Taha O, Engström M, Fagerland MW, Björkman S, Kristinsson J, Birkeland KI, Mala T, Olbers T. Weight loss, cardiovascular risk factors, and quality of life after gastric bypass and duodenal switch: a randomized trial. Ann Intern Med. 2011 Sep 6;155(5):281-91. doi: 10.7326/0003-4819-155-5-201109060-00005.

[231]. Topart P, Becouarn G, Ritz P. Weight loss is more sustained after biliopancreatic diversion with duodenal switch than Roux-en-Y gastric bypass in superobese patients. Surg Obes Relat Dis. 2013 Jul-Aug;9(4):526-30. doi: 10.1016/j.soard.2012.02.006. Epub 2012 Mar 3.

[232]. Skogar ML, Sundbom M. Duodenal Switch Is Superior to Gastric Bypass in Patients with Super Obesity when Evaluated with the Bariatric Analysis and Reporting Outcome System (BAROS). Obes Surg. 2017 Sep;27(9):2308-2316. doi: 10.1007/s11695-017-2680-z.

[233]. Angrisani L, Santonicola A, Iovino P, Vitiello A, Zundel N, Buchwald H, Scopinaro N. Bariatric Surgery and Endoluminal Procedures: IFSO Worldwide Survey 2014. Obes Surg. 2017 Sep;27(9):2279-2289. doi: 10.1007/s11695-017-2666-x.

[234]. Angrisani L, Santonicola A, Iovino P, Vitiello A, Higa K, Himpens J, Buchwald H, Scopinaro N. IFSO Worldwide Survey 2016: Primary, Endoluminal, and Revisional Procedures. Obes Surg. 2018 Dec;28(12):3783-3794. doi: 10.1007/s11695-018-3450-2.

[235]. Frezza EE, Chiriva-Internati M, Wachtel MS. Analysis of the results of sleeve gastrectomy for morbid obesity and the role of ghrelin. Surg Today. 2008;38(6):481-3. doi: 10.1007/s00595-007-3648-8. Epub 2008 May 31.

[236]. Rabben HL, Zhao CM, Hayakawa Y, Wang TC, Chen D. Vagotomy and Gastric Tumorigenesis. Curr Neuropharmacol. 2016;14(8):967-972.

[237]. Nguyen NT, Varela JE. Bariatric surgery for obesity and metabolic disorders: state of the art. Nat Rev Gastroenterol Hepatol. 2017 Mar;14(3):160-169. doi: 10.1038/nrgastro.2016.170. Epub 2016 Nov 30.

[238]. Furnes MW, Stenstrom B, Tømmerås K, Skoglund T, Dickson SL, Kulseng B, Zhao CM, Chen D. Feeding behavior in rats subjected to gastrectomy or gastric bypass surgery. Eur Surg Res. 2008;40(3):279-88. doi: 10.1159/000114966. Epub 2008 Feb 5.

[239]. Poloz Y, Stambolic V. Obesity and cancer, a case for insulin signaling. Cell Death Dis. 2015 Dec 31;6:e2037. doi: 10.1038/cddis.2015.381.

[240]. Hruby A, Hu FB. The Epidemiology of Obesity: A Big Picture. Pharmacoeconomics. 2015 Jul;33(7):673-89. doi: 10.1007/s40273-014-0243-x.

[241]. Bhupathiraju SN, Hu FB. Epidemiology of Obesity and Diabetes and Their Cardiovascular Complications. Circ Res. 2016 May 27;118(11):1723-35. doi: 10.1161/CIRCRESAHA.115.306825.

[242]. Ramos-Nino ME. The role of chronic inflammation in obesity-associated cancers. ISRN Oncol. 2013 May 30;2013:697521. doi: 10.1155/2013/697521. Print 2013.

[243]. Font-Burgada J, Sun B, Karin M. Obesity and Cancer: The Oil that Feeds the Flame. Cell Metab. 2016 Jan 12;23(1):48-62. doi: 10.1016/j.cmet.2015.12.015.

[244]. Deng T, Lyon CJ, Bergin S, Caligiuri MA, Hsueh WA. Obesity, Inflammation, and Cancer. Annu Rev Pathol. 2016 May 23;11:421-49. doi: 10.1146/annurev-pathol-012615-044359.

[245]. Kolb R, Sutterwala FS, Zhang W. Obesity and cancer: inflammation bridges the two. Curr Opin Pharmacol. 2016 Aug;29:77-89. doi: 10.1016/j.coph.2016.07.005. Epub 2016 Jul 16.

[246]. Calle EE, Rodriguez C, Walker-Thurmond K, Thun MJ. Overweight, obesity, and mortality from cancer in a prospectively studied cohort of U.S. adults. N Engl J Med. 2003 Apr 24;348(17):1625-38.

[247]. Maestro A, Rigla M, Caixàs A. Does bariatric surgery reduce cancer risk? A review of the literature. Endocrinol Nutr. 2015 Mar;62(3):138-43. doi: 10.1016/j.endonu.2014.12.005. Epub 2015 Jan 28.

[248]. Merkow RP, Ko CY. Evidence-based medicine in surgery: the importance of both experimental and observational study designs. JAMA. 2011 Jul 27;306(4):436-7. doi: 10.1001/jama.2011.1059.

[249]. Diener MK, Simon T, Büchler MW, Seiler CM. Surgical evaluation and knowledge transfer--methods of clinical research in surgery. Langenbecks Arch Surg. 2012 Dec;397(8):1193-9. doi: 10.1007/s00423-011-0775-x. Epub 2011 Mar 22.

[250]. Wang TC, Dangler CA, Chen D, Goldenring JR, Koh T, Raychowdhury R, Coffey RJ, Ito S, Varro A, Dockray GJ, Fox JG. Synergistic interaction between hypergastrinemia and Helicobacter infection in a mouse model of gastric cancer. Gastroenterology. 2000 Jan;118(1):36-47.

[251]. Tomita H, Takaishi S, Menheniott TR, Yang X, Shibata W, Jin G, Betz KS, Kawakami K, Minamoto T, Tomasetto C, Rio MC, Lerkowit N, Varro A, Giraud AS, Wang TC. Inhibition of gastric carcinogenesis by the hormone gastrin is mediated by suppression of TFF1 epigenetic silencing. Gastroenterology. 2011 Mar;140(3):879-91. doi: 10.1053/j.gastro.2010.11.037. Epub 2010 Nov 25.

[252]. Tu S, Bhagat G, Cui G, Takaishi S, Kurt-Jones EA, Rickman B, Betz KS, Penz-Oesterreicher M, Bjorkdahl O, Fox JG, Wang TC. Overexpression of interleukin-1beta induces gastric inflammation and

cancer and mobilizes myeloid-derived suppressor cells in mice. Cancer Cell. 2008 Nov 4;14(5):408-19. doi: 10.1016/j.ccr.2008.10.011.

[253]. Festing MF, Altman DG. Guidelines for the design and statistical analysis of experiments using laboratory animals. ILAR J. 2002;43(4):244-58.

[254]. Russell W.M.S., Burch R.L. The Principles of Humane Experimental Technique. Methuen & Co Ltd.; London, UK. 1959

[255]. Rowland LP. Stroke, spasticity, and botulinum toxin. N Engl J Med. 2002 Aug 8;347(6):382-3.

[256]. Dong M, Yeh F, Tepp WH, Dean C, Johnson EA, Janz R, Chapman ER. SV2 is the protein receptor for botulinum neurotoxin A. Science. 2006 Apr 28;312(5773):592-6. Epub 2006 Mar 16.

[257]. Eglen RM, Choppin A, Dillon MP, Hegde S. Muscarinic receptor ligands and their therapeutic potential. Curr Opin Chem Biol. 1999 Aug;3(4):426-32.

[258]. Ohtake A, Saitoh C, Yuyama H, Ukai M, Okutsu H, Noguchi Y, Hatanaka T, Suzuki M, Sato S, Sasamata M, Miyata K. Pharmacological characterization of a new antimuscarinic agent, solifenacin succinate, in comparison with other antimuscarinic agents. Biol Pharm Bull. 2007 Jan;30(1):54-8.

[259]. Raufman JP, Samimi R, Shah N, Khurana S, Shant J, Drachenberg C, Xie G, Wess J, Cheng K. Genetic ablation of M3 muscarinic receptors attenuates murine colon epithelial cell proliferation and neoplasia. Cancer Res. 2008 May 15;68(10):3573-8. doi: 10.1158/0008-5472.CAN-07-6810.

[260]. Okabe S, Kodama Y, Cao H, Johannessen H, Zhao CM, Wang TC, Takahashi R, Chen D. Topical application of acetic acid in cytoreduction of gastric cancer. A technical report using mouse model. J Gastroenterol Hepatol. 2012 Apr;27 Suppl 3:40-8. doi: 10.1111/j.1440-1746.2012.07070.x.

[261]. Rogers AB, Taylor NS, Whary MT, Stefanich ED, Wang TC, Fox JG. Helicobacter pylori but not high salt induces gastric intraepithelial neoplasia in B6129 mice. Cancer Res. 2005 Dec 1;65(23):10709-15.

[262]. Rogers AB, Houghton J. Helicobacter-based mouse models of digestive system carcinogenesis. Methods Mol Biol. 2009;511:267-95. doi: 10.1007/978-1-59745-447-6_11.

[263]. Ratcliffe EM, Fan L, Mohammed TJ, Anderson M, Chalazonitis A, Gershon MD. Enteric neurons synthesize netrins and are essential for the development of the vagal sensory innervation of the fetal gut. Dev Neurobiol. 2011 May;71(5):362-73. doi: 10.1002/dneu.20869.

[264]. Willert K, Brown JD, Danenberg E, Duncan AW, Weissman IL, Reya T, Yates JR 3rd, Nusse R. Wnt proteins are lipid-modified and can act as stem cell growth factors. Nature. 2003 May 22;423(6938):448-52. Epub 2003 Apr 27.

[265]. Westphalen CB, Asfaha S, Hayakawa Y, Takemoto Y, Lukin DJ, Nuber AH, Brandtner A, Setlik W, Remotti H, Muley A, Chen X, May R, Houchen CW, Fox JG, Gershon MD, Quante M, Wang TC. Long-lived intestinal tuft cells serve as colon cancer-initiating cells. J Clin Invest. 2014 Mar;124(3):1283-95.

[266]. Gershon AA, Chen J, Gershon MD. A model of lytic, latent, and reactivating varicella-zoster virus infections in isolated enteric neurons. J Infect Dis. 2008 Mar 1;197 Suppl 2:S61-5. doi: 10.1086/522149.

[267]. Japanese Gastric Cancer Association. Japanese classification of gastric carcinoma: 3rd English edition. Gastric Cancer. 2011 Jun;14(2):101-12. doi: 10.1007/s10120-011-0041-5.

[268]. Du P, Kibbe WA, Lin SM. lumi: a pipeline for processing Illumina microarray. Bioinformatics. 2008 Jul 1;24(13):1547-8. doi: 10.1093/bioinformatics/btn224. Epub 2008 May 8.

[269]. Smyth GK. Linear models and empirical bayes methods for assessing differential expression in microarray experiments. Stat Appl Genet Mol Biol. 2004;3:Article3. Epub 2004 Feb 12.

[270]. Tarca AL, Draghici S, Khatri P, Hassan SS, Mittal P, Kim JS, Kim CJ, Kusanovic JP, Romero R. A novel signaling pathway impact analysis. Bioinformatics. 2009 Jan 1;25(1):75-82. doi: 10.1093/bioinformatics/btn577. Epub 2008 Nov 5.

[271]. Iossa S, Lionetti L, Mollica MP, Barletta A, Liverini G. Energy intake and utilization vary during development in rats. J Nutr. 1999 Aug;129(8):1593-6.

[272]. Roberts SB, Dallal GE. Energy requirements and aging. Public Health Nutr. 2005 Oct;8(7A):1028-36.

[273]. Correa P, Cuello C, Duque E. Carcinoma and intestinal metaplasia of the stomach in Colombian migrants. J Natl Cancer Inst. 1970 Feb;44(2):297-306.

[274]. Ericsson P, Håkanson R, Rehfeld JF, Norlén P. Gastrin release: Antrum microdialysis reveals a complex neural control. Regul Pept. 2010 Apr 9;161(1-3):22-32. doi: 10.1016/j.regpep.2010.01.004. Epub 2010 Jan 18.

[275]. Polakis P. Drugging Wnt signalling in cancer. EMBO J. 2012 Jun 13;31(12):2737-46. doi: 10.1038/emboj.2012.126. Epub 2012 May 22.

[276]. Takahashi-Yanaga F, Kahn M. Targeting Wnt signaling: can we safely eradicate cancer stem cells? Clin Cancer Res. 2010 Jun 15;16(12):3153-62. doi: 10.1158/1078-0432.CCR-09-2943. Epub 2010 Jun 8.

[277]. Zöller M. CD44: can a cancer-initiating cell profit from an abundantly expressed molecule? Nat Rev Cancer. 2011 Apr;11(4):254-67. doi: 10.1038/nrc3023. Epub 2011 Mar 10.

[278]. Cassiman D, Libbrecht L, Sinelli N, Desmet V, Denef C, Roskams T. The vagal nerve stimulates activation of the hepatic progenitor cell compartment via muscarinic acetylcholine receptor type 3. Am J Pathol. 2002 Aug;161(2):521-30.

[279]. Revesz D, Tjernstrom M, Ben-Menachem E, Thorlin T. Effects of vagus nerve stimulation on rat hippocampal progenitor proliferation. Exp Neurol. 2008 Dec;214(2):259-65. doi: 10.1016/j.expneurol.2008.08.012. Epub 2008 Sep 4.

[280]. Salmanian S, Najafi SM, Rafipour M, Arjomand MR, Shahheydari H, Ansari S, Kashkooli L, Rasouli SJ, Jazi MS, Minaei T. Regulation of GSK-3beta and beta-Catenin by Galphaq in HEK293T cells. Biochem Biophys Res Commun. 2010 May 14;395(4):577-82. doi: 10.1016/j.bbrc.2010.04.087. Epub 2010 Apr 24.

[281]. Barker N, Clevers H. Leucine-rich repeat-containing G-protein-coupled receptors as markers of adult stem cells. Gastroenterology. 2010 May;138(5):1681-96. doi: 10.1053/j.gastro.2010.03.002.

[282]. Chen D, Nylander AG, Rehfeld JF, Axelson J, Ihse I, Håkanson R. Does vagotomy affect the growth of the pancreas in the rat? Scand J Gastroenterol. 1992 Jul;27(7):606-8.

[283]. Kodaira M, Kajimura M, Takeuchi K, Lin S, Hanai H, Kaneko E. Functional muscarinic m3 receptor expressed in gastric cancer cells stimulates tyrosine phosphorylation and MAP kinase. J Gastroenterol. 1999 Apr;34(2):163-71.

[284]. Wang L, Zhi X, Zhang Q, Wei S, Li Z, Zhou J, Jiang J, Zhu Y, Yang L, Xu H, Xu Z. Muscarinic receptor M3 mediates cell proliferation induced by acetylcholine and contributes to apoptosis in gastric cancer. Tumour Biol. 2016 Feb;37(2):2105-17. doi: 10.1007/s13277-015-4011-0. Epub 2015 Sep 7.

[285]. Oshima H, Oshima M. Mouse models of gastric tumors: Wnt activation and PGE2 induction. Pathol Int. 2010 Sep;60(9):599-607. doi: 10.1111/j.1440-1827.2010.02567.x.

[286]. Katoh Y, Katoh M. Hedgehog signaling pathway and gastric cancer. Cancer Biol Ther. 2005 Oct;4(10):1050-4. Epub 2005 Oct 18.

[287]. Lee DH, Lee SY, Oh SC. Hedgehog signaling pathway as a potential target in the treatment of advanced gastric cancer. Tumour Biol. 2017 Jun;39(6):1010428317692266. doi: 10.1177/1010428317692266.

[288]. Hirakawa S. From tumor lymphangiogenesis to lymphvascular niche. Cancer Sci. 2009 Jun;100(6):983-9. doi: 10.1111/j.1349-7006.2009.01142.x. Epub 2009 Feb 20.

[289]. Alitalo A, Detmar M. Interaction of tumor cells and lymphatic vessels in cancer progression. Oncogene. 2012 Oct 18;31(42):4499-508. doi: 10.1038/onc.2011.602. Epub 2011 Dec 19.

[290]. Oshima H, Oguma K, Du YC, Oshima M. Prostaglandin E2, Wnt, and BMP in gastric tumor mouse models. Cancer Sci. 2009 Oct;100(10):1779-85. doi: 10.1111/j.1349-7006.2009.01258.x. Epub 2009 Jun 23.

[291]. Tobler NE, Detmar M. Tumor and lymph node lymphangiogenesis--impact on cancer metastasis. J Leukoc Biol. 2006 Oct;80(4):691-6. Epub 2006 Jun 22.

[292]. Vigen RA, Kodama Y, Viset T, Fossmark R, Waldum H, Kidd M, Wang TC, Modlin IM, Chen D, Zhao CM. Immunohistochemical evidence for an impairment of autophagy in tumorigenesis of gastric carcinoids and adenocarcinomas in rodent models and patients. Histol Histopathol. 2013 Apr;28(4):531-42. doi: 10.14670/HH-28.531. Epub 2013 Feb 7.

[293]. Santarpia L, Lippman SM, El-Naggar AK. Targeting the MAPK-RAS-RAF signaling pathway in cancer therapy. Expert Opin Ther Targets. 2012 Jan;16(1):103-19. doi: 10.1517/14728222.2011.645805. Epub 2012 Jan 12.

[294]. Guo YJ, Pan WW, Liu SB, Shen ZF, Xu Y, Hu LL. ERK/MAPK signalling pathway and tumorigenesis. Exp Ther Med. 2020 Mar;19(3):1997-2007. doi: 10.3892/etm.2020.8454. Epub 2020 Jan 15.

[295]. Bikkavilli RK, Malbon CC. Mitogen-activated protein kinases and Wnt/beta-catenin signaling: Molecular conversations among signaling pathways. Commun Integr Biol. 2009;2(1):46-9.

[296]. Zhang Y, Pizzute T, Pei M. A review of crosstalk between MAPK and Wnt signals and its impact on cartilage regeneration. Cell Tissue Res. 2014 Dec;358(3):633-49. doi: 10.1007/s00441-014-2010-x. Epub 2014 Oct 14.

[297]. Takeda K, Kaisho T, Akira S. Toll-like receptors. Annu Rev Immunol. 2003;21:335-76. Epub 2001 Dec 19.

[298]. Rakoff-Nahoum S, Medzhitov R. Toll-like receptors and cancer. Nat Rev Cancer. 2009 Jan;9(1):57-63. doi: 10.1038/nrc2541. Epub 2008 Dec 4.

[299]. Kluwe J, Mencin A, Schwabe RF. Toll-like receptors, wound healing, and carcinogenesis. J Mol Med (Berl). 2009 Feb;87(2):125-38. doi: 10.1007/s00109-008-0426-z. Epub 2008 Dec 17.

[300]. Ioannou S, Voulgarelis M. Toll-like receptors, tissue injury, and tumourigenesis. Mediators Inflamm. 2010;2010. pii: 581837. doi: 10.1155/2010/581837. Epub 2010 Sep 14.

[301]. Hsieh CH, Rau CS, Kuo PJ, Liu SH, Wu CJ, Lu TH, Wu YC, Lin CW. Knockout of toll-like receptor impairs nerve regeneration after a crush injury. Oncotarget. 2017 Aug 10;8(46):80741-80756. doi: 10.18632/oncotarget.20206. eCollection 2017 Oct 6.

[302]. Okun E, Griffioen KJ, Lathia JD, Tang SC, Mattson MP, Arumugam TV. Toll-like receptors in neurodegeneration. Brain Res Rev. 2009 Mar;59(2):278-92. doi: 10.1016/j.brainresrev.2008.09.001. Epub 2008 Sep 12.

[303]. Kaczanowska S, Joseph AM, Davila E. TLR agonists: our best frenemy in cancer immunotherapy. J Leukoc Biol. 2013 Jun;93(6):847-63. doi: 10.1189/jlb.1012501. Epub 2013 Mar 8.

[304]. Stefani CB, de Oliveira RM, Silveira AA, Ferraz LF, Ribeiro ML, Gambero A, Pedrazzoli Júnior J. Expression of Toll-like receptors in enterocromaffin-like cells and their function in histamine release. Dig Dis Sci. 2012 Sep;57(9):2270-7. doi: 10.1007/s10620-012-2176-6. Epub 2012 May 23.

[305]. Goehler LE, Gaykema RP, Hansen MK, Anderson K, Maier SF, Watkins LR. Vagal immune-to-brain communication: a visceral chemosensory pathway. Auton Neurosci. 2000 Dec 20;85(1-3):49-59.

[306]. Barajon I, Serrao G, Arnaboldi F, Opizzi E, Ripamonti G, Balsari A, Rumio C. Toll-like receptors 3, 4, and 7 are expressed in the enteric nervous system and dorsal root ganglia. J Histochem Cytochem. 2009 Nov;57(11):1013-23. doi: 10.1369/jhc.2009.953539. Epub 2009 Jun 22.

[307]. Goethals S, Ydens E, Timmerman V, Janssens S. Toll-like receptor expression in the peripheral nerve. Glia. 2010 Nov 1;58(14):1701-9. doi: 10.1002/glia.21041.

[308]. Chiu IM, von Hehn CA, Woolf CJ. Neurogenic inflammation and the peripheral nervous system in host defense and immunopathology. Nat Neurosci. 2012 Jul 26;15(8):1063-7. doi: 10.1038/nn.3144.

[309]. Hosoi T, Okuma Y, Matsuda T, Nomura Y. Novel pathway for LPS-induced afferent vagus nerve activation: possible role of nodose ganglion. Auton Neurosci. 2005 Jun 15;120(1-2):104-7.

[310]. Schmausser B, Andrulis M, Endrich S, Müller-Hermelink HK, Eck M. Toll-like receptors TLR4, TLR5 and TLR9 on gastric carcinoma cells: an implication for interaction with Helicobacter pylori. Int J Med Microbiol. 2005 Jun;295(3):179-85.

[311]. So EY, Ouchi T. The application of Toll like receptors for cancer therapy. Int J Biol Sci. 2010 Nov 3;6(7):675-81.

[312]. Pimentel-Nunes P, Afonso L, Lopes P, Roncon-Albuquerque R Jr, Gonçalves N, Henrique R, Moreira-Dias L, Leite-Moreira AF, Dinis-Ribeiro M. Increased expression of toll-like receptors (TLR) 2, 4 and 5 in gastric dysplasia. Pathol Oncol Res. 2011 Sep;17(3):677-83. doi: 10.1007/s12253-011-9368-9. Epub 2011 Apr 1.

[313]. Jia D, Yang W, Li L, Liu H, Tan Y, Ooi S, Chi L, Filion LG, Figeys D, Wang L. β-Catenin and NF-κB co-activation triggered by TLR3 stimulation facilitates stem cell-like phenotypes in breast cancer. Cell Death Differ. 2015 Feb;22(2):298-310. doi: 10.1038/cdd.2014.145. Epub 2014 Sep 26.

[314]. Chen X, Cheng F, Liu Y, Zhang L, Song L, Cai X, You T, Fan X, Wang D, Gong A, Zhu H. Toll-like receptor 2 and Toll-like receptor 4 exhibit distinct regulation of cancer cell stemness mediated by cell death-induced high-mobility group box 1. EBioMedicine. 2019 Feb;40:135-150. doi: 10.1016/j.ebiom.2018.12.016. Epub 2019 Jan 22.

[315]. Frenette PS, Pinho S, Lucas D, Scheiermann C. Mesenchymal stem cell: keystone of the hematopoietic stem cell niche and a stepping-stone for regenerative medicine. Annu Rev Immunol. 2013;31:285-316. doi: 10.1146/annurev-immunol-032712-095919. Epub 2013 Jan 3.

[316]. Maryanovich M, Zahalka AH, Pierce H, Pinho S, Nakahara F, Asada N, Wei Q, Wang X, Ciero P, Xu J, Leftin A, Frenette PS. Adrenergic nerve degeneration in bone marrow drives aging of the hematopoietic stem cell niche. Nat Med. 2018 Jun;24(6):782-791. doi: 10.1038/s41591-018-0030-x. Epub 2018 May 7.

[317]. Gross ER, Gershon MD, Margolis KG, Gertsberg ZV, Li Z, Cowles RA. Neuronal serotonin regulates growth of the intestinal mucosa in mice. Gastroenterology. 2012 Aug;143(2):408-17.e2. doi: 10.1053/j.gastro.2012.05.007. Epub 2012 May 15.

[318]. Sato T, van Es JH, Snippert HJ, Stange DE, Vries RG, van den Born M, Barker N, Shroyer NF, van de Wetering M, Clevers H. Paneth cells constitute the niche for Lgr5 stem cells in intestinal crypts. Nature. 2011 Jan 20;469(7330):415-8. doi: 10.1038/nature09637. Epub 2010 Nov 28.

[319]. Powell DW, Pinchuk IV, Saada JI, Chen X, Mifflin RC. Mesenchymal cells of the intestinal lamina propria. Annu Rev Physiol. 2011;73:213-37. doi: 10.1146/annurev.physiol.70.113006.100646.

[320]. Farin HF, Van Es JH, Clevers H. Redundant sources of Wnt regulate intestinal stem cells and promote formation of Paneth cells. Gastroenterology. 2012 Dec;143(6):1518-1529.e7. doi: 10.1053/j.gastro.2012.08.031. Epub 2012 Aug 23.

[321]. Fujita M, Takami M, Usugane M, Nampei S, Taguchi T. Enhancement of gastric carcinogenesis in dogs given N-methyl-N'-nitro-N-nitrosoguanidine following vagotomy. Cancer Res. 1979 Mar;39(3):811-6.

[322]. Tatsuta M, Yamamura H, Iishi H, Ichii M, Noguchi S, Baba M, Taniguchi H. Promotion by vagotomy of gastric carcinogenesis induced by N-methyl-N'-nitro-N-nitrosoguanidine in Wistar rats. Cancer Res. 1985 Jan;45(1):194-7.

[323]. Tatsuta M, Iishi H, Yamamura H, Baba M, Taniguchi H. Effects of bilateral and unilateral vagotomy on gastric carcinogenesis induced by N-methyl-N'-nitro-N-nitrosoguanidine in Wistar rats. Int J Cancer. 1988 Sep 15;42(3):414-8.

[324]. Mordes JP, el Lozy M, Herrera MG, Silen W. Effects of vagotomy with and without pyloroplasty on weight and food intake in rats. Am J Physiol. 1979 Jan;236(1):R61-6.

[325]. Phillips RJ, Baronowsky EA, Powley TL. Regenerating vagal afferents reinnervate gastrointestinal tract smooth muscle of the rat. J Comp Neurol. 2000 Jun 5;421(3):325-46.

[326]. Phillips RJ, Baronowsky EA, Powley TL. Long-term regeneration of abdominal vagus: efferents fail while afferents succeed. J Comp Neurol. 2003 Jan 6;455(2):222-37.

[327]. CLARK CG. RECOVERY OF GASTRIC FUNCTION AFTER INCOMPLETE VAGOTOMY. Br J Surg. 1964 Jul;51:539-42.

[328]. Rivilis J. Collateral nerve sprouting and gastric secretory recovery. Surg Forum. 1969;20:317-9.

[329]. Powley TL, Chi MM, Baronowsky EA, Phillips RJ. Gastrointestinal tract innervation of the mouse: afferent regeneration and meal patterning after vagotomy. Am J Physiol Regul Integr Comp Physiol. 2005 Aug;289(2):R563-R574. Epub 2005 Apr 14.

[330]. Veenboer PW, Bosch JL. Long-term adherence to antimuscarinic therapy in everyday practice: a systematic review. J Urol. 2014 Apr;191(4):1003-8. doi: 10.1016/j.juro.2013.10.046. Epub 2013 Oct 16.

[331]. Batniji RK, Falk AN. Update on botulinum toxin use in facial plastic and head and neck surgery. Curr Opin Otolaryngol Head Neck Surg. 2004 Aug;12(4):317-22.

[332]. Duthie JB, Vincent M, Herbison GP, Wilson DI, Wilson D. Botulinum toxin injections for adults with overactive bladder syndrome. Cochrane Database Syst Rev. 2011 Dec 7;(12):CD005493. doi: 10.1002/14651858.CD005493.pub3.

[333]. Yamaguchi D, Tsuruoka N, Sakata Y, Shimoda R, Fujimoto K, Iwakiri R. Safety and efficacy of botulinum toxin injection therapy for esophageal achalasia in Japan. J Clin Biochem Nutr. 2015 Nov;57(3):239-43. doi: 10.3164/jcbn.15-47. Epub 2015 Oct 17.

[334]. Pasricha TS, Pasricha PJ. Botulinum Toxin Injection for Treatment of Gastroparesis. Gastrointest Endosc Clin N Am. 2019 Jan;29(1):97-106. doi: 10.1016/j.giec.2018.08.007. Epub 2018 Sep 28.

[335]. Topazian M, Camilleri M, De La Mora-Levy J, Enders FB, Foxx-Orenstein AE, Levy MJ, Nehra V, Talley NJ. Endoscopic ultrasound-guided gastric botulinum toxin injections in obese subjects: a pilot study. Obes Surg. 2008 Apr;18(4):401-7. doi: 10.1007/s11695-008-9442-x. Epub 2008 Feb 20.

[336]. Pero R, Coretti L, Lembo F. Botulinum Toxin A for Controlling Obesity. Toxins (Basel). 2016 Sep 26;8(10). pii: E281.

[337]. Koga S, Kawaguchi H, Kishimoto H, Tanaka K, Miyano Y, Kimura O, Takeda R, Nishidoi H. Therapeutic significance of noncurative gastrectomy for gastric cancer with liver metastasis. Am J Surg. 1980 Sep;140(3):356-9.

[338]. Bozzetti F, Bonfanti G, Audisio RA, Doci R, Dossena G, Gennari L, Andreola S. Prognosis of patients after palliative surgical procedures for carcinoma of the stomach. Surg Gynecol Obstet. 1987 Feb;164(2):151-4.

[339]. Bonenkamp JJ, Sasako M, Hermans J, van de Velde CJ. Tumor load and surgical palliation in gastric cancer. Hepatogastroenterology. 2001 Sep-Oct;48(41):1219-21.

[340]. Hartgrink HH, Putter H, Klein Kranenbarg E, Bonenkamp JJ, van de Velde CJ; Dutch Gastric Cancer Group. Value of palliative resection in gastric cancer. Br J Surg. 2002 Nov;89(11):1438-43.

[341]. DeSesso JM, Jacobson CF. Anatomical and physiological parameters affecting gastrointestinal absorption in humans and rats. Food Chem Toxicol. 2001 Mar;39(3):209-28.

[342]. Lopez PP, Nicholson SE, Burkhardt GE, Johnson RA, Johnson FK. Development of a sleeve gastrectomy weight loss model in obese Zucker rats. J Surg Res. 2009 Dec;157(2):243-50. doi: 10.1016/j.jss.2008.10.025. Epub 2008 Nov 24.

[343]. Earlam R. Bile reflux and the Roux en Y anastomosis. Br J Surg. 1983 Jul;70(7):393-7.

[344]. Stenström B, Furnes MW, Tømmerås K, Syversen U, Zhao CM, Chen D. Mechanism of gastric bypass-induced body weight loss: one-year follow-up after micro-gastric bypass in rats. J Gastrointest Surg. 2006 Dec;10(10):1384-91.

[345]. Berthoud HR. The vagus nerve, food intake and obesity. Regul Pept. 2008 Aug 7;149(1-3):15-25. doi: 10.1016/j.regpep.2007.08.024. Epub 2008 Mar 25.

[346]. Johannessen H, Revesz D, Kodama Y, Cassie N, Skibicka KP, Barrett P, Dickson S, Holst J, Rehfeld J, van der Plasse G, Adan R, Kulseng B, Ben-Menachem E, Zhao CM, Chen D. Vagal Blocking for Obesity Control: a Possible Mechanism-Of-Action. Obes Surg. 2017 Jan;27(1):177-185. doi: 10.1007/s11695-016-2278-x.

[347]. Buchwald H, Oien DM. Metabolic/bariatric surgery worldwide 2011. Obes Surg. 2013 Apr;23(4):427-36. doi: 10.1007/s11695-012-0864-0.

[348]. Clapp B, Wynn M, Martyn C, Foster C, O'Dell M, Tyroch A. Long term (7 or more years) outcomes of the sleeve gastrectomy: a meta-analysis. Surg Obes Relat Dis. 2018 Jun;14(6):741-747. doi: 10.1016/j.soard.2018.02.027. Epub 2018 Mar 6.

[349]. Lauti M, Kularatna M, Hill AG, MacCormick AD. Weight Regain Following Sleeve Gastrectomy-a Systematic Review. Obes Surg. 2016 Jun;26(6):1326-34. doi: 10.1007/s11695-016-2152-x.

[350]. Vidal J, Ibarzabal A, Romero F, Delgado S, Momblán D, Flores L, Lacy A. Type 2 diabetes mellitus and the metabolic syndrome following sleeve gastrectomy in severely obese subjects. Obes Surg. 2008 Sep;18(9):1077-82. doi: 10.1007/s11695-008-9547-2. Epub 2008 Jun 3.

[351]. Juodeikis Ž, Brimas G. Long-term results after sleeve gastrectomy: A systematic review. Surg Obes Relat Dis. 2017 Apr;13(4):693-699. doi: 10.1016/j.soard.2016.10.006. Epub 2016 Oct 17.

[352]. Johannessen H, Kodama Y, Zhao CM, Sousa MM, Slupphaug G, Kulseng B, Chen D. Eating behavior and glucagon-like peptide-1-producing cells in interposed ileum and pancreatic islets in rats subjected to ileal interposition associated with sleeve gastrectomy. Obes Surg. 2013 Jan;23(1):39-49. doi: 10.1007/s11695-012-0750-9.

[353]. Wynne K, Stanley S, McGowan B, Bloom S. Appetite control. J Endocrinol. 2005 Feb;184(2):291-318.

[354]. Watanapa P, Efa EF, Beardshall K, Calam J, Sarraf CE, Alison MR, Williamson RC. Inhibitory effect of a cholecystokinin antagonist on the proliferative response of the pancreas to pancreatobiliary diversion. Gut. 1991 Sep;32(9):1049-54.

[355]. Miazza BM, Widgren S, Chayvialle JA, Nicolet T, Loizeau E. Exocrine pancreatic nodules after longterm pancreaticobiliary diversion in rats. An effect of raised CCK plasma concentrations. Gut. 1987;28 Suppl:269-73.

[356]. Borg CM, le Roux CW, Ghatei MA, Bloom SR, Patel AG. Biliopancreatic diversion in rats is associated with intestinal hypertrophy and with increased GLP-1, GLP-2 and PYY levels. Obes Surg. 2007 Sep;17(9):1193-8.

[357]. Buchwald H, Avidor Y, Braunwald E, Jensen MD, Pories W, Fahrbach K, Schoelles K. Bariatric surgery: a systematic review and meta-analysis. JAMA. 2004 Oct 13;292(14):1724-37.

[358]. Kral JG, Buckley MC, Kissileff HR, Schaffner F. Metabolic correlates of eating behavior in severe obesity. Int J Obes Relat Metab Disord. 2001 Feb;25(2):258-64.

[359]. Takayama S, Akamine Y, Okabe T, Koya Y, Haraguchi M, Miyata Y, Sakai T, Sakura H, Sasaki T. Rate of eating and body weight in patients with type 2 diabetes or hyperlipidaemia. J Int Med Res. 2002 Jul-Aug;30(4):442-4.

[360]. Otsuka R, Tamakoshi K, Yatsuya H, Murata C, Sekiya A, Wada K, Zhang HM, Matsushita K, Sugiura K, Takefuji S, OuYang P, Nagasawa N, Kondo T, Sasaki S, Toyoshima H. Eating fast leads to obesity: findings based on self-administered questionnaires among middle-aged Japanese men and women. J Epidemiol. 2006 May;16(3):117-24.

[361]. Furnes MW, Zhao CM, Chen D. Development of obesity is associated with increased calories per meal rather than per day. A study of high-fat diet-induced obesity in young rats. Obes Surg. 2009 Oct;19(10):1430-8. doi: 10.1007/s11695-009-9863-1. Epub 2009 Jun 9.

[362]. Gudbrandsen OA, Kodama Y, Mjøs SA, Zhao CM, Johannessen H, Brattbakk HR, Haugen C, Kulseng B, Mellgren G, Chen D. Effects of duodenal switch alone or in combination with sleeve gastrectomy on body weight and lipid metabolism in rats. Nutr Diabetes. 2014 Jun 30;4:e124. doi: 10.1038/nutd.2014.22.

[363]. Furnes MW, Tømmerås K, Arum CJ, Zhao CM, Chen D. Gastric bypass surgery causes body weight loss without reducing food intake in rats. Obes Surg. 2008 Apr;18(4):415-22. doi: 10.1007/s11695-007-9392-8. Epub 2008 Feb 5.

[364]. Pories WJ. Bariatric surgery: risks and rewards. J Clin Endocrinol Metab. 2008 Nov;93(11 Suppl 1):S89-96. doi: 10.1210/jc.2008-1641.

[365]. Astrup A, Gøtzsche PC, van de Werken K, Ranneries C, Toubro S, Raben A, Buemann B. Meta-analysis of resting metabolic rate in formerly obese subjects. Am J Clin Nutr. 1999 Jun;69(6):1117-22.

[366]. Bays HE. Current and investigational antiobesity agents and obesity therapeutic treatment targets. Obes Res. 2004 Aug;12(8):1197-211.

[367]. Laurenius A, Larsson I, Bueter M, Melanson KJ, Bosaeus I, Forslund HB, Lönroth H, Fändriks L, Olbers T. Changes in eating behaviour and meal pattern following Roux-en-Y gastric bypass. Int J Obes (Lond). 2012 Mar;36(3):348-55. doi: 10.1038/ijo.2011.217. Epub 2011 Nov 29.

[368]. Bueter M, le Roux CW. Gastrointestinal hormones, energy balance and bariatric surgery. Int J Obes (Lond). 2011 Sep;35 Suppl 3:S35-9. doi: 10.1038/ijo.2011.146.

[369]. Ashrafian H, Bueter M, Ahmed K, Suliman A, Bloom SR, Darzi A, Athanasiou T. Metabolic surgery: an evolution through bariatric animal models. Obes Rev. 2010 Dec;11(12):907-20. doi: 10.1111/j.1467-789X.2009.00701.x.

[370]. Mathes CM, Spector AC. Food selection and taste changes in humans after Roux-en-Y gastric bypass surgery: a direct-measures approach. Physiol Behav. 2012 Nov 5;107(4):476-83. doi: 10.1016/j.physbeh.2012.02.013. Epub 2012 Feb 16.

[371]. Keith B, Simon MC. Hypoxia-inducible factors, stem cells, and cancer. Cell. 2007 May 4;129(3):465-72.

[372]. Filatova A, Acker T, Garvalov BK. The cancer stem cell niche(s): the crosstalk between glioma stem cells and their microenvironment. Biochim Biophys Acta. 2013 Feb;1830(2):2496-508. doi: 10.1016/j.bbagen.2012.10.008. Epub 2012 Oct 16.

[373]. Kaneko K, Yamaguchi H, Saito T, Yano T, Oono Y, Ikematsu H, Nomura S, Sato A, Kojima M, Esumi H, Ochiai A. Hypoxia imaging endoscopy equipped with laser light source from preclinical live animal study to first-in-human subject research. PLoS One. 2014 Jun 10;9(6):e99055. doi: 10.1371/journal.pone.0099055. eCollection 2014.

[374]. Gibbs-Strauss SL, Nasr KA, Fish KM, Khullar O, Ashitate Y, Siclovan TM, Johnson BF, Barnhardt NE, Tan Hehir CA, Frangioni JV. Nerve-highlighting fluorescent contrast agents for image-guided surgery. Mol Imaging. 2011 Apr;10(2):91-101.

[375]. Gray D, Kim E, Cotero V, Staudinger P, Yazdanfar S, Hehir CT. Compact Fluorescence and White Light Imaging System for Intraoperative Visualization of Nerves. Proc SPIE Int Soc Opt Eng. 2012 Feb 3;8207. doi: 10.1117/12.905354.

Paper I

CANCER

Denervation suppresses gastric tumorigenesis

Chun-Mei Zhao,[1]* Yoku Hayakawa,[2]* Yosuke Kodama,[1] Sureshkumar Muthupalani,[3] Christoph B. Westphalen,[2,4] Gøran T. Andersen,[1,5] Arnar Flatberg,[1] Helene Johannessen,[1] Richard A. Friedman,[6] Bernhard W. Renz,[2] Arne K. Sandvik,[1,7] Vidar Beisvag,[1] Hiroyuki Tomita,[8] Akira Hara,[8] Michael Quante,[9] Zhishan Li,[10] Michael D. Gershon,[10] Kazuhiro Kaneko,[11] James G. Fox,[3] Timothy C. Wang,[2†] Duan Chen[1†]

The nervous system plays an important role in the regulation of epithelial homeostasis and has also been postulated to play a role in tumorigenesis. We provide evidence that proper innervation is critical at all stages of gastric tumorigenesis. In three separate mouse models of gastric cancer, surgical or pharmacological denervation of the stomach (bilateral or unilateral truncal vagotomy, or local injection of botulinum toxin type A) markedly reduced tumor incidence and progression, but only in the denervated portion of the stomach. Vagotomy or botulinum toxin type A treatment also enhanced the therapeutic effects of systemic chemotherapy and prolonged survival. Denervation-induced suppression of tumorigenesis was associated with inhibition of Wnt signaling and suppression of stem cell expansion. In gastric organoid cultures, neurons stimulated growth in a Wnt-mediated fashion through cholinergic signaling. Furthermore, pharmacological inhibition or genetic knockout of the muscarinic acetylcholine M_3 receptor suppressed gastric tumorigenesis. In gastric cancer patients, tumor stage correlated with neural density and activated Wnt signaling, whereas vagotomy reduced the risk of gastric cancer. Together, our findings suggest that vagal innervation contributes to gastric tumorigenesis via M_3 receptor–mediated Wnt signaling in the stem cells, and that denervation might represent a feasible strategy for the control of gastric cancer.

INTRODUCTION

The nervous system regulates epithelial homeostasis in different ways, and this regulation by the nervous system partly involves modulation of stem and progenitor cells (*1*, *2*). There is also crosstalk between tumor cells and nerves, such that tumors induce active neurogenesis, resulting in increased neuronal density in preneoplastic and neoplastic tissues (*3*–*6*). In addition, activation of muscarinic receptors has been shown to promote cell transformation and cancer progression (*3*–*6*). A recent study demonstrated that prostate tumors are infiltrated by autonomic nerves contributing to cancer development and dissemination (*7*). Given the potential ability of nerves to influence gut stem and progenitor cells, and the prevailing notion that persistently elevated gut epithelial proliferation predisposes to cancer formation, it is believed that axonal reflexes could also modulate the conversion of stem or progenitor cells into cancer cells (*8*, *9*).

Gastric cancer is the fifth most common cancer and the third leading cause of cancer mortality worldwide, with a 5-year survival rate of less than 25% (*10*, *11*). It has been demonstrated that vagotomy decreases gastric mucosal thickness and cellular proliferation (*12*, *13*). An epidemiological study showed that the risk of gastric cancer [standardized incidence ratio (SIR)] after vagotomy was not reduced during the first 10-year period, but was reduced by 50% (SIR 0.5) during the second 10-year follow-up (*14*, *15*). Here, we provide evidence that proper innervation is critical for gastric tumorigenesis, and suggest that nerves may represent a therapeutic target for the treatment of gastric cancer.

RESULTS

Gastric lesser curvature has high vagal innervation and high incidence of tumors

In humans, there is a higher incidence of gastric cancer in the lesser (~80% of tumors) than the greater curvature (*16*, *17*). We also observed this distribution in the INS-GAS mouse model, a genetic mouse model of spontaneous gastric cancer (*18*, *19*), in which there was a similar prevalence (77%) of tumors in the lesser curvature (Fig. 1A). INS-GAS mice do not display obvious preneoplastic lesions until 6 months of age, but afterward, they develop gastric cancer through stages of atrophy, metaplasia, and finally, dysplasia at 12 months of age (*18*, *19*). Topographic analysis of vagus nerve fibers and terminals in the murine stomach revealed a higher density of neurons and larger ganglia in the lesser curvature compared to the greater curvature (Fig. 1B), correlating with the observed pattern of tumor formation. This possible association between the distribution of vagal nerve fibers and the appearance of gastric tumors in INS-GAS mice prompted us to study the role of nerves in gastric tumorigenesis (fig. S1 and table S1).

Surgical denervation at preneoplastic stage attenuates tumorigenesis in mouse models of gastric cancer

In the first set of experiments, vagotomy was performed in INS-GAS mice at 6 months of age. Subsequently, the effects of vagotomy were

[1]Department of Cancer Research and Molecular Medicine, Norwegian University of Science and Technology, Trondheim 7491, Norway. [2]Division of Digestive and Liver Diseases, Columbia University College of Physicians and Surgeons, New York, NY 10032–3802, USA. [3]Division of Comparative Medicine, Massachusetts Institute of Technology, Boston, MA 02139, USA. [4]Medizinische Klinik III, Klinikum der Universität München, Campus Großhadern, 81377 München, Germany. [5]Department of Surgery, St. Olavs University Hospital, Trondheim 7006, Norway. [6]Biomedical Informatics Shared Resource, Herbert Irving Comprehensive Cancer Center, Columbia University College of Physicians and Surgeons, New York, NY 10032, USA. [7]Department of Gastrointestinal and Liver Diseases, St. Olavs University Hospital, Trondheim 7006, Norway. [8]Department of Tumor Pathology, Gifu University Graduate School of Medicine, Gifu 501-1112, Japan. [9]II. Medizinische Klinik, Klinikum rechts der Isar, Technische Universität München, München 81675, Germany. [10]Department of Pathology and Cell Biology, Columbia University College of Physicians and Surgeons, New York, NY 10032, USA. [11]Department of Gastroenterology and Endoscopy Division, National Cancer Center Hospital East, Chiba 277-8577, Japan.
*These authors contributed equally to this work.
†Corresponding authors. E-mails: duan.chen@ntnu.no (D.C.); tcw21@columbia.edu (T.C.W.)

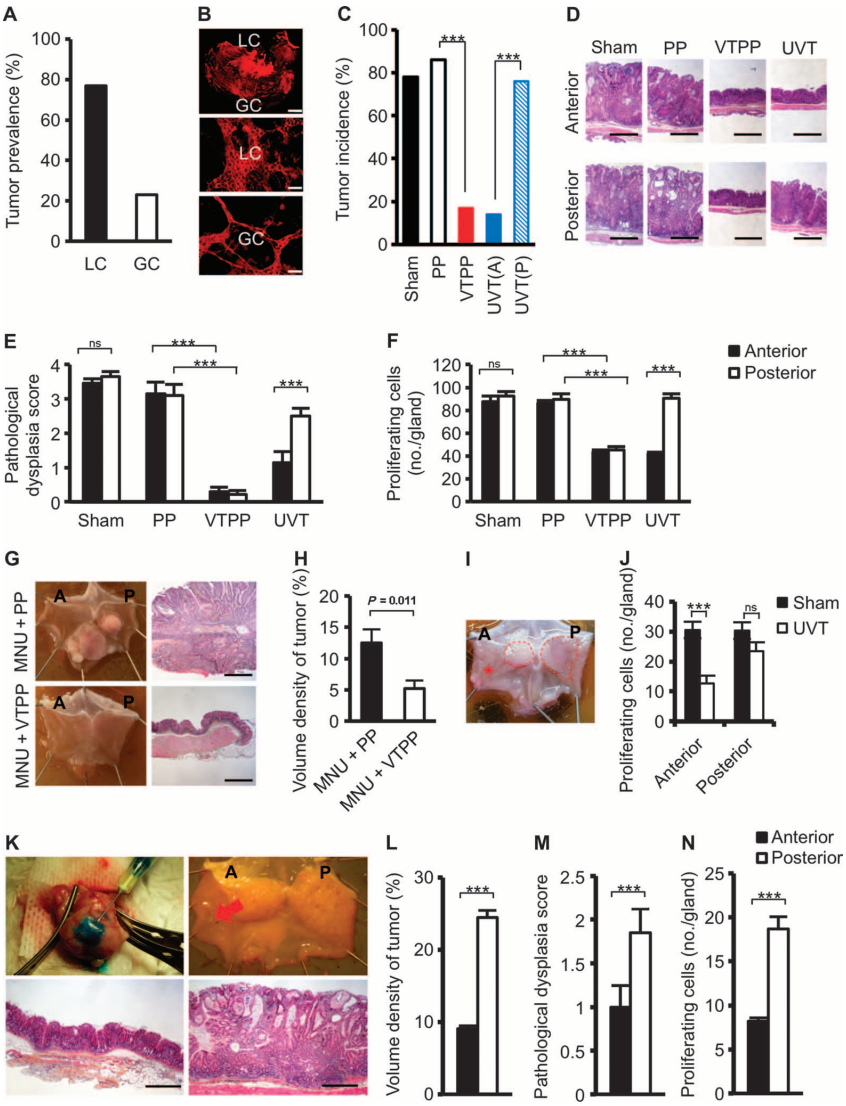

Fig. 1. Denervation attenuates tumorigenesis at the preneoplastic stage in mouse models of gastric cancer. (**A**) Tumor prevalence at the lesser curvature (LC) and greater curvature (GC) of the stomach of INS-GAS mice. (**B**) Images of carbocyanine dye (DiI)–labeled vagal terminals in an adult mouse stomach. A montage of a low-power image showing the lesser curvature and greater curvature of the gastric wall (top scale bar, 2.0 mm), and higher-power images of lesser curvature (middle) and greater curvature (bottom) show a higher density of vagal innervation in lesser curvature than in greater curvature (89 and 54% of the visual field, estimated by point counting method) (middle and bottom scale bars, 72 μm). (**C**) Tumor incidence at 12 months of age in INS-GAS mice that underwent sham operation (Sham), pyloroplasty alone (PP), bilateral vagotomy with pyloroplasty (VTPP), or anterior unilateral vagotomy (UVT) (A, anterior; P, posterior side of the stomachs) at 6 months of age. ***$P = 4.9 \times 10^{-7}$ (VTPP versus PP), $P = 1.32 \times 10^{-6}$ [UVT(A) versus UVT(P)] (Fisher's exact test). (**D**) Representative microphotographs of histopathological appearance of the anterior and posterior sides of the stomach from INS-GAS mice (at 12 months of age) that underwent sham, PP, VTPP, and UVT at 6 months of age. Scale bars, 100 μm. (**E**) Pathological score for dysplasia. Means ± SEM. Comparisons between anterior and posterior sides were performed by paired *t* test within sham ($n = 27$) and UVT ($n = 30$), or by Tukey test between PP ($n = 25$) and VTPP ($n = 25$). ***$P = 5.31 \times 10^{-5}$ (UVT), $P = 0.0001$ or 0.00006 (PP and VTPP, anterior or posterior side, respectively). ns, not significant ($P = 0.987$). (**F**) Number of proliferating cells. Means ± SEM. Comparisons between anterior and posterior sides were performed by paired *t* test within sham ($n = 27$) and UVT ($n = 30$), or by Tukey test between PP ($n = 25$) and VTPP ($n = 25$). ***$P = 5.77 \times 10^{-3}$ (UVT), $P = 1.90 \times 10^{-4}$ (anterior), and $P = 1.49 \times 10^{-3}$ (posterior) between PP and VTPP. ns, not significant ($P = 0.229$). (**G**) Representative photographs showing gross appearance of stomachs opened along the greater curvature and corresponding microphotographs of histopathological appearance of the stomachs (antrum) from mice treated with MNU + PP or MNU + VTPP. Scale bars, 100 μm. (**H**) Volume density of tumor (measured by point counting method). Means ± SEM. Student's *t* test was used to compare between MNU + PP ($n = 11$) and MNU + VTPP ($n = 9$). (**I**) Representative photograph showing gross appearance of gastric tumors (indicated by dashed line) in a stomach opened along the greater curvature from an *Hp*-infected H^+/K^+–ATPase–IL-1β mouse, which underwent UVT in the anterior side (indicated by asterisk). (**J**) Number of proliferating cells in *Hp*-infected H^+/K^+–ATPase–IL-1β mouse stomachs subjected to UVT in the anterior side. Means ± SEM. ***$P = 0.00006$ (Student's *t* test). ns, not significant ($P = 0.120$) between sham ($n = 12$) and UVT ($n = 12$) in the anterior and the posterior sides. (**K**) Photographs showing the Botox injection procedure (upper left), gross appearance of Botox-injected stomach after 6 months (A, anterior where Botox was injected; P, posterior) (upper right), and representative microphotographs of histopathological appearance of anterior (lower left) and posterior (lower right) stomach (corpus). Red arrow, injection site. Scale bars, 100 μm. (**L** to **N**) Volume density of tumor, pathological score for dysplasia, and number of proliferating cells after anterior Botox injection. Means ± SEM ($n = 16$). ***$P = 2.75 \times 10^{-11}$ (L), $P = 0.01$ (M), or $P = 0.001$ (N) between the anterior and posterior sides of the stomach (paired *t* test).

examined 6 months after surgery. One hundred seven INS-GAS mice were subjected to either subdiaphragmatic VTPP, UVT (fig. S2), sham operation, or PP. The unilateral vagotomy approach takes advantage of the fact that each (anterior or posterior) vagal trunk innervates only one-half of the stomach. Consequently, denervation of one side of the stomach does not impair the overall functional capacity of the stomach, leaving gastric acid output, circulating gastrin levels, and gastric motility unchanged (*13*, *20*).

Six months after surgery, body weight was unchanged in either male or female mice (fig. S3). Tumor incidence was 17% after VTPP versus 86% after PP alone, 14% in the anterior side versus 76% in the posterior side after anterior UVT, and 78% in the sham-operated mice (Fig. 1C). Histological examination revealed the reduction of mucosal thickness after VTPP (compared to PP) or UVT (compared to the corresponding posterior side) (Fig. 1D and fig. S4), indicating successful denervation (*12*, *13*). Pathological evaluation (*21*) revealed that vagotomy attenuated the score for dysplasia and reduced the number of proliferating cells (Fig. 1, E and F) and the scores for inflammation, epithelial defects, oxyntic atrophy, epithelial hyperplasia, pseudopyloric metaplasia, and gastric histological activity index (GHAI) (fig. S5, A to F).

To confirm these findings, we tested the surgical approach in two other mouse models of gastric cancer, namely, the carcinogen-induced [*N*-nitroso-*N*-methylurea (MNU)] (*22*) and the *Helicobacter pylori* (*Hp*)–infected H^+/K^+–ATPase (adenosine triphosphatase)–IL-1β (interleukin-1β) mouse models (*23*). In the MNU model, VTPP performed 1 week after completion of MNU treatment inhibited tumor development at 13 months of age (Fig. 1, G and H). Infection of H^+/K^+–ATPase–IL-1β mice with *Hp* accelerated gastric tumorigenesis, resembling *Hp*-related atrophy-metaplasia-dysplasia sequence in humans. UVT performed 8.5 months after *Hp* infection (at 12 months of age) reduced tumor size and number of proliferating cells in the denervated side of the stomach at 18 months of age (Fig. 1, I and J). Thus, the findings from these three independent models demonstrate the importance of functional innervation in gastric tumorigenesis.

Pharmacological denervation at an early preneoplastic stage attenuates gastric tumorigenesis

To prove that the effects of surgical denervation were primarily local (acting at vagus nerve terminals within the gastric mucosa), unilateral injection of botulinum toxin A (Botox) into the gastric wall was performed in INS-GAS mice at 6 months of age. Botox enters into the axon terminal through vesicle internalization and cleaves synaptosomal-associated protein 25, leading to impaired exocytosis of neurotransmitters, including acetylcholine (*24*). Botox was injected subserosally along the greater curvature in the anterior side of the stomach (Fig. 1K). Six months later, tumor size, score for dysplasia, and number of proliferating cells were markedly reduced in the anterior wall compared with the posterior side of the stomach (Fig. 1, L to N). Moreover, these changes were associated with attenuated scores for inflammation, epithelial defects, atrophy, hyperplasia, pseudopyloric metaplasia, and GHAI (fig. S6, A and B). Hence, these findings confirm an important role of local signaling from vagus nerve endings in early gastric tumorigenesis.

Surgical or pharmacological denervation attenuates gastric tumor progression

Because vagotomy or Botox treatment had a protective effect at preneoplastic stages, we next examined whether gastric denervation could also inhibit tumor progression at later stages. INS-GAS mice at 8, 10, or 12 months of age were subjected to anterior UVT and euthanized at 18 months of age. In these mice, the tumors were smaller with less severe dysplasia in the anterior side compared to the posterior side of the stomach, suggesting that denervation inhibits tumor progression in mice with established neoplastic changes (Fig. 2, A to C).

Whereas the average life span of wild-type FVB/N mice is well over 24 months, the survival of INS-GAS mice at 18 months of age was 53% (16 of 30 mice). Attenuation of tumor burden by UVT improved the 18-month survival when compared to age-matched INS-GAS mice: 71% when UVT was performed at 8 months, 64% when performed at 10 months, and 67% when performed at 12 months, respectively (Fig. 2D). Next, INS-GAS mice at 12 months of age were subjected to vehicle or Botox treatment unilaterally or bilaterally, with or without UVT. The tumor cell proliferation was reduced in the anterior side of the stomach where Botox was injected, when compared to the posterior side or vehicle-treated anterior side (Fig. 2E). The combination of UVT and Botox did not further reduce cellular proliferation, indicating that vagotomy and Botox likely act through the same mechanism. These results further suggest that surgical or pharmacological denervation inhibits gastric cancer progression even when applied at later stages of gastric tumorigenesis.

Denervation enhances the effect of chemotherapy in the treatment of gastric cancer

Next, we examined whether denervation could enhance the effects of systemic chemotherapy in gastric cancer. INS-GAS mice at 12 to 14 months of age received systemic administration of 5-FU + oxaliplatin or saline along with unilateral Botox treatment or UVT. The experiment was designed such that the nondenervated half of the stomach in each animal served as an internal control, either a chemotherapy-only control (the posterior side of the stomach in two of the groups received chemotherapy alone) or an untreated control. An additional group of INS-GAS mice was included as untreated controls. As early as 2 months after starting treatment, tumor size was reduced in mice treated with chemotherapy, specifically in the denervated areas of the stomach (the anterior side) after unilateral vagotomy or Botox injection (Fig. 2, F and G). The combination of either Botox or UVT with chemotherapy increased survival compared to chemotherapy alone (Fig. 2H). Together, these findings suggest that the combination of denervation and chemotherapy has an enhanced effect on tumor growth and survival.

Denervation inhibits gastric Wnt signaling and suppresses stem cell expansion through the M_3 receptor

We performed gene expression profiling in INS-GAS mice versus wild-type mice, and in unilaterally vagotomized INS-GAS mice (UVT performed at 6 months of age). Comparison between INS-GAS mice and wild-type mice showed up-regulation of the Wnt signaling pathway in INS-GAS mice (fig. S7). Comparison between the vagotomized anterior and the untreated posterior side of the same stomach revealed many differentially expressed KEGG pathways, including those involved in gastric acid secretion, mitogen-activated protein kinase signaling, cell cycle, apoptosis, autophagy, vascular endothelial growth factor signaling, and actin cytoskeleton (fig. S8). The Wnt and Notch signaling pathways were markedly inhibited in the vagotomized side [validated by quantitative reverse transcription polymerase chain reaction (qRT-PCR) arrays] (Fig. 3 and fig. S9). The inhibition of Wnt signaling was persistent at 2, 6, 8, and 10 months after vagotomy.

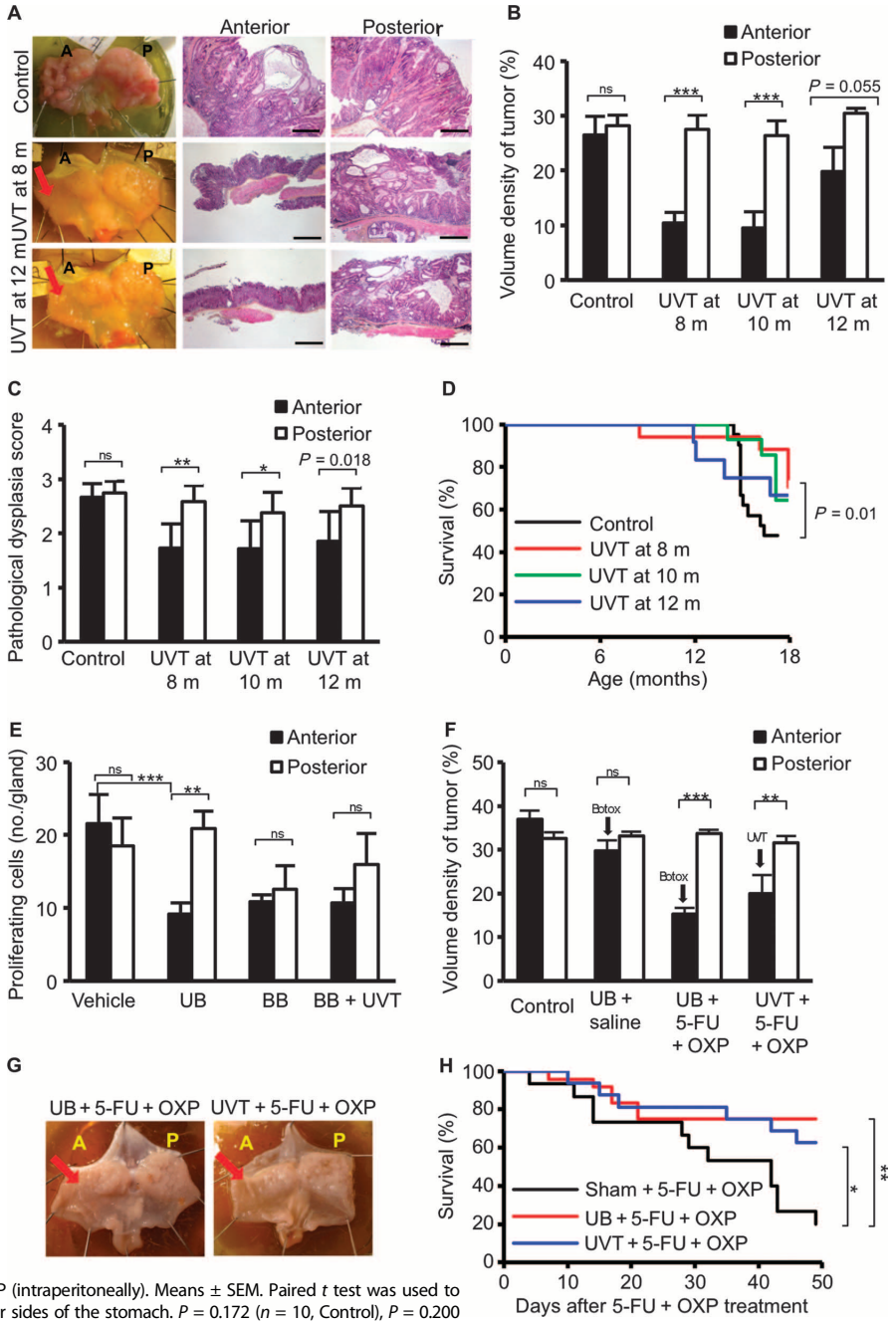

Fig. 2. Denervation attenuates gastric tumor progression in mice. (**A**) Gross appearance of mouse stomachs at 18 months of age and representative microphotographs of the histopathological appearance of the corpus region of the anterior and posterior sides of the stomach from age-matched INS-GAS mice (Control) and mice that underwent anterior UVT at 8 or 12 months of age. Scale bars, 100 μm. Red arrows, vagotomy side. (**B**) Volume density of tumor. Means ± SEM. Paired *t* test between the anterior and the posterior sides of the stomach: $P = 0.589$ ($n = 21$, Control), $P = 2.56 \times 10^{-5}$ ($n = 17$, UVT at 8 months of age), $P = 2.17 \times 10^{-4}$ ($n = 14$, UVT at 10 months), $P = 0.055$ ($n = 12$, UVT at 12 months). (**C**) Pathological score for dysplasia. Means ± SEM. Paired *t* test between the anterior and the posterior sides of the stomach: $P = 0.38$ ($n = 21$, Control), $P = 0.002$ ($n = 17$, UVT at 8 months of age), $P = 0.047$ ($n = 14$, UVT at 10 months), $P = 0.018$ ($n = 12$, UVT at 12 months). (**D**) Kaplan-Meier curves showing survival of INS-GAS mice that underwent UVT at 8 (red), 10 (green), or 12 months of age (blue), or of age-matched INS-GAS mice (Control) (black). $P = 0.01$ between control and UVT groups at 8 months. (**E**) Proliferating cells in the anterior and posterior mucosa of the stomach of INS-GAS mice at 2 months after vagotomy and/or Botox injection. Means ± SEM. Paired *t* test was used to compare the anterior and posterior sides of the stomach. $P = 0.291$ ($n = 6$, Vehicle), $P = 0.007$ [$n = 6$, unilateral anterior Botox (UB)], $P = 0.595$ [$n = 7$, bilateral Botox (BB)], $P = 0.326$ [$n = 7$, bilateral Botox plus anterior UVT (BB + UVT)], $P = 0.0007$ (Vehicle anterior versus UB anterior, Dunnett's test). (**F**) Volume density of tumor in INS-GAS mice subjected to saline (intraperitoneally) (Control), UB + saline (intraperitoneally), UB + 5-fluorouracil (5-FU) + oxaliplatin (OXP) (intraperitoneally), or UVT + 5-FU + OXP (intraperitoneally). Means ± SEM. Paired *t* test was used to compare the anterior and posterior sides of the stomach. $P = 0.172$ ($n = 10$, Control), $P = 0.200$ ($n = 10$, UB + saline), $P = 0.0004$ ($n = 24$, UB + 5-FU + OXP), $P = 0.006$ ($n = 16$, UVT + 5-FU + OXP). (**G**) Gross appearance of representative stomachs from INS-GAS mice subjected to 5-FU + OXP with UB or UVT (reduced tumor burden indicated by arrows). (**H**) Kaplan-Meier curves showing survival of INS-GAS mice that underwent sham operation and 5-FU + OXP treatment (black), UB and 5-FU + OXP (red), or anterior UVT and 5-FU + OXP (blue). *$P = 0.041$, **$P = 0.0069$.

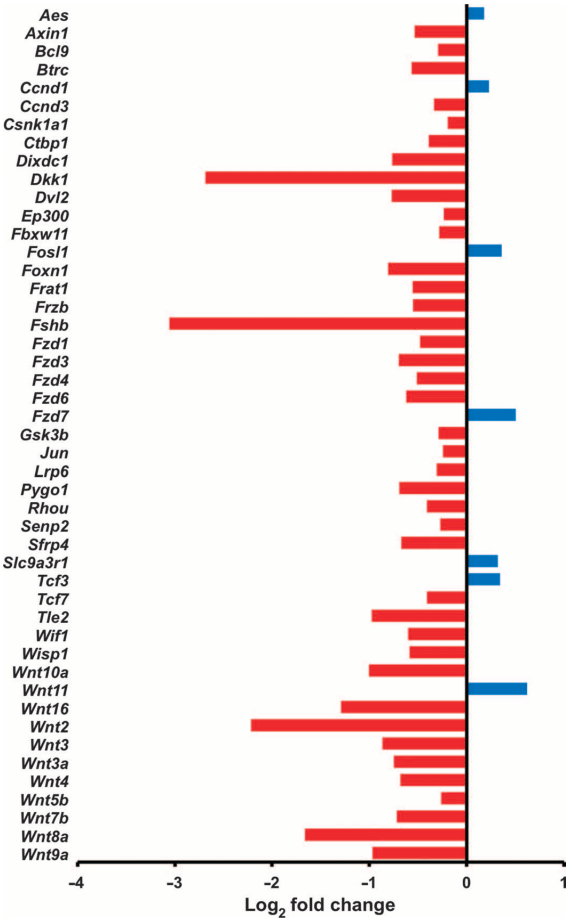

Fig. 3. Denervation leads to inhibition of Wnt signaling in the mouse model of gastric cancer. Gene expression of Wnt signaling pathway (determined by qRT-PCR array analysis) in vagotomized anterior stomach of INS-GAS mice at 12 months of age (6 months UVT). Log_2 fold changes of expressed genes in comparison with the posterior side of the same stomach are shown. Red, down-regulation; blue, up-regulation.

Inflammation-related pathways, including T cell receptor signaling, natural killer cell–mediated cytotoxicity, leukocyte transendothelial migration, and chemokine signaling, were activated at 2 months, but then inhibited at 4 and 6 months after vagotomy, whereas Toll-like receptor signaling was inhibited at all the time points (Fig. 4A).

The Wnt signaling pathway is a major regulator of gastrointestinal stem cells and tumorigenesis (*25*, *26*). CD44 is a known target of the Wnt signaling pathway (*27*) and has been shown to label a cancer-initiating cell population (*28*). Lgr5 is a marker of gastric stem cells in normal as well as cancer tissues, and also a target of the Wnt signaling pathway (*29*). Either vagotomy (VTPP and UVT) or Botox treatment induced down-regulation of CD44 (and CD44v6) in the gastric mucosa of INS-GAS mice, although the combination of vagotomy and Botox did not lead to a further decrease in CD44 expression (Fig. 4, B and C, and figs. S10 and S11). Vagotomy also reduced the expression of Wnt target genes, such as *Cyclin D1*, *Axin2*, *Myc*, *Lgr5*, and *Cd44*, in MNU-treated mice (Fig. 4D). The number of cells with nuclear translocation of β-catenin and the number of $Lgr5^+$ cells in MNU-treated mice were reduced after vagotomy (Fig. 4, E and F). These results suggest that disruption of neuronal signaling inhibits Wnt signaling and thereby stem cell expansion, resulting in the suppression of tumor development in both INS-GAS and MNU mouse models.

Wnt signaling is also known to be involved in tumor regeneration (*30*). We have established a mouse model of tumor regeneration through topical application of acetic acid in INS-GAS mice (*31*). In this model, vagotomy delayed tumor regeneration in the denervated side of the stomach (fig. S12).

We next examined whether vagotomy down-regulated *Lgr5* expression via the muscarinic acetylcholine receptors. Gastric epithelial cells from *Lgr5*-GFP mice were sorted on the basis of green fluorescent protein (GFP) expression. Afterward, gene expression of the muscarinic acetylcholine receptors was tested in *Lgr5*-negative, *Lgr5*-low, and *Lgr5*-high cell populations (Fig. 5A). We found that there was coexpression of *Lgr5* and *Chrm3*, the gene encoding muscarinic acetylcholine receptor 3 (M_3R), in the sorted cells from *Lgr5*-GFP mouse stomach, but other subtypes of muscarinic receptor were little expressed in those cells (Fig. 5, B and C), suggesting that $Lgr5^+$ stem cell function may be modulated by M_3R signaling. To investigate the involvement of M_3 receptors in gastric tumorigenesis, we treated INS-GAS mice by continuous infusion of the specific M_3 receptor antagonist, darifenacin (*32*), in combination with chemotherapy. Using an experimental design similar to that of the Botox and vagotomy experiment, we found that the combination of darifenacin and chemotherapy reduced cellular proliferation of the tumors (Fig. 5D). Furthermore, we analyzed the Wnt signaling pathway in M_3KO versus wild-type mice and found that several key genes, including one encoding β-catenin, were down-regulated (fig. S13). We then exposed M_3KO and wild-type mice to MNU treatment. At 7.5 months after MNU treatment (11 months of age), M_3KO mice had less tumor induction (57.1% versus 100%) and smaller tumor size when compared to wild-type controls (Fig. 5, E and F). Thus, the vagus nerve regulates gastric tumorigenesis at least in part through M_3 receptor–mediated Wnt signaling, which is operative in $Lgr5^+$ stem cells.

Neurons activate Wnt signaling in gastric stem cells through M_3 receptor

To demonstrate the potential regulatory role of nerves in the maintenance of gastric epithelium, we used an established in vitro culture system for gastric organoids (*9*). Primary neurons were isolated from murine spinal cord or the enteric nervous system of guinea pigs, and cocultured with gastric glands (*9*, *33*, *34*). In culture, neurons showed outgrowth of neurites and evidence of direct contact with the gastric organoids (Fig. 6, A to C). Furthermore, coculture with neurons markedly promoted gastric organoid growth (Fig. 6, D and E). The addition of either Botox or scopolamine (an unspecific muscarinic receptor antagonist) inhibited this stimulatory effect (Fig. 6, D and E), whereas pilocarpine (an unspecific muscarinic receptor agonist) stimulated organoid growth (Fig. 6F). Pilocarpine caused up-regulation of the gastric stem cell markers and Wnt target genes *Lgr5*, *Cd44*, and *Sox9* (*9*) in a dose-dependent manner. However, in gastric organoids of M_3KO mice,

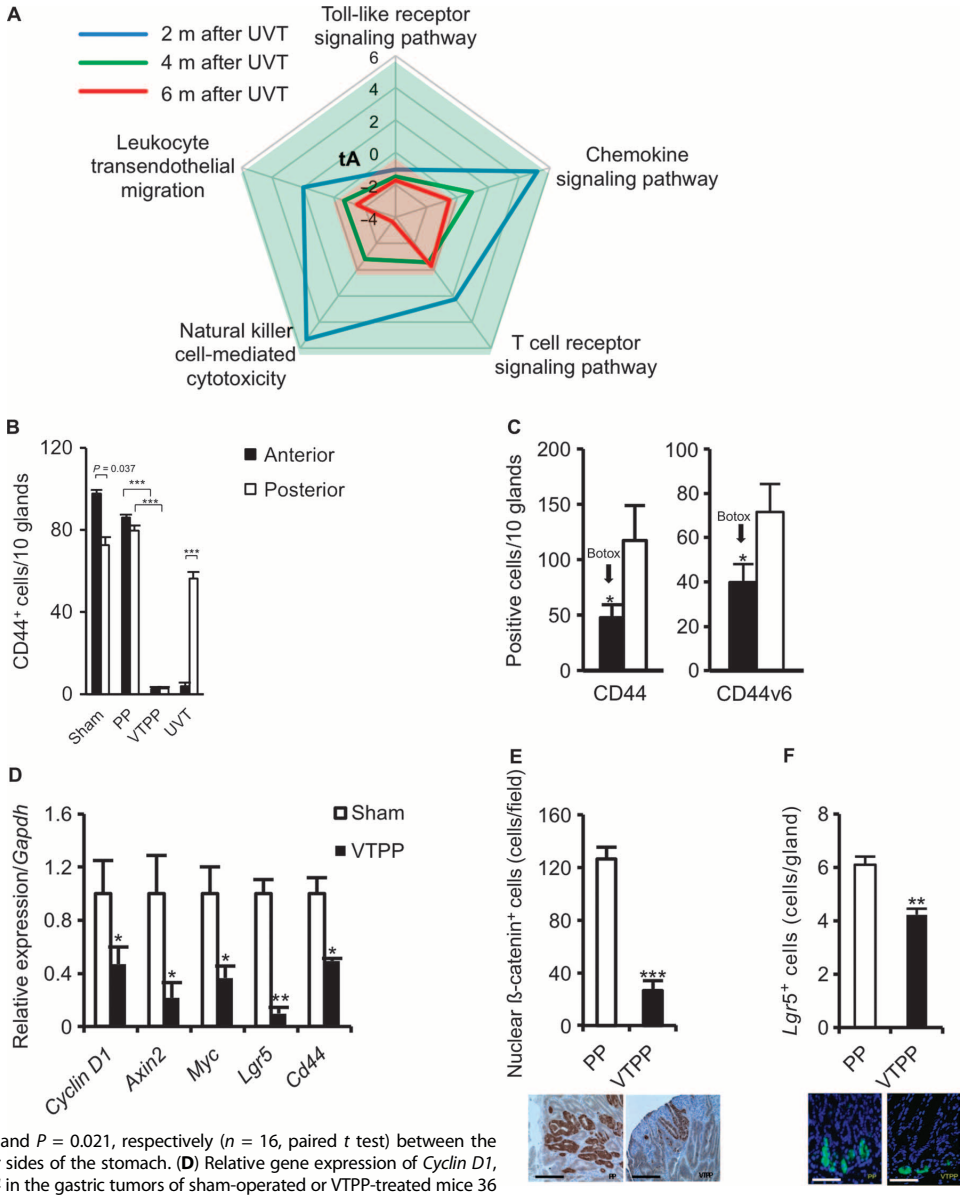

Fig. 4. Denervation alters inflammation-related signaling and suppresses stem cell expansion in mouse models of gastric cancer. (**A**) Time course of five signaling pathways determined by microarray analysis in the anterior side of the stomach at 2 (blue), 4 (green), and 6 (red) months after anterior UVT compared with the posterior side of the stomach in INS-GAS mice. Total net accumulated perturbation (expressed as tA score): −4 to 6. tA score > 0: activation; tA score < 0: inhibition. (**B**) Numbers of $CD44^+$ cells in the anterior and the posterior sides of the stomach of INS-GAS mice at 6 months after surgery. Means ± SEM. $P = 0.037$ ($n = 27$, paired t test) between the anterior and the posterior sides in sham operation (Sham), $P = 1.00 \times 10^{-6}$ or $P = 6.00 \times 10^{-6}$ ($n = 25$, Dunnett's test) between PP and VTPP (anterior and posterior sides, respectively), and $P = 1.74 \times 10^{-3}$ ($n = 30$, paired t test) between the anterior and the posterior sides within anterior UVT. (**C**) Numbers of CD44-immunoreactive cells (CD44) and CD44v6-immunoreactive cells (CD44v6) in the anterior and the posterior sides of the stomach of INS-GAS mice at 6 months after Botox injection. Means ± SEM. $P = 0.034$ and $P = 0.021$, respectively ($n = 16$, paired t test) between the anterior and the posterior sides of the stomach. (**D**) Relative gene expression of *Cyclin D1*, *Axin2*, *Myc*, *Lgr5*, and *Cd44* in the gastric tumors of sham-operated or VTPP-treated mice 36 weeks after MNU treatment ($n = 4$ per group). Means ± SEM. $P = 0.04$ (*Cyclin D1*), 0.04 (*Axin2*), 0.03 (*Myc*), 0.001 (*Lgr5*), and 0.01 (*Cd44*) (Student's t test). (**E**) Number of cells showing nuclear β-catenin accumulation in the gastric tumors of PP- or VTPP-treated mice 36 weeks after MNU treatment ($n = 4$ per group). Means ± SEM. $P = 7.00 \times 10^{-6}$ (Student's t test). Representative immunohistochemical microphotographs are shown below. Scale bars, 40 μm. (**F**) Number of $Lgr5^+$ cells in the stomachs of PP- or VTPP-treated mice 6 weeks after MNU treatment ($n = 5$ per group). Means ± SEM. $P = 4.00 \times 10^{-6}$ (Student's t test). Representative *Lgr5*-GFP^+ microphotographs are shown below. Scale bars, 20 μm.

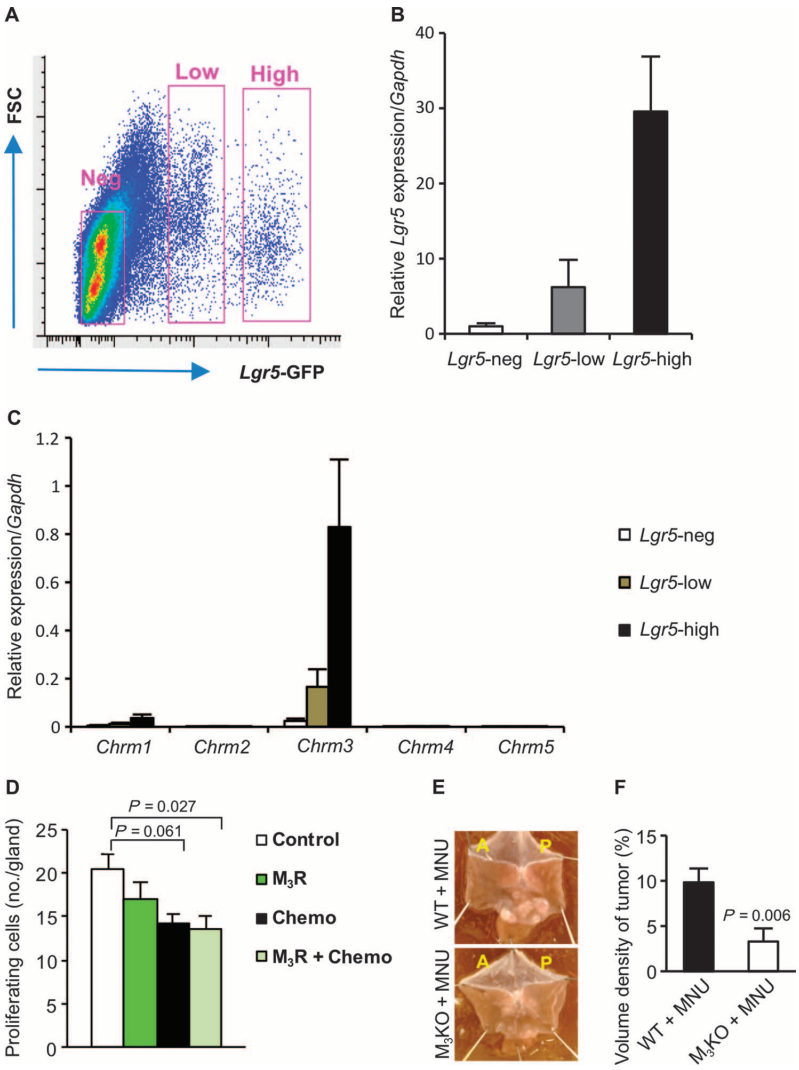

Fig. 5. M_3 receptor signaling in gastric stem cells regulates tumorigenesis in mouse models of gastric cancer. (**A**) Representative fluorescence-activated cell sorting gating showing forward scatter (FSC) and *Lgr5*-GFP expression. (**B** and **C**) Relative gene expression of *Lgr5* and muscarinic receptors (*Chrm1* to *Chrm5*) in sorted *Lgr5*-negative, *Lgr5*-low, and *Lgr5*-high populations. Means ± SEM ($n = 4$). (**D**) Number of proliferating cells in the tumors of INS-GAS mice treated with saline (Control, $n = 19$), M_3 receptor antagonist darifenacin (M_3R, $n = 15$), 5-FU + oxaliplatin (Chemo, $n = 12$), or combination of 5-FU + oxaliplatin + darifenacin (M_3R + Chemo, $n = 8$), respectively. Means ± SEM. *P* values were calculated by Dunnett's test. (**E**) Representative photographs showing gross appearance of stomachs opened along the greater curvature from wild-type (WT) or M_3 receptor knockout mice (M_3KO) treated with MNU. (**F**) Volume density of tumor in the stomachs of MNU-treated WT ($n = 13$) versus MNU-treated M_3KO mice ($n = 7$). Means ± SEM (Student's *t* test).

pilocarpine showed no effects on the expression of these genes (Fig. 6G), highlighting the importance of the M_3 receptor for stem cell expansion. Furthermore, coculture with neurons could substitute for Wnt3a in gastric organoid cultures that are otherwise strictly dependent on addition of Wnt ligands (*35*) (Fig. 6H), confirming the ability of cholinergic signaling to induce ligand-independent Wnt signaling in this in vitro system.

Gastric cancer patients display dysregulation of Wnt signaling and innervation in the tumors

To further investigate the involvement of Wnt signaling, innervation, and gastric cancer progression in humans, we evaluated three separate cohort studies of gastric cancer patients (table S2). In tumors from 17 primary gastric cancer patients, Wnt signaling, neurotrophin signaling, and axonal guidance pathways (along with other pathways) were activated in cancerous tissue when compared to adjacent noncancerous tissue (Fig. 7 and fig. S14). In another group of 120 primary gastric cancers, neuronal density was correlated with more advanced tumor stages (Fig. 8, A to C). A similar increase in neuronal density was confirmed in tumors of mice treated with MNU (Fig. 8, D to F). In the third cohort of 37 patients, who developed gastric stump cancer after distal gastrectomy with or without vagotomy, 35% (13 of 37) of patients had undergone vagotomy. Of those 13 patients, only 1 had a tumor in the posterior wall and none had tumors in the anterior wall. In the 24 patients without vagotomy, tumors were observed in both anterior and posterior walls (fig. S15).

DISCUSSION

The results of the present study, using three independent mouse models of gastric cancer, demonstrate that either surgical or pharmacological denervation suppresses gastric tumorigenesis. The effect takes place primarily on terminal and intramucosal vagal branches, as shown by the response to unilateral vagotomy and localized Botox injection. Denervation therapy was effective in both early preneoplasia and late neoplasia/dysplasia, and it enhanced the effect of chemotherapy and prolonged survival in mice with advanced tumors. Gene expression and immunohistochemical analysis of stem cell markers, along with the in vitro gastric organoid test, revealed that cholinergic nerves directly modulate epithelial stem cells through activation of Wnt signaling via the M_3 receptor. Analysis of human patients with

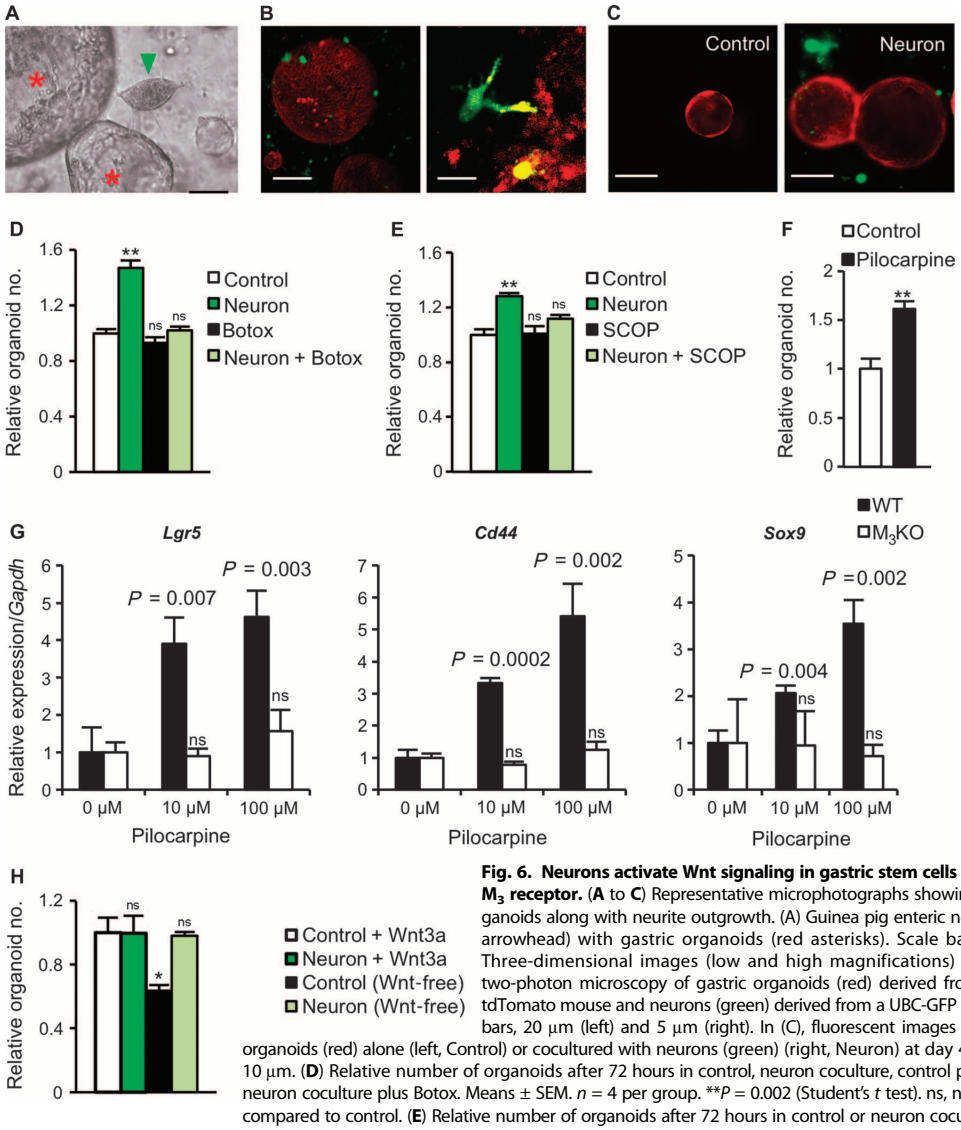

Fig. 6. Neurons activate Wnt signaling in gastric stem cells through the M_3 receptor. (**A** to **C**) Representative microphotographs showing gastric organoids along with neurite outgrowth. (A) Guinea pig enteric neuron (green arrowhead) with gastric organoids (red asterisks). Scale bar, 5 μm. (B) Three-dimensional images (low and high magnifications) obtained by two-photon microscopy of gastric organoids (red) derived from an ACTB-tdTomato mouse and neurons (green) derived from a UBC-GFP mouse. Scale bars, 20 μm (left) and 5 μm (right). In (C), fluorescent images show gastric organoids (red) alone (left, Control) or cocultured with neurons (green) (right, Neuron) at day 4. Scale bars, 10 μm. (**D**) Relative number of organoids after 72 hours in control, neuron coculture, control plus Botox, or neuron coculture plus Botox. Means ± SEM. $n = 4$ per group. $^{**}P = 0.002$ (Student's t test). ns, not significant compared to control. (**E**) Relative number of organoids after 72 hours in control or neuron coculture with or without scopolamine (SCOP) (1 μg/ml). Means ± SEM. $n = 4$ per group. $^{**}P = 0.003$ (Student's t test). ns, not significant compared to control. (**F**) Relative number of organoids at day 10 with or without 100 μM pilocarpine. Means ± SEM. $n = 4$ per group. $^{**}P = 0.006$ (Student's t test) between control and pilocarpine. (**G**) Relative mRNA expression for *Lgr5*, *Cd44*, and *Sox9* in relation to *Gapdh* on day 7 with or without 10 or 100 μM pilocarpine in gastric organoids isolated from WT or M_3KO mice. Means ± SEM. Student's t test between 0 μM and 10 or 100 μM pilocarpine. $n = 4$ per group. (**H**) Relative number of organoids at day 10 with or without neurons and/or Wnt3a. Means ± SEM. $n = 4$ per group. ns, not significant. $^{*}P = 0.030$ compared to Control + Wnt3a (Student's t test).

gastric cancer also showed correlations between neural pathways and Wnt signaling and increased innervation in more advanced tumors, with decreased tumor risk in vagotomized stomach.

In contrast to our current results, previous vagotomy studies in rat models of chemically induced gastric cancer did not reveal an inhibitory effect (*12*, *36*, *37*). This is likely due to the earlier approach of bilateral vagotomy without pyloroplasty, which delayed gastric emptying and therefore increased the exposure time of orally administered chemical carcinogens on the gastric mucosa. To ensure that dose and time of MNU exposure were equalized in all the groups and to prevent retention of gastric contents, we performed bilateral vagotomy with pyloroplasty or PP (as control) after completion of the MNU dosing

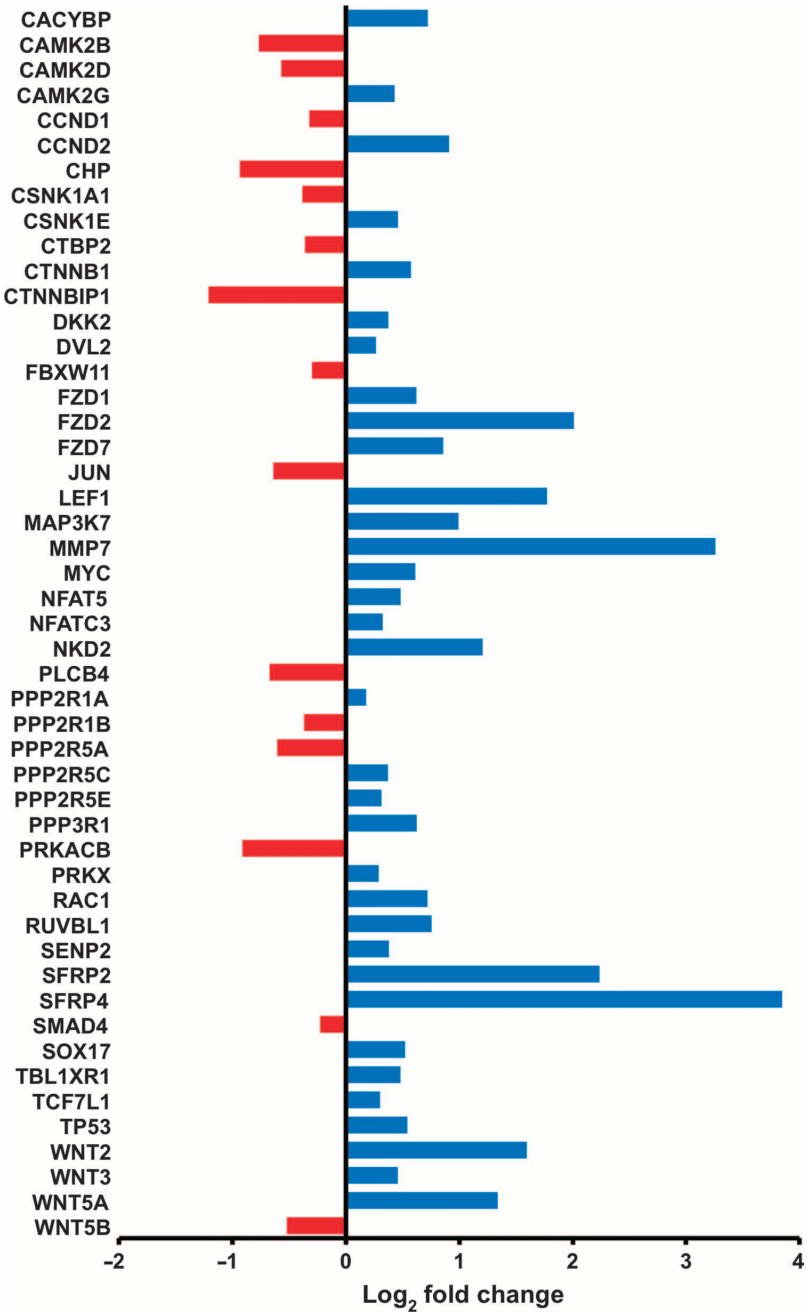

Fig. 7. Gastric cancer patients exhibit a dysregulation of Wnt signaling. Gene expression of Wnt signaling pathway (microarray analysis) in human gastric cancer tissue. The graph shows $\log_2$ fold changes of expressed genes in comparison with the adjacent noncancerous tissue of the same stomach. Red, down-regulation; blue, up-regulation.

protocol, allowing analysis of the specific effects of the vagus nerve on the gastric mucosa. Thus, we found that vagotomy inhibited gastric tumorigenesis in the MNU model. The data from two different genetically engineered mouse models of gastric cancer further established the inhibitory effect of denervation against gastric tumorigenesis. Given the limited availability of metastatic models of gastric cancer, the effect of denervation in metastatic lymph nodes or other organs remains unclear and needs to be further investigated in suitable models.

Previous studies suggested that nerves contribute to the normal stem cell niche (*1*, *2*, *38*), and a recent report has linked sympathetic nerves to prostate cancer progression (*7*). However, the stomach differs from other solid organs in that its autonomic innervation is largely parasympathetic in nature, and cholinergic nerves have been shown to regulate gastrointestinal proliferation (*39*). The present study demonstrated that *Lgr5*$^+$ gastric stem cells express the M_3 receptor, and that Wnt signaling in those cells is directly activated by cholinergic vagus stimulation, resulting in epithelial proliferation and stem cell expansion. Gastrointestinal stem cells are supported by a number of niche cells including Paneth cells, mesenchymal stem cells, myofibroblasts, smooth muscle cells, lymph and vascular endothelial cells, and bone marrow–derived stromal cells (*40*–*42*). Here, we identified nerves regulating gastric stem cell expansion during the tumorigenesis.

The vagus nerve has been shown to stimulate cell proliferation in the brain, liver, and stomach through the M_3 receptor (*43*–*45*). Furthermore, activation of muscarinic receptors in cancer cells leads to enhanced Wnt signaling independent of Wnt ligands (*46*), and M_3 receptor signaling has been implicated in the pathogenesis of intestinal neoplasia (*6*, *47*, *48*). Consistent with those findings, the present study demonstrates that genetic knockout or pharmacological inhibition of M_3 receptor suppresses gastric tumor progression, pointing to the M_3 receptor as a potential target for gastric cancer therapy. The M_3 receptor antagonist darifenacin is already in clinical use for overactive urinary bladder (*49*) and has been shown to inhibit growth of small cell lung cancer xenografts (*50*). Given

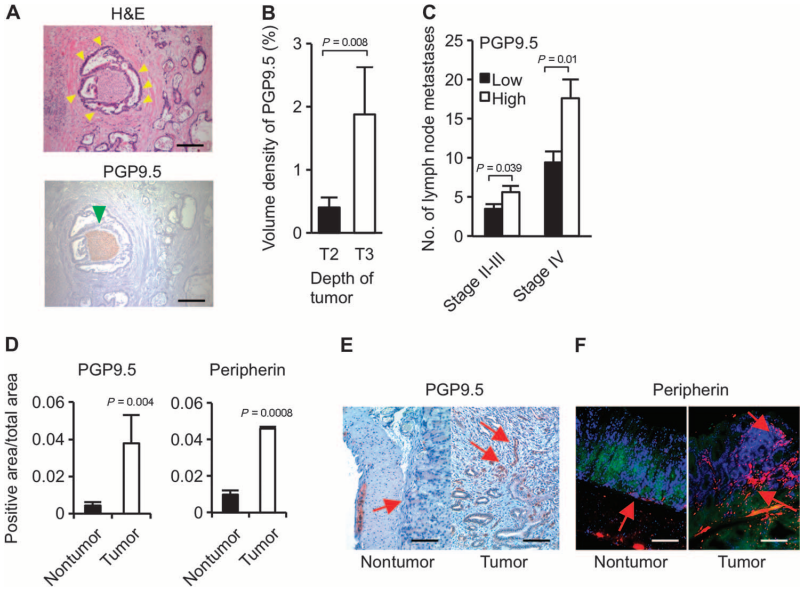

Fig. 8. PGP9.5 and peripherin may represent neural markers for gastric cancer progression. (**A**) Representative microphotographs showing human gastric cancer [indicated by yellow arrowheads, hematoxylin and eosin (H&E) staining] and PGP9.5-labeled nerve (green arrowhead). Scale bars, 50 μm. (**B**) Volume density of PGP9.5-labeled nerves in different levels of depth of tumor invasion [T2 (tumor invading muscularis propria) versus T3 (tumor penetrating subserosal connective tissue without invasion of visceral peritoneum or adjacent structures)] in the stage II and III gastric cancer patients. Means ± SEM (n = 120). P = 0.008 (Student's t test). (**C**) Number of lymph node metastases in patients with stage II and III or stage IV gastric cancer that has low or high expression of PGP9.5. Means ± SEM (n = 120). P values were calculated by Student's t test. (**D**) PGP9.5- and peripherin-immunoreactive nerve densities in gastric mucosa of control mice (nontumor) and MNU-treated mice (tumor). PGP9.5 is a ubiquitin-protein hydrolase that is expressed in the neuronal cell bodies and axons in the central and peripheral nervous system. Peripherin is a type III intermediate filament protein that is expressed in peripheral and some central nervous system neurons. Both can be used as neuronal markers in the gut. Means ± SEM (n = 6 per group). P values were calculated by Student's t test. (**E** and **F**) Representative immunohistochemical microphotographs showing PGP9.5 and peripherin (indicated by red arrows) in the nontumor and tumor areas of the mouse stomachs. Scale bars, 20 μm (E) and 40 μm (F).

that chemotherapeutic agents and darifenacin appear to show cooperative effects, M_3 receptor–targeting therapy combined with chemotherapy in unresectable gastric cancer patients could be considered in future trials, although further studies are needed to evaluate the safety and long-term effects of those regimens.

Canonical Wnt signaling controls epithelial homeostasis in the intestine and the stomach, and is thought to play a role in a subset of gastric cancers (*9*, *51*). Here, we have shown that Wnt signaling is up-regulated in the tumorigenic stomach and is down-regulated after vagotomy, suggesting that vagus nerve is a critical regulator of Wnt signaling in gastric tumorigenesis. Furthermore, gastric Wnt signaling was down-regulated in M_3KO mice, which were resistant to MNU-induced tumorigenesis. In addition, inhibition of Notch signaling was also observed after vagotomy, which is in line with both Wnt and Notch signaling promoting the initiation of intestinal tumors (*52*, *53*). Therefore, therapeutic modulation of Wnt signaling blockade using tankyrase inhibitors could also be considered, although the dose-limiting toxicity of available agents has restricted their clinical use to this point (*54*). Finally, we cannot exclude a role for additional pathways (for example, prostaglandin E_2 pathway) that may be modulated by nerves in gastric tumorigenesis.

Our finding that nerves play an important role in cancer initiation and progression highlights a component of the tumor microenvironment contributing to the cancer stem cell niche. The data strongly support the notion that denervation and cholinergic antagonism, in combination with other therapies, could represent a viable approach for the treatment of gastric cancer and possibly other solid malignancies.

MATERIALS AND METHODS

We used 581 mice divided into 14 experimental groups. In each experiment, mice were randomly divided into different subgroups (fig. S1 and table S1). INS-GAS mice with spontaneous gastric cancer were used as previously described (*18*, *19*). Denervation was achieved by subdiaphragmatic bilateral truncal vagotomy, unilateral vagotomy, or Botox local injection. The tumor prevalence/incidence, tumor size, tumor regeneration, pathological changes, gene expression profiles, and immunohistochemical biomarkers were examined after denervation. In vitro gastric organoid culture was performed as described previously (*9*). We also performed three cohort studies of human primary gastric cancer and gastric stump cancer, as well as gene expression profiling and KEGG pathway analysis. All studies and procedures involving animals and human subjects were approved by the Norwegian National Animal Research Authority, the Columbia University Institutional Animal Care and Use Committee, Gifu University, and the National Cancer Center Hospital East, Japan. Statistical comparisons were performed between experimental groups, between the anterior and posterior sides of the stomachs, and between groups of patients. See the Supplementary Materials for the complete Materials and Methods.

SUPPLEMENTARY MATERIALS

www.sciencetranslationalmedicine.org/cgi/content/full/6/250/250ra115/DC1
Materials and Methods
Fig. S1. Flowchart showing the animal study design.
Fig. S2. Anterior UVT in mice.
Fig. S3. Body weight of male and female INS-GAS mice after surgery.
Fig. S4. Thickness of the gastric oxyntic mucosa after surgery in INS-GAS mice.
Fig. S5. Pathological scores for the stomach after surgery in INS-GAS mice.

Fig. S6. Pathological scores for the stomach after Botox injection in INS-GAS mice.
Fig. S7. Wnt signaling in INS-GAS mice compared with wild-type mice.
Fig. S8. Altered signaling pathways after vagotomy in INS-GAS mice.
Fig. S9. Wnt and Notch signaling pathways after vagotomy in INS-GAS mice.
Fig. S10. Immunostaining of CD44 after vagotomy in INS-GAS mice.
Fig. S11. Numbers of CD44-immunoreactive cells after Botox treatment ± vagotomy in INS-GAS mice.
Fig. S12. Tumor regeneration in the stomach after vagotomy in INS-GAS mice.
Fig. S13. Wnt signaling KEGG pathway in M_3KO mice compared with wild-type mice.
Fig. S14. Altered signaling pathways in human gastric cancer tissue compared with adjacent noncancerous tissue.
Fig. S15. Gastric stump cancer after distal gastrectomy with or without vagotomy.
Fig. S16. Effect of 5-FU and oxaliplatin in INS-GAS mice.
Table S1. Animal experimental groups.
Table S2. Cohorts of gastric cancer patients.
Table S3. List of qRT-PCR primers used in this study.

REFERENCES AND NOTES

1. Y. Katayama, M. Battista, W. M. Kao, A. Hidalgo, A. J. Peired, S. A. Thomas, P. S. Frenette, Signals from the sympathetic nervous system regulate hematopoietic stem cell egress from bone marrow. *Cell* **124**, 407–421 (2006).
2. O. Lundgren, M. Jodal, M. Jansson, A. T. Ryberg, L. Svensson, Intestinal epithelial stem/progenitor cells are controlled by mucosal afferent nerves. *PLOS One* **6**, e16295 (2011).
3. R. R. Mattingly, A. Sorisky, M. R. Brann, I. G. Macara, Muscarinic receptors transform NIH 3T3 cells through a Ras-dependent signalling pathway inhibited by the Ras-GTPase-activating protein SH3 domain. *Mol. Cell. Biol.* **14**, 7943–7952 (1994).
4. G. E. Ayala, H. Dai, M. Powell, R. Li, Y. Ding, T. M. Wheeler, D. Shine, D. Kadmon, T. Thompson, B. J. Miles, M. M. Ittmann, D. Rowley, Cancer-related axonogenesis and neurogenesis in prostate cancer. *Clin. Cancer Res.* **14**, 7593–7603 (2008).
5. N. Shah, S. Khurana, K. Cheng, J. P. Raufman, Muscarinic receptors and ligands in cancer. *Am. J. Physiol. Cell Physiol.* **296**, C221–C232 (2009).
6. J. P. Raufman, J. Shant, G. Xie, K. Cheng, X. M. Gao, B. Shiu, N. Shah, C. B. Drachenberg, J. Heath, J. Wess, S. Khurana, Muscarinic receptor subtype-3 gene ablation and scopolamine butylbromide treatment attenuate small intestinal neoplasia in $Apc^{min/+}$ mice. *Carcinogenesis* **32**, 1396–1402 (2011).
7. C. Magnon, S. J. Hall, J. Lin, X. Xue, L. Gerber, S. J. Freedland, P. S. Frenette, Autonomic nerve development contributes to prostate cancer progression. *Science* **341**, 1236361 (2013).
8. R. Pardal, M. F. Clarke, S. J. Morrison, Applying the principles of stem-cell biology to cancer. *Nat. Rev. Cancer* **3**, 895–902 (2003).
9. N. Barker, M. Huch, P. Kujala, M. van de Wetering, H. J. Snippert, J. H. van Es, T. Sato, D. E. Stange, H. Begthel, M. van den Born, E. Danenberg, S. van den Brink, J. Korving, A. Abo, P. J. Peters, N. Wright, R. Poulsom, H. Clevers, $Lgr5^{+ve}$ stem cells drive self-renewal in the stomach and build long-lived gastric units in vitro. *Cell Stem Cell* **6**, 25–36 (2010).
10. J. Ferlay, H. R. Shin, F. Bray, D. Forman, C. Mathers, D. M. Parkin, Estimates of worldwide burden of cancer in 2008: GLOBOCAN 2008. *Int. J. Cancer* **127**, 2893–2917 (2010).
11. A. Jemal, M. M. Center, C. DeSantis, E. M. Ward, Global patterns of cancer incidence and mortality rates and trends. *Cancer Epidemiol. Biomarkers Prev.* **19**, 1893–1907 (2010).
12. R. Håkanson, S. Vallgren, M. Ekelund, J. F. Rehfeld, F. Sundler, The vagus exerts trophic control of the stomach in the rat. *Gastroenterology* **86**, 28–32 (1984).
13. J. Axelson, M. Ekelund, R. Håkanson, F. Sundler, Gastrin and the vagus interact in the trophic control of the rat oxyntic mucosa. *Regul. Pept.* **22**, 237–243 (1988).
14. G. Lundegårdh, A. Ekbom, J. K. McLaughlin, O. Nyrén, Gastric cancer risk after vagotomy. *Gut* **35**, 946–949 (1994).
15. S. Bahmanyar, W. Ye, P. W. Dickman, O. Nyrén, Long-term risk of gastric cancer by subsite in operated and unoperated patients hospitalized for peptic ulcer. *Am. J. Gastroenterol.* **102**, 1185–1191 (2007).
16. P. Correa, C. Cuello, E. Duque, Carcinoma and intestinal metaplasia of the stomach in Colombian migrants. *J. Natl. Cancer Inst.* **44**, 297–306 (1970).
17. M. Cassaro, M. Rugge, O. Gutierrez, G. Leandro, D. Y. Graham, R. M. Genta, Topographic patterns of intestinal metaplasia and gastric cancer. *Am. J. Gastroenterol.* **95**, 1431–1438 (2000).
18. T. C. Wang, C. A. Dangler, D. Chen, J. R. Goldenring, T. Koh, R. Raychowdhury, R. J. Coffey, S. Ito, A. Varro, G. J. Dockray, J. G. Fox, Synergistic interaction between hypergastrinemia and *Helicobacter* infection in a mouse model of gastric cancer. *Gastroenterology* **118**, 36–47 (2000).
19. J. G. Fox, T. C. Wang, Inflammation, atrophy, and gastric cancer. *J. Clin. Invest.* **117**, 60–69 (2007).
20. P. Ericsson, R. Håkanson, J. F. Rehfeld, P. Norlén, Gastrin release: Antrum microdialysis reveals a complex neural control. *Regul. Pept.* **161**, 22–32 (2010).
21. A. B. Rogers, N. S. Taylor, M. T. Whary, E. D. Stefanich, T. C. Wang, J. G. Fox, *Helicobacter pylori* but not high salt induces gastric intraepithelial neoplasia in B6129 mice. *Cancer Res.* **65**, 10709–10715 (2005).
22. H. Tomita, S. Takaishi, T. R. Menheniott, X. Yang, W. Shibata, G. Jin, K. S. Betz, K. Kawakami, T. Minamoto, C. Tomasetto, M. C. Rio, N. Lerkowit, A. Varro, A. S. Giraud, T. C. Wang, Inhibition of gastric carcinogenesis by the hormone gastrin is mediated by suppression of *TFF1* epigenetic silencing. *Gastroenterology* **140**, 879–891 (2011).
23. S. Tu, G. Bhagat, G. Cui, S. Takaishi, E. A. Kurt-Jones, B. Rickman, K. S. Betz, M. Penz-Oesterreicher, O. Bjorkdahl, J. G. Fox, T. C. Wang, Overexpression of interleukin-1β induces gastric inflammation and cancer and mobilizes myeloid-derived suppressor cells in mice. *Cancer Cell* **14**, 408–419 (2008).
24. D. Dressler, F. Adib Saberi, Botulinum toxin: Mechanisms of action. *Eur. Neurol.* **53**, 3–9 (2005).
25. P. Polakis, Drugging Wnt signalling in cancer. *EMBO J.* **31**, 2737–2746 (2012).
26. F. Takahashi-Yanaga, M. Kahn, Targeting Wnt signaling: Can we safely eradicate cancer stem cells? *Clin. Cancer Res.* **16**, 3153–3162 (2010).
27. M. Zöller, CD44: Can a cancer-initiating cell profit from an abundantly expressed molecule? *Nat. Rev. Cancer* **11**, 254–267 (2011).
28. S. Takaishi, T. Okumura, S. Tu, S. S. Wang, W. Shibata, R. Vigneshwaran, S. A. Gordon, Y. Shimada, T. C. Wang, Identification of gastric cancer stem cells using the cell surface marker CD44. *Stem Cells* **27**, 1006–1020 (2009).
29. J. Schuijers, H. Clevers, Adult mammalian stem cells: The role of Wnt, Lgr5 and R-spondins. *EMBO J.* **31**, 2685–2696 (2012).
30. J. Chen, Y. Li, T. S. Yu, R. M. McKay, D. K. Burns, S. G. Kernie, L. F. Parada, A restricted cell population propagates glioblastoma growth after chemotherapy. *Nature* **488**, 522–526 (2012).
31. S. Okabe, Y. Kodama, H. Cao, H. Johannessen, C. M. Zhao, T. C. Wang, R. Takahashi, D. Chen, Topical application of acetic acid in cytoreduction of gastric cancer. A technical report using mouse model. *J. Gastroenterol. Hepatol.* **27** (Suppl. 3), 40–48 (2012).
32. P. Song, H. S. Sekhon, X. W. Fu, M. Maier, Y. Jia, J. Duan, B. J. Proskosil, C. Gravett, J. Lindstrom, G. P. Mark, S. Saha, E. R. Spindel, Activated cholinergic signaling provides a target in squamous cell lung carcinoma. *Cancer Res.* **68**, 4693–4700 (2008).
33. C. B. Westphalen, S. Asfaha, Y. Hayakawa, Y. Takemoto, D. J. Lukin, A. H. Nuber, A. Brandtner, W. Setlik, H. Remotti, A. Muley, X. Chen, R. May, C. W. Houchen, J. G. Fox, M. D. Gershon, M. Quante, T. C. Wang, Long-lived intestinal tuft cells serve as colon cancer–initiating cells. *J. Clin. Invest.* **124**, 1283–1295 (2014).
34. A. A. Gershon, J. Chen, M. D. Gershon, A model of lytic, latent, and reactivating varicella-zoster virus infections in isolated enteric neurons. *J. Infect. Dis.* **197** (Suppl. 2), S61–S65 (2008).
35. N. Barker, H. Clevers, Leucine-rich repeat-containing G-protein-coupled receptors as markers of adult stem cells. *Gastroenterology* **138**, 1681–1696 (2010).
36. M. Tatsuta, H. Yamamura, H. Iishi, M. Ichii, S. Noguchi, M. Baba, H. Taniguchi, Promotion by vagotomy of gastric carcinogenesis induced by *N*-methyl-*N*′-nitro-*N*-nitrosoguanidine in Wistar rats. *Cancer Res.* **45**, 194–197 (1985).
37. M. Tatsuta, H. Iishi, H. Yamamura, M. Baba, H. Taniguchi, Effects of bilateral and unilateral vagotomy on gastric carcinogenesis induced by *N*-methyl-*N*′-nitro-*N*-nitrosoguanidine in Wistar rats. *Int. J. Cancer* **42**, 414–418 (1988).
38. P. S. Frenette, S. Pinho, D. Lucas, C. Scheiermann, Mesenchymal stem cell: Keystone of the hematopoietic stem cell niche and a stepping-stone for regenerative medicine. *Annu. Rev. Immunol.* **31**, 285–316 (2013).
39. E. R. Gross, M. D. Gershon, K. G. Margolis, Z. V. Gertsberg, R. A. Cowles, Neuronal serotonin regulates growth of the intestinal mucosa in mice. *Gastroenterology* **143**, 408–417.e2 (2012).
40. T. Sato, J. H. van Es, H. J. Snippert, D. E. Stange, R. G. Vries, M. van den Born, N. Barker, N. F. Shroyer, M. van de Wetering, H. Clevers, Paneth cells constitute the niche for Lgr5 stem cells in intestinal crypts. *Nature* **469**, 415–418 (2011).
41. D. W. Powell, I. V. Pinchuk, J. I. Saada, X. Chen, R. C. Mifflin, Mesenchymal cells of the intestinal lamina propria. *Annu. Rev. Physiol.* **73**, 213–237 (2011).
42. H. F. Farin, J. H. Van Es, H. Clevers, Redundant sources of Wnt regulate intestinal stem cells and promote formation of Paneth cells. *Gastroenterology* **143**, 1518–1529.e7 (2012).
43. D. Revesz, M. Tjernstrom, E. Ben-Menachem, T. Thorlin, Effects of vagus nerve stimulation on rat hippocampal progenitor proliferation. *Exp. Neurol.* **214**, 259–265 (2008).
44. D. Cassiman, L. Libbrecht, N. Sinelli, V. Desmet, C. Denef, T. Roskams, The vagal nerve stimulates activation of the hepatic progenitor cell compartment via muscarinic acetylcholine receptor type 3. *Am. J. Pathol.* **161**, 521–530 (2002).
45. T. Aihara, T. Fujishita, K. Kanatani, K. Furutani, E. Nakamura, M. M. Taketo, M. Matsui, D. Chen, S. Okabe, Impaired gastric secretion and lack of trophic responses to hypergastrinemia in M_3 muscarinic receptor knockout mice. *Gastroenterology* **125**, 1774–1784 (2003).
46. S. Salmanian, S. M. Najafi, M. Rafipour, M. R. Arjomand, H. Shahheydari, S. Ansari, L. Kashkooli, S. J. Rasouli, M. S. Jazi, T. Minaei, Regulation of GSK-3β and β-catenin by Gαq in HEK293T cells. *Biochem. Biophys. Res. Commun.* **395**, 577–582 (2010).

47. E. R. Spindel, Muscarinic receptor agonists and antagonists: Effects on cancer. *Handb. Exp. Pharmacol.* 451–468 (2012).
48. J. P. Raufman, R. Samimi, N. Shah, S. Khurana, J. Shant, C. Drachenberg, G. Xie, J. Wess, K. Cheng, Genetic ablation of M_3 muscarinic receptors attenuates murine colon epithelial cell proliferation and neoplasia. *Cancer Res.* **68**, 3573–3578 (2008).
49. P. W. Veenboer, J. L. Bosch, Long-term adherence to antimuscarinic therapy in everyday practice: A systematic review. *J. Urol.* **191**, 1003–1008 (2014).
50. P. Song, H. S. Sekhon, A. Lu, J. Arredondo, D. Sauer, C. Gravett, G. P. Mark, S. A. Grando, E. R. Spindel, M3 muscarinic receptor antagonists inhibit small cell lung carcinoma growth and mitogen-activated protein kinase phosphorylation induced by acetylcholine secretion. *Cancer Res.* **67**, 3936–3944 (2007).
51. H. Oshima, M. Oshima, Mouse models of gastric tumors: Wnt activation and PGE_2 induction. *Pathol. Int.* **60**, 599–607 (2010).
52. J. H. van Es, P. Jay, A. Gregorieff, M. E. van Gijn, S. Jonkheer, P. Hatzis, A. Thiele, M. van den Born, H. Begthel, T. Brabletz, M. M. Taketo, H. Clevers, Wnt signalling induces maturation of Paneth cells in intestinal crypts. *Nat. Cell Biol.* **7**, 381–386 (2005).
53. S. Fre, S. K. Pallavi, M. Huyghe, M. Laé, K. P. Janssen, S. Robine, S. Artavanis-Tsakonas, D. Louvard, Notch and Wnt signals cooperatively control cell proliferation and tumorigenesis in the intestine. *Proc. Natl. Acad. Sci. U.S.A.* **106**, 6309–6314 (2009).
54. L. Lehtiö, N. W. Chi, S. Krauss, Tankyrases as drug targets. *FEBS J.* **280**, 3576–3593 (2013).

Acknowledgments: We thank A. Øverby, O. D. Røe, and J. E. Gronbech at Norwegian University of Science and Technology (NTNU) for valuable assistance and discussions; A. A. Diacou at Columbia University for extraction of enteric nervous system; and K. Takeuchi at Kyoto Pharmaceutical University for providing M_3KO mice. The microarray and part of the bioinformatics work were provided by Norwegian Microarray Consortium–NTNU, a national technology platform supported by Functional Genomics Programme (FUGE) of Research Council of Norway (RCN) and NTNU. **Funding:** Supported by the RCN (D.C.), Joint Programme of the Medical Faculty of NTNU and St. Olavs University Hospital, Liaison Committee between the Central Norway Regional Health Authority and NTNU (C.-M.Z.), U.S. NIH (grants 1U54CA126513, RO1CA093405, and RO1CA120979) (T.C.W.), Clyde Wu Family Foundation (T.C.W.), Mitsukoshi Health and Welfare Foundation (Y.H.), Japan Society for the Promotion of Science Postdoctoral Fellowships for Research Abroad (Y.H.), and Uehara Memorial Foundation (Y.H.). Y.K., H.J., and G.T.A. are supported by Ph.D. fellowships from the FUGE of RCN, the European Union Seventh Framework Programme (FP7/2007-2013, no. 266408), and the St. Olavs Hospital, respectively. C.B.W. and M.Q. are supported by the Max Eder Program of the Deutsche Krebshilfe. C.B.W. is supported by the German Research Foundation. **Author contributions:** C.-M.Z. and Y.H. contributed equally to the design of the experiments, performance of the animal experiments and histology, the in vitro experiments, flow cytometry, and qRT-PCRs and contributed collection and analysis of the data. Y.K. performed the animal experiments (except for nos. 3 and 9 to 14 in table S1) and qRT-PCR arrays and contributed to collection and analysis of the data. A.F. and R.A.F. performed the bioinformatics analysis. S.M. and J.G.F. performed the pathological evaluation of mice. A.K.S. and V.B. performed the microarray experiments of mice and humans. G.T.A., H.J., and B.W.R. performed part of animal experiments. H.T. and A.H. performed the pathological evaluation of humans. C.B.W., M.Q., and H.T. performed some of the immunohistochemical analyses of mice and humans. Z.L. and M.D.G. performed the vagus nerve mapping. K.K. performed the analysis of human gastric stump cancer. T.C.W. and D.C. were joint senior authors; contributed to the study supervision, coordination, and performance of experiments; and wrote the manuscript. All authors contributed to the discussion of results and the preparation of the final manuscript. **Competing interests:** The authors declare that they have no competing interests. **Data and materials availability:** Mouse microarray data are available through Gene Expression Omnibus (GEO) database, accession no. GSE30295, and human data are in ArrayExpress, accession no. E-MTAB-1338.

Submitted 19 May 2014
Accepted 15 July 2014
Published 20 August 2014
10.1126/scitranslmed.3009569

Citation: C.-M. Zhao, Y. Hayakawa, Y. Kodama, S. Muthupalani, C. B. Westphalen, G. T. Andersen, A. Flatberg, H. Johannessen, R. A. Friedman, B. W. Renz, A. K. Sandvik, V. Beisvag, H. Tomita, A. Hara, M. Quante, Z. Li, M. D. Gershon, K. Kaneko, J. G. Fox, T. C. Wang, D. Chen, Denervation suppresses gastric tumorigenesis. *Sci. Transl. Med.* **6**, 250ra115 (2014).

Science Translational Medicine
AAAS

Denervation suppresses gastric tumorigenesis
Chun-Mei Zhao *et al.*
Sci Transl Med **6**, 250ra115 (2014);
DOI: 10.1126/scitranslmed.3009569

Editor's Summary

Treating Cancer by Getting on Its Nerves

The nervous system plays a role in the regulation of many different organs, including the gut. Now, Zhao *et al*. have shown that the vagal nerve, which signals to the stomach through muscarinic receptors, contributes to the growth of gastric tumors. The authors demonstrated that vagotomy (surgical interruption of the vagal nerve) can prevent gastric cancer in mice and reduce the recurrence of gastric tumors in human patients. Moreover, the same result can be achieved in mice treated with Botox or anticholinergic drugs to inhibit vagal nerve signaling, raising the hope of a safer treatment for gastric cancer without irreversible side effects.

Science Translational Medicine (print ISSN 1946-6234; online ISSN 1946-6242) is published weekly, except the last week in December, by the American Association for the Advancement of Science, 1200 New York Avenue NW, Washington, DC 20005.

www.sciencetranslationalmedicine.org/cgi/content/full/6/250/250ra115/DC1

Supplementary Materials for

Denervation suppresses gastric tumorigenesis

Chun-Mei Zhao, Yoku Hayakawa, Yosuke Kodama, Sureshkumar Muthupalani, Christoph B. Westphalen, Gøran T. Andersen, Arnar Flatberg, Helene Johannessen, Richard A. Friedman, Bernhard W. Renz, Arne K. Sandvik, Vidar Beisvag, Hiroyuki Tomita, Akira Hara, Michael Quante, Zhishan Li, Michael D. Gershon, Kazuhiro Kaneko, James G. Fox, Timothy C. Wang,* Duan Chen*

*Corresponding author. E-mail: duan.chen@ntnu.no (D.C.); tcw21@columbia.edu (T.C.W.)

Published 20 August 2014, *Sci. Transl. Med.* **6**, 250ra115 (2014)
DOI: 10.1126/scitranslmed.3009569

The PDF file includes:

Supplementary Materials and Methods

Animals

The insulin-gastrin (INS-GAS) transgenic mice were generated by Dr. T.C. Wang (*18*), and imported to Norway by Dr. D. Chen for these studies. Animals were further bred through sibling mating for more than 20 generations. 829 INS-GAS mice have been examined during the past 9 years. The percentage of the mice without preneoplastic lesions was 3.7% at 6 months of age, and the prevalence of spontaneous gastric cancer increased from 75% (at the beginning of this study in Jan. 2005) to 100% (May 2013) at 12 months of age without an additional infection with *Helicobacter pylori*. 187 INS-GAS mice were examined at 1 to 20 months of age during 2005, and 61 mice were found to have gastric tumors after 9 months of age (see Fig. 1A: the tumor prevalence at the lesser or greater curvature of the stomach). During 2012, 139 INS-GAS mice were examined at 12 months of age and all mice had gastric tumors. M_3KO mice were obtained from Dr. Koji Takeuchi at Kyoto Pharmaceutical University (*45*). M_3KO mice had higher water intake than age- and sex-matched wild type mice (14.62±1.71 *vs.* 6.48±1.00 mL/100 g body weight/24 hours, Means ± SEM (N=8), p = 0.01 (Student's t test). The chemically-induced gastric cancer model was established according to our previous report (*22*). In brief, mice were exposed to N-Methyl-N-nitrosourea (MNU, Sigma Chemicals), which was dissolved in distilled water at a concentration of 240 ppm and freshly prepared twice per week for administration in drinking water in

light-shielded bottles *ad libitum.* Starting at 4 weeks of age, mice were given drinking water containing MNU on alternate weeks for a total of 10 weeks. *H. pylori* infection was induced in H^+/K^+-ATPase-IL-1ß mice (*23*) by inoculation with pre-mouse Sydney strain 1 [PMSS1]). Three inocula (0.2 mL of *Hp*, 10^{10} colony-forming units/mL) were delivered every other day by oral gavage using a sterile gavage needle.

In the present study, animals were housed 3-4 mice per cage on wood chip bedding with a 12-hour light/dark cycle, room temperature of 22°C and 40-60% relative humidity. INS-GAS mice and FVB wild-type (WT) mice were housed at the standard housing conditions in a specific pathogen-free environment. M_3KO mice, *Hp*-infected H^+/K^+-ATPase-IL-1ß mice, and WT controls (C57BL/6 mice, Taconic, Denmark) were housed in a guaranteed animal facility at Comparative Medicine Core Facility at Norwegian University of Science and Technology All the mice had free access to tap water and standard pellet food (RM1 801002, Scanbur BK AS). Animal experiments were approved by the Norwegian National Animal Research Authority (Forsøksdyrutvalget, FDU) and by the Columbia University Institutional Animal Care and Use Committee (IACUC).

Experimental designs

581 mice were divided into 14 experimental groups (Table S1). In each experiment, mice were randomly divided into different subgroups. The animals, samples, and treatments were coded until the data were analyzed.

In the 1st experiment, 107 INS-GAS mice underwent bilateral truncal vagotomy with pyloroplasty (VTPP) (6 males, 19 females), pyloroplasty alone (PP) (7 males, 18 females), unilateral anterior truncal vagotomy (UVT) (11 males, 19 females), or sham operation (11 males, 16 females) at 6 months of age. Six months after surgery (at 12 months of age), the animals were euthanized, and the anterior and posterior parts of the stomachs were collected for histopathological and immunohistochemical analyses.

In the 2nd experiment, 20 WT mice (FVB, the same genetic background as INS-GAS mice) were exposed to MNU for one week every other week for 5 cycles (10 weeks). At 3.5 months of age, half of the MNU-treated mice underwent VTPP and the other half underwent a sham operation (PP). All the mice were euthanized at 13 months of age, and the stomachs were examined macroscopically and collected for histopathological analysis.

In the 3rd experiment, 24 H^+/K^+-ATPase-IL-1ß mice (14 males and 10 females, backcrossed to C57BL/6 for 10 generation) were inoculated with *Hp* at 3.5 months of age. At 12 months of age, half of the infected mice underwent UVT and the other half underwent a sham operation (laparotomy). All the mice were euthanized 6 months later. The stomachs were examined macroscopically and collected for histopathological analysis.

In the 4th experiment, 16 INS-GAS mice (5 males and 11 females) at 6 months of age underwent unilateral Botox treatment and were euthanized at 12 months of age. The anterior and posterior parts of the stomachs were collected for histopathological analysis.

In the 5th experiment, 64 INS-GAS mice at 8 months (7 males and 10 females), 10 months (6 males and 8 females) and 12 months (6 males and 6 females) of age underwent UVT, and 21 age-matched mice (8 males and 13 females) had no surgery. At 18 months of age, all surviving mice including 12 (6 males and 6 females) from the 8-month group, 9 from the 10-month group (3 males and 6 females), 8 from the 12-month group (4 males and 4 females), and 10 from the un-operated group (4 males and 6 females) were euthanized, and the anterior and posterior parts of the stomachs were collected for histopathological analysis and genome-wide gene expression profiling analysis. Survival analysis was also performed.

In the 6th experiment, 26 INS-GAS mice at 12 months of age underwent Botox treatments (only anterior or both anterior and posterior sides of the stomach with or without UVT) or vehicle injection (both anterior and posterior sides of the stomach). Mice were euthanized at 14 months of age. Both the anterior and posterior parts of the stomachs were collected for histopathological analysis.

In the 7th experiment, 133 INS-GAS mice at 12-14 months of age received no treatment (6 males and 6 females), saline (5 males and 5 females), 5-fluorouracil (5-FU) (5 males and 5 females), oxaliplatin (5 males and 8 females), saline + unilateral Botox treatment (4 males

and 6 females), unilateral Botox treatment + 5-FU (4 males and 6 females), unilateral Botox treatment + oxaliplatin (6 males and 7 females), sham operation (laparotomy) + 5-FU + oxaliplatin (6 males and 9 females), unilateral Botox treatment + 5-FU + oxaliplatin (11 males and 13 females), or UVT+ 5-FU + oxaliplatin (6 males and 10 females).Denervation treatment was applied to only half of the stomach, such that the non-denervated half of the stomach in each animal served as a control, either as chemotherapy only or as an untreated control. All mice were euthanized 2 months after starting the treatments, except for mice that died before the end of study, and both the anterior and posterior parts of the stomachs were collected for histopathological analysis. Survival analysis was also performed.

In the 8th experiment, 16 INS-GAS mice at 6 months of age underwent UVT and were euthanized at 2 months (1 male and 4 females), 4 months (2 males and 3 females), or 6 months (2 males and 4 females) postoperatively. The anterior and posterior parts of the stomachs were collected for genome-wide gene expression profiling.

In the 9th experiment, 44 INS-GAS mice at 12-14 months of age received saline (3 males and 3 females), 5-FU + oxaliplatin (5 males and 8 females), darifenacin (6 males and 6 females), or a combination of 5-FU + oxaliplatin and darifenacin (8 males and 5 females). Two months after starting the treatments, the mice were euthanized, and both the anterior and posterior parts of the stomachs were collected for histopathological analysis.

In the 10th experiment, both INS-GAS mice (6 males and 6 females) and WT mice (10 males and 10 females) were subjected either to UVT or no treatment. Six months after surgery (at 12 months of age), the animals were euthanized and the anterior and posterior parts of the stomachs were collected for gene expression analysis.

In the 11th experiment, 12 MNU-treated mice (6 males and 6 females) were subjected to PP or VTPP at 6 months of age and euthanized 4 months later. The stomachs were collected for qRT-PCR analysis.

In the 12th experiment, 7 M_3KO mice (4 males and 3 females) and 13 WT mice (5 males and 8 females) (C57BL/6, the same genetic background as M_3 KO mice) were exposed to MNU and euthanized at 11 months of age. The stomachs were examined macroscopically and were collected for histopathological analysis.

In the 13th experiment, 37 mice (20 males, 17 females) at 12-18 months of age underwent a topical application of acetic acid on the anterior side of the stomach with or without simultaneous UVT and were euthanized 1 week (5 males, 7 females), 2 weeks (3 males, 9 females), or 3 weeks (12 males, 1 female) later, and the anterior parts of the stomachs were collected for histopathological analysis.

In the 14th experiment, 10 Lgr5-GFP mice (all males) were treated with MNU at 2 months of age, subjected to PP or VTPP at 19 weeks of age, and euthanized at 25 weeks of age.

Animal surgery

All surgical procedures were performed under isoflurane inhalation anesthesia (2-3 %), with buprenorphine (0.1 mg/kg subcutaneously) given as postoperative analgesia. The abdominal cavity was accessed through a midline incision. The sham operation consisted of a laparotomy with mild manipulation of organs, including identification of the vagus nerve. PP was done by longitudinal incision of the pyloric sphincter followed by transverse suturing. VTPP was performed by subdiaphragmatic dissection of both the anterior and posterior vagal trunks and simultaneous PP to prevent post-vagotomy delayed gastric emptying. In UVT, only the anterior truncal vagus nerve was cut (Fig. S2), leading to a specific vagal denervation of the anterior aspects of the stomach, with preserved pyloric function making PP unnecessary. Sample collection was done under inhalation anesthesia as described, and the animals were euthanized by exsanguination while still under anesthesia.

Botox treatment

Botox 100 U (Botox Allergan Inc.) was dissolved in 0.9% cold saline and 1% methylene blue (to visualize the injection), achieving a concentration of 0.25 U of Botox/mL. The Botox solution was injected subserosally along the greater curvature into the anterior (unilateral Botox treatment) or both anterior and posterior sides (bilateral Botox treatment) of the stomach (only the corpus area where tumor developed) at the dose of 0.05 U/mouse (0.2

mL/mouse) or 0.1 U/mouse (0.4 mL/mouse), respectively, once per month until the end of the study. In the control group, the vehicle solution was prepared with 0.9% saline and 1% methylene blue and injected into both anterior and posterior sides of the stomach (only the corpus area where tumor developed) at a volume of 0.4 mL/mouse.

Chemotherapy and M_3 receptor antagonist treatment

5-Fluorouracil (5-FU, Flurablastin, Pfizer, Inc.) was diluted in saline and given at a dose of 25 mg/kg in a volume of 1 mL. Oxaliplatin (Hospira, Inc.) was diluted in saline and given at 5 mg/kg in 1 mL. Combination of 5-FU (25 mg/kg in 0.5 mL) and oxaliplatin (5 mg/kg in 0.5 mL) was given at the same time, but the drugs were injected separately. Chemotherapy was given by intraperitoneal injection weekly in 2 cycles, namely 3 injections in the 1st month (starting one week after the 1st Botox, UVT, or the 1st osmotic mini-pump implantation), and 3 injections in the 2nd month (starting at one week after the 2nd Botox, no UVT, or the 2nd mini-pump). Age- and sex-matched mice received intraperitoneal injection of saline (1 mL) as controls. The injection needle was 27 G. The dosages and regimens were made based on our pilot experiments for selecting the doses. There was no effect on tumor size by 5-FU or oxaliplatin alone (Fig. S16).

Darifenacin hydrobromide (Santa Cruz Biotechnology) was given at a dose of 1 mg/kg/h for 2 months via an osmotic mini-pump (ALZET 2006) as reported previously (*48*).

Tumor regeneration model

Topical application of acetic acid was found to promptly cause necrosis in the tumor tissue in INS-GAS mice. Under isoflurane anesthesia, the stomach was exposed through a midline abdominal incision, and 60% acetic acid was topically applied to the serosa of the anterior side of the stomach for 60 seconds using a 5 mm internal diameter cylindrical metal mold. In the experiment combining acetic acid-induced necrotic ulcers with UVT, the mice underwent acetic acid application during the UVT surgery.

Pathological and immunohistochemical analyses

The stomachs were removed, opened along the greater curvature, washed in 0.9% NaCl, and pinned flat on a petri-dish-silicone board. Each stomach was photographed digitally; the tumor profiles in both anterior and posterior sides of the stomach were drawn separately and subjected to morphometric analysis of the volume density (expressed as the percentage of glandular volume occupied by the tumor) using point-counting technique with a test grid comprised of a 1.0 cm square lattice. This grid was placed over each photograph (40 x 30 cm^2), and the numbers of test points overlying the tumor and gastric glandular area were determined. The samples for histology comprised multiple linear strips along the greater curvature of the stomach wall, extending from the squamocolumnar junction through the

antrum. Samples were fixed in 4% formaldehyde for 8-12 hours at room temperature and embedded in paraffin. Sections (4 µm thick) were stained with hematoxylin and eosin. Pathological evaluation was performed by comparative pathologists and a histologist who were blinded to the sample source. The gastric lesions were scored on an ascending scale from 0 to 4, using criteria adopted from previous reports (*21)*. Inflammation scoring were assigned for patchy infiltration of mixed leukocytes in mucosa and/or submucosa (1), multifocal-to-coalescing leukocyte infiltration not extended below submucosa (2), marked increase in leukocytes with lymphoid follicles +/- extension into tunica muscularis (3), or effacing transmural inflammation (4). The epithelial defects were defined as gland dilatation, surface erosions and gland atrophy, and ulceration and fibrosis. Immunohistochemistry was performed using a DAKO AutoStainer (Universal Staining System with DAKO EnVision System, Dako). Antibodies used were Ki67 (1:100; code M7249, Dako), PCNA (1:100, code M0879, Dako), CD44 (1:100, code 550538, BD Pharmingen), CD44V6 (1:200, code AB2080, Millipore), PGP9.5 (1:1000, code Z5116, Dako, and code 7863-0504, AbD Serotec), peripherin (1:500, code AB1530, Millipore), ß-catenin (1:500, code 610654, BD Transduction Laboratories), Alexa Fluor 488 Phalloidin (1:200, code A12379, Life Technologies), Alexa Fluor 555 Goat Anti-Rabbit IgG (H+L)(1:200, code A21428, Life Technologies). Cellular proliferation is expressed as the number of Ki67 or PCNA immunoreactive cells/gland. There was no difference between the two markers between two

labs (TW and DC). Slides were visualized on a Nikon TE2000-U and representative microhistophotos were taken. Positive-stained cells with nuclei were counted only in dysplastic glands, with least 50 glands counted per animal in a blinded fashion, and results are expressed as numerical densities (number of cells per gland, number of cells per 10 glands or per object field). Positive-stained nerves were quantitated by ImageJ software and are expressed as positive area per total mucosal area.

Vagus nerve fibers and terminals in the mouse stomach traced with carbocyanine dye (DiI)

The esophagus, diaphragm and stomach were removed from adult mice and fixed for 3 days with formaldehyde. DiI crystals were placed on the anterior and posterior thoracic vagal trunks about 1 cm above the diaphragm, which was left undisturbed. The preparation was incubated at 37°C in PBS containing 0.5% sodium azide in a sealed container for 3 months. After incubation, the stomach was opened along the greater curvature, the mucosa and submucosa were removed, and the preparations were mounted, serosal side up, in buffered glycerol for microscopic examination. DiI fluorescence was viewed with a Leica CTR6000 microscope equipped with a cooled CCD camera and computer assisted video imaging. The entire gastric wall was scanned with a 2.5x objective, and a montage was made from the resulting images. In order to observe the density of DiI-labeled vagal fibers within the

myenteric plexus, additional images were obtained at higher magnification in the lesser curvature close to the esophagogastric junction and in the greater curvature. The density of DiI-labeled fibers was estimated by point counting technique. A test system comprising a 1.0 cm square lattice was placed over each photograph, and the numbers of test points overlying the DiI-labeled fibers and the visual field were determined.

RNA isolation, gene expression profiling by microarray, qRT-PCR arrays and qRT-PCR in mice and humans

The collected mouse and human stomach samples were kept frozen at -80°C until further processing. Total RNA from the frozen stomach samples was isolated and purified using an Ultra-Turrax rotating-knife homogenizer and the mirVana miRNA Isolation Kit (AM1560, Ambion) according to the manufacturer's instructions. Concentration and purity of total RNA were assessed using a NanoDrop photometer (NanoDrop Technologies, Inc.). The A260/280 ratios were 2.05 ± 0.01 for mouse samples and 1.96 ± 0.10 for human samples (mean ± SEM). RNA integrity was assessed using a Bioanalyzer (Agilent Technologies) and found satisfactory, with RNA integrity number (RIN) values 9.1 ± 0.1 for mouse samples, and 8.7 ± 0.9 for human samples (means ± SEM). The microarray gene expression analysis followed standard protocols, analyzing 300 ng total RNA per sample with the Illumina MouseWG-6 and HumanHT-12 Expression BeadChips (Illumina). Microarray data were confirmed by

qRT-PCR array (RT^2 Profiler PCR Array, SABiosciences) (StepOnePlus™, Applied Biosystems). Mouse microarray data were deposited in the Gene Expression Omnibus (GEO accession no. GSE30295), and human data in ArrayExpress (accession no. E-MTAB-1338). Longitudinal strips of gastric tissue from the anterior wall as well as the posterior wall were harvested and snap-frozen in dry ice and kept in a -80°C freezer until processed for analysis. Total RNA was extracted with Nucleospin RNA II kit (Clontech), and cDNA was synthesized by Superscript III First-strand Synthesis System for RT-PCR (Invitrogen). See Table S3 for primer sequences used. Expression levels of indicated genes were quantified by real-time PCR assays with SYBR Green dye and the Applied Biosystems 7300 Real Time PCR System.

Fluorescence-activated cell sorting (FACS)

Single epithelial cells were isolated from *Lgr5*-GFP mouse stomachs. Isolated crypts were dissociated with TrypLE Express (Invitrogen) including 1 mg/ml DNase I (Roche Applied Science) for 10 minutes at 37°C. Dissociated cells were passed through a 20-μm cell strainer, washed with 2% FBS/PBS, and sorted by FACS (BD FACSAria Cell Sorter III). Viable single epithelial cells were gated by forward scatter, side scatter and a pulse-width parameter, and negative staining for propidium iodide. Cells expressing high and low levels of GFP and

GFP-negative cells were sorted separately, and RNA was isolated by using RNAqueous-Micro Kit (Ambion).

***In vitro* culture system**

Wild-type (WT), Ubiquitin C-green fluorescent protein (UBC-GFP), or Gt(ROSA)26Sortm4(ACTB-tdTomato,-EGFP)Luo/J mice (The Jackson laboratory) were used for *in vitro* culture. Gastric gland isolation and culture were performed as described previously (*9*), with minor modifications. Stomachs removed from WT and M_3KO mice were opened longitudinally, chopped into approximately 5 mm pieces, and incubated in 8 mM EDTA in PBS for 60 minutes on ice. The tissue fragments were vigorously suspended, yielding supernatants enriched in gastric glands. Gland fractions were centrifuged at 900 rpm for 5 minutes at 4°C and diluted with advanced DMEM/F12 (Invitrogen) containing B27, N2, 1 μM n-Acetylcysteine, 10 mM HEPES, penicillin/streptomycin, and Glutamax (all Invitrogen). Glands were embedded in extracellular matrix (Fisher Bioservices/NCI Frederick Central Repository) and 400 crypts/well were seeded on pre-warmed plates. Advanced DMEM/F12 medium containing 50 ng/mL EGF, 100 ng/mL Noggin, and 1 μg/mL R-spondin1 was applied. Wnt3a (PeproTech) was added at 100 ng/mL when indicated. Growth factors were added every other day, and the entire medium was changed twice a week. Passage was performed at day 7 as described previously (*9*). Mouse primary neuronal cells were prepared following the protocol described previously (*33*). Neuronal cells were

mixed with extracted gastric crypts in the extracellular matrix at the ratio of crypt:neuron 1:5. The enteric nervous system was isolated from guinea pigs as described previously (*34*). Botox, scopolamine hydrochloride, and pilocarpine hydrochloride (Sigma) were dissolved in PBS and added in the cultured medium every other day. The images of gastric organoids were acquired using fluorescent microscopy (Nikon, TE2000-U) and two-photon microscopy (Nikon, A1RMP). Isolation of mRNA from cultured organoids was performed with a NucleoSpin RNA XS kit (Clontech Laboratories Inc.) according to manufacturer's instructions. The first-strand complementary DNA was synthesized using the ImProm-II Reverse Transcription System (Promega). Amplification was performed using the ABI PRISM 7300 Quantitative PCR System (Applied Biosystems).

Patients and methods

Three cohort studies were included (Table S2). In the 1st study, human stomach specimens (both tumors and the adjacent non-tumor tissues) were taken immediately after gastrectomy from 17 patients during 2005 to 2010 at St. Olav's University Hospital, Trondheim, Norway for gene expression profiling analysis. All patients were diagnosed histologically as primary gastric carcinoma of stage I-IV. 10 of 17 patients were *H. pylori* positive at the time of surgery. In the 2nd study, human stomach tissues were obtained from 120 gastric cancer patients who underwent curative surgical resection from 2001 to 2008 at Gifu University

Hospital, Gifu, Japan. All patients were diagnosed histologically as primary gastric carcinoma of stage II, III, or IV. Immunohistochemical analysis of the nerve density was performed with PGP9.5 antibody. Low and high expression of PGP9.5 were defined with respect to the median of the volume density of PGP9.5. In the 3rd study, clinical data of 37 patients with gastric stump cancer (GSC) who had received distal gastrectomy with or without vagotomy during 1962 to 1995 at the National Cancer Center Hospital East, Chiba, Japan were evaluated. GSC was defined as gastric cancer that occurred ≥ 5 years (from 5 to 36 years) after curative distal gastrectomy, regardless of the original benign or malignant disease. GSC included in this study was adenocarcinoma infiltrating the mucosal or submucosal layer. The tumor location was recorded according to the recommendation by the Japanese Gastric Cancer Association: anterior or posterior wall, or lesser or greater curvature (Fig. S15). All the study protocols were approved by the ethics committees in Japan and Norway, and written informed consent was obtained from patients.

Data analysis and statistics

Values were expressed as means ± SEM. Pairwise comparisons between experimental groups and between anterior and posterior sides of the stomach were performed with the paired and unpaired *t*-test as appropriate. All tests were two sided with a significance cutoff of 0.05. Comparisons between more than 2 groups were performed by ANOVA, followed by

Dunnett's test or Tukey's test as appropriate. Comparisons with categorical independent variables were performed using Fisher's exact test. Kaplan-Meier survival curves were calculated and were analyzed by the Cox proportional hazard method. Tumor prevalence/incidence was analyzed by Fisher's exact test. Affymetrix microarray data were normalized using RMA, and Illumina microarray data was analyzed using Lumi. Both qRT-PCR and microarray data were analyzed on the $\log_2$ scale. The significance of differential expression of qRT-PCR data was analyzed using parametric frequentist statistics, and microarray data were analyzed using the empirical Bayesian method implemented in Limma. Gene expression profiles from both microarray and qRT-PCR were analyzed independently by a paired robust *t*-test for mouse samples or a paired *t*-test for human samples. Paired *t*-statistics were computed by fitting a linear robust or non-robust regression to the anterior and posterior stomach samples within each mouse or to the cancer and the adjacent non-cancerous tissue samples within each patient. For microarray data, transcripts with Benjamini-Hochberg false discovery rates less than 0.05 were considered to be differentially expressed. Regulated KEGG (Kyoto Encyclopedia of Genes and Genomes) pathways were identified using Signaling Pathway Impact Analysis. All of the above calculations were performed in the R/Bioconductor software environment.

Supplementary figures and tables

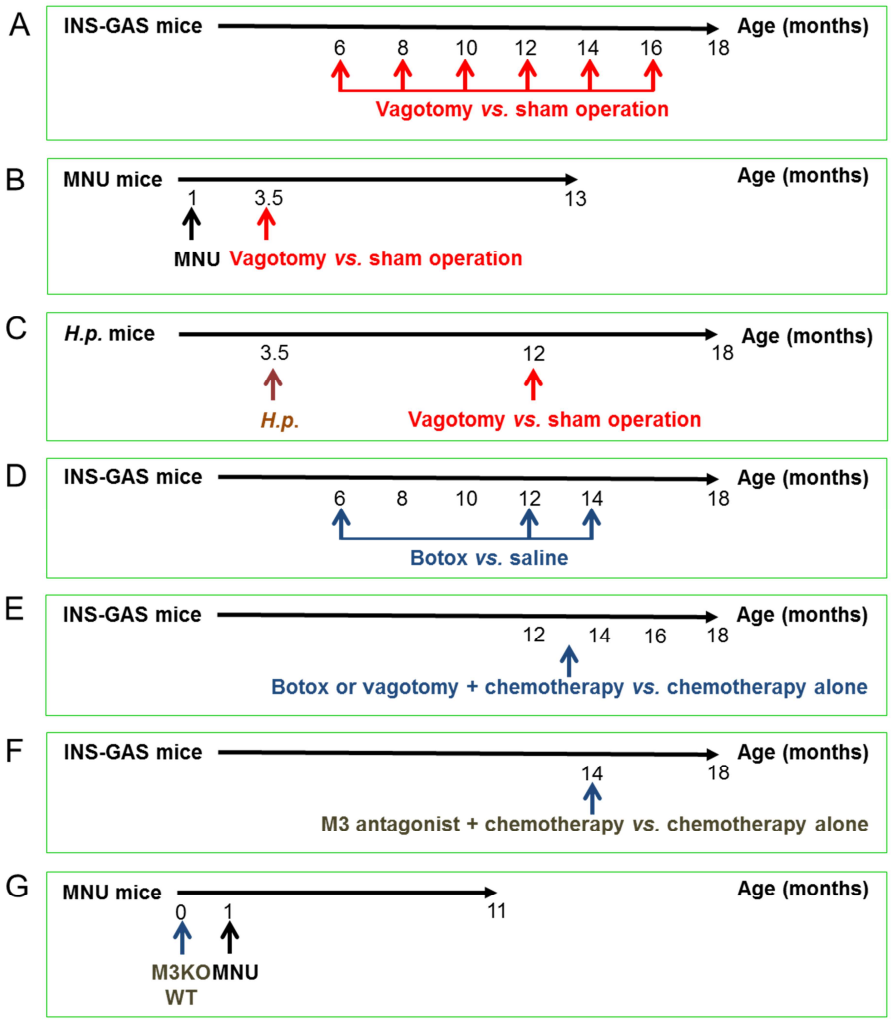

Fig. S1. Flowchart showing the animal study design.

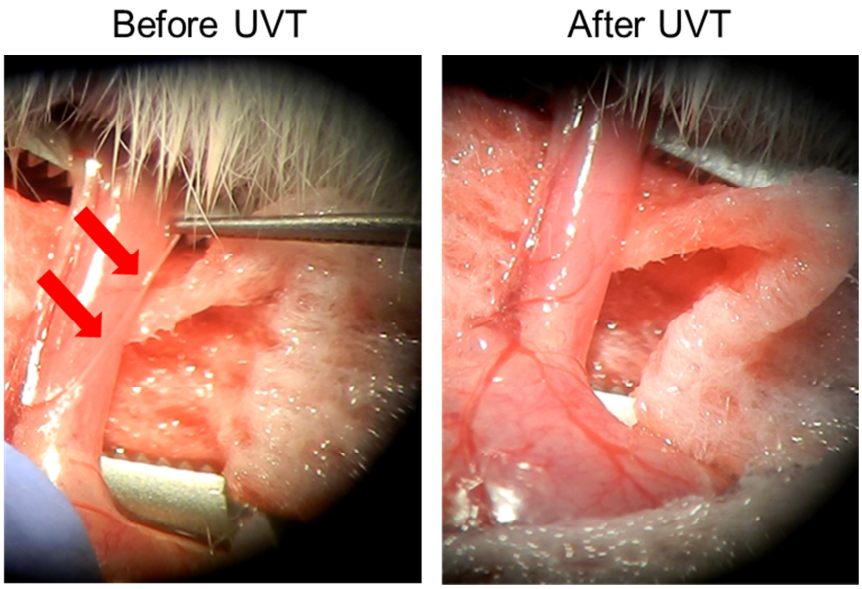

Figure S2: Anterior UVT in mice. Photographs showing dissected vagus nerve (indicated by arrows) before and after anterior unilateral truncal vagotomy (UVT) are shown.

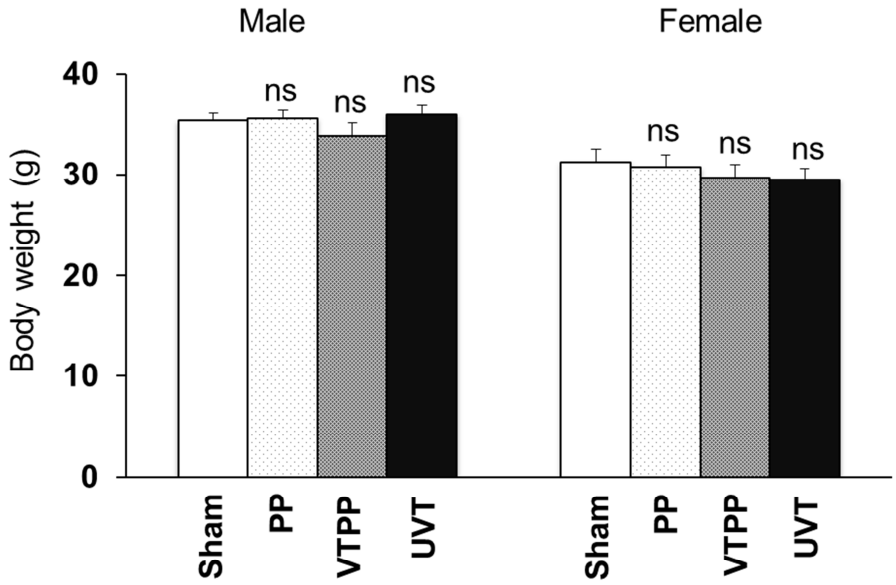

Figure S3: Body weight of male and female INS-GAS mice after surgery. Body weight of sham (Sham), pyloroplasty (PP), bilateral vagotomy with pyloroplasty (VTPP), and anterior unilateral vagotomy (UVT)-operated INS-GAS mice at 12 months of age (6 months postoperatively). Means ± SEM. ns: not significantly different between Sham (*N* = 11 males, 16 females) and PP (*N* = 7 males, 18 females), VTPP (*N* = 6 males, 19 females), or UVT (*N* = 11 males, 19 females) (Dunnett's test).

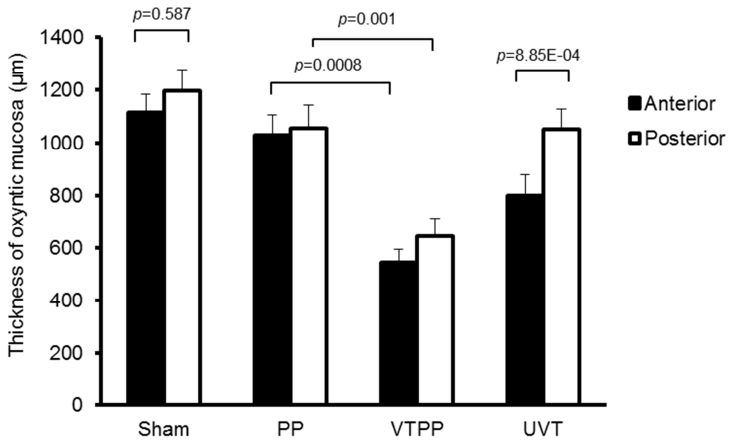

Figure S4: Thickness of the gastric oxyntic mucosa after surgery in INS-GAS mice. Thickness of the oxyntic mucosa in sham (Sham), pyloroplasty (PP), bilateral vagotomy with pyloroplasty (VTPP), and anterior unilateral vagotomy (UVT)-operated INS-GAS mice at 12 months of age (6 months postoperatively). Means ± SEM. Tukey test: between PP (N = 25) and VTPP (N = 25). Paired t test: between anterior vs. posterior sides within Sham (N = 27) and UVT (N = 30).

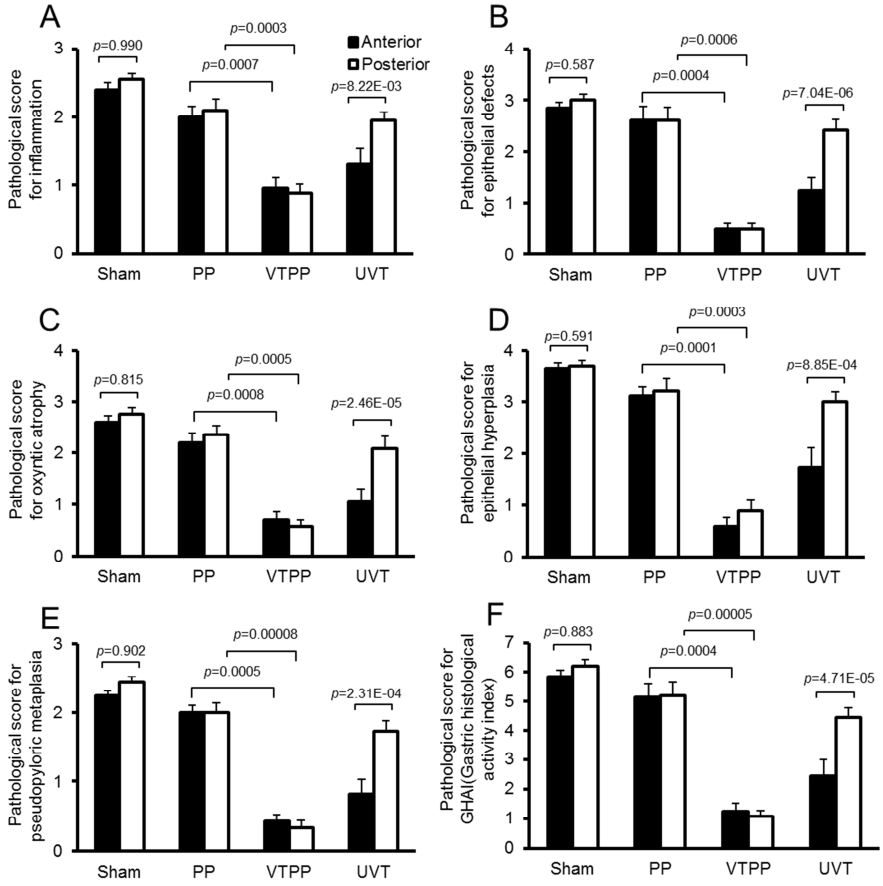

Figure S5: Pathological scores for the stomach after surgery in INS-GAS mice. Pathological scores for inflammation (A), epithelial defects (B), oxyntic atrophy (C), epithelial hyperplasia (D), pseudopyloric metaplasia (E), and GHAI (gastric histological activity index) (F) in sham (Sham), pyloroplasty (PP), bilateral vagotomy with pyloroplasty (VTPP), and anterior unilateral vagotomy (UVT)-operated INS-GAS mice at 12 months of age (at 6 months after surgery). Means ± SEM. Tukey test: between PP (N = 25) and VTPP (N = 25). Paired t test:

between anterior *vs.* posterior sides within Sham (N = 27) and UVT (N = 30).

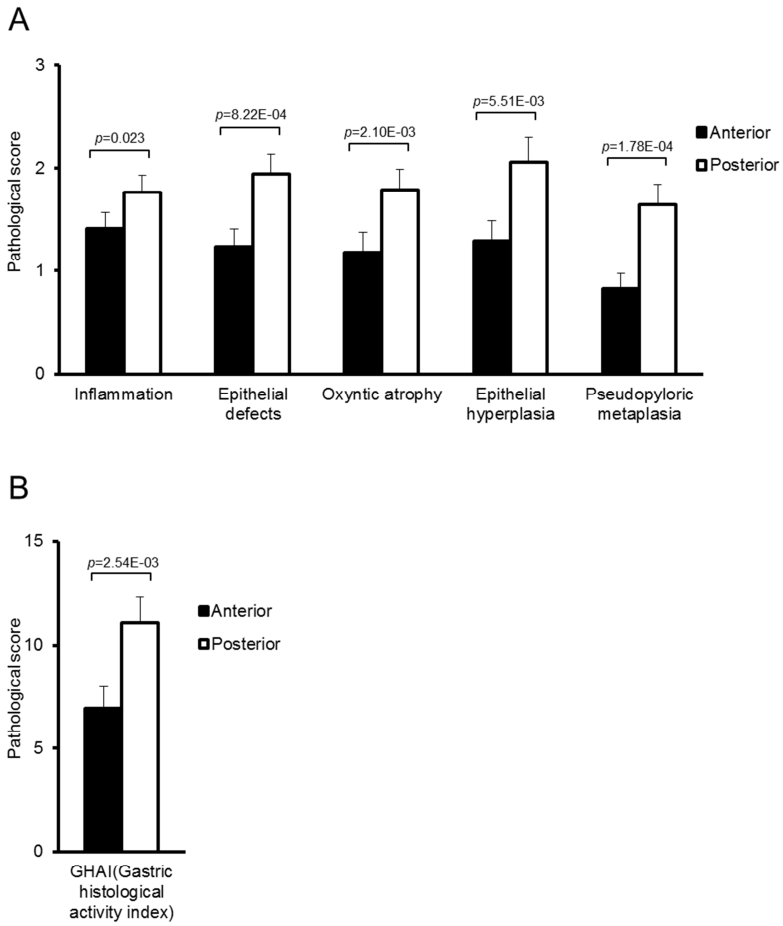

Figure S6: Pathological scores for the stomach after Botox injection in INS-GAS mice. Pathological scores for inflammation, epithelial defects, oxyntic atrophy, epithelial hyperplasia, pseudopyloric metaplasia (A), and GHAI (gastric histological activity index) (B) in Botox-injected (in anterior side of the stomach) INS-GAS mice at 12 months of age (monthly Botox injection starting at 6 months of age). Means ± SEM (N = 16). Paired t test between anterior *vs.* posterior sides.

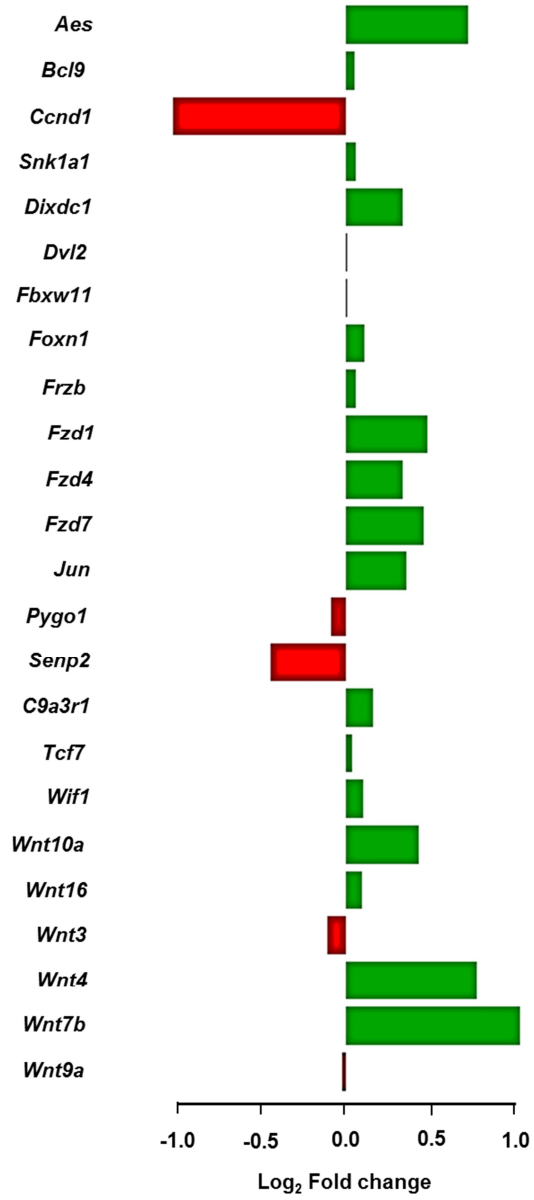

Figure S7: Wnt signaling in INS-GAS mice compared with wild-type mice. Fold changes of Wnt-related genes: upregulated (indicated by red) and downregulated (green).

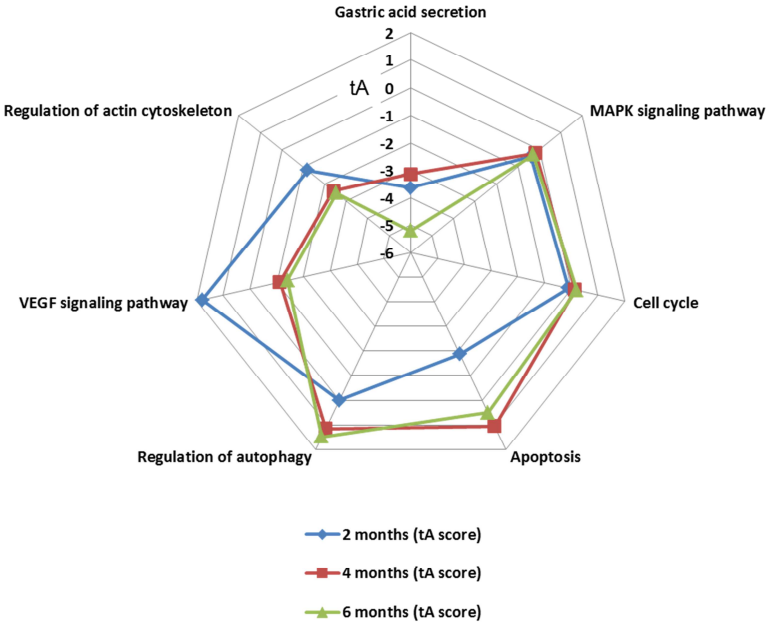

Figure S8: Altered signaling pathways after vagotomy in INS-GAS mice. Altered signaling pathways involved gastric acid, MAPK signaling, and tissue homeostasis at 2 (blue), 4 (green), and 6 (red) months in the anterior oxyntic mucosa of the stomach after anterior unilateral vagotomy compared with posterior side. tA score: -4 to 6. tA score>0: activation; tA score<0: inhibition.

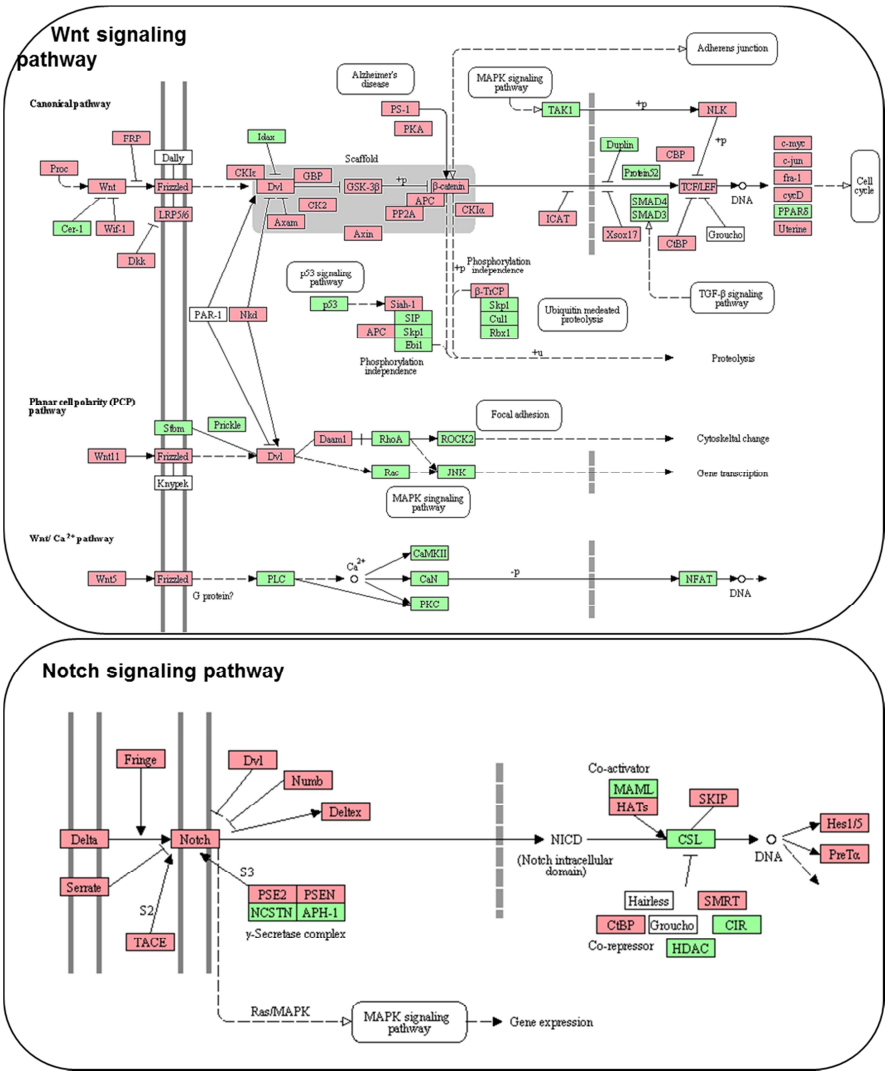

Figure S9: Wnt and Notch signaling pathways in the stomach after vagotomy in INS-GAS mice. Wnt and Notch signaling KEGG pathways in the anterior oxyntic mucosa after anterior unilateral vagotomy compared with the posterior side at 6 months postoperatively. Down-regulated genes (p<0.05) are indicated by pink; unchanged genes are green.

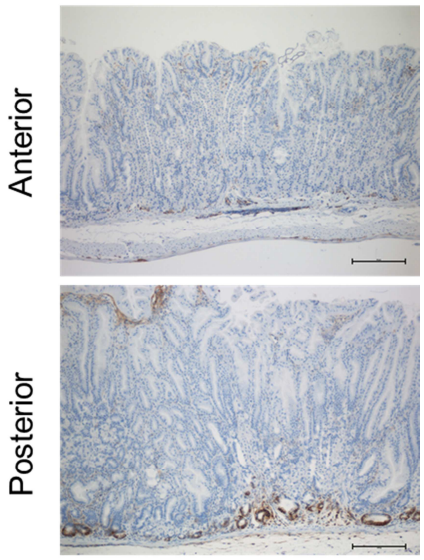

Figure S10: Immunostaining of CD44 after vagotomy in INS-GAS mice. Representative microphotographs of CD44+ cells in the oxyntic mucosa of the anterior and the posterior regions of the same stomach in a mouse subjected to unilateral anterior vagotomy (UVT). Scale bars = 25 μm.

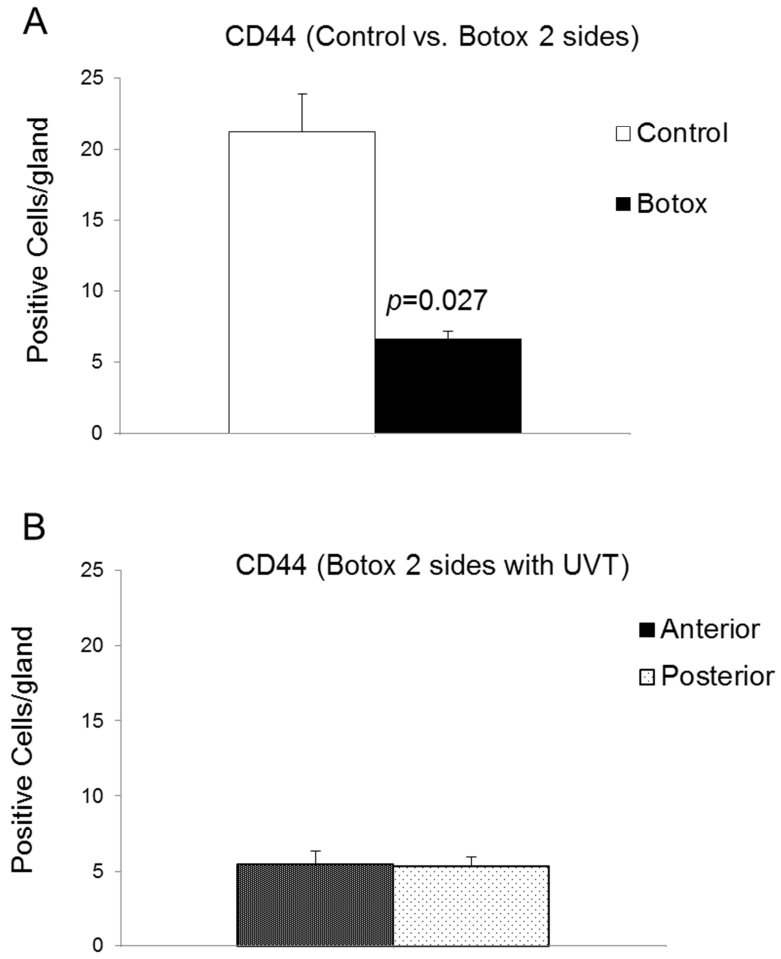

Figure S11: Numbers of CD44-immunoreactive cells after Botox treatment ± vagotomy in INS-GAS mice. CD44-immunoreactive cells in mice subjected to saline (control) or Botox injection into anterior and posterior sides of the stomach (A) and Botox injection into anterior and posterior sides plus anterior UVT (B). Means ± SEM. Student's *t* test was used to compare control ($N = 6$) and Botox ($N = 7$).

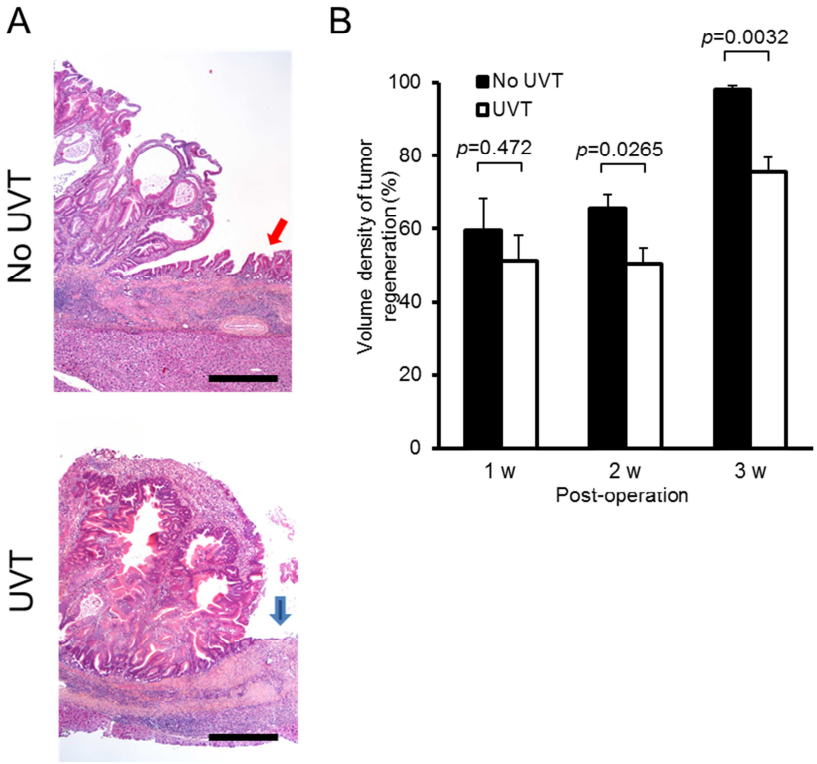

Figure S12: Tumor regeneration in the stomach after vagotomy in INS-GAS mice. (A) Microphotographs showing histopathological appearances of tumor regeneration at 3 weeks after acetic acid-induced necrotic ulcer. Note regeneration (indicated by red arrow) without unilateral vagotomy (No UVT) and no regeneration (blue arrow) after UVT. Scale bars: 50 µm. (B) Volume density of tumor regeneration 1, 2, and 3 weeks after application of acetic acid in mice with or without UVT. Means ± SEM. Student's *t* test was used to compare no UVT and UVT (*N* = 6, except *N* = 8 or 5, respectively, at 3 weeks).

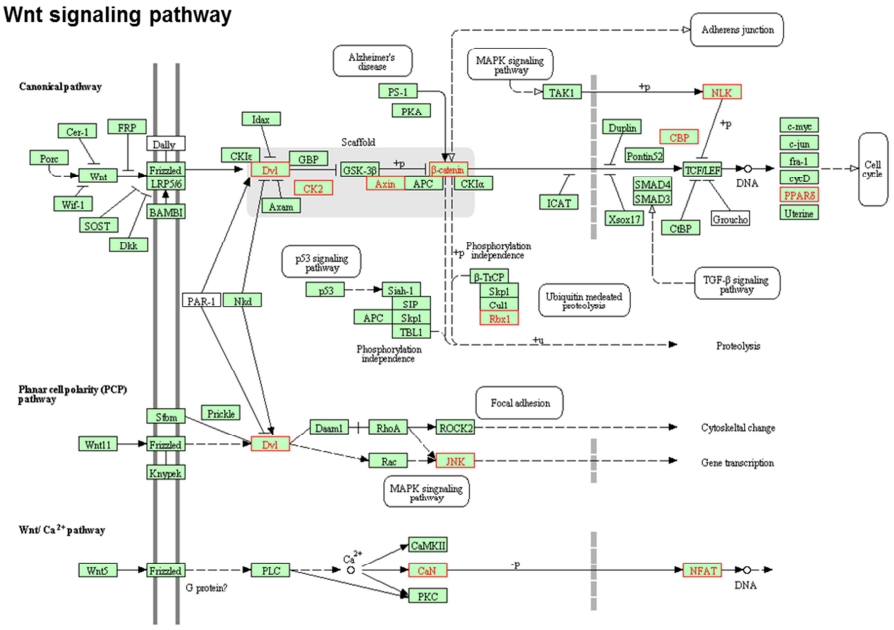

Figure S13: Wnt signaling KEGG pathway in M_3KO mice compared with wild-type mice. Downregulated genes ($p < 0.05$) are indicated by red, unchanged genes are green.

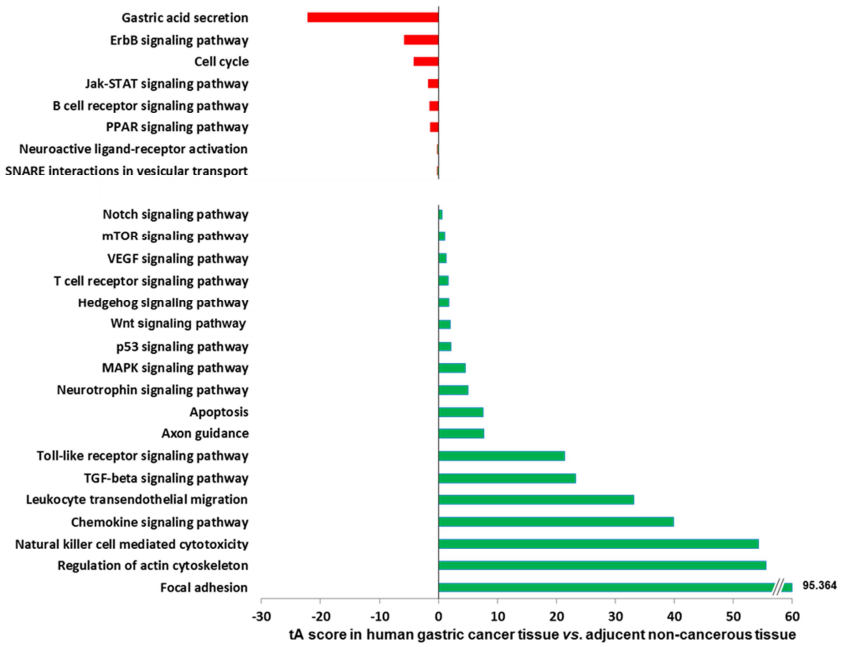

Figure S14: Altered signaling pathways in human gastric cancer tissue compared with adjacent noncancerous tissue. tA score>0: activation (indicated by green); tA score<0: inhibition (red)

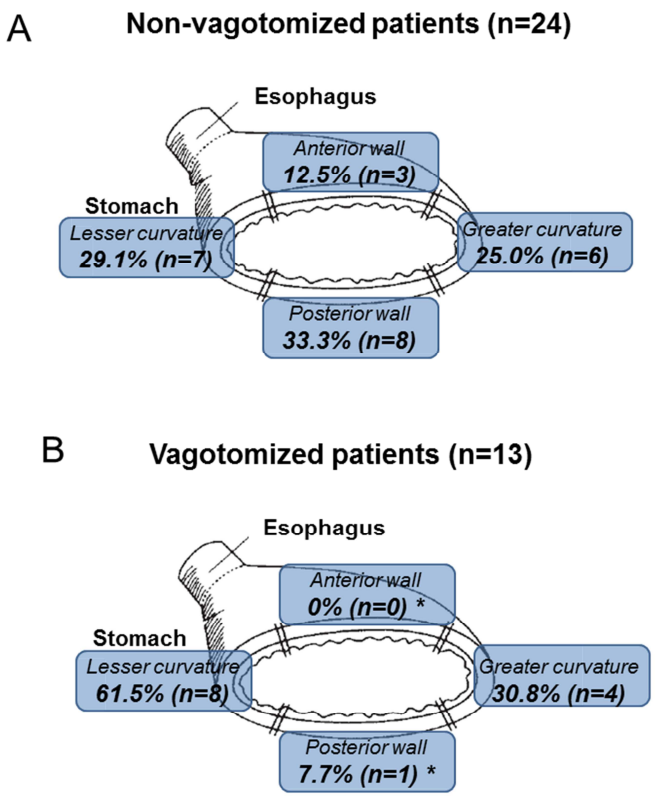

Fig. S15. Gastric stump cancer after distal gastrectomy with or without vagotomy. (A) Tumors in both anterior and posterior walls in 24 patients without vagotomy. (B) No tumors in anterior and one tumor in a posterior wall among 13 patients who underwent vagotomy. $p = 0.01898$ or $p = 0.02718$ for anterior or posterior wall of vagotomized patients compared with non-vagotomized patients (Fisher test).

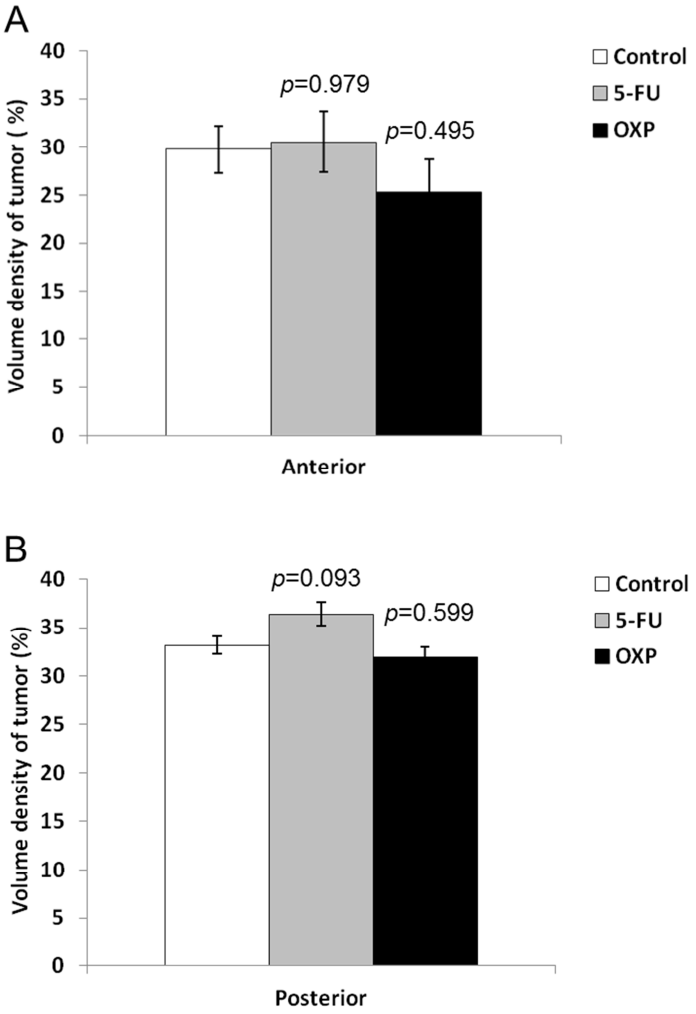

Fig. S16. Effect of 5-FU and oxaliplatin on INS-GAS mice. Tumor size in the anterior (A) or posterior (B) sides of stomachs in mice treated with saline (Control, *N* = 10), 5-FU (*N* = 10), or oxaliplatin (OXP, *N* = 13). Means ± SEM. P values were calculated by Dunnett's test.

Table S1. Animal experimental groups.

	Mouse (*N*)	Group (*N*)	Age* at operation (months)	Age* at examination (months)
1	INS-GAS (107)			
		Sham (27)	6	12
		PP (25)	6	12
		UVT (30)	6	12
		VTPP (25)	6	12
2	MNU (FVB)(20)			
		MNU+ PP(11)		13
		MNU+VTPP (9)	3.5	13
3	*H.p.*-infection (24)			
		Sham (12)	12	18
		UVT (12)	12	18
4	INS-GAS (16)			
		UB (16)	6	12
5	INS-GAS (64)			
		No surgery (21)		18
		UVT (17)	8	18
		UVT (14)	10	18
		UVT (12)	12	18
6	INS-GAS (26)			
		Vehicle (6)	12	14
		UB (6)	12	14
		BB (7)	12	14
		BB+UVT (7)	12	14
7	INS-GAS (133)			
		No treatment (12)	12-14	14-16
		Saline (10)	12-14	14-16
		5-FU (10)	12-14	14-16
		OXP (13)	12-14	14-16
		UB+Saline (10)	12-14	14-16
		UB+5-FU (10)	12-14	14-16
		UB+OXP (13)	12-14	14-16
		Sham+5-FU+OXP (15)	12-14	14-16
		UB+5-FU+OXP (24)	12-14	14-16

		UVT+5-FU+OXP (16)	12-14	14-16
8	INS-GAS (16)			
		UVT (5)	6	8
		UVT (5)	6	10
		UVT (6)	6	12
9	INS-GAS (64)			
		Saline (19)	12-14	14-16
		5-FU+OXP (12)	12-14	14-16
		Darifenacin (15)	12-14	14-16
		5-FU+OXP+darifenacin (8)	12-14	14-16
10	INS-GAS (12)	INS-GAS - No treatment (6)	6	12
	FVB (20)	INS-GAS - UVT (6)	6	12
		WT- No treatment (10)	6	12
		WT- UVT (10)	6	12
11	MNU (12)			
		PP (6)	6	10
		VTPP (6)	6	10
12	M3KO (7)	M3KO+MNU (7)		11
	C57BL/6 (13)	WT+MNU (13)		11
13	INS-GAS (37)			
		Regeneration** 1 week (6)	12-18	12-18+1week
		Regeneration 1 week after UVT (6)	12-18	12-18+1week
		Regeneration 2 weeks (6)	12-18	12-18+2weeks
		Regeneration 2 weeks after UVT (6)	12-18	12-18+2weeks
		Regeneration 3 weeks (8)	12-18	12-18+3weeks
		Regeneration 3 weeks after UVT (5)	12-18	12-18+3weeks
14	Lgr5-GFP (10)			
		MNU + PP (5)	4,75	6,25
		MNU+ VTPP (5)	4,75	6,25

PP: Pyloroplasty, UVT: Unilateral vagotomy, VTPP: Bilateral vagotomy+pyloroplasty
UB: Unilateral Botox injection, BB: Bilateral Botox injection, OXP: Oxaliplatin
*Preneoplasia at 6 months and neoplasia at 12 months of age in INS-GAS mouse. **Tumor regeneration was induced by topical application of acetic acid.

Table S2. Cohorts of gastric cancer patients.

	1st cohort	**2nd cohort**	**3rd cohort**
Country	Norway	Japan	Japan
Purpose	Gene expression profiling	Innervation and tumorigenesis	Stump cancer after vagotomy
Study period	2005-2010	2001-2008	1962-1998
Patient			
Number (male:female)	17 (14:3)	120 (78:42)	37 (31:6)
Age (y.o.)	49-86	31-92	69-90
Pathological stage	I-IV	II-IV	I-II
H.pylori status	10/17 positive	n.d.	n.d.

Table S3. List of qRT-PCR primers used in this study.

Gene	Forward (5'->3')	Reverse (5'->3')
Lgr5	TCCAACCTCAGCGTCTTC	TGGGAATGTGTGTCAAAG
Cd44	CACATATTGCTTCAATGCCTCAG	CCATCACGGTTGACAATAGTTATG
Axin2	ACTGACCGACGATTCCATGT	TGCATCTCTCTCTGGAGCTG
Myc	AGAGCTCCTCGAGCTGTTTG	TGAAGTTCACGTTGAGGGG
Cyclin D1	TCCTCTCCAAAATGCCAGAG	GGGTGGGTTGGAAATGAAC
Sox9	AGGAAGCTGGCAGACCAGTA	TCCACGAAGGGTCTCTTCTC
Chrm1	CAGAAGTGGTGATCAAGATGCCTAT	GAGCTTTTGGGAGGCTGCTT
Chrm2	TGGAGCACAACAAGATCCAGAAT	CCCCTGAACGCAGTTTTCA
Chrm3	CCAGTTGGTGTGTTCTTCCTT	AGGAAGAGCTGATGTTGGGA
Chrm4	GTGACTGCCATCGAGATCGTAC	CAAACTTTCGGGCCACATTG
Chrm5	GGCCCAGAGAGAACGGAAC	TTCCCGTTGTTGAGGTGCTT
Gapdh	TCATTGTCATACCAGGAAATGAG	AGAAACCTGCCAAGTATGATGAC

Paper II

J Gastrointest Surg
DOI 10.1007/s11605-010-1315-7

2010 SSAT PLENARY PRESENTATION

Eating Behavior in Rats Subjected to Vagotomy, Sleeve Gastrectomy, and Duodenal Switch

Yosuke Kodama · Chun-Mei Zhao · Bård Kulseng · Duan Chen

Received: 26 April 2010 / Accepted: 9 August 2010

Abstract
Background/Aim Food intake, eating behavior, and metabolic parameters in rats that underwent bilateral truncal vagotomy, sleeve gastrectomy, and duodenal switch procedures were examined.
Methods Rats were subjected to bilateral truncal vagotomy plus pyloroplasty (VTPP), pyloroplasty (PP), laparotomy, sleeve gastrectomy (SG), or duodenal switch (DS; with and without SG).
Results VTPP, but neither PP nor laparotomy, reduced body weight (BW; 10%) transiently (1 week postoperatively). SG reduced BW (10%) for 6 weeks, while DS alone or SG followed by DS led to a continuous BW loss from 15% at 1 week to 50% at 8 weeks postoperatively. Food intake was higher and the satiety ratio was lower during the night than the day for all groups of surgeries. Neither VTPP nor SG had measurable effect on food intake, eating behavior and metabolic parameters. DS reduced daily food intake by more than 50%, which was associated with hypercholecystokinin(CCK)emia, reduced meal size and increased satiety ratio, and increased fecal energy content (measured at 8 weeks).
Conclusions Weight loss after VTPP, SG, or DS differed in terms of degree, duration, and underlying mechanisms. DS without SG was most effective in the long-term, probably due to hyperCCKemia-induced reduction in food intake and long-limb intestinal bypass-induced malabsorption.

Keywords Body weight · Food intake · Obesity surgery

Y. Kodama · C.-M. Zhao · B. Kulseng · D. Chen
Department of Cancer Research and Molecular Medicine,
Norwegian University of Science and Technology,
Trondheim, Norway

B. Kulseng
Departments of Surgery and Endocrinology,
St. Olavs University Hospital,
Trondheim, Norway

D. Chen (✉)
Department of Cancer Research and Molecular Medicine,
Faculty of Medicine,
Norwegian University of Science and Technology,
Laboratory Centre (3rd Floor-East Side),
Erling Skjalgssons Gate 1,
7006 Trondheim, Norway
e-mail: duan.chen@ntnu.no

Introduction

During the evolution of surgery for morbid obesity, many different surgical procedures have been developed in order to reduce food intake and/or nutrition absorption. For instance, gastric bypass surgery is designed to create a small pouch in the stomach to produce early satiety and a consequent reduction in food intake, and moreover to induce malabsorption by creating a short gut syndrome and/or by accomplishing distal mixing of bile acid and pancreatic juice with ingested nutrients, thereby reducing absorption. It has also been demonstrated that weight loss surgery, including gastric bypass, changes the perception of food and thus eating behavior, leading to the concept of "behavior surgery".[1] We recently reported that rats developed an altered eating behavior for the short term, but not the long term after gastric bypass. Gastric-bypassed rats ate more during the daytime than sham-operated control rats and were unable to keep up with the control rats with respect to meal size and eating rate during the night. More

Published online: 08 September 2010

interestingly, neither their food intake nor absorption was reduced, despite the fact that the rats had a loss in body weight following the gastric bypass.[2]

Based on the hypothesis that "common obesity" has hypothalamic origins, truncal vagotomy was used for treatment of severe obesity.[3] Based on the understanding that the vagus nerve controls satiety/hunger and energy homeostasis, an alternative minimally invasive treatment, the so-called "Vagal BLocking for Obesity Control" (VBLOC), has been developed to intermittently block vagal nerve trunks with high frequency and low power electrical signals through the laparoscopically implanted device.[4] Hence, the first aim of the present study was to analyze the eating behavior and energy expenditure in rats subjected to bilateral truncal vagotomy. The measurements were performed by utilizing a state-of-the-art method known as a comprehensive laboratory animal metabolic monitoring system (CLAMS), as performed in our previous studies.[2,5,6]

Laparoscopically assisted vertical gastrectomy using a Dexterity Pneumo Sleeve device, the so-called sleeve gastrectomy, was originally proposed as the first stage followed by Roux-en-Y gastric bypass or duodenal switch as the second stage.[7,8] This procedure has been recently considered as an independent weight loss surgery, based on clinical outcomes and presumably underlying mechanism in which the ghrelin-rich gastric fundus is eliminated and the volume of the stomach is reduced.[9–12] Previously, we compared the eating behavior in rats that underwent a total gastrectomy vs. gastric bypass (i.e., end-to-end anastomosis of esophagus–proximal jejunum) and found that the food intake and meal size were reduced after gastrectomy but not gastric bypass, thus suggesting that the control of food intake was independent of the food reservoir function of the stomach.[5] Therefore, the second aim of the present study was to analyze the eating behavior and energy expenditure in rats subjected to sleeve gastrectomy.

The duodenal switch procedure was originally created as a surgical solution for primary bile reflux gastritis and/or to decrease post-gastrectomy symptoms after distal gastrectomy and gastroduodenostomy.[13] Currently, a combined procedure of sleeve gastrectomy and duodenal switch has been applied to the treatment of morbid obesity based on the rationale that the sleeve gastrectomy preserves the pylorus and first portion of the duodenum which negates the possibility of dumping symptoms and reduces the risk of marginal ulcers.[8] The duodenal switch procedure achieves complete pancreaticobiliary diversion. As a result, postprandial biliary and pancreatic secretion will be reduced or eliminated, and the negative feedback effect of the bile acid and pancreatic juice on cholecystokinin (CCK)-producing cells in the duodenum and jejunum will be deprived, thereby leading to an increase in circulating CCK levels. Since CCK is well known as a satiety hormone, we hypothesized that the duodenal switch procedure could be an independent weight loss surgery because this procedure would reduce the food intake due to hyperCCKemia and induce malabsorption due to long-limb intestinal bypass. Hence, the third aim of the present study was to evaluate the effects of a duodenal switch with and without a sleeve gastrectomy on body weight, eating behavior, serum CCK levels, fecal energy content, and energy expenditure.

Materials and Methods

Animals

Male rats (Sprague–Dawley, 3 months old) were purchased from Taconic M&B, Skensved, Denmark. The males were preferred because females change their food intake during ovulation and males grow faster than females, making it easier to detect body weight change. The rats were housed in individually ventilated Makrolon cages with 12 h light/dark cycle, room temperature of 22°C and 40–60% relative humidity. They were allowed free access to tap water and standard rat pellet food (RM1 801002, Scanbur BK AS, Sweden). The study was approved by the Norwegian National Animal Research Authority (Forsøksdyrutvalget, FDU).

Experimental Design

The animals were divided into the following groups: laparotomy (LAP), pyloroplasty (PP), bilateral truncal vagotomy plus pyloroplasty (VTPP), sleeve gastrectomy (SG), duodenal switch alone (DS), SG as the first stage and then DS as the second stage (SG_1+DS_2), and SG and DS simultaneously (SG+DS). In consideration of the "3Rs" for the human use of animals (e.g., reduction of animal numbers to the minimum consistent with achieving the scientific purposes of the experiment),[14] rats in control groups have been re-used after a 9-week recovery from previous operation and revealed an unchanged eating behavior and metabolic parameters. The rats were first subjected to LAP ($n=7$), PP ($n=7$), or VTPP ($n=7$), respectively. After 9 weeks, LAP and PP rats were subjected to SG and DS, respectively. After an additional 11 weeks, SG rats were subjected to DS, and VTPP rats were simultaneously subjected to both SG and DS. An additional group of age-matched rats were subjected to LAP ($n=7$).

Each rat was monitored weekly with respect to the body weight development throughout the study period. Each rat was placed in the CLAMS cage three times for 48 h, i.e., 1 week before surgery, 1–2 and 8–11 weeks after surgery for measurements of the eating and metabolic parameters.

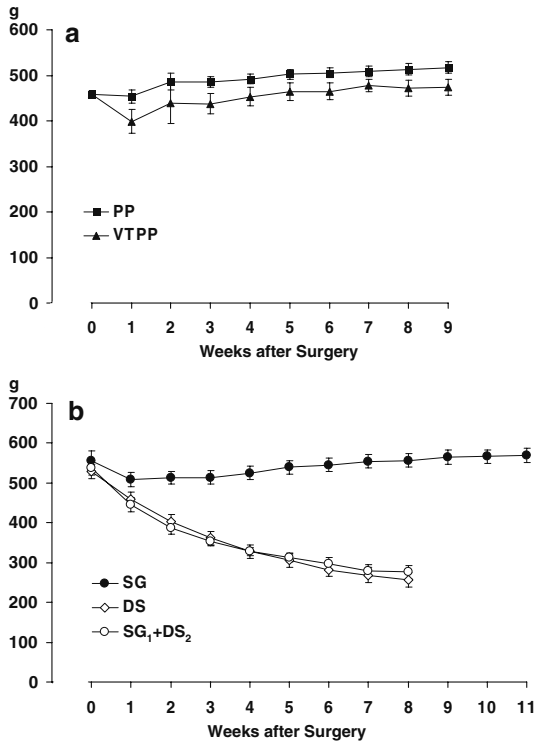

Fig. 1 Body weight developments after pyloroplasty (PP) and bilateral truncal vagotomy plus pyloroplasty (VTPP) (**a**), and after sleeve gastrectomy (SG), duodenal switch alone (DS) and SG as the first stage and then DS as the second stage ($SG_{1+}DS_2$) (**b**). Data are expressed as mean ± SEM

Surgery

Rats were deprived of food but not water for 12 h pre- and 24 h post-operation. All operations were performed under general anesthesia with isofluran (4% for induction and 2% for maintenance). Buprenorphine (0.05 mg/kg) was administrated as a pain reliever subcutaneously immediately after surgery. LAP was performed through middle-line incision. PP was performed by cutting off the pyloric sphincter (2 mm) and suturing it vertically against the incision. VTPP was achieved by cutting both the anterior and posterior vagal trunks immediately below the diaphragm and, while at the same time performing a PP to prevent gastroparesis-induced food retention and gastric dilation. SG was performed by resecting 70% of the glandular stomach along the greater curvature. DS was constructed by transecting the duodenum 1 cm to the pylorus, and a common channel was created by dividing the ileum 5 cm proximal to the ileocecal junction (rats have a much longer jejunum than humans). The distal limb of the ileum was anastomosed to the post-pyloric duodenum in an end-to-end manner, and the stump of the duodenum was closed with cross-suture. The distal anastomosis was performed by joining the distal biliopancreatic limb at 1 cm to the ileocecal junction in an end-to-side manner.

Eating and Metabolic Parameters

Eating and metabolic parameters were automatically recorded by the comprehensive laboratory animal monitoring system (CLAMS; Columbus Instruments International, Columbus, OH, USA). This system is composed of a four-chamber indirect calorimeter designed for the continuous monitoring of individual rats from each chamber. An air sample was withdrawn every 5 min. The energy expenditure (kcal/h) was calculated according to equation: $(3.815+1.232\ RER)\times VO_2$, where the respiratory exchange ratio (RER) was the volume of CO_2 produced per volume of O_2 consumed. VO_2 was the volume of O_2 consumed per hour per kilogram of mass of the animal. The energy expenditure is expressed as kcal/h/100 g body weight. Urine production was automatically recorded by weight. In order for rats to acclimate to this system, they were placed in these metabolic cages for 24 h before the first CLAMS monitoring. The high-resolution eating data was generated by monitoring all eating balances every 0.5 s, providing accumulated food intake, meal size, and meal duration. The end of an eating event (meal) was when the balance was stable for more than 10 s and a minimum of 0.05 g was

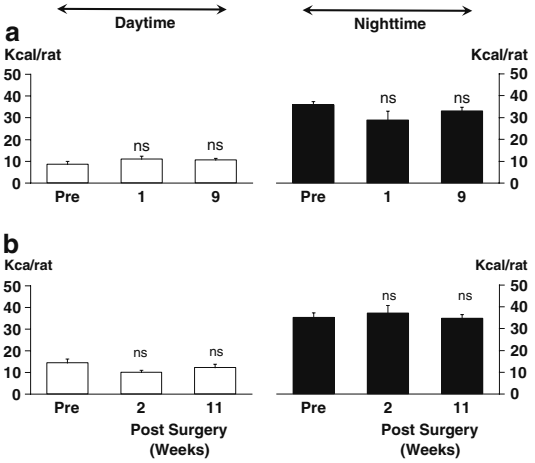

Fig. 2 Calories intake (kcal/rat) during the day and the night at 1 week before (Pre), 1 and 9 weeks after bilateral truncal vagotomy plus pyloroplasty (VTPP) (**a**), 1 week before (Pre), 2 and 11 weeks after sleeve gastrectomy (SG) (**b**). Data are expressed as mean ± SEM. *ns* not significant between pre- vs. post-operation

eaten. Parameters during daytime and nighttime for each rat included: meal size, meal duration, accumulated food intake, intermeal interval, rate of eating, and satiety ratio. The intermeal interval was defined as the interval in minutes between two meals. The rate of eating was calculated by dividing meal size by meal duration. The satiety ratio, an index of non-eating time produced by each gram of food consumed, was calculated as intermeal interval divided by meal size. The rats were placed in the CLAMS chambers for 48 h (data from the first 24 h were not used in the analysis) with free access to standard rat powder food (RM1 811004, Scanbur BK AS, Sweden) and tap water. The total metabolizable energy was 2.57 kcal/g for both RM1 801002 and 811004.

Determination of Energy Content in Feces

Feces were collected when the rats were placed in CLAMS cages 8 weeks after DS or age-matched control LAP, and dried for 72 h at 60°C. The energy content was determined by means of an adiabatic bomb calorimeter (IKA-Calorimeter C 5000, IKA-Werke GmbH & Co. KG, Staufen, Germany).

Determination of Serum CCK Levels

CCK levels in serum were analyzed by radioimmunoassay with sulfated CCK-8 as standard, using a CCK kit (Eurodiagnostica AB, Malmö, Sweden).

Statistical Analysis

The data were expressed as mean ± SEM. Comparisons between surgical groups and between three time points (1 week before, 1–2 and 8–11 weeks after surgery) were performed using an independent sample *t* test or ANOVA followed by a Tukey's test when applicable. $p<0.05$ was considered statistically significant.

Table 1 Eating and metabolic parameters at 1 week before VTPP, 1 and 9 weeks after VTPP

	Parameters	1 W before VTPP	1 W after VTPP	9 W after VTPP
Daytime	Food intake (g)	3.37±0.51	4.27±0.53 ns	4.08±0.31 ns
	Food intake (g/100 g body weight)	0.74±0.11	1.11±0.18 ns	0.86±0.07 ns
	Calories intake (kcal)	8.66±1.30	10.97±1.37 ns	10.49±0.79 ns
	Calories intake (kcal/100 g body weight)	1.91±0.29	2.86±0.46 ns	2.20±0.18 ns
	Number of meals	13.86±1.77	12.43±1.73 ns	15.57±1.95 ns
	Meal size (g/meal)	0.25±0.03	0.39±0.07 ns	0.28±0.03 ns
	Meal duration (min/meal)	1.00±0.20	1.81±0.52 ns	1.12±0.14 ns
	Intermeal interval (min)	51.86±6.11	59.91±10.49 ns	46.82±6.47 ns
	Satiety ratio (min/g)	230.76±43.10	165.10±20.64 ns	166.71±13.47 ns
	Rate of eating (g/min)	0.27±0.02	0.27±0.04 ns	0.26±0.02 ns
Nighttime	Food intake (g)	13.90±0.63	11.18±1.61 ns	12.80±0.70 ns
	Food intake (g/100 g body weight)	3.06±0.15	2.72±0.26 ns	2.68±0.14 ns
	Calories intake (kcal)	35.72±1.62	28.73±4.14 ns	32.89±1.80 ns
	Calories intake (kcal/100 g body weight)	7.87±0.39	6.99±0.66 ns	6.88±0.36 ns
	Number of meals	31.00±3.04	24.29±3.02 ns	31.00±5.32 ns
	Meal size (g/meal)	0.46±0.03	0.48±0.06 ns	0.50±0.10 ns
	Meal duration (min/meal)	1.96±0.29	2.64±0.46 ns	2.12±0.32 ns
	Intermeal interval (min)	21.78±1.92	29.97±5.48 ns	25.66±5.36 ns
	Satiety ratio (min/g)	46.70±2.27	65.33±10.13 ns	50.59±2.40 ns
	Rate of eating (g/min)	0.25±0.02	0.20±0.03 ns	0.24±0.02 ns
24 h	Energy expenditure (kcal/h/100 g body weight)	0.39±0.01	0.43±0.01 ns	0.36±0.01*
	RER	0.95±0.01	0.93±0.01 ns	0.95±0.01 ns
	Ambulatory activity	7,494.14±1,240.97	6,902.00±923.12 ns	6,504.00±999.08 ns

Data are expressed as mean ± SEM

ns not significant

*$p<0.01$ (1 W vs. 9 W)

Results

Mortality

There was no mortality in rats that underwent LAP, PP, or VTPP. The mortality rate was one of seven in rats subjected to SG, two of seven to DS alone, one of six to SG_1+DS_2, and six of seven to SG+DS simultaneously.

Body Weight

Both LAP and PP had no effect on body weight development. VTPP transiently reduced the body weight (about 10% at 1 week postoperatively; Fig. 1a). SG reduced the body weight (approximately 10%) for about 6 weeks (Fig. 1b). DS alone or SG followed by DS reduced the body weight in a similar manner: a rapid and continuous weight loss of about 10% at 1 week and 50% at 8 weeks postoperatively (Fig. 1b).

Food Intake, Eating Behavior, Energy Expenditure, and Fecal Energy Content

Food intake was higher and the satiety ratio was lower during the night than the day for each rat.

There were no differences between LAP and PP in terms of food intake and eating behavior parameters at either 1 or 9 weeks postoperatively (data not shown).

VTPP was without any measurable effects on food intake, eating behavior, and metabolic parameters measured at either 1 or 9 weeks postoperatively (Fig. 2a; Table 1).

SG had no effects on food intake and eating behavior parameters, except for meal duration during the night measured at 2 weeks (Fig. 2b; Table 2). In addition, SG reduced the water intake during one interval (0.91±0.07 vs. 0.47±0.07 mL at 2 weeks and vs. 0.45±0.08 mL at 11 weeks, both $p<0.01$). Energy expenditure was increased at 2 weeks and RER was increased at 11 weeks postoperatively (Table 2).

Table 2 Eating and metabolic parameters at 1 week before SG, 2 and 11 weeks after SG

	Parameters	1 W before SG	2 W after SG	11 W after SG
Daytime	Food intake (g)	5.62±0.70	3.92±0.38 ns	4.76±0.63 ns
	Food intake (g/100 g body weight)	1.01±0.15	0.77±0.07 ns	0.83±0.10 ns
	Calories intake (kcal)	14.43±1.79	10.08±0.97 ns	12.24±1.62 ns
	Calories intake (kcal/100 g body weight)	2.60±0.38	1.97±0.18 ns	2.13±0.27 ns
	Number of meals	13.83±1.83	9.83±1.42 ns	11.17±1.54 ns
	Meal size (g/meal)	0.41±0.01	0.44±0.08 ns	0.43±0.04 ns
	Meal duration (min/meal)	1.52±0.13	1.72±0.20 ns	1.29±0.07 ns
	Intermeal interval (min)	51.45±7.09	70.24±8.34 ns	62.28±7.13 ns
	Satiety ratio (min/g)	124.13±14.28	170.13±18.28 ns	149.69±23.39 ns
	Rate of eating (g/min)	0.28±0.02	0.25±0.03 ns	0.33±0.02 ns
Nighttime	Food intake (g)	13.61±0.89	14.41±1.39 ns	13.47±0.69 ns
	Food intake (g/100 g body weight)	2.43±0.17	2.80±0.22 ns	2.34±0.09 ns
	Calories intake (kcal)	34.97±2.28	37.04±3.57 ns	34.63±1.78 ns
	Calories intake (kcal/100 g body weight)	6.23±0.43	7.19±0.56 ns	6.01±0.22 ns
	Number of meals	28.50±3.40	23.17±3.59 ns	28.00±4.27 ns
	Meal size (g/meal)	0.50±0.06	0.73±0.15 ns	0.53±0.07 ns
	Meal duration (min/meal)	1.69±0.19	2.88±0.47*	1.77±0.18 ns
	Intermeal interval (min)	24.46±2.86	31.58±5.83 ns	26.76±5.05 ns
	Satiety ratio (min/g)	48.93±3.63	45.93±4.93 ns	48.68±2.50 ns
	Rate of eating (g/min)	0.30±0.00	0.25±0.02 ns	0.30±0.01 ns
24 h	Energy expenditure (kcal/h/100 g body weight)	0.34±0.01	0.38±0.00*	0.37±0.01 ns
	RER	0.96±0.01	0.94±0.01 ns	1.02±0.01**, ***
	Ambulatory activity	7,014.50±1,001.57	6,721.17±807.00 ns	5,094.67±549.75 ns

Data are expressed as mean ± SEM

ns not significant

*$p<0.05$

**$p<0.01$ (pre vs. 2 W or 11 W)

***$p<0.01$ (2 W vs.11 W)

DS regardless of whether it was accompanied by SG reduced the daily food/calories intake by approximately 50% when measured at 2 as well as 8 weeks postoperatively (Fig. 3a; Table 3). The reduced food intake was associated with a reduced meal size and an increased satiety ratio, but not with the number of meals (Fig. 3b–d; Table 3). The fecal energy content of DS rats was higher than that of control LAP rats (20411.15±177.86 J/g vs. 18756.36±51.61 J/g, $p<0.001$) at 8 weeks. It was difficult to collect the feces at 2 weeks after DS due to a severe diarrhea. There were no differences between DS and SG_1+DS_2 in terms of food intake and eating behavior parameters, except RER and energy expenditure at 2 weeks and water intake at 8 weeks postoperatively.

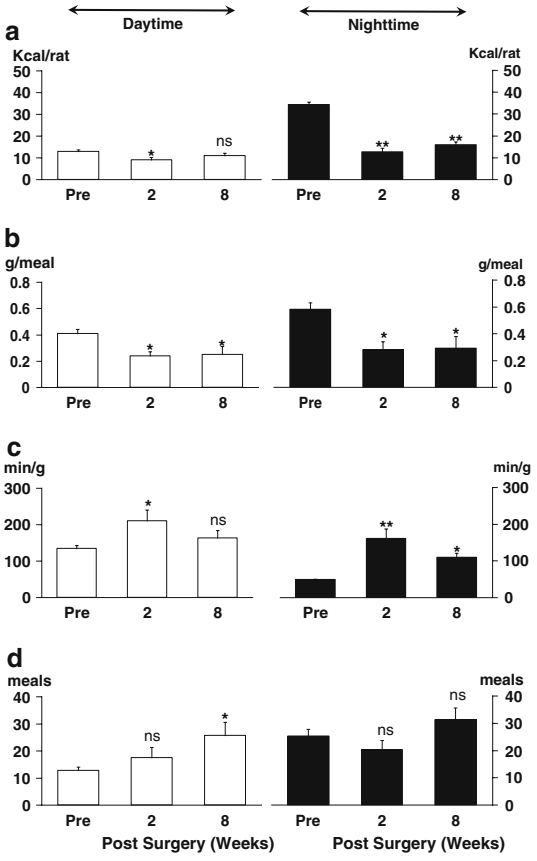

Fig. 3 Calories intake (kcal/rat) (**a**), meal size (g/meal) (**b**), satiety ratio(min/g) (**c**), number of meals (meals) (**d**) during the day and the night at 1 week before (Pre), 2 and 8 weeks after duodenal switch (DS)(regardless of whether it was accompanied by SG). Data are expressed as mean ± SEM. *$p<0.05$, **$p<0.01$, *ns* not significant between pre- vs. 2 W or 8 W postoperatively

One surviving rat that was subjected to SG+DS had reduced food intake and altered eating behavior, much like the rats subjected to SG_1+DS_2. However, this was not analyzed statistically.

Circulating CCK Levels

Serum CCK levels were 12.6±3.0 pmol/L in SG_1+DS_2 rats. This was more than ten times higher than the value of rats subjected to the sham operation in our previous report (plasma CCK levels were 1.1±0.5 pmol/L).[15] Unfortunately, there was a technical error in the determination of the CCK levels in age-matched control LAP and DS rats in the present study.

Discussion

The role of vagus in physiologically controlling eating behavior has been studied during the past decades. It is believed that food interacts with the gut to provide the brain via vagal afferents with information regarding food composition, amount of ingested food and energy content. The brain determines the rate of nutrient absorption, partitioning, storage, and mobilization through vagal efferents as well as the sympathetic nervous system and hormonal mechanisms.[16] This food–gut-brain axis is considered as an autonomic neurohumoral pathway regulating energy homeostasis. In the present study, disruption of the gut-brain axis by VTPP was without any measureable effect on the energy homeostasis. The body weight loss was slight (about 15%) and transient (1 week postoperatively). This may explain why vagotomy as treatment for obesity has received little attention since it was used 30 years ago.[3] However, with the substantial need for effective treatment of obesity at younger ages and the improved safety of laparoscopic procedures, it has been suggested that surgical treatment can be justified at lower levels of BMI, before the eating disorder has become intractable and requires malabsorptive operations. The possibility for utilizing a laparoscopic abdominal vagotomy has been well discussed elsewhere.[17]

SG weight loss surgery is believed to be restrictive as well as a neurohormone-mediated procedure. The early clinical results seem promising, but long-term data is still needed to define the place of LSG within the bariatric surgery armamentarium.[18,19] In the present study, SG reduced the body weight by about 10% in the short-term (1–6 weeks) but not in the long-term (after 7 weeks). The reduction was not associated with reduced food intake but possibly with increased energy expenditure, which is in line with previous observations in rats subjected to total gastrectomy or gastric bypass.[5] The underlying physiological mechanisms are still unknown. It should also be

Table 3 Eating and metabolic parameters at 1 week before DS both with and without SG, 2 and 8 weeks after DS both with and without SG

	Parameters	1 W before operation	2 W after operation	8 W after operation
Daytime	Food intake (g)	4.99±0.31	3.54±0.44*	4.30±0.44 ns
	Food intake (g/100 g body weight)	0.92±0.05	0.87±0.11 ns	1.60±0.20**, ****
	Calories intake (kcal)	12.83±0.79	9.11±1.14*	11.05±1.14 ns
	Calories intake (kcal/100 g body weight)	2.36±0.13	2.25±0.28 ns	4.10±0.51**, ****
	Number of meals	12.80±1.18	17.50±3.79 ns	25.70±4.86*
	Meal size (g/meal)	0.41±0.03	0.24±0.03*	0.25±0.06*
	Meal duration (min/meal)	1.33±0.10	2.35±0.41 ns	3.74±1.82 ns
	Intermeal interval (min)	54.01±4.00	54.86±14.48 ns	42.19±12.04 ns
	Satiety ratio (min/g)	134.37±8.03	210.35±29.60*	163.30±20.66 ns
	Rate of eating (g/min)	0.31±0.01	0.13±0.03**	0.10±0.01**
Nighttime	Food intake (g)	13.34±0.43	4.89±0.73**	6.16±0.54**
	Food intake (g/100 g body weight)	2.47±0.12	1.19±0.17**	2.20±0.15****
	Calories intake (kcal)	34.29±1.10	12.56±1.86**	15.82±1.38**
	Calories intake (kcal/100 g body weight)	6.35±0.30	3.07±0.44**	5.65±0.39****
	Number of meals	25.20±2.62	20.30±3.43 ns	31.20±4.48 ns
	Meal size (g/meal)	0.58±0.05	0.28±0.06*	0.29±0.09*
	Meal duration (min/meal)	1.96±0.19	3.64±1.28 ns	3.84±1.58 ns
	Intermeal interval (min)	28.19±2.96	40.29±6.97 ns	27.13±7.01 ns
	Satiety ratio (min/g)	48.90±1.66	161.24±26.37**	109.27±11.90*
	Rate of eating (g/min)	0.30±0.01	0.10±0.01**	0.09±0.01**
24 h	Energy expenditure (kcal/h/100 g body weight)	0.37±0.01	0.38±0.02 ns	0.43±0.01*, ***
	RER	0.99±0.02	0.90±0.03 ns	1.11±0.07****
	Ambulatory activity	5,410.30±696.92	5,773.60±891.92 ns	3,533.70±618.31 ns

Data are expressed as mean ± SEM

ns not significant

*$p<0.05$

**$p<0.01$ (pre vs. 2 W or 8 W)

***$p<0.05$

****$p<0.01$ (2 W vs. 8 W)

mentioned that SG rats, like totally gastrectomized rats, seemed to drink frequently postoperatively, probably owing to lower ghrelin and obestatin levels.[5,20,21]

In the present study, DS alone and SG+DS exhibited well-matched postoperative effects on body weight, metabolic parameters and eating behavior, leading to a long lasting and effective body weight loss. More interestingly, the results of the present study support our hypothesis that the DS procedure per se could be considered as an independent weight loss surgery because this procedure reduces the food intake due to hyperCCKemia and induces malabsorption due to intestinal bypass. As expected after pancreaticobiliary diversion,[15,22–24] circulating CCK levels were elevated after SG_1+DS_2, which in turn increased the satiety ratio and reduced meal size. Malabsorption is believed to be due to long-limb intestinal bypass after DS. In fact, DS patients also showed a decreased appetite and continuously body weight loss.[25] In addition to CCK, glucagon-like peptide-1 (GLP-1) levels in the circulation have been reported to be elevated in rats subjected to pancreaticobiliary diversion, which could have a beneficial effect on ß cells in the pancreas.[26,27] Unfortunately, GLP-1 was not measured in the present study, thus it will be of interest for future study.

In conclusion, VTPP, SG, and DS, like gastric bypass, reduced the body weight, though the effectiveness and underlying mechanisms appear different. Since obesity is believed to a multifactorial disease, the options for the treatment, including various surgical procedures, should be individualized.

Acknowledgments The authors thank Dr. Catia Martins for determination of CCK levels, Jostein Johansen for assistance of data analysis at Department of Cancer Research and Molecular Medicine, and Morten Grønli, and Erik Langørgen for assistance of bomb calorimeter at Department of Energy and Process Engineering, Norwegian University of Science and Technology.

References

1. Miras AD, le Roux CW. Bariatric surgery and taste: novel mechanisms of weight loss. Curr Opin Gastroenterol. 2010;26(2):140–5.
2. Furnes MW, Tømmerås K, Arum CJ, Zhao CM, Chen D. Gastric bypass surgery causes body weight loss without reducing food intake in rats. Obes Surg. 2008;18(4):415–22.
3. Kral JG. Vagotomy for treatment of severe obesity. Lancet. 1978;1 (8059):307–8.
4. Camilleri M, Toouli J, Herrera MF, Kulseng B, Kow L, Pantoja JP, Marvik R, Johnsen G, Billington CJ, Moody FG, Knudson MB, Tweden KS, Vollmer M, Wilson RR, Anvari M. Intra-abdominal vagal blocking (VBLOC therapy): clinical results with a new implantable medical device. Surgery. 2008;143(6):723–31.
5. Furnes MW, Stenstrom B, Tømmerås K, Skoglund T, Dickson SL, Kulseng B, Zhao CM, Chen D. Feeding behavior in rats subjected to gastrectomy or gastric bypass surgery. Eur Surg Res. 2008;40 (3):279–88.
6. Furnes MW, Zhao CM, Chen D. Development of obesity is associated with increased calories per meal rather than per day. A study of high-fat diet-induced obesity in young rats. Obes Surg. 2009;19(10):1430–8.
7. Naitoh T, Gagner M. Laparoscopically assisted gastric surgery using dexterity pneumo sleeve. Surg Endosc. 1997;11(8):830–3.
8. Anthone GJ. The duodenal switch operation for morbid obesity. Surg Clin North Am. 2005;85(4):819–33
9. Rosen DJ, Dakin GF, Pomp A. Sleeve gastrectomy. Minerva Chir. 2009;64(3):285–95.
10. Rubino F, Schauer PR, Kaplan LM, Cummings DE. Metabolic surgery to treat type 2 diabetes: clinical outcomes and mechanisms of action. Annu Rev Med. 2010;61:393–411.
11. Bohdjalian A, Langer FB, Shakeri-Leidenmühler S, Gfrerer L, Ludvik B, Zacherl J, Prager G. Sleeve gastrectomy as sole and definitive bariatric procedure: 5-year results for weight loss and ghrelin. Obes Surg. 2010;20(5):535–40.
12. Abu-Jaish W, Rosenthal RJ. Sleeve gastrectomy: a new surgical approach for morbid obesity. Expert Rev Gastroenterol Hepatol. 2010;4(1):101–19.
13. DeMeester TR, Fuchs KH, Ball CS, Albertucci M, Smyrk TC, Marcus JN. Experimental and clinical results with proximal end-to-end duodenojejunostomy for pathologic duodenogastric reflux. Ann Surg. 1987;206(4):414–26.
14. Russell WMS, Burch RL. The Principles of Humane Experimental Technique. London: Methuen & Co. LTD. 1959.
15. Chen D, Nylander A-G, Rehfeld JF, Axelson J, Ihse I, Hakanson R. Does vagotomy affect the growth of the pancreas in the rat? Scand J Gastroenterol 1992;27:606–608.
16. Berthoud HR. The vagus nerve, food intake and obesity. Regul Pept. 2008;149(1–3):15–25.
17. Kral JG. Psychosurgery for obesity. Obes Facts. 2009;2(6):339–41.
18. Ward M, Prachand V. Surgical treatment of obesity. Gastrointest Endosc. 2009;70(5):985–90.
19. Frezza EE, Chiriva-Internati M, Wachtel MS. Analysis of the results of sleeve gastrectomy for morbid obesity and the role of ghrelin. Surg Today. 2008;38(6):481–3.
20. Samson WK, White MM, Price C, Ferguson AV. Obestatin acts in brain to inhibit thirst. Am J Physiol Regul Integr Comp Physiol. 2007;292(1):R637–43.
21. Hashimoto H, Fujihara H, Kawasaki M, Saito T, Shibata M, Otsubo H, Takei Y, Ueta Y. Centrally and peripherally administered ghrelin potently inhibits water intake in rats. Endocrinology. 2007;148(4):1638–47.
22. Chen D, Nylander AG, Rehfeld JF, Sundler F, Håkanson R. Hypercholecystokininemia produced by pancreaticobiliary diversion causes gastrin-like effects on enterochromaffin-like cells in the stomach of rats subjected to portacaval shunting or antrectomy. Scand J Gastroenterol. 1993;28(11):988–92.
23. Chen D, Andersson K, Iovanna JL, Dagorn JC, Håkanson R. Effects of hypercholecystokininemia produced by pancreaticobiliary diversion on pancreatic growth and enzyme mRNA levels in starved rats. Scand J Gastroenterol. 1993;28(4):311–4.
24. Chen D, Nylander AG, Norlén P, Håkanson R. Gastrin does not stimulate growth of the rat pancreas. Scand J Gastroenterol. 1996;31(4):404–10.
25. Marceau P, Hould FS, Simard S, Lebel S, Bourque RA, Potvin M, Biron S. Biliopancreatic diversion with duodenal switch. World J Surg. 1998;22(9):947–54.
26. Borg CM, le Roux CW, Ghatei MA, Bloom SR, Patel AG. Biliopancreatic diversion in rats is associated with intestinal hypertrophy and with increased GLP-1, GLP-2 and PYY levels. Obes Surg. 2007;17(9):1193–8.
27. Miazza BM, Widgren S, Chayvialle JA, Nicolet T, Loizeau E. Exocrine pancreatic nodules after long-term pancreaticobiliary diversion in rats. An effect of raised CCK plasma concentrations. Gut. 1987;28 Suppl:269–73.

Discussant

DR. THOMAS H. MAGNUSON (Baltimore, MD): I would like to thank Dr. Kodama and congratulate him on an excellent presentation, and he and his coauthors on an excellent manuscript. They have given us some important insights into how some these bariatric operations work from a metabolic perspective. This is an important topic, with the ultimate goal of better selecting the right operation for each individual patient.

They found, interestingly, that vagotomy alone or sleeve gastrectomy alone seemed to have little impact on weight loss or eating behavior, but the duodenal switch operation did have a dramatic impact on weight loss and also altered energy expenditure.

I have a couple quick questions.

First, with regards to your sleeve gastrectomy model, it looks like this didn't work very well, but yet there's other animal models, obese rats and mice for example, as well as our human clinical experience, showing that the sleeve works pretty well as an operation for weight loss. I wonder if you could comment briefly on why your results differ from that of others. Did you measure circulating levels of ghrelin, which has been implicated as being important in the function of the sleeve gastrectomy as an appetite suppressant?

The second question involves your duodenal switch model. It looks like these animals lost dramatic weight, but was this really a physiologic model? It seems like most of these animals had severe diarrhea and over 30 or 40% of your animals actually died in the study. Was this due to severe malnutrition? Did you measure nutritional parameters, such as serum albumin levels, to make sure this wasn't a model of severe protein calorie malnutrition contributing to the deaths and the severe diarrhea?

In addition, you measured CCK levels and postulated that that might be an effect of the duodenal switch and its impact on satiety, but did you think about measuring other GI peptides. GLP-1, adiponectin, NPY and PYY have all been implicated as being important to weight loss in animal models that bypass variable lengths of intestine.

Once again, I enjoyed your presentation.

Closing discussant

DR. YOSUKE KODAMA: Thank you very much for your comments. In this study with normal rats, duodenal switch, but not vagotomy or sleeve gastrectomy, resulted in the dramatic weight loss. It will be of interest to repeat this study but with obese rats to see whether the effect differs. We did not measure ghrelin levels in this study, because we did not see a significant weight loss after the sleeve gastrectomy.

As reported in our manuscript, 2 of 7 rats died after duodenal switch procedure alone, and 1 of 6 rats died after sleeve gastrectomy as the first stage and duodenal switch as the second stage. Such mortality is generally acceptable in the experimental surgery with small animals. All survived animals from duodenal switch had severe diarrhea but it lasted only for a short time period (e.g. 2 weeks). We did not measure the serum albumin levels. In the case that the two procedures were performed at the same time, 6 of 7 rats died, which was most likely due to surgical trauma.

This was our first experimental study suggesting that duodenal switch alone might be used as an independent weight loss surgery. The underlying mechanism should be further investigated, for example, by measuring not only CCK but also other GI hormones as you have suggested.

Paper III

OPEN ACCESS Freely available online

PLOS ONE

Mechanistic Comparison between Gastric Bypass vs. Duodenal Switch with Sleeve Gastrectomy in Rat Models

Yosuke Kodama[1], Helene Johannessen[1], Marianne W. Furnes[1], Chun-Mei Zhao[1], Gjermund Johnsen[2], Ronald Mårvik[2], Bård Kulseng[1,2], Duan Chen[1,2]*

1 Department of Cancer Research and Molecular Medicine, Norwegian University of Science and Technology, Trondheim, Norway, **2** Department of Surgery, Saint Olav's University Hospital, Trondheim, Norway

Abstract

Background: Both gastric bypass (GB) and duodenal switch with sleeve gastrectomy (DS) have been widely used as bariatric surgeries, and DS appears to be superior to GB. The aim of this study was to better understand the mechanisms leading to body weight loss by comparing these two procedures in experimental models of rats.

Methods: Animals were subjected to GB, DS or laparotomy (controls), and monitored by an open-circuit indirect calorimeter composed of comprehensive laboratory animal monitoring system and adiabatic bomb calorimeter.

Results: Body weight loss was greater after DS than GB. Food intake was reduced after DS but not GB. Energy expenditure was increased after either GB or DS. Fecal energy content was increased after DS but not GB.

Conclusion: GB induced body weight loss by increasing energy expenditure, whereas DS induced greater body weight loss by reducing food intake, increasing energy expenditure and causing malabsorption in rat models.

Citation: Kodama Y, Johannessen H, Furnes MW, Zhao C-M, Johnsen G, et al. (2013) Mechanistic Comparison between Gastric Bypass vs. Duodenal Switch with Sleeve Gastrectomy in Rat Models. PLoS ONE 8(9): e72896. doi:10.1371/journal.pone.0072896

Editor: Yvette Tache, University of California, Los Angeles, United States of America

Received April 9, 2013; **Accepted** July 13, 2013; **Published** September 9, 2013

Funding: The present research has been supported by funding from the Central Norway Regional Health Authority, and the European Union Seventh Framework Programme (FP7/2007–2013) under grant agreement n 266408. The funders had no role in study design, data collection and analysis, decision to publish, or preparation of the manuscript.

Competing Interests: The authors have declared that no competing interests exist.

* E-mail: duan.chen@ntnu.no

Introduction

Various bariatric surgical procedures, such as gastric banding, gastric bypass (GB) and duodenal switch with sleeve gastrectomy (DS), have been developed in order to reduce food intake and/or lead to malabsorption [1]. GB was invented by Dr. Edward Mason as a bariatric surgery in 1965, and later it was converted to Roux-en-Y procedure which was created by Dr. Cesar Roux already in 1897. Recently, a laparoscopic mini-GB procedure has been shown to be regarded as a simpler and safer alternative to laparoscopic Roux-en-Y with similar efficacy at 5 or 10 year experience [2]. However, the different procedures have shown different efficacy in individual patients, and the underlying mechanisms are not yet clear. Therefore, it is a challenge to select the most effective bariatric procedure for individual patients.

Various rat models of bariatric surgery have been developed in order to understand the underlying physiological mechanisms of different surgical procedures. There have been many studies in the literature reporting the surgical procedures (such as Roux-en-Y) in rats that are made as same as they are used in humans [3,4]. However, there is a significant difference in the anatomy and physiology of the gastrointestinal tract between rats and humans, which should be kept in mind when creating the surgical models in rats and translating findings from animals and humans. For instance, the rat stomach consists of antrum, fundus (also called corpus) and rumen (forestomach), while the human stomach is divided into antrum, body and fundus (Fig 1A, E). The rat jejunum represents almost 90% of the small intestine, the human jejunum about 40% [5]. Unlike humans, rats are nonemetic (not vomiting) and has no gallbladder. The Roux-en-Y reconstruction was initially created to prevent post-gastrectomy bile vomiting in patients [6]. Apparently, it is not necessary to create the Roux-en-Y reconstruction in rats that are subjected to GB [7–9]. The duodenal switch procedure was originally created as a surgical solution for primary bile reflux gastritis and/or to decrease postoperative symptoms after distal gastrectomy and gastroduodenostomy [10]. In patients, the operation usually consists of a 75% longitudinal gastrectomy (the so-called sleeve gastrectomy), creation of an alimentary limb approximately 50% of total small bowel length (i.e. bypassing jejunum), a common channel length of 100 cm, and cholecystectomy. In the present study using rats, GB was performed without the Roux-en-Y reconstruction and the postsurgical anatomy was similar to mini-GB on humans, and DS was performed according to the rat anatomy (Fig 1A–H) [11].

GB is the most common procedure because of relatively high efficacy and safety, whereas DS seems to be even more effective, particularly in super-obese patients [12]. Both GB and DS are believed to cause restriction in food intake and malabsorption by decreasing stomach size and bypassing part of the small intestine. In patients, DS is superior to GB in body weight loss as well as in

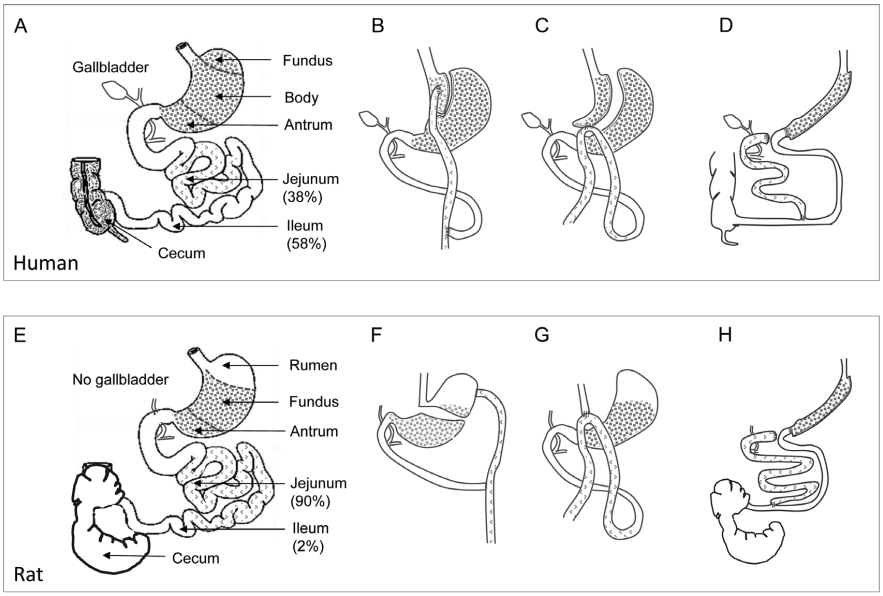

Figure 1. Schematic drawing of anatomy. The gastrointestinal tract of human (**A–D**) and rat (**E–H**) before (**A, E**) and after Roux-en-Y gastric bypass (GB) (**B, F**), mini-GB (**C, G**), and duodenal switch (**D, H**). Glandular stomach is indicated by grid gray and jejunum by light grid gray. The rumen of rat stomach is non-glandular (white area). Note: In **A, E**, percentages mean % of small intestine, e.g. in **E**, jejunum is 90% of total small intestine in rats based on [11]; in **F**, rat Roux-en-Y GB [3], and in **G**, Mini-GB used in the present study.
doi:10.1371/journal.pone.0072896.g001

improvement of comorbidities such as diabetes, hypertension and dyslipidemia [12–18]. Mechanisms underlying the postoperative weight loss and possible regain remain unclear. Whether this is due to biological or behavioral factors is one of the major debates [19]. The aim of the present study was to compare the postoperative effects of GB *vs.*DS on eating behavior and energy expenditure in rat models.

Materials and Methods

Animals and Experimental Design

Adult rats (male, Sprague-Dawley, 6–12 months of age) were purchased from Taconic M&B, Skensved, Denmark and housed in ventilated cages in a specific pathogen free environment with room temperature of 22°C, 40–60% relative humidity and 12 hr day/night cycle with 1 hr dusk/dawn. The rats had free access to tap water and standard rat pellet food (RM1 801002, Scanbur BK AS, Sweden). In our previous studies, we have reported that the male rats gained body weight mainly as a result of continuous expansion of the fat compartment after puberty (8 weeks of age with 200 g body weight), and that the male rats that were fed a high-fat diet starting at 5 weeks of age gained body weight up to ~650 g at 40 weeks of age as a result of increased fat mass [7,8]. In the present study, normal adult male rats (~600 g body weight) were chosen after considerations of the small difference in body weight (~650 g *vs.* ~600 g induced by high-fat diet) and the experimental efforts in terms of time-consuming and financial expense (Fig 2A). Furthermore, the body weight development of naïve rats reaches a plateau (580±20 g) at 40 weeks of age, and laparotomy performed at 13 weeks of age did not affect the development of body weight (Fig 2A).

Thirty-four rats, at 587.0±8.1 g body weight, were randomly divided into experimental (GB and DS) as well as control groups (laparotomy, LAP): GB (14 rats), DS (7 rats), and LAP (13 rats). The body weight was not different between the groups before surgery ($p = 0.276$). Because of markedly loss of body weight after DS, the group of DS rats, together with age-matched group of laparotomized rats (LAP_{DS}, 7 rats), were followed up only for 8 weeks, while GB rats and the rest of laparotomized rats (LAP_{GB}, 6 rats) were followed up for 14 weeks. In consideration of the "3Rs" for the human use of animals (i.e., reducing the number of animals while achieving the scientific purposes of the experiment), rats that had been used for studies of the effects of individual surgical procedures were re-used [8,20]. The study was approved by the Norwegian National Animal Research Authority (Forsøksdyrutvalget, FDU).

Surgery

All operations were performed under general anesthesia with isofluran (4% for induction and 2% for maintenance) (Baxter Medical AB, Kista, Sweden). Buprenorphine (0.05 mg/kg) (Schering-Plough Europe, Brussels, Belgium) was administrated as an analgesic agent subcutaneously immediately during surgery. LAP was performed through a middle-line incision with gentle manipulation of viscera. A rat model of Roux-en-Y GB procedure has been described by Stylopoulos and his colleagues [3]. Gastric pouch in that rat model was created at the site of rumen which does not exist in humans (Fig 1F). In the present study, GB was

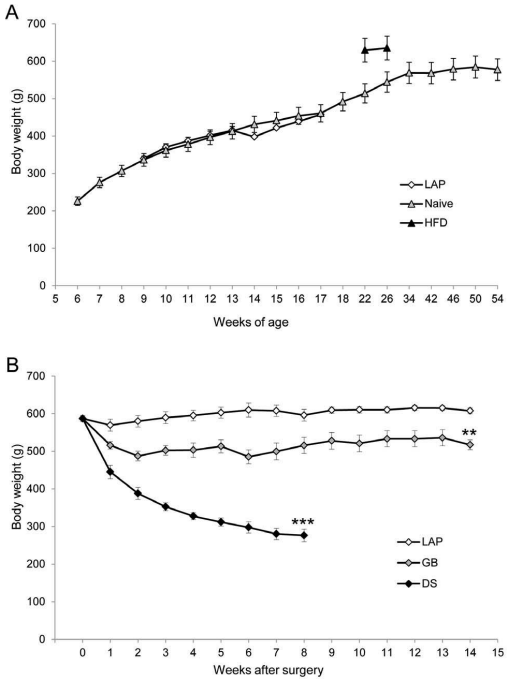

Figure 2. Body weight. Naïve rats (data from Taconic), rats that underwent laparotomy (LAP) at 13 weeks (LAP) and rats that have had high-fat since 5 weeks of age (data from [31]) (**A**)**.** Rats after gastric bypass (GB), duodenal switch (DS) and laparotomy (LAP) (**B**). Data are expressed as means ± SEM. **: $p<0.01$, ***: $p<0.001$ between LAP *vs.* GB or DS.
doi:10.1371/journal.pone.0072896.g002

performed by anastomosing the distal esophagus to the proximal jejunum about 2–3 cm distal to the Treitz ligament in an end-to-side manner (Fig 1G) as described previously [7,8]. DS was achieved in two stages. The two-stage procedure has been recommended in patients because the single-stage procedure increases the risk of postoperative complications and staged DS may avoid biliopancreatic diversion in some patients [21]. In the present study, sleeve gastrectomy was performed by resecting approximately 90% of the rumen and 70% of the glandular stomach along the greater curvature. Three months later, duodenal switch was achieved by creating biliopancreatic limb, alimentary limb (bypassing jejunum) and common channel length of 5 cm (Fig 1H). The duration of surgical time was 30–60 min for GB or DS. In all surgeries performed in the present study, proper aseptic surgical techniques were applied, and therefore, neither prophylactic nor postoperative antibiotics were used. This was done according to the guidelines and recommendations by the Federation of European Laboratory Animal Science Associations (FELASA 2008) and the guide for the care and use of laboratory animals by the Committee of USA National Research Council (2010). After recovering from anesthesia, the animals were placed 2–4 per cage throughout the study period.

Measurements of Eating Behavior and Energy Expenditure Parameters

These were monitored by the Comprehensive Laboratory Animal Monitoring System (CLAMS, Columbus Instruments International, Columbus, OH, USA) 2–3 weeks after GB, DS or LAP and 14 weeks after GB, 8 weeks after DS or 8–14 weeks after LAP. The CLAMS is composed of a 4-chamber indirect calorimeter designed for the continuous monitoring of individual rats from each chamber. The eating data was generated by monitoring all feed balances every 0.5 s. In CLAMS program used in the present study, the end of an eating event (meal) was when the balance was stable for more than 10 s and a minimum of 0.05 g was eaten. The eating parameters during daytime and nighttime (12 hr each time) for each rat included: accumulated food intake (g or kcal), number of meals, meal size (g/meal), meal duration (min/meal), intermeal interval (min), rate of eating (g/min), and satiety ratio (min/g). The intermeal interval was defined as the interval in minutes between two meals. The rate of eating was calculated by dividing meal size by meal duration. The satiety ratio, an index of non-eating time produced by each gram of food consumed, was calculated as intermeal interval divided by meal size [22]. The volume of O_2 consumption (VO_2 mL/kg/hr) and the volume of CO_2 production (VCO_2 mL/kg/hr) were measured by an air sample withdrawn every 5 min from each chamber through the gas dryer. The energy expenditure (kcal/hr) was calculated according to equation: $(3.815+1.232\ \mathrm{RER}) \times VO_2$, where the respiratory exchange ratio (RER) was obtained by VCO_2 divided by VO_2. In order for rats to acclimate to CLAMS, they were placed in these metabolic chambers for 24 hr one week before the first CLAMS monitoring. For the measurement of eating and metabolic parameters, the rats were placed in the CLAMS for 48 hr. In order to minimalize possible effect of stress, only data from the last 24 hr in CLAMS were used for the analysis. An analysis of eating pattern in control rats over a time period from day 1 and 21 showed no significant differences in any parameters, indicating that the animals had acclimated to CLAMS (Table S1). The rats have had free access to standard rat powder food (RM1 811004, Scanbur BK AS, Sweden) and tap water while they were in CLAMS. The total metabolizable energy was 2.57 kcal/g for both the pellet food (RM1 811002) and the powder food (RM1 811004).

Determination of Fecal Energy Density

Feces were collected while the rats were placed in CLAMS chambers and dried for 72 hr at 60°C. The energy density was determined by means of an adiabatic bomb calorimeter (IKA-Calorimeter C 5000, IKA-Werke GmbH & Co. KG, Staufen, Germany).

Determination of Plasma Levels of Cytokines

Blood was drawn from the abdominal aorta under the anesthesia just before the animals were killed, and plasma was stored at −80°C until determination of levels of cytokines. The multiplex cytokine assay was used (Cat no:171-K1002M, Bio-plex Pro Rat Cytokine Th1/Th2 12-plex Panel; Bio-Rad Laboratories, Hercules, CA, USA). It contained the following analytics: IL-1α, IL-1β, IL-2, IL-4, IL-5, IL-6, IL-10, IL-13, granulocyte-macrophage colony stimulating factor (GM-CSF), interferon gamma (IFNγ), and tumor necrosis factor alpha (TNFα).

Statistical Analysis

The values were expressed as means ± SEM. Two-tailed independent-samples *t*-test or Mann Whitney U test was

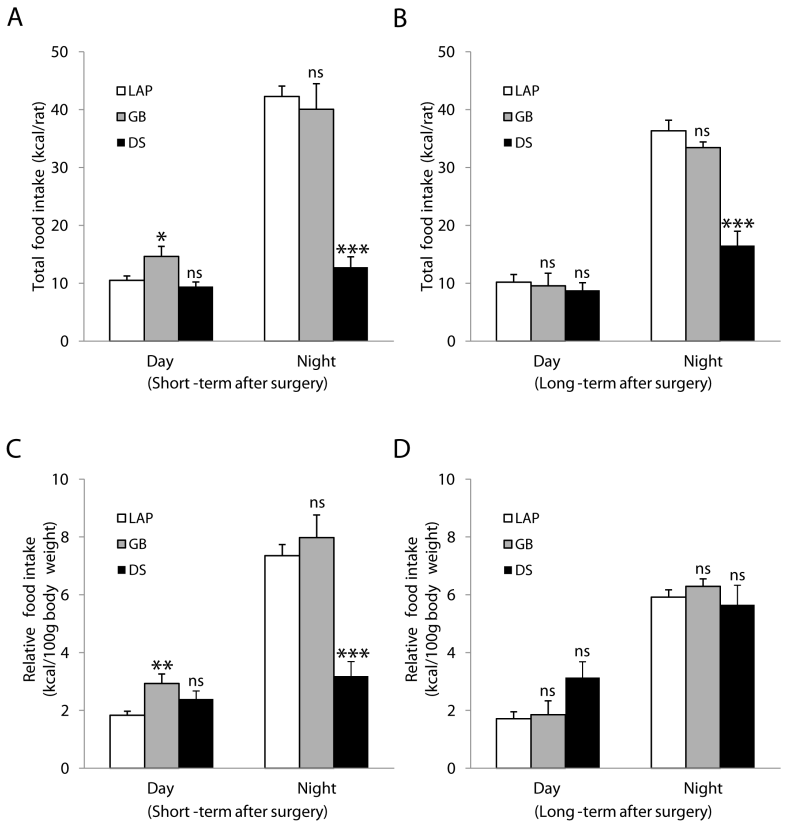

Figure 3. Food intake. Total food intake (kcal/rat) (**A,B**) and relative food intake (kcal/100 g body weight) (**C,D**) during day- and night-time. Short-term after surgery: 3 weeks after gastric bypass (GB), 2 weeks after duodenal switch (DS) or 2–3 weeks after lapatoromy (LAP). Long-term after surgery: 14 weeks after GB, 8 weeks after DS or 8–14 weeks after LAP. Data are expressed as means ± SEM. *: $p<0.05$, **: $p<0.01$, ns: not significant between LAP (n = 13) *vs.* GB (n = 8) or DS (n = 5).
doi:10.1371/journal.pone.0072896.g003

performed for two-group comparisons. ANOVA followed by Bonferroni test was performed for multiple comparisons. Homogeneity of regression assumption test and ANCOVA were performed for analysis of energy expenditure. SPSS version 19.0 (SPSS Inc. Chicago, IL, USA) was used. A p-value of <0.05 was considered statistically significant.

Results

Mortality

No one died after LAP alone, 6 after GB, and 2 after DS due to surgical complications, trauma and learning curve factors.

Body Weight

LAP alone did not reduce body weight during the study period (maximum 14 weeks). GB caused approximately 20% weight loss throughout the study period (14 weeks). DS induced approximately 50% weight loss within 8 weeks (Fig 2B).

Food Intake and Eating Behavior

In comparison with LAP, GB increased daytime (but not nighttime) food intake (expressed as either kcal/rat or kcal/100 g body weight) at 3 weeks, and had no effects afterwards (14 weeks postoperatively). In contrast, DS reduced nighttime (but not daytime) food intake (kcal/rat at both 2 and 8 weeks or kcal/100 g body weight at 2 weeks). The food intake (kcal/100 g) at 8 weeks was not reduced because of markedly loss of the body weight after DS (Fig 3).

GB was without effects neither on satiety ratio (min/g) nor rate of eating (g/min), whereas DS increased satiety ratio during nighttime, and decreased rate of eating during both daytime and nighttime at 2 weeks and 8 weeks postoperatively (Fig 4) (Tables 1,2).

Energy Expenditure

Age-matched control rats that underwent LAP only were included for comparisons because metabolic parameters are age-dependent [23,24]. GB increased nighttime energy expenditure

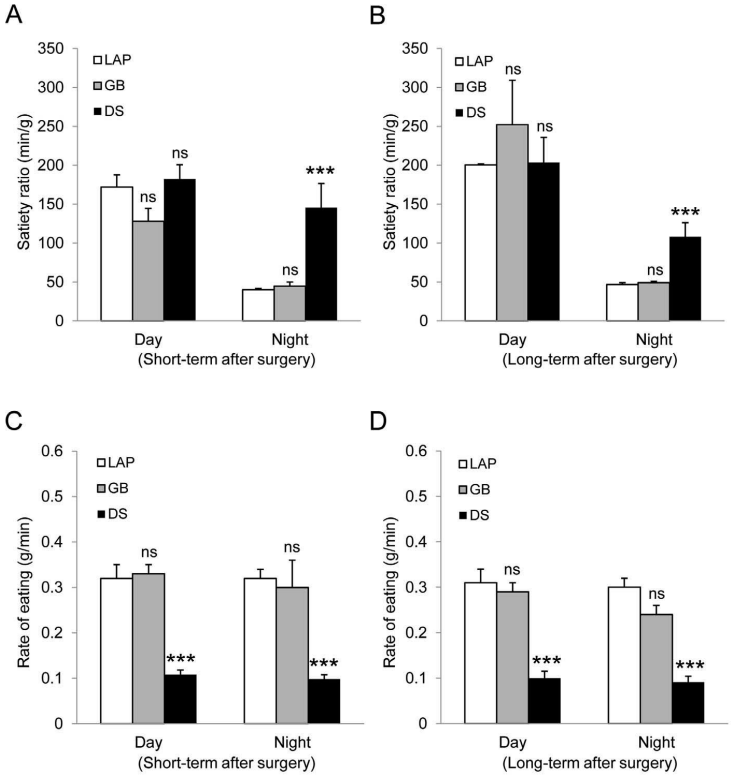

Figure 4. Eating behavior. Satiety ratio (min/g) (**A,B**) and rate of eating (g/min) (**C,D**) during day- and night-time**.** Short-term after surgery: 3 weeks after gastric bypass (GB), 2 weeks after duodenal switch (DS) or 2–3 weeks after lapatoromy (LAP). Long-term after surgery: 14 weeks after GB, 8 weeks after DS or 8–14 weeks after LAP. Data are expressed as means ± SEM. ***: $p<0.001$, ns: not significant between LAP (n = 13) *vs.* GB (n = 8) or DS (n = 5).
doi:10.1371/journal.pone.0072896.g004

(kcal/hr/100 g body weight) at 3 weeks and daytime energy expenditure at 14 weeks postoperatively (Fig 5A, C) (Tables 3, 4). RER was unchanged after GB. DS increased daytime energy expenditure both at 2 and 8 weeks as well as nighttime energy expenditure at 8 weeks postoperatively (Fig 5B, D) (Tables 3, 4). RER tended to be reduced during nighttime at 2 weeks after DS ($p = 0.051$) (Table 3).

Analysis of the homogeneity of regression slopes indicated that there was positive correlation between the body weight and energy expenditure (kcal/hr) particularly in LAP_{DS} rats and similar regression slopes between LAP and GB or DS ($p>0.05$) (Fig S1). ANCOVA showed that there was no significant difference in adjusted energy expenditure between LAP and GB or DS ($p>0.05$) (Fig S2).

Fecal Energy Density

There was no change in the fecal energy density after GB. DS had severe diarrhea within 2 weeks postoperatively, so that it was difficult to collect the fecal samples. At 2 months, the solid feces were collected and the energy density was increased (Fig 6).

Plasma Levels of Cytokines

There was no difference between LAP *vs.* GB or DS in the plasma levels of the 11 cytokines measured (Table S2).

Discussion

The present study shows that the rat models provide results that are in accordance with results from clinical series in patients , i.e. greater weight loss by DS than GB [17,18,25]. Furthermore, the results of the present study show different postsurgical effects of GB *vs.* DS in terms of food intake, eating rate, energy expenditure and absorption.

It is a common dogma that to reduce size of stomach by surgery would lead to early satiety and consequently reduce food intake. Regardless of difference in surgical procedure, either GB or DS reduces stomach size and bypasses part of the small intestine (duodenum and most of the jejunum). Previously, we have found that the food intake was independent on the size of stomach by comparing gastrectomy and GB in rat models [9]. In clinical studies, the size of pouch after GB was found not to correlate with weight loss outcome in patients [25,26]. In our previous and the

Table 1. Eating behavior.

	Parameter	LAP	GB	DS
Day	Food Intake (g)	4.08±0.3	5.69±0.68*	3.67±0.31†
	Food Intake (g/100g body weight)	0.7±0.06	1.14±0.13**	0.93±0.11
	Food intake (kcal)	10.5±0.76	14.62±1.74*	9.42±0.80†
	Food intake (kcal/100g body weight)	1.83±0.14	2.93±0.33**	2.39±0.28
	Number of meals	12.15±0.97	18.29±2.48*	16.6±0.92
	Meal size (g/meal)	0.35±0.03	0.32±0.02	0.22±0.021*
	Meal size (kcal/meal)	0.91±0.08	0.82±0.05	0.57±0.05*
	Meal duration (min)	13.5±1.39	17.96±2.82	34.47±3.29***,†††
	Meal duration (min/meal)	1.14±0.1	0.98±0.08	2.13±0.29***,†††
	Intermeal interval (min)	57.5±4.42	40.37±5.38*	39.38±2.04
	Satiety ratio (min/g)	171.89±15.81	127.93±16.63	182.34±18.24
	Rate of eating (g/min)	0.32±0.03	0.33±0.02	0.11±0.01***,†††
Night	Food Intake (g)	16.45±0.69	15.58±1.72	4.96±0.70***,†††
	Food Intake (g/100g body weight)	2.86±0.15	3.11±0.30	1.24±0.19***,†††
	Food intake (kcal)	42.28±1.77	40.05±4.41	12.76±1.81***,†††
	Food intake (kcal/100g body weight)	7.35±0.39	7.98±0.78	3.19±0.50***,†††
	Number of meals	34.38±3.92	31.71±3.01	24.40±3.85
	Meal size (g/meal)	0.57±0.09	0.51±0.07	0.21±0.03*
	Meal size (kcal/meal)	1.47±0.22	1.30±0.17	0.55±0.08*
	Meal duration (min)	54.21±4.54	56.25±5.13	53.21±9.39
	Meal duration (min/meal)	1.88±0.36	1.82±0.18	2.20±0.28
	Intermeal interval (min)	22.6±3.08	21.36±1.97	29.43±5.57
	Satiety ratio (min/g)	40±1.86	44.64±5.41	145.51±31.17***,†††
	Rate of eating (g/min)	0.32±0.02	0.30±0.06	0.10±0.01***,††

Parameters during day- and night-time at 3 weeks after gastric bypass (GB), 2 weeks after duodenal switch (DS) and 2–3 weeks after laparotomy (LAP). Data are expressed as means ± SEM. *: $p<0.05$, **: $p<0.01$, ***: $p<0.001$ between LAP *vs.* GB or DS. †: $p<0.05$, ††: $p<0.01$, †††: $p<0.001$ between GB *vs.* DS.
doi:10.1371/journal.pone.0072896.t001

present studies, GB did reduce body weight but not food intake in rats [7–9]. Behavior of rats is mostly driven on instincts, while behavior of humans is much more complicated. In fact, there is still an open question: "Does GB reduce food intake in humans?". A recent review shows that large and persistent alterations in macronutrient intake after GB have not generally been reported, and when the changes do occur, they are either transient or relatively modest. The authors argue for more direct measures of food intake in human studies that are similar to those used in animal studies [27]. Food intake in patients is also affected by following the "postoperative instruction" to achieve the best possible conditions for weight reduction and to minimize side-effects like gastro-esophageal reflux and dumping syndrome which unlikely occur in rats. Recently, a human study of eating behavior and meal pattern following GB was still performed by manually weighing differences to determine food and water intake and by the Three-Factor Eating Questionnaire to evaluate eating behavior [28]. However, in that human study, the food intake was not reported, but *ad libitum* meal size was reduced while number of meals per day was increased, and hunger and satiety scores did not change after GB, which are in line with our findings in rats following GB [8]. Methods with more direct measures of food intake (and food-selection and taste-related behavior) for humans are needed in order to facilitate translation between findings from animal models and clinical research [27].

Unlike GB, DS does reduce the food intake. Previously, we have shown that food intake was reduced by duodenal switch alone but not by sleeve gastrectomy alone by comparing sleeve gastrectomy only *vs.* duodenal switch without sleeve gastrectomy in rats [20]. In the present study, DS markedly reduced food intake and increased satiety ratio particularly during nighttime. The rate of eating has also impacts on body weight. It has been reported that there is a correlation between rate of eating and body weight or body mass index (BMI) [29,30]. Previously, we have shown that high-fat-diet-induced obesity was associated with increased rate of eating, increased size of meals, but not with daily calories intake [31]. In the present study, DS decreased the eating rate during both day- and night-time.

Mechanisms underlying postoperative weight loss and possible regain remain unclear. A major point of controversy is whether this is due to biological or behavioral factors [19,32]. We and others have shown that GB increased the energy expenditure in rats and mice, which could be one of the mechanisms explaining the physiologic basis of weight loss after this procedure [8,33,34]. The increased resting energy expenditure in the animal models after GB is in accordance with some, but not all, reports in humans. The discrepancies in the clinical studies may include the heterogeneity of patient populations and measurements of energy expenditure for a limited time using portable metabolic carts under artificial rather than "free-living" conditions [35]. Nerve-less, resting energy expenditure has been suggested to be a

Table 2. Eating behavior.

	Parameter	LAP	GB	DS
Day	Food Intake (g)	3.97±0.51	3.71±0.85	3.42±0.50
	Food Intake (g/100g body weight)	0.66±0.09	0.72±0.19	1.22±0.21
	Food intake (kcal)	10.19±1.32	9.54±2.18	8.78±1.29
	Food intake (kcal/100g body weight)	1.71±0.24	1.85±0.48	3.14±0.54
	Number of meals	10.92±1.29	11.25±1.81	18.60±4.50
	Meal size (g/meal)	0.4±0.06	0.34±0.06	0.23±0.05
	Meal size (kcal/meal)	1.03±0.17	0.86±0.15	0.59±0.12
	Meal duration (min)	13.54±1.74	13.89±3.86	37.17±6.92***,†††
	Meal duration (min/meal)	1.37±0.22	1.23±0.22	2.34±0.45
	Intermeal interval (min)	68.39±7.92	73.68±16.91	50.16±17.90
	Satiety ratio (min/g)	200.34±27.9	252.16±57.01	203.50±32.22
	Rate of eating (g/min)	0.31±0.03	0.29±0.02	0.10±0.01***
Night	Food Intake (g)	14.15±0.71	13.00±0.38	6.43±0.96***,†††
	Food Intake (g/100g body weight)	2.3±0.1	2.45±0.10	2.20±0.26
	Food intake (kcal)	36.35±1.82	33.42±0.98	16.52±2.46***,†††
	Food intake (kcal/100g body weight)	5.92±0.25	6.29±0.26	5.65±0.68
	Number of meals	26.92±2.76	26.50±3.69	34.20±7.13
	Meal size (g/meal)	0.59±0.06	0.58±0.09	0.24±0.07*,†
	Meal size (kcal/meal)	1.52±0.15	1.48±0.23	0.61±0.19*,†
	Meal duration (min)	50.66±4.57	56.36±2.96	70.58±5.38*
	Meal duration (min/meal)	2.01±0.18	2.53±0.47	2.39±0.44
	Intermeal interval (min)	27.78±3.84	27.91±4.11	21.49±4.03
	Satiety ratio (min/g)	46.78±2.4	49.20±1.56	108.18±17.98***,†††
	Rate of eating (g/min)	0.3±0.02	0.24±0.02	0.09±0.01***,††

Parameters during day- and night-time at 14 weeks after gastric bypass (GB), 8 weeks after duodenal switch (DS) and 8–14 weeks after laparotomy (LAP). Data are expressed as mean ± SEM. *: $p<0.05$, **: $p<0.01$, ***: $p<0.001$ between LAP *vs.* GB or DS. †: $p<0.05$, ††: $p<0.01$, †††: $p<0.001$ between GB *vs.* DS.

doi:10.1371/journal.pone.0072896.t002

therapeutic target for obesity [32,36]. In the present study, we further showed that the increased energy expenditure took place only during nighttime (relevant to active energy expenditure) shortly after GB (weeks) and switched to daytime (resting energy expenditure) after months, whereas the energy expenditure was increased during daytime shortly after DS and during both day- and night-time months after DS.

The most extensively used method for calculation of energy expenditure is dividing O_2 consumption by body weight or body surface area [37]. In the present study, the energy expenditure was calculated by taking into account both O_2 consumption and CO_2 production, and expressed as kcal/hr/rat, kcal/hr/100 g body weight, and kcal/hr/cm^2 body surface. Dividing the energy expenditure by body weight does not take into account differences in body composition, and therefore, the fat-free mass or lean body mass (as denominator) has often been used in both human and mouse studies. However, this could be inappropriate because brown fat can be the most metabolically active tissue in the body [37]. ANCOVA has been suggested to be appropriate method for analysis of the mouse energy expenditure, but it cannot be used when the samples sizes are small [37,38]. In rat studies, ANCOVA has not been used with the exception of a few reports including our previous study of ileal interposition associated with sleeve gastrectomy [5,39]. The reasons for not widely use of ANCOVA than ANOVA in rat studies might be less statistical power when sample size is small and nonlinear relationship between covariate (s) and dependent variable. Another reason may be that ANCOVA is best used with quasi-experimental data, such as genetically-modified mice [37] or humans [40,41]. The results of the present study showed that there were highly correlation between the body weight and the energy expenditure (kcal/hr/rat) in control LAP rats, and significant increases in the energy expenditure (kcal/hr and/or kcal/hr/100 g body weight) after GB or DS (by ANOVA). However, ANCOVA showed no significant difference in the energy expenditure (kcal/hr) between LAP and GB or DS. The difference in terms of p values by ANOVA *vs.* ANCOVA (i.e. testing the body-weight independent differences) can be interpreted as that GB or DS increases the energy expenditure (possible cause) while reducing the body weight (effect), which is at odds with the positive correlation between the body weight and the energy expenditure in control animals (LAP).

Both GB and DS are designed for restriction and malabsorption by creating the alimentary limb. However, DS, but not GB, caused diarrhea shortly after surgery (2 weeks) and malabsorption (measured at 2 months postoperatively) in rats, which is in line with observations in patients [42].

It should be noticed that in the present study, neither prophylactic nor postoperative antibiotics were used and none of the 11 plasmas cytokines measured was changed after surgery, indicating no or little impact of microflora and inflammation on the eating behavior and the body weight changes. Recently, a mouse study showed that specific alterations in the gut microbiota

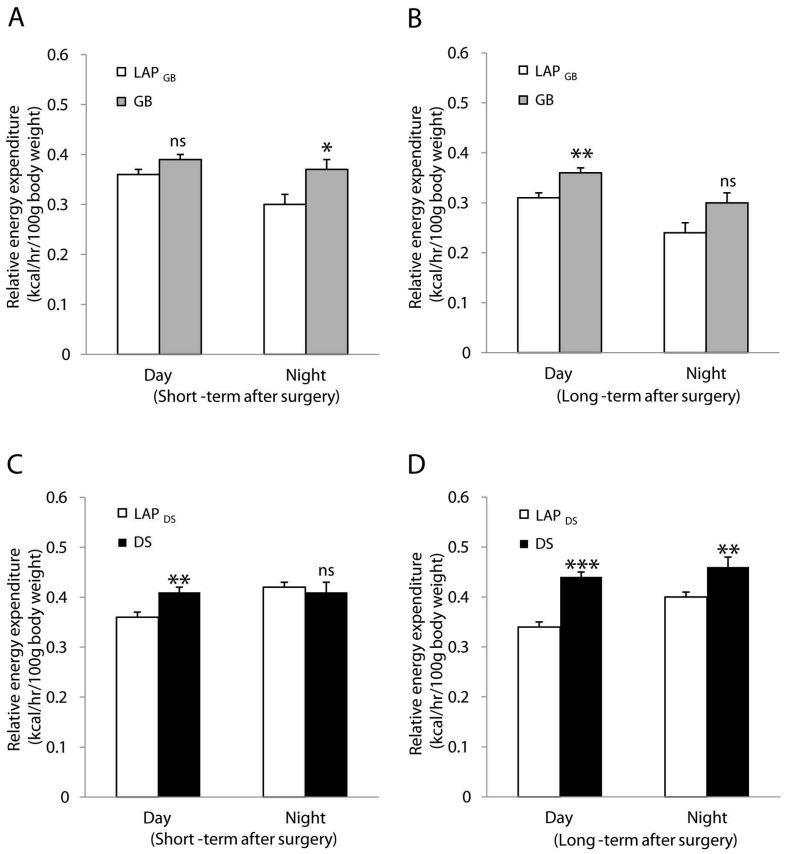

Figure 5. Energy expenditure during day- and night-time. Short-term after surgery: 3 weeks after gastric bypass (GB), 2 weeks after duodenal switch (DS) or 2–3 weeks after laparotomy (LAP). Long-term after surgery: 14 weeks after GB, 8 weeks after DS or 8–14 weeks after LAP. Data are expressed as means ± SEM. *: $p<0.05$, **: $p<0.01$, ***: $p<0.001$, ns: not significant between LAP_{GB} (n = 7) *vs.* GB (n = 8) or LAP_{DS} (n = 6) *vs.* DS (n = 5).
doi:10.1371/journal.pone.0072896.g005

contributed to the beneficial effect of bariatric surgery on energy balance [43]. Whether GB or DS alters the gut microbiota and consequently leads to the weight loss via same or different pathways might be of interest for future study.

There are several limitations of the present study. 1) The rats used were not obese. Whether or not the postsurgical effects of these two procedures are different between normal and obese rats that are induced by high-fat diet or developed spontaneously (e.g. Zucker, Otsuka Long-Evans Tokushima Fatty, Obese SHR, or Wistar Ottawa Karlsburg W rats), and which animal model of obesity best mimics the obese humans in response to the bariatric surgery could be the subjects for further research. 2) GB procedure used in rats was not exactly the same as it was applied in humans. Fig 1 shows different procedures of GB. A laparoscopic mini-gastric bypass procedure (which is similar with one used in the present study) has been shown to be regarded as a simpler and safer alternative to laparoscopic Roux-en-Y procedure with similar efficacy at 5 or 10 year experience [2,44]. It may be of interest to compare different GB procedures in the future, if there is any clinical relevancy. 3) Although the size of gastric pouch after GB does not correlate with weight loss outcome in patients [25,26], it cannot be excluded whether lack of the pouch in GB has impact on food intake, satiety and eating behavior. 4) The differences between rats and humans are not only in terms of the GI anatomy but also the responses to surgery. For instance, sleeve gastrectomy only (without duodenal switch) works in some patients but not in rats [20,45]. It may be of interest to directly compare the effects of sleeve only *vs.* sleeve with duodenal switch (one or two-staged) in the future.

In general, research in patients is directly clinical relevant. However, studies in animals provide much greater latitude in control and experimental manipulation of the system, and ultimately help to reveal the underlying mechanisms and to adopt the protocols and methods that are tested in animals to humans [46]. Research using animal models is an excellent way of developing and learning bariatric surgical techniques as well as understanding the postsurgical physiology [47]. Taken the data from the previous and the present studies together, the

Table 3. Metabolism.

		3 weeks after surgery		2 weeks after surgery	
	Parameter	**LAP_{GB}**	**GB**	**LAP_{DS}**	**DS**
Day	Energy expenditure (kcal/hr)	2.08±0.03	1.93±0.06	2.08±0.07	1.66±0.12**
	Energy expenditure (kcal/hr/100g body weight)	0.36±0.01	0.39±0.01	0.36±0.01	0.41±0.01**
	Energy expenditure (kcal/hr/cm^2 body surface)	0.003±0.0001	0.004±0.0001	0.003±0.0001	0.004±0.0002
	RER	0.94±0.01	0.93±0.02	1.02±0.03	0.96±0.03
	VO_2	726.68±15.56	779.91±23.26	705.18±18.00	823.91±31.49**
	VCO_2	682.50±12.08	727.85±23.54	717.08±26.45	791.69±26.59
Night	Energy expenditure (kcal/hr)	1.75±0.14	1.85±0.10	2.45±0.08	1.66±0.10***
	Energy expenditure (kcal/hr/100g body weight)	0.30±0.02	0.37±0.02*	0.42±0.01	0.41±0.02
	Energy expenditure (kcal/hr/cm^2 body surface)	0.003±0.0002	0.003±0.0002	0.004±0.0001	0.004±0.0002*
	RER	1.00±0.01	1.01±0.03	1.07±0.03	0.97±0.04
	VO_2	600.02±36.70	737.88±43.20*	820.65±20.88	823.94±35.51
	VCO_2	594.19±37.54	735.07±35.39*	877.73±35.71	803.06±49.36

Parameters during day- and night-time at 3 weeks after gastric bypass (GB) and the age-matched laparotomy-operated group (LAP_{GB}), and at 2 weeks after duodenal switch (DS) and the age-matched laparotomy-operated group (LAP_{DS}). Data are expressed as means ± SEM. *: $p<0.05$, **: $p<0.01$, ***: $p<0.001$ between LAP_{GB} *vs.* GB or LAP_{DS} *vs.* DS.

doi:10.1371/journal.pone.0072896.t003

appropriately designed rat models provide significant insights into the mechanisms of bariatric surgery which explain well the clinical observations, e.g. that DS is superior to GB in body weight loss. The results of the present study may suggest further that GB induces body weight loss by increasing energy expenditure, whereas DS induces greater body weight loss by reducing food intake, increasing energy expenditure and causing malabsorption.

Table 4. Metabolism.

		14 weeks after surgery		8 weeks after surgery	
	Parameter	**LAP_{GB}**	**GB**	**LAP_{DS}**	**DS**
Day	Energy expenditure (kcal/hr)	1.92±0.08	1.90±0.05	2.10±0.06	1.27±0.07***
	Energy expenditure (kcal/hr/100g body weight)	0.31±0.01	0.36±0.01**	0.34±0.01	0.44±0.01***
	Energy expenditure (kcal/hr/cm^2 body surface)	0.003±0.0001	0.003±0.0000*	0.003±0.0000	0.003±0.0001
	RER	0.98±0.03	0.91±0.05	0.99±0.03	0.98±0.01
	VO_2	622.25±27.61	720.95±14.41**	681.99±13.62	873.32±25.35***
	VCO_2	605.31±17.73	652.48±25.93	675.60±23.89	853.15±25.17***
Night	Energy expenditure (kcal/hr)	1.48±0.11	1.60±0.10	2.45±0.12	1.34±0.01***
	Energy expenditure (kcal/hr/100g body weight)	0.24±0.02	0.30±0.02	0.40±0.01	0.46±0.02***
	Energy expenditure (kcal/hr/cm^2 body surface)	0.002±0.0002	0.003±0.0002	0.004±0.0001	0.004±0.0001*
	RER	0.97±0.06	1.04±0.05	1.06±0.03	0.99±0.03
	VO_2	475.14±36.56	598.36±45.29	778.37±16.51	919.50±28.99**
	VCO_2	487.63±35.15	609.64±55.95	825.43±27.97	906.74±39.86

Parameters during day- and nighttime at 14 weeks after gastric bypass (GB) and the age-matched laparotomy-operated group (LAP_{GB}), and at 8 weeks after duodenal switch (DS) and the age-matched laparotomy-operated group (LAP_{DS}). Data are expressed as means ± SEM. *: $p<0.05$, **: $p<0.01$, ***: $p<0.001$ between LAP_{GB} *vs.* GB or LAP_{DS} *vs.* DS.

doi:10.1371/journal.pone.0072896.t004

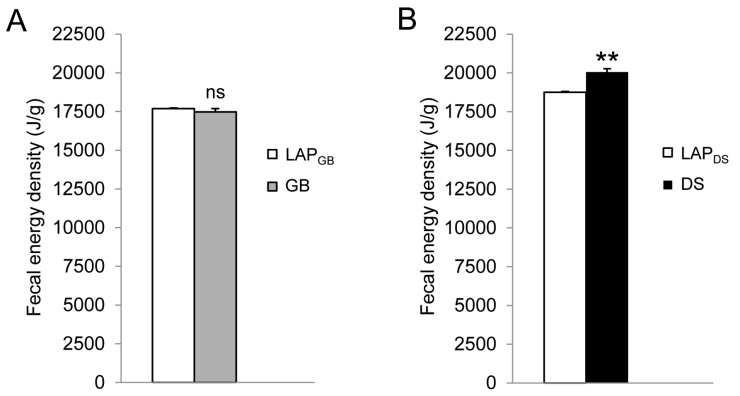

Figure 6. Fecal energy density. Three weeks after gastric bypass (GB) or laparotomy (LAP_{GB}) (**A**) and eight weeks after duodenal switch (DS) or laparotomy (LAP_{DS}) (**B**). Data are expressed as mean ± SEM. **: $p<0.01$, ns: not significant between LAP_{GB} (n = 7) *vs.* GB (n = 8) or LAP_{DS} (n = 6) *vs.* DS (n = 5).
doi:10.1371/journal.pone.0072896.g006

Supporting Information

Figure S1 Scatterplot of energy expenditure against body weight. $LAP_{GB\ or\ DS}$: laparotomy as control for GB or DS; GS: gastric bypass; DS: Duodenal switch.
(TIF)

Figure S2 Adjust energy expenditure by ANCOVA. $LAP_{GB\ or\ DS}$: laparotomy as control for GB or DS; GS: gastric bypass; DS: Duodenal switch. Means ± SEM.
(TIF)

Table S1 CLAMS measurements of normal rats. Data at day 1 and 21 one week after 24 hours training with CLAMS cage are expressed as means ± SEM. ns: not significant between day 1 vs. day 21.
(DOC)

Table S2 Plasma levels of cytokines. Data of rats after gastric bypass (GB) and duodenal switch (DS) compared with the age-matched laparotomy-operated groups (LAP_{GB} or LAP_{DS}, respectively) are expressed as means ± SEM. ns: not significant between LAP_{GB} vs. GB or LAP_{DS} vs. DS.
(DOC)

Acknowledgments

The authors thank Morten Grønli and Erik Langørgen for assistance of bomb calorimeter at Department of Energy and Process Engineering, and Terje Espevik and Liv Ryan for analysis of cytokines at Centre of Molecular Inflammation Research, Department of Cancer Research and Molecular Medicine, Norwegian University of Science and Technology.

Author Contributions

Conceived and designed the experiments: YK HJ MWF C-MZ GJ RM BK DC. Performed the experiments: YK HJ DC. Analyzed the data: YK HJ DC. Contributed reagents/materials/analysis tools: MWF C-MZ BK DC. Wrote the paper: YK HJ C-MZ GJ BK DC.

References

1. Ward M, Prachand V (2009) Surgical treatment of obesity. Gastrointest Endosc 70: 985–990.
2. Noun R, Skaff J, Riachi E, Daher R, Antoun NA, et al. (2012) One thousand consecutive mini-gastric bypass: short- and long-term outcome. Obes Surg 22: 697–703.
3. Stylopoulos N, Hoppin AG, Kaplan LM (2009) Roux-en-Y gastric bypass enhances energy expenditure and extends lifespan in diet-induced obese rats. Obesity (Silver Spring) 17: 1839–1847.
4. Sabench Pereferrer F, Hernandez Gonzalez M, Del Castillo Dejardin D (2011) Experimental metabolic surgery: justification and technical aspects. Obes Surg 21: 1617–1628.
5. Johannessen H, Kodama Y, Zhao CM, Sousa MM, Slupphaug G, et al. (2013) Eating behavior and glucagon-like peptide-1-producing cells in interposed ileum and pancreatic islets in rats subjected to ileal interposition associated with sleeve gastrectomy. Obes Surg 23: 39–49.
6. Earlam R (1983) Bile reflux and the Roux en Y anastomosis. Br J Surg 70: 393–397.
7. Stenstrom B, Furnes MW, Tommeras K, Syversen U, Zhao CM, et al. (2006) Mechanism of gastric bypass-induced body weight loss: one-year follow-up after micro-gastric bypass in rats. J Gastrointest Surg 10: 1384–1391.
8. Furnes MW, Tømmerås K, Arum CJ, Zhao CM, Chen D (2008) Gastric bypass surgery causes body weight loss without reducing food intake in rats. Obes Surg 18: 415–422.
9. Furnes MW, Stenström B, Tømmerås K, Skoglund T, Dickson SL, et al. (2008) Feeding behavior in rats subjected to gastrectomy or gastric bypass surgery. Eur Surg Res 40: 279–288.
10. DeMeester TR, Fuchs KH, Ball CS, Albertucci M, Smyrk TC, et al. (1987) Experimental and clinical results with proximal end-to-end duodenojejunostomy for pathologic duodenogastric reflux. Ann Surg 206: 414–426.
11. DeSesso JM, Jacobson CF (2001) Anatomical and physiological parameters affecting gastrointestinal absorption in humans and rats. Food Chem Toxicol 39: 209–228.
12. Anthone GJ, Lord RV, DeMeester TR, Crookes PF (2003) The duodenal switch operation for the treatment of morbid obesity. Ann Surg 238: 618–627; discussion 627–618.
13. Laurenius A, Taha O, Maleckas A, Lonroth H, Olbers T (2010) Laparoscopic biliopancreatic diversion/duodenal switch or laparoscopic Roux-en-Y gastric bypass for super-obesity-weight loss versus side effects. Surg Obes Relat Dis 6: 408–414.
14. Strain GW, Gagner M, Inabnet WB, Dakin G, Pomp A (2007) Comparison of effects of gastric bypass and biliopancreatic diversion with duodenal switch on weight loss and body composition 1–2 years after surgery. Surg Obes Relat Dis 3: 31–36.
15. Prachand VN, Davee RT, Alverdy JC (2006) Duodenal switch provides superior weight loss in the super-obese (BMI > or = 50 kg/m2) compared with gastric bypass. Ann Surg 244: 611–619.

16. Prachand VN, Ward M, Alverdy JC (2010) Duodenal switch provides superior resolution of metabolic comorbidities independent of weight loss in the super-obese (BMI > or = 50 kg/m2) compared with gastric bypass. J Gastrointest Surg 14: 211–220.
17. Sovik TT, Taha O, Aasheim ET, Engstrom M, Kristinsson J, et al. (2010) Randomized clinical trial of laparoscopic gastric bypass versus laparoscopic duodenal switch for superobesity. Br J Surg 97: 160–166.
18. Sovik TT, Aasheim ET, Taha O, Engstrom M, Fagerland MW, et al. (2011) Weight loss, cardiovascular risk factors, and quality of life after gastric bypass and duodenal switch: a randomized trial. Ann Intern Med 155: 281–291.
19. Hill JO, Wyatt HR (1999) Relapse in obesity treatment: biology or behavior? Am J Clin Nutr 69: 1064–1065.
20. Kodama Y, Zhao CM, Kulseng B, Chen D (2010) Eating behavior in rats subjected to vagotomy, sleeve gastrectomy, and duodenal switch. J Gastrointest Surg 14: 1502–1510.
21. Dapri G, Cadiere GB, Himpens J (2011) Superobese and super-superobese patients: 2-step laparoscopic duodenal switch. Surg Obes Relat Dis 7: 703–708.
22. Zorrilla EP, Inoue K, Fekete EM, Tabarin A, Valdez GR, et al. (2005) Measuring meals: structure of prandial food and water intake of rats. Am J Physiol Regul Integr Comp Physiol 288: R1450–1467.
23. Iossa S, Lionetti L, Mollica MP, Barletta A, Liverini G (1999) Energy intake and utilization vary during development in rats. J Nutr 129: 1593–1596.
24. Roberts SB, Dallal GE (2005) Energy requirements and aging. Public Health Nutr 8: 1028–1036.
25. Topart P, Becouarn G, Ritz P (2012) Weight loss is more sustained after biliopancreatic diversion with duodenal switch than Roux-en-Y gastric bypass in superobese patients. Surg Obes Relat Dis.
26. MacLean LD, Rhode BM, Nohr CW (2000) Late outcome of isolated gastric bypass. Ann Surg 231: 524–528.
27. Mathes CM, Spector AC (2012) Food selection and taste changes in humans after Roux-en-Y gastric bypass surgery: a direct-measures approach. Physiol Behav 107: 476–483.
28. Laurenius A, Larsson I, Bueter M, Melanson KJ, Bosaeus I, et al. (2012) Changes in eating behaviour and meal pattern following Roux-en-Y gastric bypass. Int J Obes (Lond) 36: 348–355.
29. Otsuka R, Tamakoshi K, Yatsuya H, Murata C, Sekiya A, et al. (2006) Eating fast leads to obesity: findings based on self-administered questionnaires among middle-aged Japanese men and women. J Epidemiol 16: 117–124.
30. Takayama S, Akamine Y, Okabe T, Koya Y, Haraguchi M, et al. (2002) Rate of eating and body weight in patients with type 2 diabetes or hyperlipidaemia. J Int Med Res 30: 442–444.
31. Furnes MW, Zhao CM, Chen D (2009) Development of obesity is associated with increased calories per meal rather than per day. A study of high-fat diet-induced obesity in young rats. Obes Surg 19: 1430–1438.
32. Astrup A, Gotzsche PC, van de Werken K, Ranneries C, Toubro S, et al. (1999) Meta-analysis of resting metabolic rate in formerly obese subjects. Am J Clin Nutr 69: 1117–1122.
33. Bueter M, Lowenstein C, Olbers T, Wang M, Cluny NL, et al. (2010) Gastric bypass increases energy expenditure in rats. Gastroenterology 138: 1845–1853.
34. Nestoridi E, Kvas S, Kucharczyk J, Stylopoulos N (2012) Resting Energy Expenditure and Energetic Cost of Feeding Are Augmented after Roux-en-Y Gastric Bypass in Obese Mice. Endocrinology.
35. Bueter M, le Roux CW (2011) Gastrointestinal hormones, energy balance and bariatric surgery. Int J Obes (Lond) 35 Suppl 3: S35–39.
36. Bays HE (2004) Current and investigational antiobesity agents and obesity therapeutic treatment targets. Obes Res 12: 1197–1211.
37. Tschop MH, Speakman JR, Arch JR, Auwerx J, Bruning JC, et al. (2012) A guide to analysis of mouse energy metabolism. Nat Methods 9: 57–63.
38. Butler AA, Kozak LP (2010) A recurring problem with the analysis of energy expenditure in genetic models expressing lean and obese phenotypes. Diabetes 59: 323–329.
39. Zelova J, Sumbera R, Okrouhlik J, Skliba J, Lovy M, et al. (2011) A seasonal difference of daily energy expenditure in a free-living subterranean rodent, the silvery mole-rat (Heliophobius argenteocinereus; Bathyergidae). Comp Biochem Physiol A Mol Integr Physiol 158: 17–21.
40. Miller GA, Chapman JP (2001) Misunderstanding analysis of covariance. J Abnorm Psychol 110: 40–48.
41. Owen SV, Froman RD (1998) Uses and abuses of the analysis of covariance. Res Nurs Health 21: 557–562.
42. Leff DR, Heath D (2009) Surgery for obesity in adulthood. BMJ 339: b3402.
43. Liou AP, Paziuk M, Luevano JM, Jr., Machineni S, Turnbaugh PJ, et al. (2013) Conserved shifts in the gut microbiota due to gastric bypass reduce host weight and adiposity. Sci Transl Med 5: 178ra141.
44. Lee WJ, Ser KH, Lee YC, Tsou JJ, Chen SC, et al. (2012) Laparoscopic Roux-en-Y Vs. Mini-gastric Bypass for the Treatment of Morbid Obesity: a 10-Year Experience. Obes Surg.
45. Victorzon M (2012) An update on sleeve gastrectomy. Minerva Chir 67: 153–163.
46. Mathes CM, Spector AC (2012) Food selection and taste changes in humans after Roux-en-Y gastric bypass surgery: A direct-measures approach. Physiol Behav.
47. Ashrafian H, Bueter M, Ahmed K, Suliman A, Bloom SR, et al. (2010) Metabolic surgery: an evolution through bariatric animal models. Obes Rev 11: 907–920.

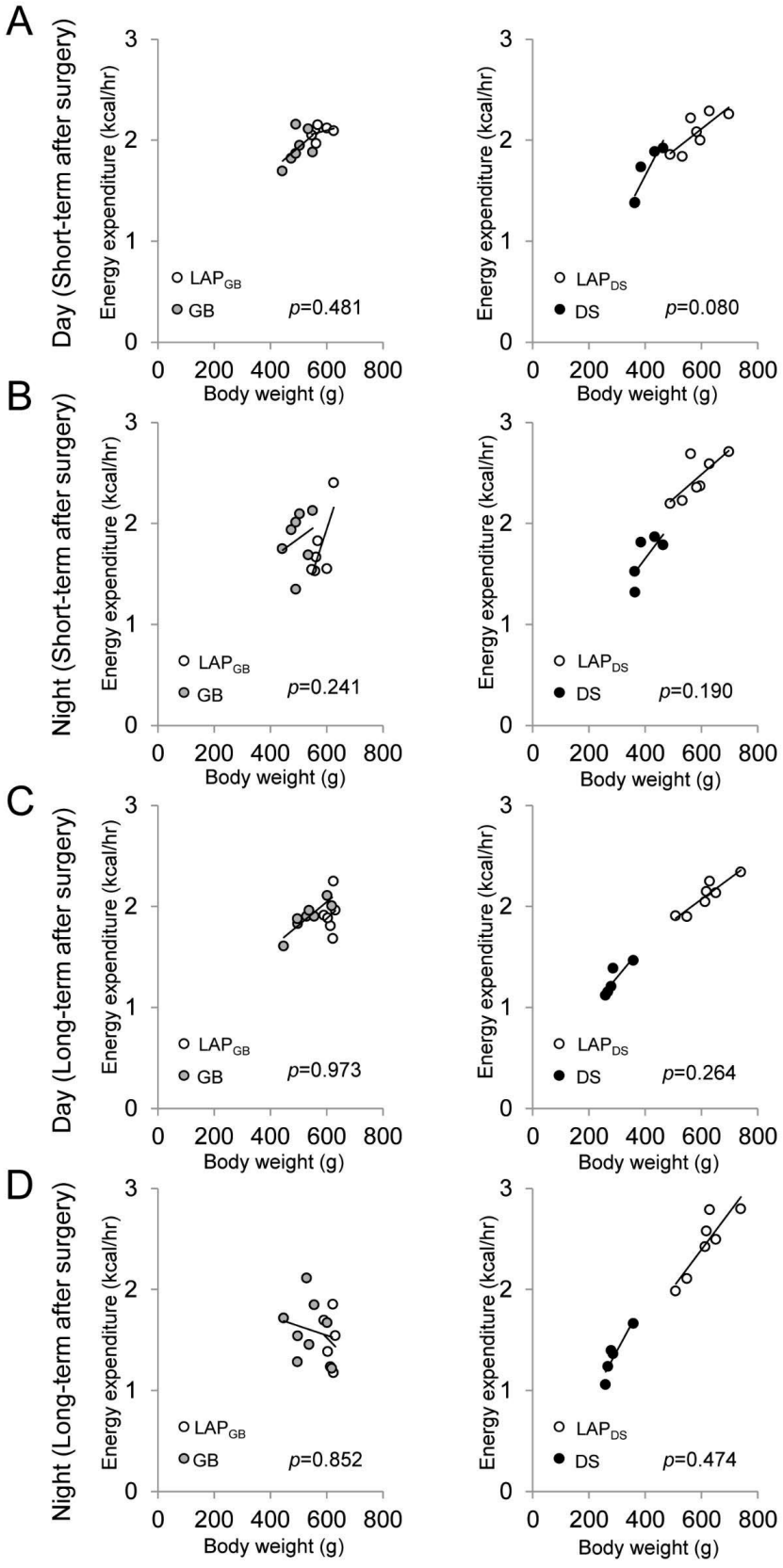

Supplementary Fig. 1: Scatterplot of energy expenditure against body weight for each of the experimental groups. LAP $_{GB\ or\ DS}$: laparotomy as control for GB or DS; GS: gastric bypass; DS: Duodenal switch.

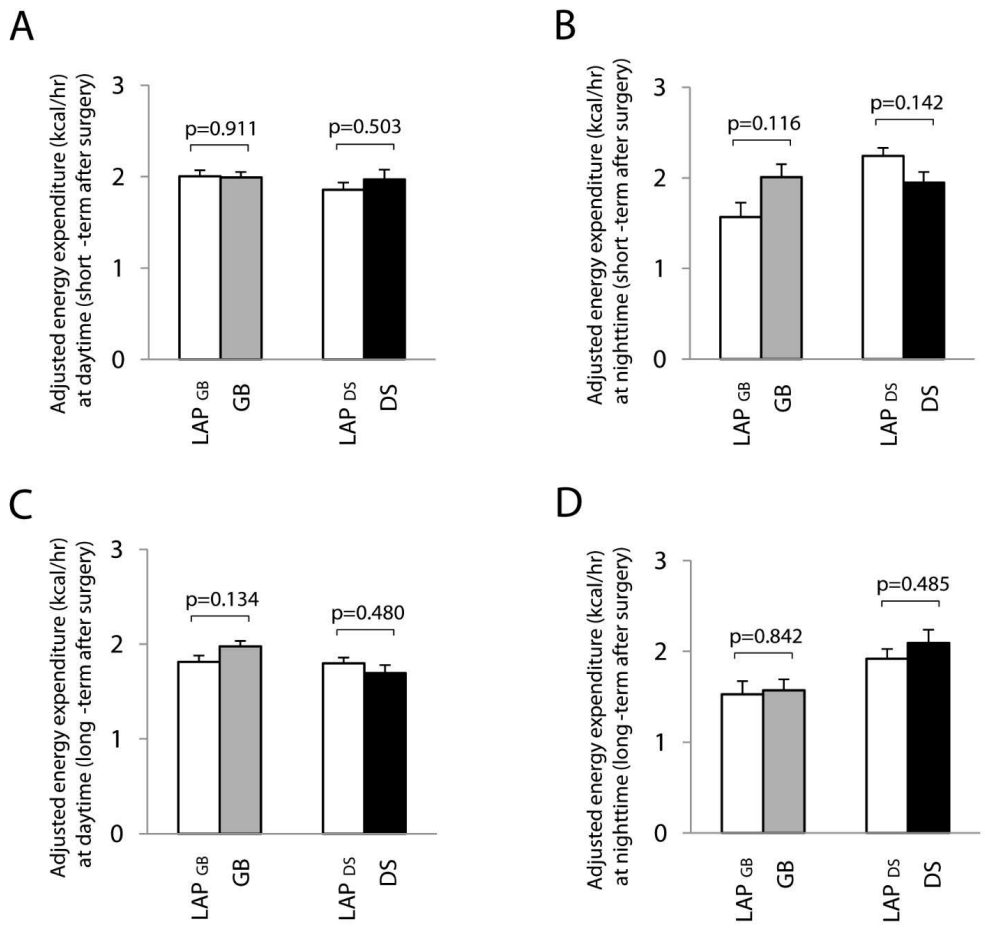

Supplementary Fig. 2: Adjust energy expenditure (kcal/hr) by ANCOVA (data from Figure. 5). LAP $_{GB\ or\ DS}$: laparotomy as control for GB or DS; GS: gastric bypass; DS: Duodenal switch. Means ± SEM

Supplementary Table 1. CLAMS measurements of normal rats at day 1 and 21 one week after 24 hours training with CLAMS cage. Data are expressed as means ± SEM. ns: not significant between day 1 *vs.* day 21.

	Parameter	Day 1	Day 21
Day	Food Intake (g)	6.76±0.67	7.36±0.60 ^{ns}
	Food Intake (g/100g body weight)	1.38±0.14	1.46±0.14 ^{ns}
	Food intake (kcal)	17.36±1.72	18.90±1.53 ^{ns}
	Food intake (kcal/100g body weight)	3.54±0.35	3.74±0.36 ^{ns}
	Number of meals	14.17±1.66	13.50±1.48 ^{ns}
	Meal size (g/meal)	0.52±0.10	0.56±0.05 ^{ns}
	Meal size (kcal/meal)	1.34±0.25	1.45±0.12 ^{ns}
	Meal duration (min)	18.98±2.07	21.10±1.95 ^{ns}
	Meal duration (min/meal)	1.45±0.27	1.61±0.15 ^{ns}
	Intermeal interval (min)	49.44±5.95	50.43±4.48 ^{ns}
	Satiety ratio (min/g)	101.03±9.37	90.73±6.44 ^{ns}
	Water intake (mL)	2.17±0.64	2.24±0.42 ^{ns}
	Water intake (mL/100g body weight)	0.45±0.13	0.45±0.09 ^{ns}
	Water intake during one interval (mL/time)	0.25±0.07	0.28±0.05 ^{ns}
	Ambulatory activity	1305.17±318.30	1451.17±326.57 ^{ns}
Night	Food Intake (g)	19.38±0.72	21.07±0.78 ^{ns}
	Food Intake (g/100g body weight)	3.94±0.13	4.15±0.19 ^{ns}
	Food intake (kcal)	49.80±1.85	54.16±2.00 ^{ns}
	Food intake (kcal/100g body weight)	10.13±0.33	10.67±0.50 ^{ns}
	Number of meals	29.17±2.65	28.83±3.89 ^{ns}
	Meal size (g/meal)	0.68±0.04	0.79±0.09 ^{ns}
	Meal size (kcal/meal)	1.75±0.11	2.02±0.24 ^{ns}
	Meal duration (min)	62.62±3.01	63.66±2.10 ^{ns}
	Meal duration (min/meal)	2.21±0.15	2.36±0.24 ^{ns}
	Intermeal interval (min)	22.57±1.80	23.88±2.95 ^{ns}
	Satiety ratio (min/g)	32.98±1.22	30.20±1.05 ^{ns}
	Water intake (mL)	16.14±0.74	17.70±0.60 ^{ns}
	Water intake (mL/100g body weight)	3.28±0.12	3.48±0.13 ^{ns}
	Water intake during one interval (mL/time)	0.87±0.15	0.89±0.09 ^{ns}
	Ambulatory activity	5292.00±1166.98	4484.00±833.95 ^{ns}

Supplementary Table 2. Plasma levels of cytokines in rats after gastric bypass (GB) and duodenal switch (DS) compared with the age-matched laparotomy-operated groups (LAP_{GB} or LAP_{DS}, respectively). Data are expressed as means ± SEM. ns: not significant between LAP_{GB} *vs.* GB or LAP_{DS} *vs.* DS.

Cytokine	LAP_{GB}	GB	LAP_{DS}	DS
IL1α (pg/mL)	66.20±21.31	33.48±21.01 ^{ns}	94.34±33.31	124.84±19.20 ^{ns}
IL-1β (pg/mL)	74.06±22.89	32.63±11.51 ^{ns}	310.22±175.16	215.53±87.70 ^{ns}
IL-2 (pg/mL)	201.62±59.23	112.19±46.99 ^{ns}	190.21±40.10	373.21±69.13 ^{ns}
IL-4 (pg/mL)	10.62±2.48	27.33±22.06 ^{ns}	39.37±17.56	41.69±9.90 ^{ns}
IL-5 (pg/mL)	38.08±8.80	41.19±10.48 ^{ns}	129.45±26.03	106.05±18.71 ^{ns}
IL-6 (pg/mL)	111.53±51.69	208.33±176.17 ^{ns}	216.85±82.11	158.36±49.23 ^{ns}
IL-10 (pg/mL)	213.33±29.71	145.88±31.72 ^{ns}	534.60±139.86	588.50±74.00 ^{ns}
IL-13 (pg/mL)	19.52±8.16	4.47±1.23 ^{ns}	61.05±33.76	55.41±19.65 ^{ns}
GM-CSF (pg/mL)	9.42±4.59	1.23±0.41 ^{ns}	41.06±24.68	30.81±12.69 ^{ns}
IFNγ (pg/mL)	53.90±25.31	106.47±105.90 ^{ns}	76.90±38.39	75.45±24.11 ^{ns}
TNFα (pg/mL)	9.25±6.98	3.72±0.35 ^{ns}	65.66±46.06	56.94±29.70 ^{ns}